INVESTIGATION INTO THE EFFECTS OF THE TROPOSPHERE ON VHF AND UHF RADIO PROPAGATION AND INTERFERENCE BETWEEN CO-FREQUENCY FIXED LINKS

Thesis submitted for the degree of

Doctor of Philosophy

at the University of Leicester

by

Naveed Mufti

Department of Engineering

University of Leicester

October 2011

ABSTRACT

Previous studies on anomalous, over-sea propagation have been either focused on single links employing space/antenna diversity or on point-to-multipoint links, usually involving single frequency. Measurements on two co-linear, trans-horizon paths (50km and 140 km long) over the English Channel have been made over periods in excess of a year in order to investigate the propagation characteristics of VHF and UHF signals propagating over the sea. The setup comprises a transmitter located on Jersey and receivers on Alderney and Portland. Signal strengths, meteorological factors within the lowest 1 km as well as their mutual relationships have been studied.

Signal strength enhancements have been observed on both paths, primarily in the late afternoon and evening periods, in the spring and summer months. These enhancements occur for different percentages of time between 12% and 21%. It was observed that the enhancements at both receiving sites and both frequencies may/may not be concurrent, leading to a probability of interference. The values of median lapse rate of refractivity in lowest 1km of atmosphere, effective earth radius factor and surface refractivity significantly less than those used by ITU have been observed. Refractivity gradients indicative of super-refraction and ducting are observed between heights of 52m and 84m for considerable amounts of time. Different current propagation models have been used to predict the median propagation loss values, which do not always clearly point out the dominant propagation mechanisms.

This study has made available further results regarding enhanced signal strength events, has improved the values of some critical parameters linked to tropospheric propagation and has identified certain trends relating weather to signal level enhancements. These issues bear direct relevance to radio propagation in marine and coastal areas.

ACKNOWLEDGEMENTS

First and foremost, all praise, thanks and acknowledgements to the Almighty, Who gifted me with the priceless bounties throughout my life and continues to shower countless blessings. It is only the physical and mental strengths gifted to me by the Almighty that enabled me to be what I am.

This research and the resulting thesis are a culmination of an effort that involved invaluable help from many individuals and organizations.

To start off, I would like to express my heartfelt thanks and gratitude to my family, friends and well-wishers. My family, being closest to me, were, in one way or other, involved with and affected while I was pursuing my PhD. In particular, I can never repay the love, affection, unconditional support, encouragement, prayers and faith given to me by my parents Mr. & Mrs. Saeed Mufti and the pride they feel because of me. I am also indebted to my beloved wife, whose support through kith and kin, sacrifices and compromises so that my research does not get compromised enabled me to reach this stage.

I am indebted to the University of Engineering and Technology, Peshawar, Pakistan for providing me with financial support during the first three years of my PhD, and to the Higher Education Commission, Government of Pakistan, for taking initiatives while the country is going through very hard times.

I offer my sincerest gratitude to my supervisors, Professor Dr. Mike Warrington and Dr. David Siddle, for their continued support coming in many forms from start till end.

I am indebted to Dr. Warrington' vision, thought-provoking queries and patience whilst providing me with the room to work at my own pace and in my own way, and Dr. Siddle's enthusiasm, guidance and an ever-ready and willing-to-help-immediately approach to my incessant inputs, not to forget the support beyond normal expectations from a supervisor.

I owe gratitude to Dr. Alan Stocker, for his informal chats and valuable technical support including critical data backups and recovery as well as sorting out network and software update issues, and Dr. Salil Gunashekar, for his continuous encouragement, always urging me to take initiatives and lifting me up whenever I felt low. I also thank Dr. Bo Wang from Department of Mathematics for helping me with understanding certain aspects of statistics.

This project could not be implemented without the able and experienced hands of Mr. Julian Jones, Technician, Department of Engineering, who was instrumental in setting-up the transmitter and receiver sites in the Channel Islands and who had to visit the Channel Islands a few times, owing to recurrent technical problems. I am also grateful to Mr. Bilal Haveliwala at Radio Systems Lab for providing local technical support whenever required.

I would like to take this opportunity to express my gratitude to Portland Bill Lighthouse, Ronez Quarry (Jersey) and Isl de Raz (Alderney) for allowing me to install my project equipment.

Additionally, I would also like to thank Mr. R Barry Hall, Climate Enquiry Officer at the UK Met Office, and Mr. Scott E. Stephens, Meteorologist at NOAA's National Climatic Data Center, for providing us with valuable weather data.

I also wish to thank National Data Buoy Centre for providing data from the Channel Lightship in the English Channel, British Atmospheric Data Centre for allowing us to utilize high-resolution UK radiosonde data and British Oceanographic Data Centre for providing recorded tidal data.

I also thank Mr. Shane Lin, Mr. Bill Finger, Mr. Chris D. Larson, Mr. Frederic Moisy and Mr. Ben Barrowes for sharing their MATLAB codes whose modified versions I used in this research to carry out certain analysis.

Finally, I remain indebted to the efforts of my elders, teachers and honest friends, who have, over the years, shaped me into the person that I am today. Thanks to each and every one of them.

Naveed Mufti

October 2011

TABLE OF CONTENTS

GLOSSARY

°C	Degree Centigrade
°K	Degree Kelvin
AGC	Automatic Gain Control
AMSL	Above Mean Sea Level
ANAPROP	Anomalous Propagation
Anticyclone	A large-scale circulation of winds around a central region of high atmospheric pressure, clockwise in the Northern Hemisphere, counter-clockwise in the Southern Hemisphere
ASTD	Air-Sea Temperature Difference
Atemp	Air Temperature
BBC	British Broadcasting Corporation
BODC	British Oceanographic Data Centre
BTL	Basic Transmission Loss
CCIR	Comité consultatif international pour la radio (International Radio Consultative Committee), now known as ITU-R
CG	CLV-Guernsey
CLV	Channel Light Vessel
CP	CLV-Portland
CW	Continuous Wave (or Continuous Waveform)- A signal of constant frequency and amplitude
d.p.	Decimal Places
dB	Decibels
DC	Direct Current
Decile	Any of the nine values that divide the sorted data into ten equal parts, so that each part represents 1/10 of the sample

Dewp	Dewpoint Temperature
Diurnal cycle	Any pattern that recurs daily
educt	Evaporation duct
Effective Conductivity	A measure of a material's ability to conduct electricity
EIRP	Effective Isotropic Radiated Power
ERP	Effecative Radiated Power
ESS	Enhanced Signal Strengths
FSL	Free Space Loss
GHz	Giga-Hertz (1x10^9 Hertz)
GPS	Global Positioning System
hPa	Hecto Pascals
Humid	Relative Humidity (%)
IDR	Inter-Decile Range is the difference between the first and the ninth deciles (the values exceeded 90% and 10% of time)
IPS	Integrated Propagation System
IQR	Inter-Quartile Range (also called the midspread or middle fifty) is the difference between the values exceeded 75% and 25% of time
ITU	International Telecommunication Union
ITU-R	International Telecommunication Union Radiocommunication Sector
JG	Jersey-Guernsey
k/k-factor	Effective Earth Radius Factor
kHz	Kilo-Hertz (1x10^3 Hertz)
km	kilometres
LIDAR	Light Detection & Ranging
LOS	Line-of-Sight

MATLAB	Matrix Laboratory, a programming language suite developed by MathWorks
mbar	Millibars
MetOffice/UKMO	United Kingdom Meteorological Office
MHz	Mega-Hertz (1x10^6 Hertz)
N/A	Not applicable
N0	Sea Level Surface Refractivity
NaN	Not a Number (used for missing/invalid values)
NBS	National Bureau of Standards, USA
NCDC	National Climatic Data Centre, NOAA, USA
NDBC	National Data Buoy Centre
NNDC	NOAA National Data Cente, USA
NOAA	National Oceanic and Atmospheric Administration, USA
NPS	Naval Postgraduate School
Ns	Surface Refractivity
NTIS	National Technical Information Service, USA
P-J Model	Paulus-Jeske Model (to calculate evaporation duct height)
PJ	Portland-Jersey
Press	Atmospheric Pressure
Quartile	Quartiles of a set of values are the three points that divide the data set into four equal groups, each representing a fourth of the population being sampled.
RADAR	Radio Detection and Ranging
Relative Permittivity	The ratio of the amount of electrical energy stored in a material by an applied voltage, relative to that stored in a vacuum.
RH	Relative Humidity (%)
RS-232	Recommended Standard 232-A serial port standard
Rx	Receiver

SFN	Single Frequency Network
SINAD	Signal-to-noise and distortion ratio
SRTM	Shuttle Radar Topography Mission
SSB	Single Side Band (A type of Amplitude Modulation)
Stemp	Sea Temperature
Temp	Atmospheric Temperature
TN-101	Technical Note 101
Tx	Transmitter
UHF	Ultra High Frequency (300 MHz - 3 GHz)
UK	United Kingdom
URSI	International Union of Radio Science
UT	Universal Time
VHF	Very High Frequency (30 MHz - 300 MHz)
w.r.t	With respect to
Wdir	Wind Direction
WS	Wind Speed
Wspd	Wind Speed
ΔN	Lapse Rate of Refractivity in the lowest 1 km of atmosphere
μV	Micro-Volt (1x10^-6 Volt)

1. INTRODUCTION

Telecommunications are now established as an industry, playing a significant role in national economies. Telecommunications-related revenues have increased globally, mobile and broadband communications being the leading contributors, with the number of mobile subscribers exceeding those on fixed lines in many countries [1]. Over 80 million 'active' mobile subscribers contributed nearly £ 4 billion of revenues in third quarter of Year 2011 alone, whereas during the same time period, fixed voice services generated £2.2 billion of revenues. In addition, the number of 'active' mobile broadband customers exceeded 5 million in Year 2011 [107].

Telecommunications systems have been served well by advances in science and technology, progressing both in wire-line and wireless methods of information exchange. Wireless has become more dominant than ever, and its importance in today's world cannot be undermined. Wireless communications now play a critical role in many different applications, ranging from public mobile telephony, internet and broadband access, fixed telephony forward haul and backhaul, national trunks, international communications, satellite, military, cordless telephony, radio-controlled applications, missile control, wireless networking and so on. The radio frequency spectrum contributed almost 3 % of the UK's Gross Domestic Product [2]. UK's communications sector revenues (which include telecommunications, television and radio) were nearly £39 billion in the Year 2010 [108].

The radio frequency spectrum holds the key to wireless communications. However, it is a limited but re-useable resource. Propagation and interference research and modelling makes possible more efficient use of this valuable resource. VHF and UHF offer reasonable compromises between propagation loss and potential bandwidth and hence are currently the most valuable frequencies for commercial applications.

With reference to radio propagation, the lowest part of the atmosphere- troposphere- plays a vital role. Weather, most of which happens within the troposphere, affects propagation such that a particular propagation mechanism or a combination of propagation mechanisms influenced by weather conditions could enable propagation of signals over the surface of the Earth.

The troposphere has a complex structure at coastal areas. Marine and coastal areas are subject to constantly changing weather conditions and hence are prone to abnormal propagation conditions, such as atmospheric radio ducts that enable anomalous propagation. Anomalous propagation can enable long distance communications beyond horizon, which can create potential interference as well as ‘false echoes’ as have been observed by radars. Hence, the planning and management of communication systems in such environments need to be addressed. There are propagation models like ITU-R P.617 [20] and P.452 [21] to model over-sea UHF propagation. Most of the models are (semi) empirical (based on experimental data) and hence need radio-meteorological statistics over long periods of time to address their

deficiencies and improve reliability in their prediction procedures. In this regard, the ITU, from time to time, poses ‘questions’ to be addressed and studied.

This opens up the opportunity to investigate the propagation of radio signals between coastal stations, or in other words, the radio signal propagation over the sea. The Radio Systems Group at the University of Leicester has made measurements across the Channel Islands in excess of a year to investigate the propagation characteristics of VHF and UHF signals propagating over the sea. A transmitter at Jersey and receivers at Alderney and Portland form a network of two collinear point-to-point links, namely Jersey – Portland and Jersey – Alderney. The main objectives of this research were to implement a measurement campaign to investigate in detail anomalous propagation of VHF and UHF signals over the sea. Another issue was that of interference between links operating on the same frequency but over different paths - the novel collinear experimental configuration employed also allowed some aspects of this problem to be investigated. During the course of investigations, the meteorology of the region was extensively analysed. The relationships between signal levels received and the local meteorological variables were also investigated. Certain aspects of currently active ITU-R questions [109, 110, 111, 112] relevant to radio-communications were also addressed in the course of investigation. This involved gathering statistics of signal propagation at different frequencies on two different paths and their analysing dependence on weather conditions, testing the currently used propagation and interference

prediction model(s) for relevant frequencies and paths and the improving the understanding of over sea wireless propagation.

Various aspects of propagation investigated by this research have direct bearing on planning and management of VHF and UHF radio communication systems, including but not limited to inter-ship communications, cellular mobile communications in marine and coastal areas, ship-to-coast communications, search-and-rescue operations in sea and marine radar communications. The results are more relevant to the southern coast of UK.

This thesis provides the reader with relevant technical background, followed by a review of the relevant studies and research undertaken previously. The experimental arrangement of the research setup implemented in the English Channel is then explained, followed by observations on the received signal strength. A detailed analysis of the results, followed by investigation of correlations between different parameters and received signal levels precede the conclusions and recommendations for future work.

2. GENERAL ASPECTS OF TRANS-HORIZON PROPAGATION

The journey of a radio signal from one point to another is commonly known as propagation. Radio signals can travel up to horizon and also beyond horizon. Radio signal propagation is dependent on mechanisms such as reflection, refraction, diffraction, absorption and scattering. Radio signal propagation is possible through one or combination of these mechanisms.

2.1. Free Space Propagation

Free-space propagation serves as a benchmark for radio-frequency engineering and the Free Space Loss (which is the loss through air, implying that the path taken by radio signals is unobstructed) is given by [3]:

$$FSL = 32.44 + 20 \log d + 20 \log f \quad \text{dB} \quad (2.01)$$

Where:

d is the distance (km)

f is the frequency (MHz)

In situations where transmitter and receiver antennas are visible to each other, propagation is line-of-sight. However, interference caused by signals reaching receiver from potential reflected paths could cause departures from expected free space loss value. For these reasons, the line-of-sight region is also known as interference region [113].

2.2. Trans-Horizon Propagation

Scattering from troposphere and diffraction around the earth's curvature are the major mechanisms for trans-horizon communication. Ducting and layer reflection/refraction can also extend communication range for small percentages of time [21].

2.2.1. Tropospheric propagation

The troposphere is the lowest layer of the atmosphere, extending to heights of 8 to 10 km at polar latitudes, 10 to 12 km at middle latitudes and up to 18 km at the Equator. Within the troposphere, temperature decreases with height at an average gradient of 6 to 7 °C per kilometre. The water vapour content of the troposphere decreases rapidly with height and at 1.5 km above the surface is usually half of that at the surface. Pressure also decreases rapidly with altitude in the troposphere, at nearly linear rate up to about 6 km height from the Earth's surface [81].

Normally, weather variations and effects felt on the Earth occur in the troposphere. Fluctuations in weather variables cause changes in the refractive index of atmosphere. This makes the troposphere the most important region of the atmosphere for VHF and UHF propagation. The troposphere can enable beyond-horizon communications through refraction and scattering.

2.2.1.1. Refraction through the troposphere

Refraction is the propagation mechanism by which a medium causes electromagnetic rays to bend as they pass through the medium. The index of refraction 'n' is a measure of the amount of refraction. It is defined as the ratio of the speed of propagation in free space, 'c', to that experienced in a medium, 'v':

$$n = \frac{c}{v} \tag{2.02}$$

When an electromagnetic ray passes from one medium into another, it can bend if the refractive indices of the two media are not the same. The extent of refraction depends upon difference in refractive indices of the two media, discovered by Snell. Figure 2.1 illustrates simplified Snell's Law [114]:

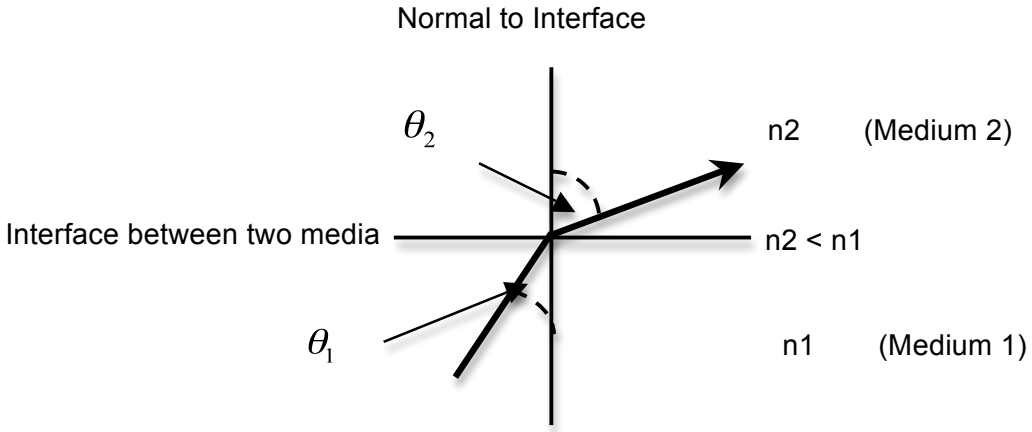

Figure 2-1: **Refraction – Snell's law**

In terms of mathematical relation,

$$\frac{\sin\theta_1}{\sin\theta_2} = \frac{v_1}{v_2} = \frac{n_2}{n_1} \tag{2.03}$$

Where:

θ_2 is the angle from normal in medium 2

θ_1 is the angle from normal in medium 1

n2 is the refractive index of medium 2

n1 is the refractive index of medium 1

v1 is the speed of the electromagnetic wave in medium 2

v2 is the speed of the electromagnetic wave in medium 1

This effectively means that when the ray travels from a medium with higher value of refractive index (denser medium) to a medium with lower refractive index (rarer medium), the refracted ray is bent away from the normal, and vice versa.

The refractive index of the troposphere changes with height and weather conditions, depending on pressure, temperature and relative humidity [60]. Generally, as height increases, pressure, temperature and relative humidity tend to decrease in such a way that the refractive index within the troposphere also decreases. In the absence of more reliable local data, the ITU-R Recommendation ITU-R P.835 [63] can be used to determine the temperature, pressure and water-vapour pressure as functions of altitude.

As a radio signal travels up through the troposphere in normal conditions, it tends to get refracted downwards, extending the range of propagation. Hence radio signals tend to travel beyond the geometric horizon, up to ‘radio horizon’, as shown in Figure 2-2:

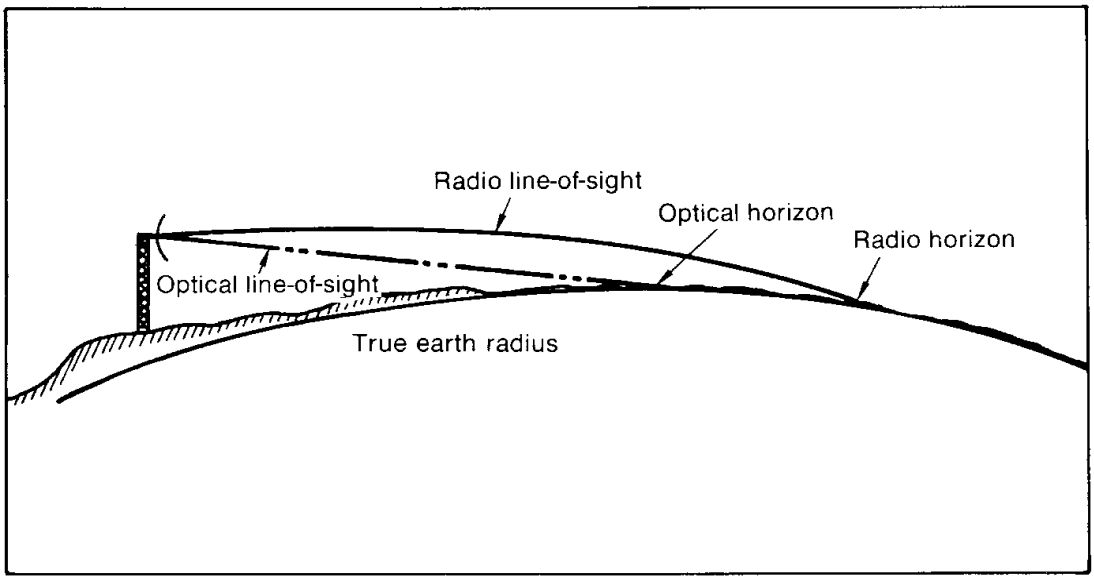

Figure 2-2: **Optical and radio horizons [17]**

The value of the refractive index of air for VHF and UHF signals near the surface of earth is of the order of 1.0003. Any changes in value of 'n' near Earth are not more than a few units in 10000, hence it is convenient to use the term Refractivity. Refractivity, N, is related to refractive index by the formula [48]:

$$N = (n-1) \times 10^6 \quad \text{N-units} \qquad (2.04)$$

The Modified Refractivity 'M' is defined as [18]:

$$M(h) = N(h) + 157h \quad \text{M-units} \qquad (2.05)$$

Where:

h is height in km

Refractivity is dependent on atmospheric pressure, temperature and water vapour pressure, according to the following equation [18,60]:

$$N = \underbrace{77.6\frac{P}{T}}_{Dry\,Term} + \underbrace{3.73*10^5\,\frac{e}{T^2}}_{Wet\,Term} \qquad (2.06)$$

Where:

P is the pressure (hPa)

T is the absolute temperature (°K)

e is the water vapour pressure (hPa)

The relationship between water vapour pressure and relative humidity is [17]:

$$e = \frac{H\,e_s}{100} \qquad (2.07)$$

where:

H is the relative humidity (%)

e_s is the saturation vapour pressure (hPa) at temperature T (°C)

Refractivity 'N' can be directly measured using refractometer or indirectly by measuring temperature, pressure and humidity and consequently determining 'N' using Eq. 2.06. Different methods used are discussed in Chapter 4.

Usually, "Surface Refractivity", N_s, and "Surface Refractivity reduced to Sea Level", N_0, are used in radio-propagation studies. The ITU provides global values of N_0 [18].

COST 255 Report [64] observes that in a standard atmosphere, the model temperature decreases linearly within the troposphere, pressure decreases

rapidly at nearly exponential rate and water vapour variation is usually more volatile as a function of time. The variability of the 'wet term' of refractivity (refer to Eq. 2.06) is more than the 'dry term'. The vapour pressure is seen to increase strongly with increasing ambient temperature.

The dependence of refractive index upon height is exponential [18]:

$$n(h) = 1 + N_0 * 10^{-6} * \exp(-h / h_0) \qquad (2.08)$$

In accordance with the above equation, the value of refractivity at height 'h' (km) above mean sea level can be determined by the following equation [18]:

$$N(h) = N_0 \exp(-h / h_0) \qquad (2.09a)$$

Or, in terms of N_s & N_0:

$$N_s = N_0 \exp(-h_s / h_0) \qquad (2.09b)$$

Where:

h_0 is the scale height (km)

h is the height above Earth's surface (km)

h_s is the height of the Earth's surface above sea level (km)

Scale height is that height at which value of N(h) is 1/e of the value of N_0. The reference values for terrestrial paths are N_0= 315, h_0= 7.35 km [18, 72].

A radio ray passing through the troposphere undergoes bending caused by the gradient of refractivity. Hence, this gradient of refractivity near the surface

of the Earth is of particular importance in many applications of telecommunications. A useful parameter used for refraction studies is the lapse of refractivity in the lowest 1 km of troposphere, ΔN. In the absence of more reliable data, ITU ΔN maps can be used [18], which use equation 2.10:

$$\Delta N = N_s - N_1 \qquad (2.10)$$

Where:

N_1 is the refractivity at 1 km above surface of the Earth

The refractivity gradient obviously has two components – vertical and horizontal. Since the refractive index varies mainly with altitude, only the vertical gradient of the refractive index is generally considered. The horizontal gradient is normally negligibly small [17], especially over oceans [73]. Glevy investigated effects of horizontal changes in refractivity on radio propagation [75] and observed that the assumption of horizontal homogeneity was correct in 86 percent of cases [73]. Hitney et al performed a similar analysis of five years of data to reach a similar conclusion [73]. Hence, for tropospheric studies, the curvature of a radio ray at a point (discussed later in equations 2.11 to 2.14) is considered in vertical plane only, assuming that the atmosphere is horizontally homogeneous.

In the light of above, statistics of vertical gradient of refractivity become important for the estimation of propagation effects. It is not practical to always measure and model the refractive effects on case-to-case basis. Also, many current propagation models (discussed in Chapters 3 and 6) are statistical. Refractivity gradient statistics for the lowest 100 metres from the surface of

the Earth are used to estimate the probability of occurrence of ducting and multipath conditions [21]. Extreme values of these 'initial' refractivity gradients are responsible for much of the unusual behaviour of radio systems [43]. ITU has published statistics related to vertical refractivity gradient in lowest 100m of atmosphere [18].

The curvature of a radio ray, C, is given by [17]:

$$C = -\frac{1}{n}\frac{dn}{dh}\cos\theta \qquad (2.11)$$

Where:

C is the radius of curvature of the ray path
n is the refractive index of atmosphere
dn/dh is the vertical gradient of refractive index
θ is the local elevation angle of the ray
h is the height of the point above the Earth's surface

C is defined as positive for rays bending towards the surface of the Earth. If the path is approximately horizontal, then $\cos\theta=1$ as θ is close to 0, and since refractivity is very close to 1, the equation can be simplified to give:

$$C = -\frac{dn}{dh} \qquad (2.12)$$

If the vertical gradient is constant, the ray trajectories are arcs of a circle. If an Earth suitably larger than the actual Earth is assumed such that the curvature of the ray is absorbed in curvature of the effective Earth, then the relative curvature of the two remains the same. Also, if the height profile of refractivity is assumed linear, it implies that the refractivity gradient is constant along the ray path. These assumptions allow radio rays to be drawn as straight lines

over the Earth, rather than curved rays over the actual Earth. This is the classic method of accounting for the effects of atmospheric refraction of radio waves as this maintains the relative curvature between the Earth and radio ray [17]:

Curvature of the Earth - Curvature of Radio Ray = Curvature of the Effective Earth (2.13)

Hence, Using Equation 2.11, Equation 2.13 can be mathematically written as:

$$\frac{1}{a} + \frac{1}{n}\frac{dn}{dh}\cos\theta = \frac{1}{ka} \tag{2.14}$$

Where:

a is the Earth's radius (km)

k is the effective Earth radius factor, a scaling factor that helps quantifying the curvature of propagated ray.

If Equation 2.12 is used instead of Equation 2.11, then the expression is:

$$\frac{1}{a} + \frac{dn}{dh} = \frac{1}{ka} \tag{2.15}$$

The variation of refractive index (or refractivity) with height is exponential. If it is assumed that refractive index of air varies linearly with height and does not vary horizontally, then 'k'– the effective Earth radius factor – is given by:

$$k \cong \frac{1}{1 + a\frac{dn}{dh}} \tag{2.16}$$

This method simplifies the height distribution of refractive index in atmosphere. At heights up to 1 km and for terrestrial radio paths, the exponential lapse rate in refractive index may be approximated by a linear one [17, 18, 72].

On average, and in normal atmospheric conditions, successful communications have been observed beyond the optical line of sight by almost 15% [17]. This means that in these conditions, k=1.33 or 4/3, the value for k used normally.

Using equations 2.03 and 2.13, the value of Earth's radius a ≈ 6370 km and converting from refractive index 'n' to refractivity 'N', the expression for 'k' is given by:

$$k \approx \left[1 + \left(\left(\frac{\Delta N}{\Delta h}\right)/157\right)\right]^{-1} \qquad (2.17)$$

Where:

$\frac{\Delta N}{\Delta h}$ is the vertical refractivity gradient within the troposphere

In the troposphere, $\frac{\Delta N}{\Delta h}$ can vary anywhere from -500 to 1000 N-units/km [17].

Of the three atmospheric variables affecting refractivity, relative humidity has the greatest effect on refraction, followed by temperature and then pressure. Pressure variations alone provide no significant change in refraction [45].

In free space, electromagnetic signals would travel in straight line. The refractive index of air is slightly higher than that of free space (vacuum), meaning that the speed of electromagnetic signals as they travel through atmosphere is slightly less than that within free space. Hence, a propagating electromagnetic signal is bound to bend downwards (towards the Earth's surface) as it travels through normal atmosphere [45].

A gradual decrease in pressure, temperature and humidity (and hence refractivity) with increasing height is termed as normal atmospheric condition. During such condition, the curvature of ray is slightly less than the Earth's curvature. Under standard atmospheric conditions, $\frac{\Delta N}{\Delta h}$ = -40 N-units/km.

If the decrease in magnitude of refractivity with height is less than normal or when temperature and humidity variation is such that refractivity is increasing with height [45], then the beam bends less than normal and climbs excessively skyward. This is known as sub-refraction. In some situations, signals might turn away from Earth towards sky. Sub-refractive conditions can greatly reduced radio horizons, as the bulge of the Earth causes the direct path between the transmitter and receiver to be obscured, resulting in a considerable decrease in the received signal strength. In this situation, diffraction around the Earth's curvature is the dominant propagation mechanism and may result in diffraction fading on normally line-of-sight microwave paths [43]. Bean et al [43] observed that the surface conditions conducive to sub-refractive gradients are of two opposite types:

(a) temperature > 30°C; relative humidity < 40 percent;

(b) temperature 10° to 30°C; relative humidity > 60 percent;

If the decrease in refractivity due to decrease in pressure, temperature and humidity is more than normal (i.e. more than the normal gradual trend), super-refraction occurs. Increasing temperature with height and/or sharp decrease in humidity with height can cause super-refraction [45]. In this case, radio waves are bending more than normal (expected). This can reduce the radio horizon. However, in certain cases, this super-refraction can bend the radio wave equal to or more than the Earth's curvature. Super refractive gradients are responsible for greatly extended service horizons, and may cause interference between widely separated radio links operating on the same frequency [43].

Ducting is a phenomenon by which radio wave gets trapped into a structure and is able to travel long distances without significant loss in signal power. Hence, ducts give rise to anomalous propagation. Ducting is an extension of super-refraction. The difference is that the conditions that form a ducting layer are more intense than those that form a super-refractive layer [45].

These different refractive conditions are summarised in Table 2-1 and illustrated in Figure 2-3:

Parameter	Refractive Condition				
	Sub	Standard	Normal	Super	Ducting
ΔN/Δh	> 0 N-units/km	-39 N-units/km	0 to >-79 N-units/km	-79 to >-157 N-units/km	≤ -157 N-units/km
ΔM/Δh	>157 M-units/km	118 M-units/km	>78 to 157 M-units/km	>0 to 78 M-units/km	≤ 0 M-units/km
k	<1	1.33	1 to 2	2 to <∞	∞ @ ΔM/Δh=0, otherwise < 0

Table 2-1: Refractive conditions, based on refractivity gradients [from 106]

From Table 2-1, it is evident that ducts exist whenever vertical refractivity gradient at a certain height and location is less than or equal -157 N-units/km. If it equals -157, the ray has same curvature as the Earth and appears like straight-line propagation over flat Earth, as also illustrated in Figure 2-3:

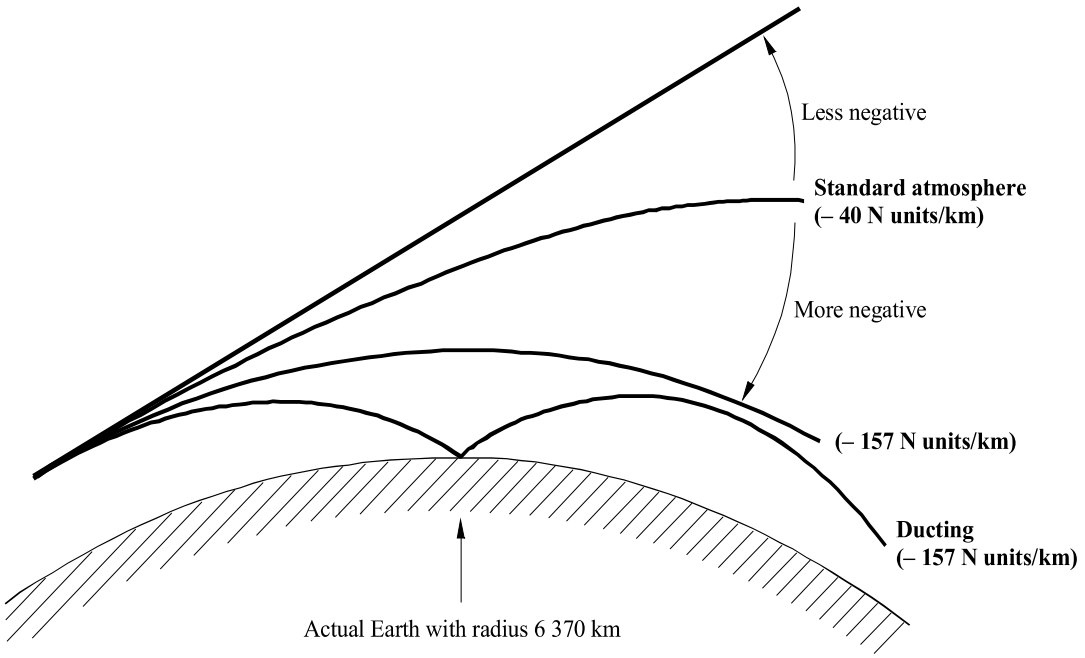

Figure 2-3: **Effects of atmospheric refraction on radio propagation [13]**

2.2.1.2. Ducting within the troposphere

There could be three different types of ducts in a marine environment: Evaporation, Surface-based and Elevated.

Evaporation duct forms immediately over the surface of sea and other large bodies of water. It is caused by steep humidity gradients immediately above the sea-surface [77]. It exists primarily because the amount of water vapour present in the air decreases rapidly with height in the first few metres above the surface of the sea. The air that is in immediate contact with the sea surface is saturated with water vapour (i.e. the relative humidity is almost 100%) as a consequence of the process of evaporation, hence the name evaporation duct. As the height increases, the water vapour pressure in the atmosphere rapidly decreases until it reaches an ambient value at which it remains more or less static for a further increase in height [73].

The overall modified refractivity profile of an evaporation duct is a log-linear variation. The point at which the 'M' gradient changes from negative to positive is referred to as the evaporation duct height (or thickness) [77]. It is the same height at which 'M' reaches its minimum value and is taken as a measure of the strength of the evaporation duct.

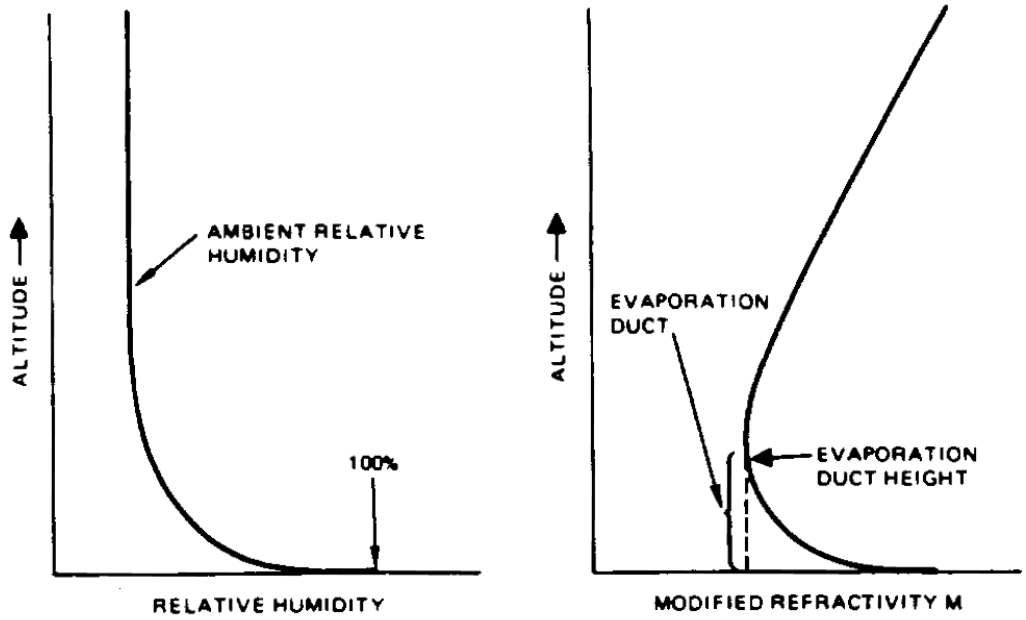

Figure 2-4: **Vertical profiles of relative humidity and modified refractivity, also showing evaporation duct height [73]**

Given the nature of this duct, it is a near-permanent feature on over-sea paths. It has been observed that the height and strength of the duct vary with wind speed, with stronger winds generally resulting in stronger signals [87]. The same effect has been observed by Gunashekar [50]. Hitney and Vieth performed statistical assessment of evaporation ducting, using data from experiments performed earlier at Aegean Sea and North Sea. They concluded that evaporation ducting was dominantly present as trans-horizon propagation mechanism at frequencies above 2 GHz [77].

Surface-based ducts can be caused by trapping layers extending several hundred metres in height from the surface. If the trapping layer is close to the surface, it can be simply referred to as surface duct [73]:

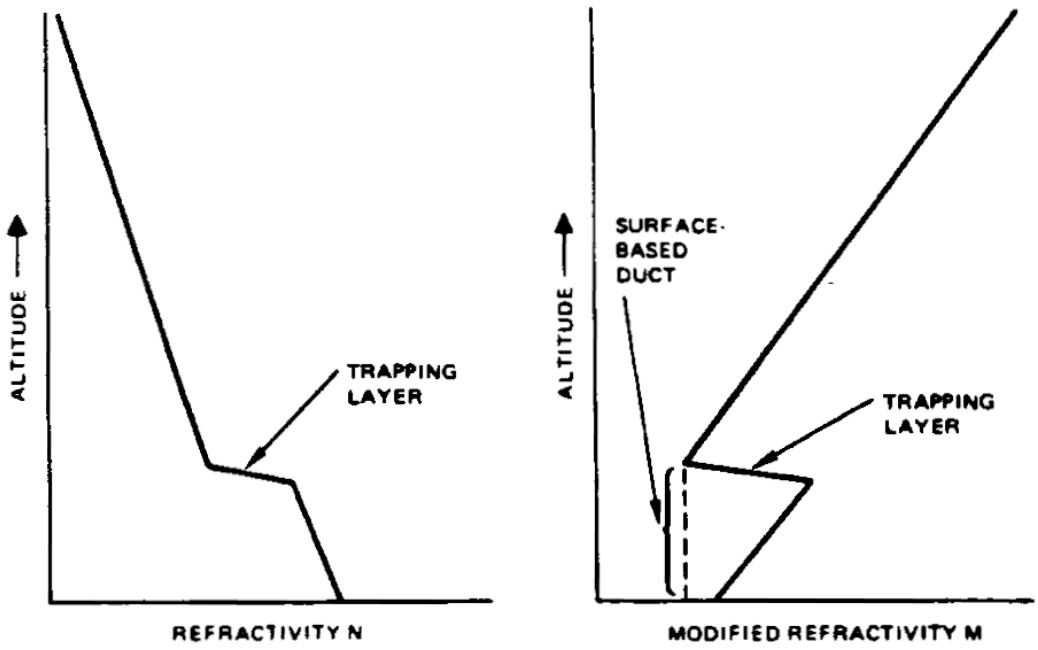

Figure 2-5: **Refractivity profiles showing surface-based duct [73]**

Surface ducts exist when the value of modified refractivity 'M' at top of trapping layer is less than value of 'M' at the surface [73].

Surface ducts on over-water paths can extend from sea surface up to 20 metres. They are persistent during fair weather and tend to reform after showers. ITU provides ducting statistics based on 20 years (1977-1996) of radiosonde observations from 661 sites [18]. For the English Channel, surface ducting is expected 20% of time in average year, with an annual average height of 50m from the surface. Hitney and Vieth note that surface based ducts occur in the North Sea area about 1.7 % of time [77]. Paulus [79] observed that surface-based ducts would form in oceanic regions under a continental influence due to the advection of warm and dry air over the cooler sea surface. In this situation, surface ducting takes over evaporation ducting as the dominant propagation mechanism. Evaporation ducts are more

effective for frequencies above 1 GHz while surface-based ducts can support frequencies as low as 100 MHz [77].

Elevated ducts are created by elevated trapping layers in similar fashion to surface-based ducts; it extends from top of the trapping layer down to a height where value of 'M' is equal to the value of 'M' at the top of the layer [73]:

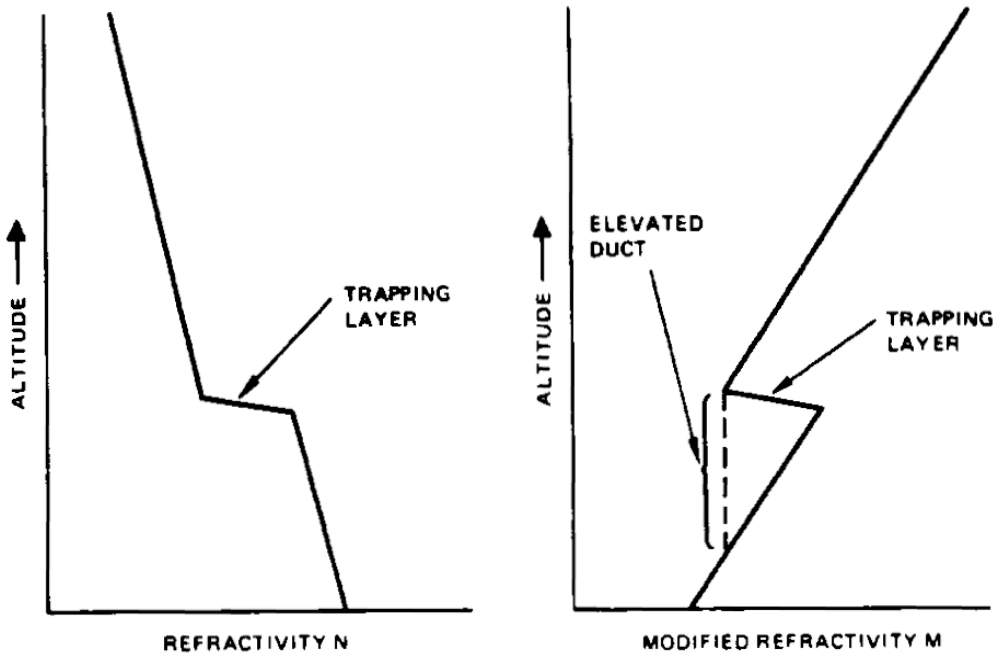

Figure 2-6: **Refractivity profiles showing elevated duct [73]**

The average year elevated duct occurrence is 15% for the English Channel, with annual mean duct thickness of 150m and annual mean base height of 1.2 km from surface [18].

Both surface-based and elevated ducts support long-range communications for frequencies above 100 MHz [73]. Ducts can become a means of causing interference on trans-horizon paths and fading and enhancements on line-of-

sight paths. They can also allow radars to track objects many hundreds of kilometres beyond the normal radio horizon [43].

Radio rays can get trapped in a duct if the transmitting antenna is within a duct and elevation angles are low. Assuming normal refractivity conditions with fixed refractivity gradient, the critical elevation angle for trapping rays is [23]:

$$\alpha = \sqrt{2 * 10^{-6} \Delta h \left| \frac{dM}{dh} \right|} \quad \text{radians} \qquad (2.18)$$

Where:

dM/dh is the vertical gradient of modified refractivity

Δh is the height of top of duct above transmitting antenna

However, getting trapped in a duct does not guarantee successful long-range communications without much signal strength loss. For this, in addition to satisfying the elevation angle criteria above, frequency of signal must also be above a threshold value, which depends on the refractivity profile and the physical depth of the duct. If the frequency were below minimum trapping frequency, energy would continue to leak through duct boundaries [23]. Figure 2-7 shows the minimum trapping frequency for surface ducts and elevated ducts:

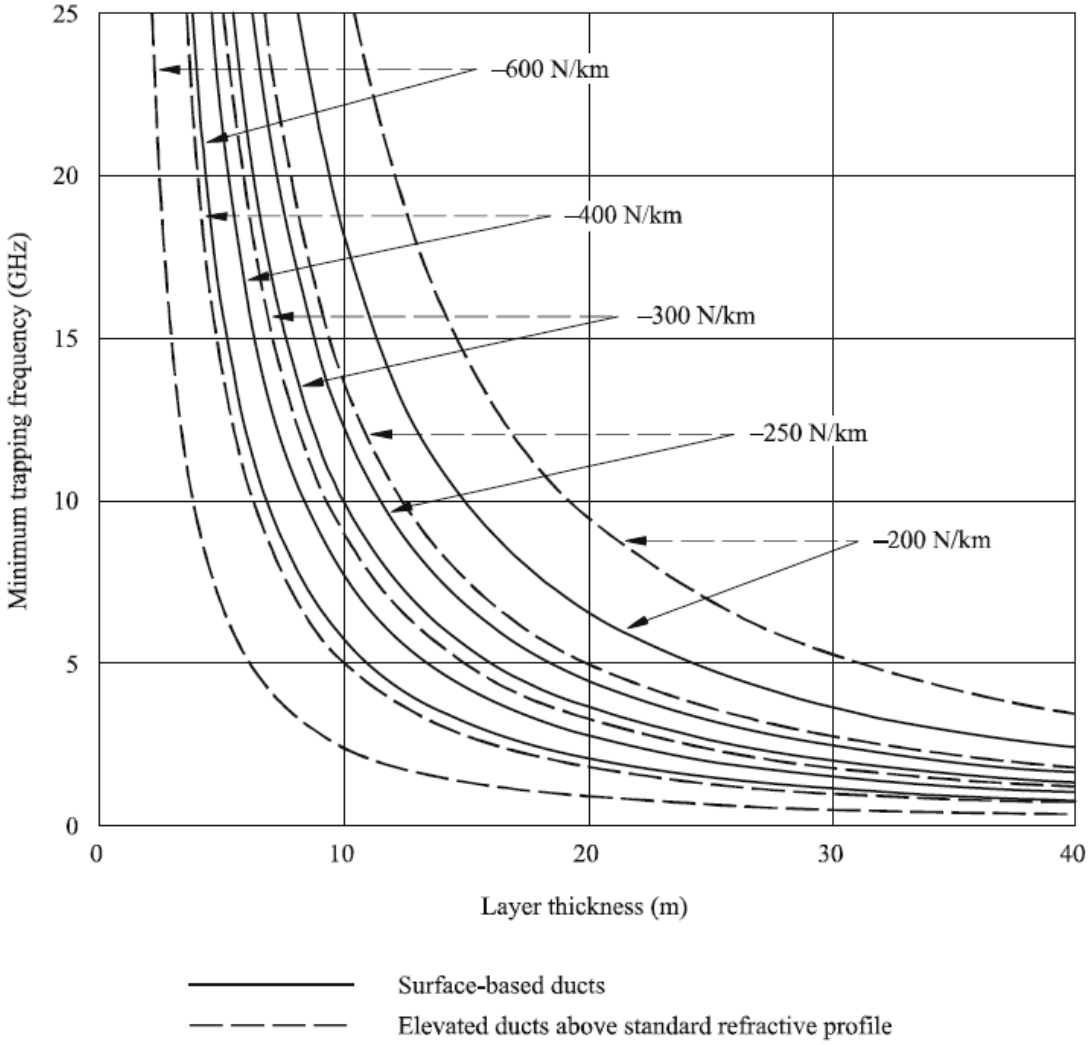

Figure 2-7: **Minimum frequency for trapping in surface and elevated ducts of constant refractivity gradients [23]**

However, unlike standard waveguide propagation, the cut-off wavelength for ducting does not sharply divide the regions of propagation and no propagation [87]. Gunashekar observed that the cut-off wavelength/frequency determined by equations is not a definite value and just gives a rough idea. For instance, as observed by Gunashekar, the calculated values of evaporation duct should not support 2-GHz propagation for 83% of time, whereas this was observed to be a nearly permanent propagation mechanism during that investigation [50]. It was also observed that it is not essential for the antennas to be located within the duct for the signal to get trapped within the duct, although it was

acknowledged that if antennas are located within the duct, the possibility of signal getting trapped within duct and propagating without considerable loss increases.

A possible cause of ducting is temperature inversion. Under normal conditions, as height above the Earth's surface increases, temperature and humidity decrease. Temperature inversion is an area within atmosphere where temperature reverses its normal variation with height, i.e. it starts increasing with height. Temperature inversions are stable structures that can spread over a large area and can remain for long periods of time. They can enable development of strong humidity gradients, which can further lead to development of trapping layers exhibiting strong super-refraction leading to ducting. These temperature inversions can be near surface level or at some heights above surface. Temperature inversions are formed as a result of the processes of radiation, advection and subsidence [16]. It has been observed during over-sea measurements that ducting due to temperature inversion effects is more pronounced for higher frequencies [73].

Radiation refers to the cooling of the earth's surface as heat flows into the space above the surface. This is the most common type of temperature inversion, forming mostly during the night. Clear sky and light surface winds at night cool the land surface and the layer of air closest to it. Air is a poor conductor of heat and hence the air above remains largely unaffected (i.e. warmer than the air close to the surface). This leads to the formation of temperature inversion. Radiation between day and night times is different,

causing diurnal variations in refractive conditions. During the day, at the time when surface temperature is maximum, there might be a sub-refractive layer present.

Advection is the process whereby dry air above the warm land surface flows out over the cold sea. This is typical of the English Channel during summer when clear sunny weather has persisted for a few days [16]. Advection results in a layer of warm dry air above cold damp air, resulting in a strong refractivity gradient. Advection results in the formation of low-altitude ducts (advection ducts). Coastal regions are particularly prone to advection ducts.

Subsidence is the descent of air from a high-level, high-pressure system in the atmosphere. This air volume can get heated by compression to slowly spread out in a layer well above the Earth's surface. This air is dry and can produce temperature inversion as it settles over a cooler, moist air mass. This leads to an elevated super-refractive layer, with temperature above and below this layer decreasing with height. During the day, land becomes warmer than sea. The air above land rises, and is replaced by air from the sea, a phenomenon called sea breeze. In the night, land becomes colder than sea and land breeze in opposite direction is set up. With a sea breeze, a duct may be formed over water due to subsidence. Subsidence can destroy sub-refractive layers and intensify super-refractive layers.

Another type of inversion is called frontal inversion. It occurs when two air masses of different temperatures comes together and do not mix freely.

Hence a transition zone called a “front” forms between these two air masses of different temperature. Fronts are commonly zones of steep horizontal temperature gradients and therefore are associated with strong winds and causes complex inversion. These conditions are generally developed only for a short period of time, along a limited path, that is fairly significant [11]. Frontal systems are prevalent in the UK.

To summarise, there is a higher possibility of anomalous propagation through ducting if the signal satisfies appropriate angle and frequency criteria.

2.2.1.3. Scattering through the troposphere

Scattering due to the troposphere is the dominant propagation mechanism for trans-horizon paths that extend well beyond horizon, when loss due to diffraction is very high (diffraction discussed later in Section 2.2.2). The troposcatter mechanism exists due to variations in vertical profile of the atmosphere, mainly pressure, humidity and temperature. With respect to a point on the surface of the Earth, the atmosphere is always in motion. This motion causes changes in refractivity, called “blobs”. These blobs introduce a different refractivity structure than the surrounding medium. These relatively abrupt changes in refractivity produce a scattering effect on an incident radio beam. Only small amount of energy is scattered back to the Earth [17].

The strength of the signal received by the mechanism of troposcatter depends on scatter volume and the scatter angle, as shown in Figure 2-8. The two

antenna beams meet at common scattering volume between 3 to 8 km above the Earth's surface. As the scatter angle increases, the strength of signal received due to scatter decreases.

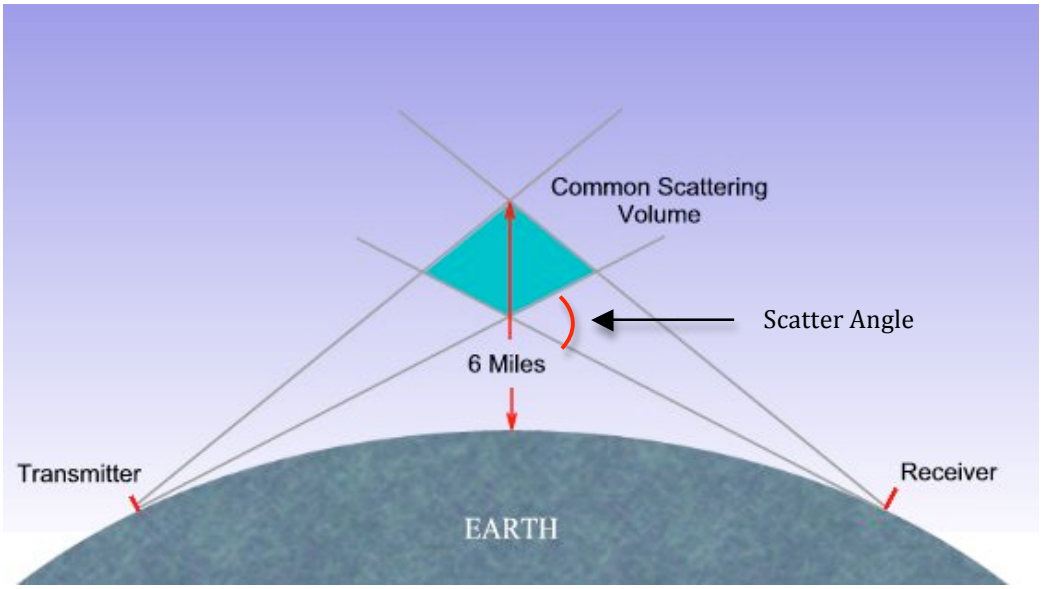

Figure 2-8: Tropospheric scattering of non-line of sight signal [IV]

There is considerable short-term and long-term fading with troposcatter, requiring diversity for reliability [7].

Hydrometeor[1] scatter is a less frequent phenomenon, almost always dominant in cloudy, rainy conditions. Being less reliable, this propagation mechanism is not employed for radio frequency planning, but is considered for interference studies.

There is a possibility of reflection within the troposphere when there is a sharp change in the refractive index between two regions of the troposphere

[1] Hydrometeor - Liquid and frozen water particles, i.e. clouds, rain and snow

separated by a relatively small distance. The ability of the process of layer reflection to support propagation beyond the horizon has been noted by Shen and Vilar [55].

2.2.2. Diffraction

A signal transmitted from a fixed terminal does not just travel in a straight line following a direct Line-of-Sight (LOS) path but spreads out into a space after it leaves the antenna. This space can be split into Fresnel Zones, which are concentric ellipsoids, having common focal points at transmitter and receiver antennas, as shown by Figure 2-9:

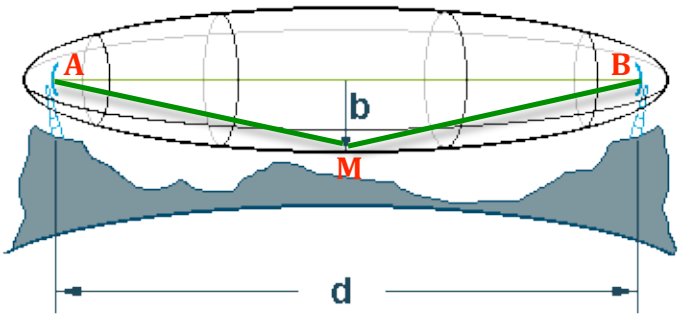

Figure 2-9: **Fresnel zones [III]**

Any point M on any ellipsoid satisfies the equation:

$$AM + MB = AB + n\lambda/2 \qquad (2.19a)$$

Where:

λ is the wavelength of the transmitted signal (m)

d is the total path length (m)

b is the radius of the Fresnel Zone (m)

n corresponds to the ellipsoid or the Fresnel Zone (n=1 is first Fresnel zone) such that n represents the number of half-wavelength multiple (nλ/2) that represents the difference in path length from the direct LOS path [117]

AM is the distance of point 'M' from point 'A' (m)

MB is the distance of the point 'M' from point 'B' (m)

The radius 'b' of any Fresnel Zone is given by:

$$b = \sqrt{\frac{n * \lambda * AM * MB}{AM + MB}} \text{ metres} \qquad (2.19b)$$

The first 'Fresnel Zone' contains most of the signal power transmitted that reaches the receiver. Reflections within this ellipsoid interfere constructively with the direct ray reaching receiving antenna. As a general rule of thumb, if less than 60% of the first Fresnel Zone is obstructed for minimum value of effective earth radius factor 'k' suggested for the path, the signal could reach the receiver without noticeable losses due to the diffraction caused by the obstacle. For k=4/3, 100% of the first zone should be clear of obstacles for normal propagation avoiding losses. The higher the frequency, the narrower is the Fresnel Zone [15, 117].

In case of trans-horizon paths, the Earth's bulge is the major cause of loss due to diffraction, and it tends to obstruct considerable part of the Fresnel zones. In fact, the curvature of the Earth introduces the horizon as obstacle. As a result, the radio waves diffract (bend) around the bulge of the Earth, undergoing loss due to this diffraction. The signal strength can still be high

enough to reach distant receivers. However, diffraction loss increases rapidly with distance [73]. The distance to horizon is related to antenna height, so this restriction can be extended with higher antennas. However, in that case, signals can only travel farther if power input is higher. It can be shown that the maximum line-of-sight distance (geometric horizon) between transmitting and receiving antennas is:

$$d_{glos} = \sqrt{2ah_T} + \sqrt{2ah_R} \quad \text{km} \quad (2.20)$$

The radio horizon distance uses effective radius of Earth:

$$d_{rlos} = \sqrt{2a_e h_T} + \sqrt{2a_e h_R} \quad \text{km} \quad (2.21)$$

Where:

d_{glos} is the geometric horizon distance between transmitter and receiver (km)

d_{rlos} is the radio horizon distance between transmitter and receiver (km)

h_R is the height of receiving antenna above ground (km)

h_T is the height of transmitting antenna above ground (km)

a is the radius of the Earth (km)

a_e is the effective radius of the Earth (km) and is equal to k.a

Figure 2-10 illustrates the different types of trans-horizon diffraction paths:

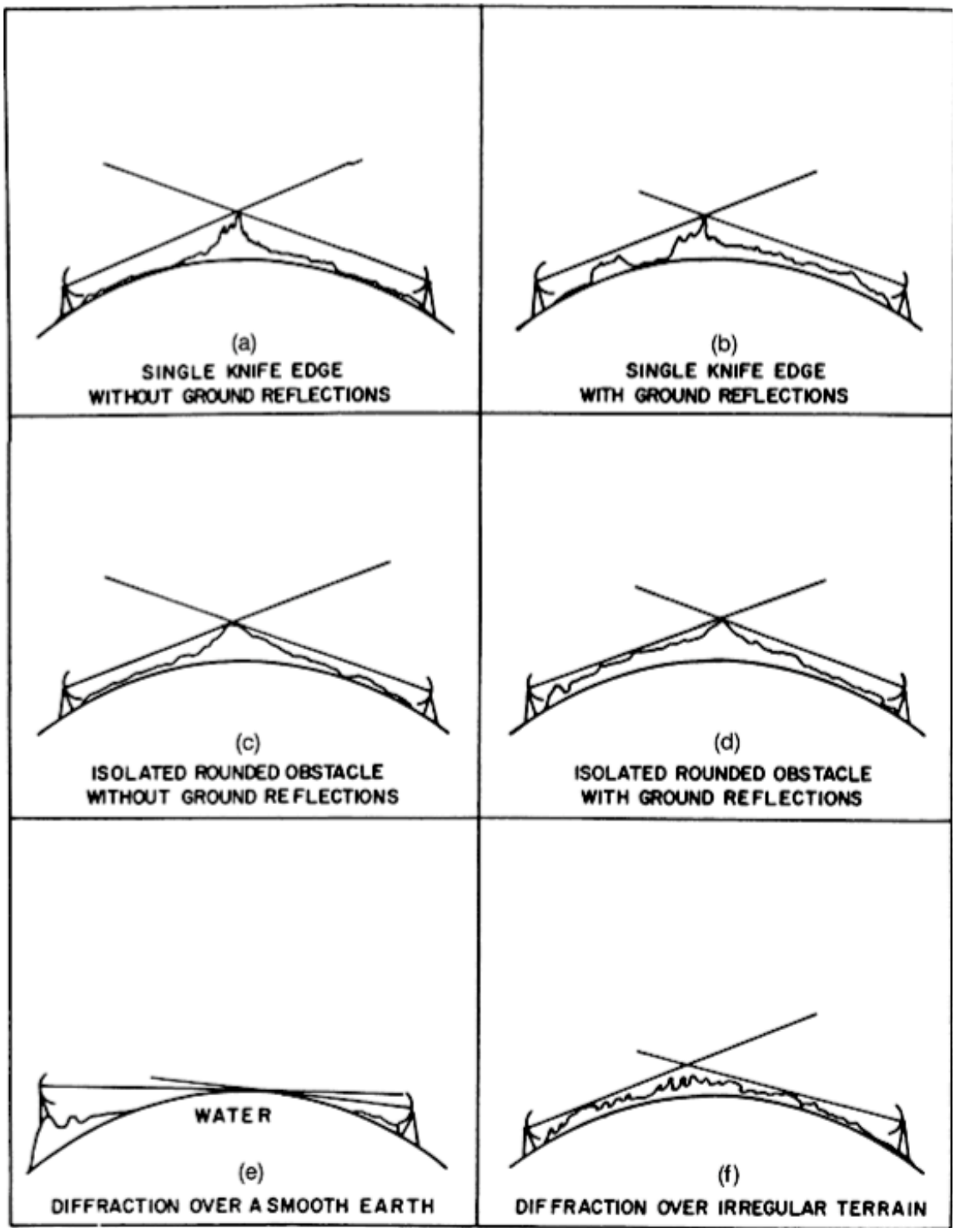

Figure 2-10: **Types of trans-horizon diffraction paths [17]**

As evident from the figure, the type of path for this research is type (e) – diffraction over a smooth earth.

2.3. Time-Dependent Classification of Propagation Mechanisms

It has been observed that any of the line-of-sight (LOS), diffraction and troposcatter mechanisms can exist for dominant percentages of time on a particular path. For this reason, they are referred to as long-term propagation/interference mechanisms [21]. They are also termed as standard propagation mechanisms because they can exist in standard atmosphere, where refractivity decreases exponentially with height in such a manner that this decrease is linear in lowest part of atmosphere [73]. Other propagation mechanisms like ducting, elevated layer reflection/refraction have been observed to occur for smaller percentages of time, and hence are termed as short-term propagation/interference mechanisms.

2.4. Interim Conclusions

In case of paths extending beyond the horizon (i.e. trans-horizon paths), the most common mechanisms and modes of propagation for VHF and UHF frequencies are diffraction due to curvature of the Earth and refraction and scattering through the troposphere while ducting near surface of the Earth or at heights above the Earth's surface can enable enhanced signal strengths.

3. REVIEW OF STUDIES INTO ANOMALOUS PROPAGATION

Anomalous propagation of wireless signals usually occurs when the modifications in the refractive index of air by changes in temperature gradient, pressure or water vapour content cause sub-refraction, super-refraction and trapping leading to ducting. The term ‘anomalous propagation’ is most often used to describe the conditions resulting in increase or reduction of propagation range.

Sub-refraction can lead to shortened radio horizons and decreased propagation range. Altitude errors for height-finding radars also occur in sub-refractive conditions [81]. In contrast, wireless signals are able to travel long distances during super-refractive conditions. Ducting, an extreme case of super-refraction, can enable long-distance propagation without considerable loss of signal strength. This can also enhance the signal strengths received even to the extent of exceeding free space loss predictions. This enhancement and extension in range can be a potential source of interference to geographically distant areas using similar frequencies.

The implications of anomalous propagation include over-reaches, radar holes and shadow zones in radars [81].

Experimental investigation into the propagation of wireless signals on trans-horizon paths has been carried out since the middle of the twentieth century. Studies of meteorological effects leading to tropospheric ducting on over-sea

paths raised particular interest because of the anomalous propagation of signals. The application and validity of these studies to radars ensured that long-range propagation in the marine environment remained in continuous focus. The historical development of studies into anomalous propagation in the marine environment has been discussed by Hitney et al [73].

3.1. Dominant Trans-Horizon Propagation Mechanism

According to the Technical Note 101, troposcatter and diffraction losses are approximately equal at [17]:

$$d_e = 65 * \left(\frac{100}{f}\right)^{1/3} \quad \text{km} \quad (3.01)$$

Where:

d_e is the effective distance at which basic median transmission losses associated with diffraction and troposcatter are equal (km)

f is the frequency (MHz)

If path distance is more than d_e, troposcatter dominates otherwise diffraction dominates. If there is a difference of 15 dB or more between the basic median transmission loss values from both modes, the one with lesser loss value dominates.

Gunashekar identified diffraction and evaporation ducting as the dominant propagation mechanisms on paths less than 50km long during periods of normal signal reception while enhanced signal reception, observed for almost

9% of time, was attributed to ducting [50]. This does not agree with the hypothesis presented by Equation 3.01.

Sim conducted statistical studies of VHF/UHF radio wave propagation on two over sea paths of around 33 and 48 km across the English Channel [11]. Two frequencies (VHF/UHF) were used in this experiment, 248.375 MHz and 341.375 MHz with both horizontal and vertical polarisation. The path of more relevance to this research is the longer path, Jersey to Alderney, for which 8 months of data was available, from November 2001 until September 2002. High-magnitude, fast fading observed on Jersey-Alderney path (~48 km) led Sim to the conclusion that diffracted and troposcattered fields had comparable field strengths. In addition, the consistency between the measurements and simulated results (based on ITU-R P.526 [12]) suggested that the dominating propagation mechanism for Jersey-Guernsey path (~33 km) during calm sea days (i.e. when sea wave heights are minimal) was smooth earth diffraction. Both of these results agree with the assumptions made in accordance with Equation 3.01.

Gough [90] concluded that at average atmospheric conditions, if the diffracted signal is 50 dB below the free space level, tropospheric scattering becomes dominant as the distance increases. For lapse rates of refractivity between -40 N/km and -100 N/km, tropospheric scattering dominates diffraction at all ranges. Lapse rates that are less than -150 N/km will enable mechanisms causing higher received signal levels (such as ducting) to always dominate scatter at short to medium ranges.

Roda [93] suggested that for a beyond-the-horizon path, at minimum scatter angle (less than 1°), diffraction is the dominant propagation mechanism and is much more stable than troposcatter. Its variations are mainly due to the changes in the refractivity of the air.

A 3-year investigation (1991-1994) was carried out on multi-link, over-sea path in the English Channel between Portsmouth and Cap d' Antifer (155km) at 11.65 GHz to study trans-horizon propagation [55]. Troposcatter propagation has been identified as the dominant mechanism during normal atmospheric conditions. Enhancement of the received signal above normal troposcatter medians is termed as anomalous propagation.

Typical features of signal received due to each type of mechanism were identified. According to the type of 'signature' observed in the received signal, signal enhancements were attributed to particular mechanisms (ducting, layer reflection and high k-factor diffraction). In case of troposcatter, the received signal amplitude has scintillations, with a noisy envelope with variation ~5dB (a). Signal received via ducting shows a multipath-fading pattern, with a degree of stability in signal levels (b). Typical signature due to layer reflections shows short-lived, frequent high variations (like impulses) added to troposcatter envelope (c). Diffraction due to high k-factor is a gradual phenomenon, hence showing a bridge-shaped signal signature, with smooth start/end, with troposcatter scintillation still evident (d). Figure 3-1 shows these typical signatures:

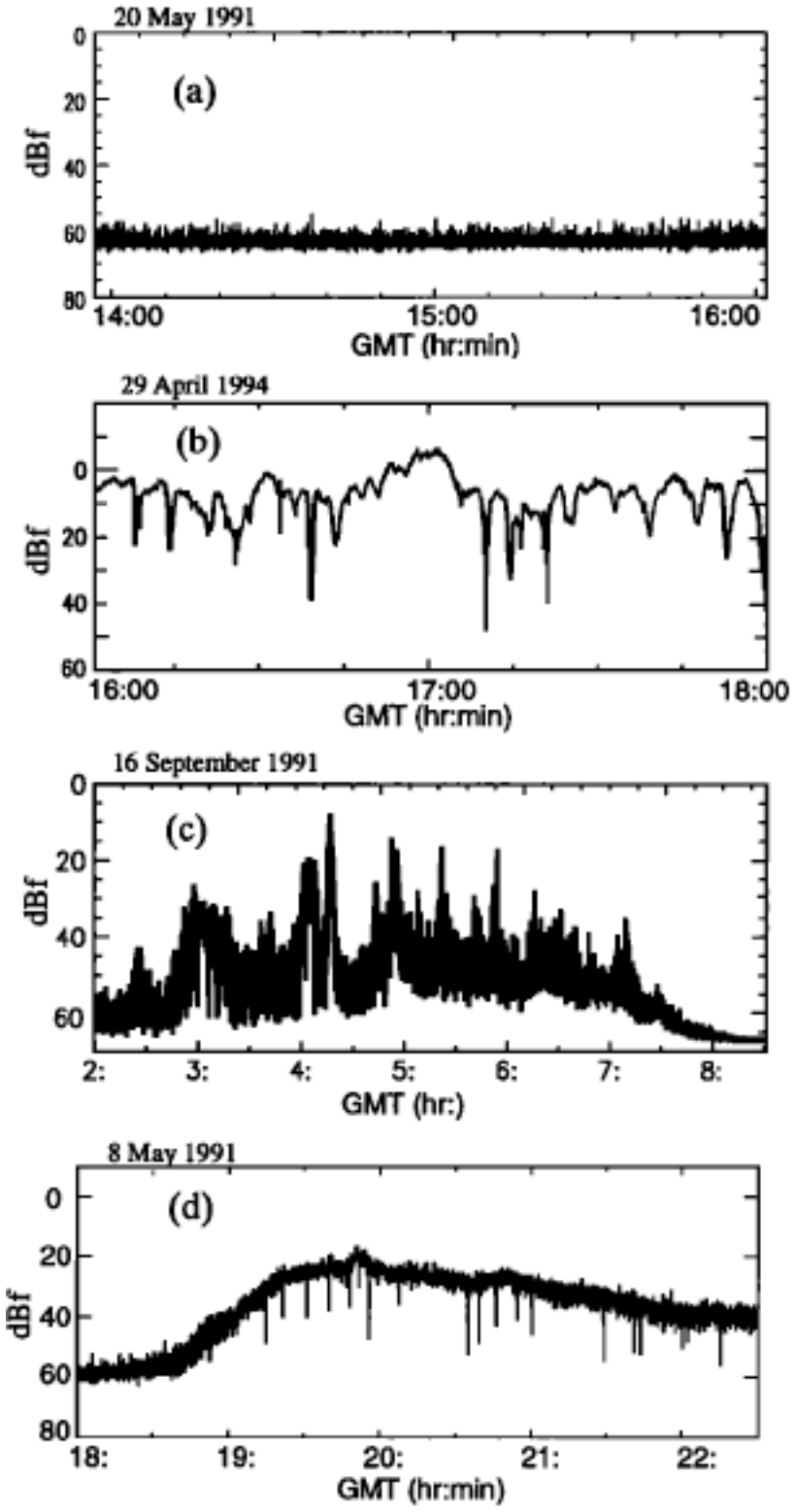

Figure 3-1: Typical signatures for different propagation mechanisms [55] –

(a). Troposcatter 'normal' reception

(b). Ducting enhancement

(c). Layer reflection enhancement

(d). High k-factor diffraction enhancement

It was concluded that troposcatter was the dominant mechanism, existing for 56% of time, followed by diffraction, which was observed for 23% of time, followed by ducting (10% of time) and layer reflections (6% of time). In most of enhancement events, one propagation mechanism was observed as dominant. However, at times it was observed that more than one mechanism was responsible. 'Mixed' propagation accounted for almost 4.4% of time.

It was acknowledged that the behaviour of a trans-horizon channel could change dramatically, depending on the mechanism dominant at a certain time. Hence, it becomes vital that each mechanism is identified, the path loss due to each mechanism be calculated and statistics related to each mechanism be studied.

Joy [57] investigated long-range propagation of 3 GHz horizontally polarised signals on over-sea paths in the North Sea and the English Channel during 1940s and 1950s. Coastal transmitters and on-ship receivers were used. High signal levels were observed for 'considerable' amounts of time in summer for distances up to 90 nautical miles in the North Sea experiments. These were attributed to super-refractive conditions. In the absence of super-refraction, troposcatter is believed to be the dominant mode. Super-refraction was not observed on the English Channel measurements carried out in May through to December of 1952 and no reason could be attributed. However, large day-to-day variations in the signal level were noticed.

Stark conducted a simultaneous prolonged measurement over the North Sea at 5 different receiving sites at 560 MHz and 774 MHz using paths from 200 km to 950 km. The results showed that the ratio of field strength exceeded for a specified time percentage is slightly higher at higher frequency. Assumptions were made that the median field strengths were predominantly due to scattering in turbulent conditions whereas the propagation mechanism for small time percentages was refraction or layer reflection [92].

A year-long investigation into signal level statistics for 128-km trans-horizon path in Atlantic operating at C-band (4.7 GHz) was carried out by Goldhirsh and Musiani [94]. It concluded that during the spring-summer period, received signal levels were due to ducting whereas the fall-winter levels may be due to troposcatter from irregularities of the refractive index.

Tawfik and Vilar conducted over-sea measurements at X-band frequencies (10.7 and 11.6 GHz) in the English Channel during an experiment conducted in 1987 – 1991 [100]. Two paths, Cap d' Antifer-Portsmouth (155 km) and Brittany-Dorset (254 km), were used, with antenna and frequency diversity employed for shorter path. The measured path loss was compared to the values predicted by then ITU models. The path loss was observed to be normally distributed, with three regions: (1) troposcatter-dominated region of probability greater than about 50%, (2) the region of probability less than 50% and greater than 1% not dominated by any particular mechanism (blended

mode), and (3) the probability region less than 1% of the time linked to anomalous propagation mechanisms.

3.2. Effective Earth Radius Factor

BBC also carried out long-term measurements on over-sea paths in the English Channel within TV Bands IV & V (500-750 MHz) to determine the most suitable path that could serve as a re-broadcasting link between mainland UK and Channel Islands [53]. Receiving sites at Alderney at 90m and 69m AMSL (diversity) and Guernsey at 80m AMSL while transmitters at Rowbridge, Caradon Hill, Stockland Hill and Portland Bill with respective heights 280m, 602m, 461m & 156m AMSL were used. The path lengths varied from 95 km to 174 km.

The study by BBC [53] compared median measured field strength with predicted field strength derived from Curves in CCIR (now ITU) & Japanese Ministry of Postal Services Atlases of Propagation assuming standard atmosphere. The results indicate that the measured field strength exceeds predicted values for all paths except Portland-Alderney, where measured and predicted values are comparable. Based on these results, the report suggests that the annual median refractive index lapse rate over the English Channel is somewhat greater than the value of k=4/3.

3.3. Typical Transmission Loss

Freeman [17] observed that diffraction could be the dominant propagation mechanism for paths less than 160 km long, displaying long-term median transmission loss around 170-190 dB. On paths from 160 km to 800 km and beyond, troposcatter is dominant, exhibiting long-term median transmission loss of 180-260 dB.

Boithias and Battesti observed that long-term and seasonal propagation characteristics due to troposcatter depend on climatic zone [80]. It was observed that usually transmission loss reaches one maximum and one minimum annually, being greatest during: (i) the rainy season for tropical and equatorial climates, (ii) the hot season for desert areas, and (iii) the cold season for non-desert areas. Diurnal variations exist in all climates, with maximum transmission loss in late afternoon and minimum in morning. For temperate climates, the variation of hourly median transmission loss is ~10 dB in summer and much smaller in winter.

Frazier [67] compiled curves of path loss using IPS, which was developed by NTIS, United States Department of Commerce. IPS was based on then available ITU-R Recommendations (1984) and predicted the median value of radio wave propagation loss at far field distances over a spherical earth for the line-of-sight modes of surface wave, free space, and multipath; and for the beyond-line-of-sight modes of smooth earth diffraction and tropospheric scatter. The curves of path loss (in dB) were for 100 MHz, 1,000 MHz, and

10,000 MHz. Effects of terrain roughness, mixed path surfaces, vegetation, fading relative to the median loss, and tropospheric ducting were not included whereas terrain roughness, mixed path surface, foliage, rain, and long-term time-dependent power fading had to be determined from other sources and added to the smooth-earth transmission loss predictions.

The results by Castel [91] show that the path loss over the sea is around 10 dB less than over the land when transmitting at 400 MHz:

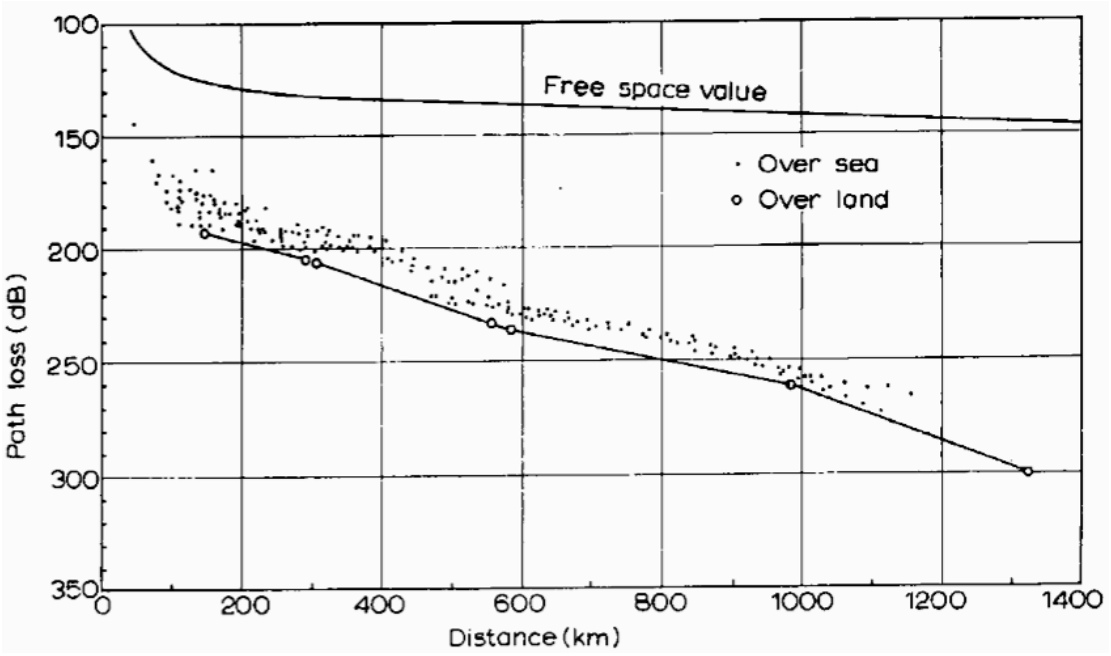

Figure 3-2: Path loss between over-sea/over-land propagation paths [91]

3.4. Indirect Measurement of Refractivity

The values of refractivity taken at different heights above the surface of the Earth can help determine the refractivity gradients prevailing at different heights and times. Knowledge of these initial gradients (up to a height of

around 1 km above the surface of the Earth) can help understand the refractive conditions prevalent in the troposphere.

Levy et al conducted airborne measurements over the English Channel to study anomalous propagation in the summer of 1989, at heights from approximately 60m to 1500m AMSL [52]. A 250 km over-sea path between Bournemouth, UK and Lannion, France was chosen for the flights. A 400 MHz receiver was also used on-board for signal strength measurements. Attempts were made to fly during times of predicted anti-cyclonic conditions. Direct measurements of refractivity were made using a refractometer for only part of campaign with simultaneous measurements of weather variables. It was observed that indirect measurements of refractivity through pressure, temperature and dew-point temperature were consistent with direct measurements using the refractometer within the lowest 1 km of atmosphere. The study used indirect measurements for their subsequent analysis.

Bye et al [42] observed that radiosonde readings of pressure, temperature and relative humidity (to get values of refractivity) are usually not taken at the times of sunrise and sunset, which is when gradients of heating and cooling of atmosphere and thus variation in refractivity gradients are expected to be maximum. Also, finer details in vertical profile of the atmosphere can be lost with the ‘normal’ radiosonde readings usually taken with vertical resolution greater than 10 metres. Hence, there could be a degree of ‘generalisation’ and ‘inaccuracy’ of refractivity statistics based on radiosonde data. In spite of these deficiencies, most of the previous research and pioneering studies into

vertical profiling of atmosphere, like Bean et al [43], are based on radiosonde data.

3.5. Signal Enhancement

Gunashekar observed [50] signal enhancement for almost 9% of time in his study on propagation of 2 GHz signal on over-sea path. Almost 91% of these enhanced signal cases occur when refractivity gradient in lowest 100m is indicative of super-refraction or ducting. While super-refractive and ducting refractivity gradients were observed for almost 40% of time, signal strength enhancement was only observed for almost 9% of time. Almost 54% of time with ducting refractivity gradient and 37% of time with super-refractive gradient was enhanced signal strength observed. This indicates that although ducting and super-refraction are primarily responsible for the occurrence of enhanced signal strengths (ESS) on trans-horizon over-sea paths, they do not necessarily always result in ESS (though the likelihood of ESS reception increases).

In this study, there are 119 days on which signal strength enhancements are observed at both the high and low antennas at Alderney. Furthermore, of these 119 days, there are 78 (66%) days on which enhanced signal strength (ESS) occurs for four hours or more consecutively. In terms of the hourly duration of each ESS event, approximately 82% of the cases persist for four hours or longer. This suggests that ESS is being caused by relatively slow-moving physical mechanisms. The simultaneous signal strength

enhancements at Alderney, Guernsey and Sark indicate that the physical mechanisms responsible for ESS exist on a relatively large scale. Study of synoptic weather charts indicated strong correlation between the occurrence of enhanced signal strengths and the existence of high-pressure centres, which are often associated with anti-cyclonic conditions, which usually extend over large regions and are slow-moving phenomena. 77% of days when ESS were observed at Alderney, high pressure cells were observed either directly over or close to the Channel Islands area. In addition, it has also been observed that the presence of high-pressure cells does not always result in ESS. While at times marginal increase in received signal levels has been observed, at other times no enhancement has been observed while synoptic charts indicated the presence of high-pressure cells in the region.

The presence of frontal activity in the English Channel has been observed to be correlated with the occurrence of enhanced signal strengths, to a lesser extent [50].

Diurnal and seasonal patterns were observed in enhancement (i.e. late afternoons and evenings in summers and springs). For the Jersey-Alderney path, the conditions observed to be prevalent at times of signal enhancement were: increase in air and sea temperatures, positive air-sea temperature difference, existence of high pressure centres over the region, enhancement in absolute humidity of air above the sea surface and calm sea conditions or low velocity winds flowing from continental Europe.

A ducting/super-refractive layer between the approximate altitudes of Guernsey Airport (102m) and Alderney Airport (88.7m) was identified. This higher ducting layer correlates very well with signal strength enhancements.

It was also observed by Gunashekar that a stable atmosphere (sea temperature lower than the air temperature) correlates well with the occurrence of enhanced signals.

Sim studied propagation on over-sea trans-horizon paths for frequencies around 300 MHz with transmitter at Jersey and receivers at Alderney and Guernsey [11]. Enhancement in received signal levels (ESS) was observed at both sites, citing surface ducting and super-refraction as possible explanation. ESS occurred for higher percentages of time in summer, around 43 to 76% and 31 to 48% of the total time (percentage of days) during summer 2001 and 2002 respectively. In comparison, the total time was below 10% during winter period.

Correlation was observed between signal enhancements at both receiving sites. The received signal levels were compared to the predictions by ITU-R P.526 [12].

Nuaimi et al studied a 63 km trans-horizon link operating at 11 GHz over the Bristol Channel in the UK for two years. A closer investigation of six days chosen as a sample representative of signal trends with reference to prevailing meteorological conditions (cloud base height and horizontal

visibility) was made [118]. The results indicated positive correlation between signal levels received and the cloud base height and height of horizontal visibility as observed by the nearest weather stations.

It has been noted from Gunashekar [50] that Wickerts and Nilsson conducted long-term radio-meteorological experiments at frequencies ranging from 60 MHz to 5 GHz in the Baltic Sea [89]. Signal strength enhancements were observed on a 160 km path, predominantly in the summer. Additionally, different propagation mechanisms dominated the different transmission frequencies. For instance, at 5 GHz, ducting was the primary mechanism responsible for the occurrence of enhanced signals. At 170 MHz however, layer reflections produced high signal levels.

The study by Rudd [51] on a 200km over-sea path in the English Channel observed enhancements in UHF signal in the evening and early part of the night. This has been attributed to changes in temperature differential between warmer continental air and colder sea surface air. In addition, it was observed that 50% of enhancement events lasted for 6 hours or more.

Tawfik et al [105] observed enhancements well above the troposcatter level throughout the year of study. Diurnal enhancements in signal have been observed in early morning and night (0500 and 2000 hours GMT), attributed to subsidence and surface ducting due to evaporation and advection. Investigations were made into correlation of signal level strength with localised meteorological parameters temperature, pressure and humidity. The data

used for the correlation studies was the daily average signal level strength and daily average local temperature, pressure, humidity, refractivity (wet and dry terms), and maximum daily temperature for the long link (254 km). It was observed that signal enhancements occurred only when surface atmospheric pressure was greater than about 995 mbars. The majority of enhancements occurred between 1010 and 1025 mbars. A positive correlation between signal levels and daily average local temperature was noticed. A higher (positive) correlation was observed with maximum daily local temperatures. There was some correlation with refractivity, but not very good. High correlation between 1-week and 2-week averaged signal and meteorological parameters indicated that averaging over a period of 1 to 2 weeks is appropriate for the correlation process.

The BBC conducted propagation measurements at frequencies between 40 and 600 MHz on trans-horizon paths in the UK, the North Sea and the English Channel during the years 1946-57 [76]. The measured 187-MHz field strength values exceeded for 1% and 10% of time, for a 200-km over-sea path, for summer, were higher than the values predicted by the then relevant ITU procedure (CCIR London 1953).

During a series of investigations by the BBC on over-sea paths, signal level enhancements were observed [53]. Table 3-1 summarises the percentage of times signal levels on all paths exceeded the free space field strength:

Path	Path length (km)	Freq (MHz)	Duration of measurements	Percent of time free space field strength exceeded
Rowbride-Guernsey	167	501.25	3.5 years (Feb 67 – Sep 70)	3
Caradon Hill-Guernsey	174	533.25	2 years (July 69 – July 71)	4
Rowbridge-Alderney	121	501.25	2 years (Feb 67 – Feb 69)	9 (90m) 4 (69m)
Portland-Alderney (90m)	95	666	10 months (Feb 70 – Nov 70)	6 (Vertical) 1.2 (Horizontal) 4 (Combined)
Stockland Hill-Alderney	137	756	4 months (Aug 70-Nov 70)	10

Table 3-1: English Channel paths- signal exceedance time percentages [53]

Analysis of monthly field strength variations revealed considerable month-to-month variation, emphasising the need to have measurements over long periods of time. The variation of median monthly field strength value is summarised in Table 3-2, for measurements of at least 2 years:

Path	Variation of monthly median field strength
Rowbride-Guernsey	35 dB
Caradon Hill-Guernsey	32 dB
Rowbridge-Alderney	20 dB (90m), 15 dB (69m)

Table 3-2: English Channel paths - variation of monthly median field strength [53]

Based on these results, the research further suggests that anomalous propagation exists in some summer months for more than half the time.

The study by Ames et al [54] specifically observed that high signal levels were reached for short periods of time during summer, the values of signal strength exceeded for 1% of time in summer coming to within 17 dB of free space loss (FSL) level whereas the median value in summer was ~ 48 dB below FSL.

The research by Shen & Vilar [55] investigated seasonal occurrence of enhancement events due to ducting, layer reflection and high k-factor diffraction. The results indicate that (a) a majority of ducting events occurred in summer, (b) layer-reflection events were present throughout the year except October, November and December, reaching maximum during the summer and (c) diffraction events due to high k-factor occurring throughout the year. Figure 3-3 shows the total monthly duration (number of hours) of signal enhancements due to different enhancement events (diffraction, ducting and layer-reflection). If these distributions are combined, there are indications of signal level enhancement throughout the year:

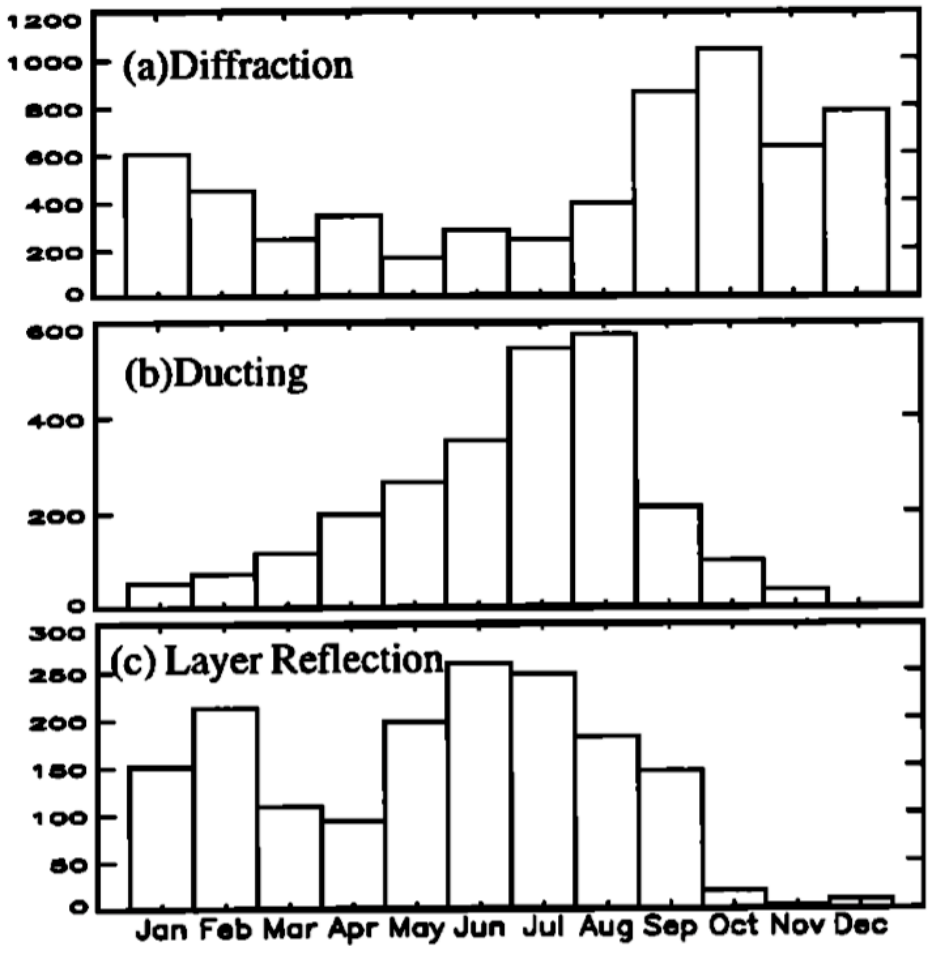

Figure 3-3: Monthly distribution of duration of enhancement events due to different mechanisms [55]

Investigation by Shen and Vilar [56] into statistics of path loss on over-sea path in the English Channel reveals that enhancement due to ducting, diffraction and layer reflection decreases as the distance to horizon increases.

A multi-frequency propagation experiment was conducted in 1989 (mid-Sep to mid- Dec) on a 27.7 km over-the-horizon path offshore of Lorient, France [97]. Paulus and Anderson compared the results for 3 GHz, 5.6 GHz, 10.5 GHz and 16 GHz, noting that higher signal enhancements were observed for the higher frequencies [96].

During investigation into X-band propagation on over-sea paths by Tawfik and Vilar [100], path loss was observed to be less than free space path loss for 1% of time at lower antennas in the shorter path, 0.1% of time at higher antennas in shorter path and for less than 0.01% of time for the longer path. A comparison of path loss exceeded for 0.1% of time in July and December revealed that the seasonal range for the longer path (254 km) is about 40 dB, whereas for the 155-km shorter path of Cap d' Antifer-Portsmouth the range is about 25 dB.

Long-term strong signals were attributed to anti-cyclonic conditions over the paths, whereas the daily variability was assumed to be due to the incidence of ducting in the afternoon, particularly over the sea areas. Increase in temperature and humidity differentials between the advected (overland) air and that close to the sea were cited as the possible causes and a delay of 3 to 4 hours was expected between the time at which the land is at its hottest and

the time the heated advected air moves over the sea to produce enhanced ducting conditions [100].

3.6. Ducting

The ITU has also made available the annual statistics of ducting characteristics in the form of maps and text files. These statistics are derived from 20 years (1977-1996) of radiosonde observations from 661 global sites. According to this data, surface and elevated ducts can occur in UK coastal areas for almost 20% and 15% of time respectively, in a year [18].

The studies by Bean et al [43] indicate that for Bordeaux, France (which is nearest site in this study to project sites for this particular statistic), the median and minimum trapping frequencies of ducting layers are given by Table 3-3:

February		**May**		**August**		**November**	
Med	Min	Med	Min	Med	Min	Med	Min
1300	190	565	99	402	89	442	186

Table 3-3: Median & minimum trapping frequency of ducting layers-Bordeaux, France (MHz) [43]

Rudd conducted a study into short-term variability in interference due to tropospheric enhancement at UHF on over-sea path in the English Channel [51]. A transmitter was placed in Caen, France and receivers in Brighton, UK (almost 200km path length). A time series of power received from a Single-

Frequency Network[1] (SFN) during a ducting event shows a fast fading pattern of +/- 2dB (i.e. a variation of 4 dB) with varying frequency, as depicted in Figure 3-4:

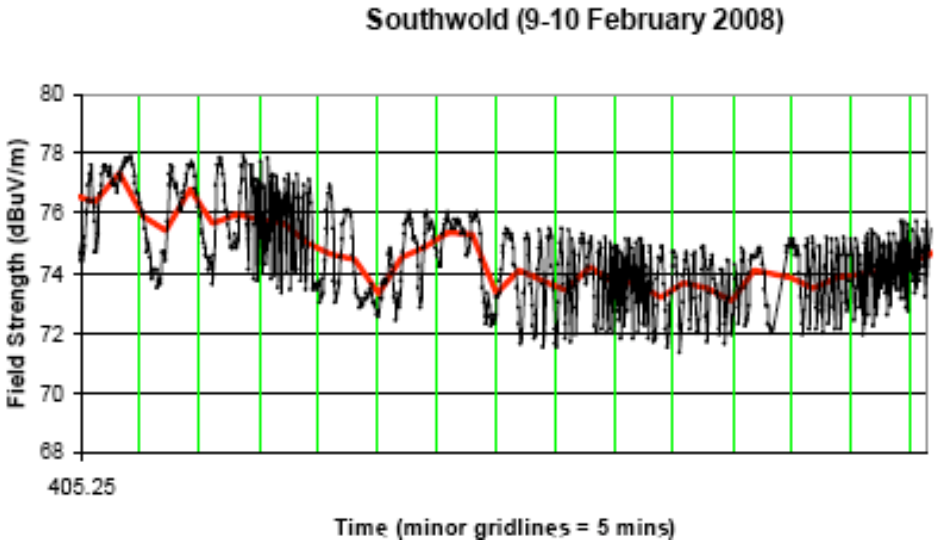

Figure 3-4: Interference pattern due to SFN [51]

This indicates that ducting can enable a fading phenomenon, whose frequency varies as different sources of the SFN couple more or less strongly into the duct.

Study by Levy et al [52] during summer observed a strong elevated duct and a corresponding inhomogeneous refractivity layer at 1km height above Bournemouth. The duct was detected by radiosonde measurements while the inhomogeneous refractivity layer was detected through airborne measurements.

[1] SFN - Single Frequency Network - A broadcast network where multiple transmitters simultaneously use the same frequency

Gunashekar [50] observed evaporation ducting most of the time and also a ducting/super-refractive layer between the approximate altitudes of Guernsey Airport (102.0 m) and Alderney Airport (88.7 m). This higher ducting layer correlates very well with the occurrence of signal strength enhancements. Analysis of meteorological data from neighbouring radiosonde stations reveals that the occurrence trend of surface-based ducts in this region agrees well with the seasonal pattern of enhanced signal strength incidences. Ducting gradients in lowest 100m of atmosphere were observed for almost 9% of time (though signal enhancement was only evident for almost 54% of these cases when ducting gradients were present).

Since evaporation ducting is a weather-dependent phenomenon, it is difficult to measure its characteristics using any instruments. Hitney conducted an assessment of evaporation ducting based on bulk meteorological data from buoys and concluded that high-quality meteorological measurements made via oceanographic buoys are very suitable for assessing evaporation ducting conditions [82].

Jeske devised a method to determine the evaporation duct height using measured values of sea temperature, air temperature, relative humidity, and wind speed [78]. Later, Paulus applied a correction to Jeske's method to address the anomalies arising as a result of errors in the air-sea temperature difference [79]. Babin et al observed that this correction often results in an underestimation of the duct height [83]. In spite of this, the Paulus-Jeske method is the most widely implemented model [77,84,85,86].

A pioneering study into evaporation ducting throughout the world for almost 300 oceanic areas, using 15 years of data, by Hitney and Vieth has been made using Paulus-Jeske (P-J) method [77]. The analysis of Aegean Sea and North Sea paths show that path loss decreases monotonically across the entire range of duct heights for frequencies less than 3 GHz, and that evaporation ducting is dominant at frequencies above 2 GHz for trans-horizon, over-sea paths.

Meteorological data from NCDC for the period 1970 to 1984 was used to construct an evaporation duct climatology [95], which has been used by Paulus and Anderson [96] to predict propagation loss on both a monthly and annual basis in coastal regions strongly under continental influence. Climatological predictions were compared to measurements over trans-horizon over-sea paths in France and USA [94, 97, 98]. It was concluded that the evaporation duct climatology could be used to predict median signal level propagation, even in coastal environments strongly under a coastal zone influence.

Evaporation ducting markedly tends to extend radio communications for frequencies beyond 3 GHz [73].

It was observed by Gunashekar [50] that signal strength levels are higher than diffraction and lower than free space levels, indicating that evaporation ducting is causing signal strength enhancements to some extent, extending radio horizon and enabling propagation to ranges inaccessible without ducting.

Positive correlation was observed between the radio data and evaporation ducting conditions during periods of normal reception. During periods of normal reception (non enhanced signal strength), it has been observed that higher (i.e. stronger) evaporation ducts support higher signal strengths at most times. By considering only the non-ESS data, the signal strength at the Alderney high antenna increases at the rate of 0.61 dB per metre increase in duct height. In cases of enhanced signal strength, however, no correlation was observed between signal strength and calculated evaporation duct height, implying that a mechanism other than evaporation ducting is active and dominant.

Sea-based surface duct (i.e. evaporation duct) events have also been identified by Shen and Vilar [55] by observing ducting events with concurrent, synchronised sharp fadings, attributed to ship movements in the English Channel.

Hitney et al [73] observed that it was not necessary for an antenna to be within the evaporation duct to receive enhanced signal due to evaporation ducting; however, the probability of receiving a higher signal increases if the antenna is located within the duct. Gunashekar had similar observations during his study on over-sea propagation [50].

3.7. Fading Statistics

Freeman observed that the amplitude of short-term fades for troposcatter links follows a Rayleigh Distribution [17]. A similar observation has been made by Boithias et al [80]. The typical short-term fading range is around 13.5 dB. It has been observed that short-term fading is more prevalent on shorter paths when fade rate goes up to 20 fades per second. Freeman explains that this could be because the scattering properties of troposphere are more volatile at lower altitudes and tend to become more uniform at higher altitudes [17].

On the other hand, long-term fading (variation in hourly median value) is caused by overall (slow) changes in refractive conditions of troposphere. It is characterised by day-to-day fades and seasonal fades. Daily variations are attributed to changes in properties of scatter volume (temperature, density, humidity, altitude of scattering layers) while seasonal variations are due to seasonal changes to these properties [17].

It has been observed that the amplitude of long-term fading generally follows a lognormal distribution, with the fading decreasing with increasing path length, e.g. the fading range is ~30 dB for 80 km path and ~11 dB for a 500 km path [17]. The frequency of fading is greatest when the hourly median transmission loss is greater than the long-term median transmission loss.

Castel [91] showed that the probability of fading increases dramatically over the sea/coast than over land as the propagation path length increases, as

shown by Figure 3-5. In this case, the frequency used was 400 MHz and the antenna height for both transmitter and receiver was fixed at 10 metres.

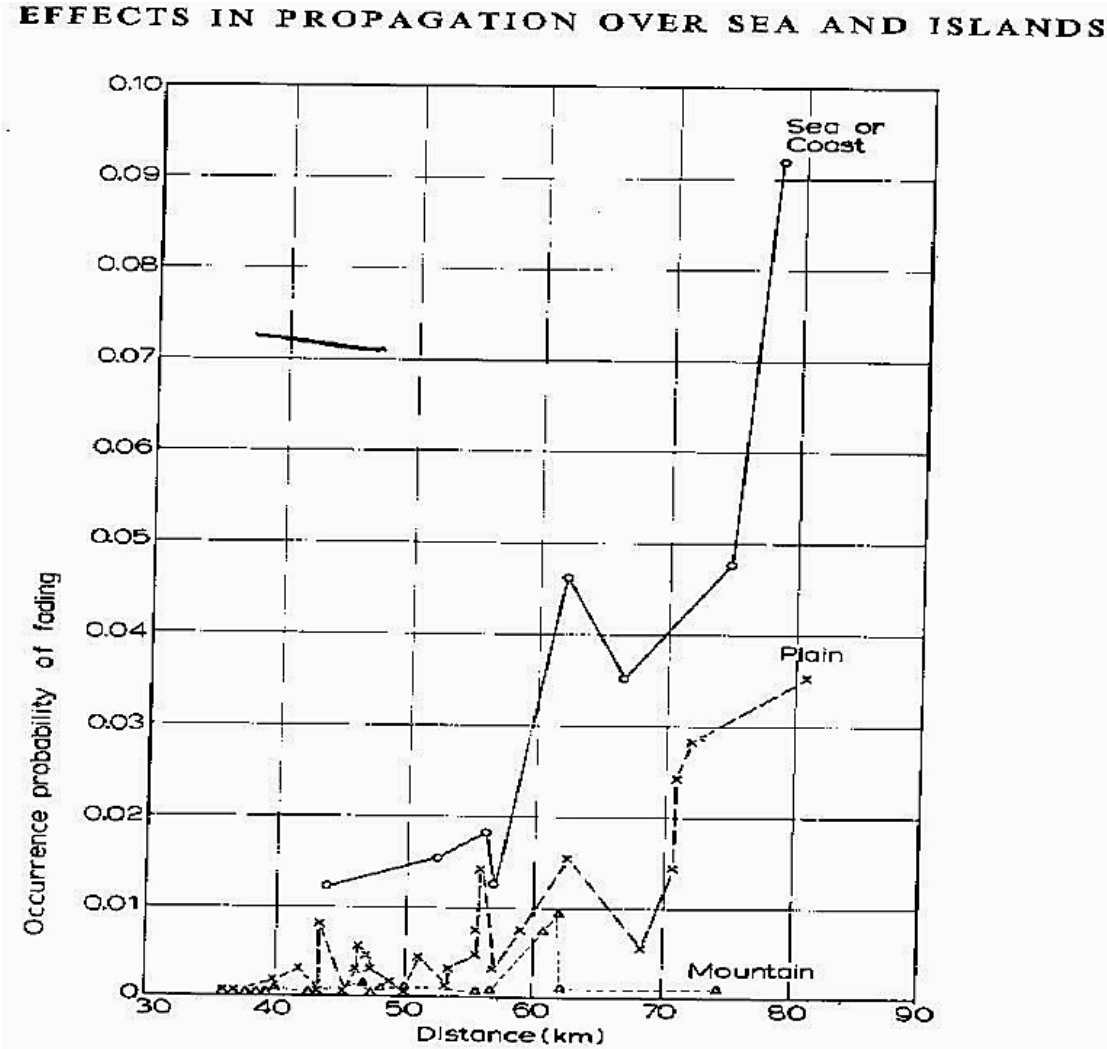

Figure 3-5: Fading effects in propagation over sea and islands [91]

Previous research carried out in the UK using VHF frequencies for 140km path for a day in September 1959 has shown some interesting signal behaviour in relation to pressure [16] (See Figure 3-6). The day starts with clear sky conditions and a steady high signal level, which begins to fall as the pressure at the transmitter begins to decrease:

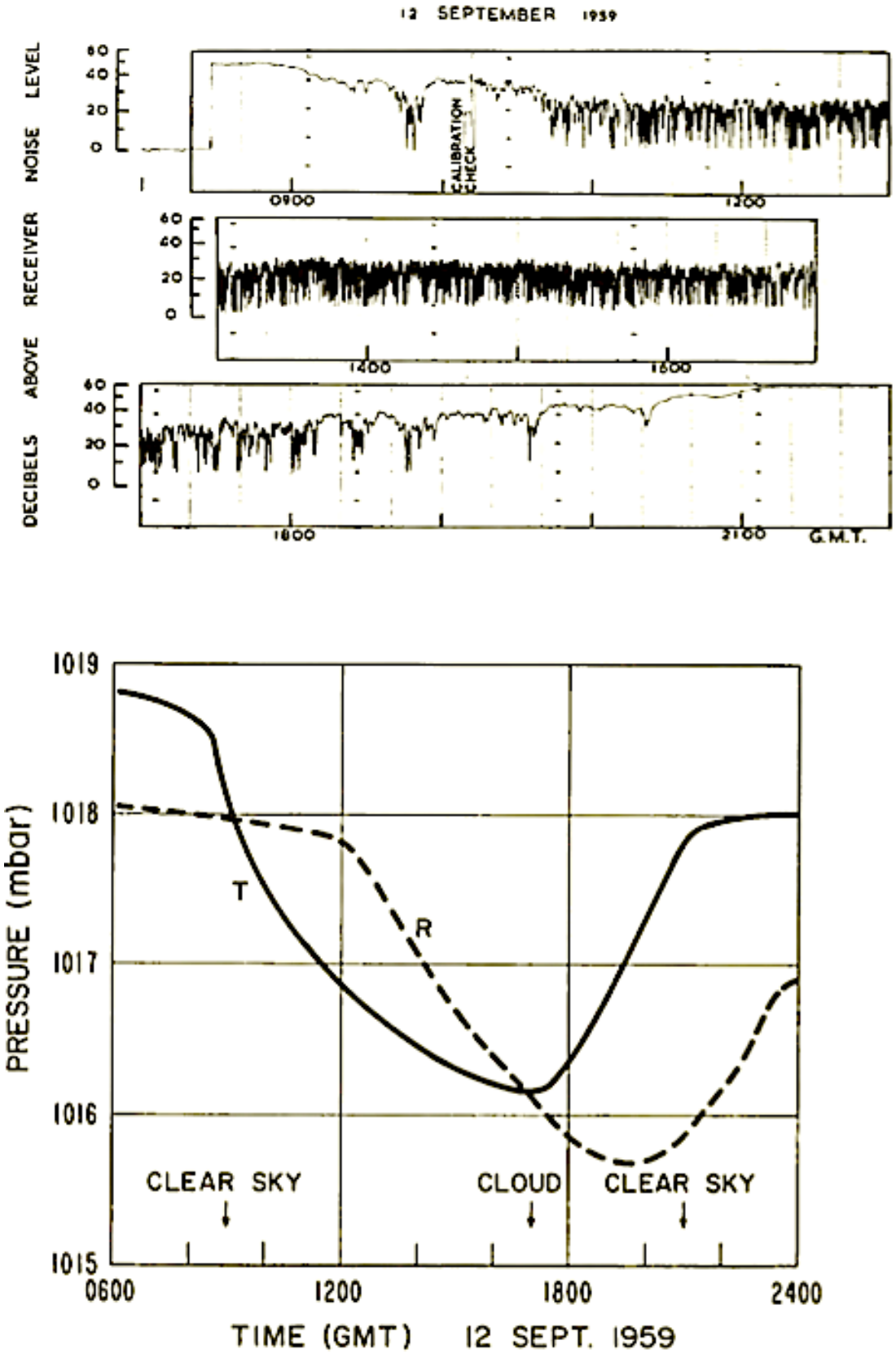

Figure 3-6: Signal level and pressure variations at transmitter (T) and receiver (R) on 140-km path at frequency=186 MHz [16]

At about 1030 hours the median level and fading rate change abruptly as the pressure at the midpoint falls. The fading rate increases while signal level drops. Between 1200 and 1700 hours the pressure over the whole path is falling, and the signal characteristics remain essentially uniform, with rapid fading and lower-than-morning signal level. However, a significant increase in median level and a reduction in fading rate are evident at 1700 hours as the pressure begins to increase at the transmitter. As pressure at receiver starts to increase around 2000 hours, fading rate is further reduced and signal level increases. By about 2300 hours the pressure at the centre of the path has reached a steady value and the signal level is again high with negligible fading.

This variation in signal behaviour has been attributed to the vertical motion of atmosphere and correlation between hourly median field strength and calculated values of vertical velocity has been observed [16].

The BBC conducted experiments to study the effects of tides on VHF and UHF propagation of television signals over the sea [99]. Line of sight paths were used, based on the theoretical consideration that the received field strength is the vector sum of direct component and indirect component reflected from sea surface. Sea-level variations were expected to cause signal strength variations. Severe fading of more than 40 dB was observed for UHF in un-obstructed paths, reducing as range increases from line of sight to beyond horizon.

Ames et al carried out VHF signal measurements for summer and winter representative months (August 1953 and January 1954) for trans-horizon over-sea paths in the North-Atlantic Ocean at 220 MHz [54]. The paths investigated were 320 & 650 km long. The results were compared to similar measurements on over-land paths. Airborne measurements of signal strength were also made at heights from 150m to 4.5km.

Airborne measurements at altitude of 150m along trans-horizon path recorded fading rates of 1-3 cycles per minute within the line of sight region, no fading within the diffraction region and minute-to-minute variation of 10 to 20 dB beyond the diffraction region.

A study of fading statistics on an over-sea trans-horizon path in the English Channel by Ndzi et al [58] reveals slow fading during ducting with fade depths up to 50 dB. The results during troposcatter conditions indicate rapid fading with small fade depths. A strong negative correlation has been observed between fading depth and signal level.

Sim observed that high fading occurred at around 35 to 55% of the time during summer, decreasing to around 10% during the period from Nov 2001 until Jan 2002 [11]. Average fading ranges of around 10 and 7 dB during autumn and summer respectively were also observed, with a maximum fading level of 12 dB in autumn. In terms of fading duration, an average fading period of around 7 seconds was observed, with a maximum fading period of 22 seconds during the autumn period.

3.8. Correlation Between Lapse Rate and Surface Refractivity

Lane [49] observed a high correlation (0.85) between the average annual surface refractivity and the average annual lapse rate in the first kilometre for the British Isles.

Studies based on 5 years of radiosonde data (1997-2002) in Barcelona, Spain (also a coastal station) observed significant correlations between monthly averages of surface refractivity and vertical refractivity gradients [44].

For the English Channel and the North Sea, Bean et al [43] observed high correlation between the monthly mean refractive index lapse rate $\overline{\Delta N}$ and the monthly mean surface refractivity $\overline{N_S}$, with a correlation coefficient value of 0.9.

3.9. Correlation Between Surface Refractivity/Lapse Rate and Signal Level

A number of studies have reported correlation between the surface refractivity or the lapse rate of refractivity and the signal level [16, 50, 55, 80].

Previous research on different trans-horizon paths in diverse climates has shown correlations between monthly median values of ΔN/surface refractivity and field strength, ranging from 0.4 to 0.95 [16].

It has been concluded further that this correlation between field strength and surface refractivity:

(i). increases with increasing variation in the field strength and the surface refractivity

(ii). is greater for the summer diurnal cycles than the winter ones

(iii). is greater for the seasonal cycles of night-time values of the variables than for the midday values

Also, these results are found to be consistent with the assumption that N decreases exponentially with height.

The research by Gunashekar [50] investigates the correlation coefficients between hourly, diurnal, weekly and monthly variation of some of the important weather parameters (pressure, temperature, humidity, refractivity, wind speed) and signal strength at Alderney. The lapse rate of refractivity calculated from refractivity values at Guernsey and Channel Light Vessel gave the best correlation.

Low correlation (0.112) is observed between surface refractivity and signal strength, when using hourly data. However, monthly mean values of surface refractivity and signal strength show increased correlation (0.568). The study also observes that the presence of inversions in modified refractivity between the surface (CLV) and the altitude of Jersey Airport (i.e. 84.0 m) correlate strongly with occurrence of enhanced signal strength.

Shen and Vilar [55] investigated correlation between surface refractivity at receiver sites and different enhancement events. The enhancement due to high-factor diffraction showed a correlation of 0.67. Ducting enhancements have low correlation 0.35, while layer reflection enhancements have a reasonable correlation of 0.55.

Boithias et al [80] observed that for Dakar, Senegal, correlation between Ns and enhanced signal levels is evident only during winter months.

Hence, correlation between signal level and surface refractivity seems to depend on season, propagation mechanism, time of day etc. Low values of correlation may not be surprising because propagation might be enabled by a phenomenon located higher up in the troposphere and may not be correlated with a meteorological parameter measured at ground. However, if surface refractivity is correlated to a certain characteristic of higher atmosphere and the signal is correlated to that characteristic, then it in turn would imply that signal and surface refractivity are correlated. Analysis of surface refractivity and measured field strength at frequencies near 100 MHz on 20 paths, 130 to 446 km long, located in various part of the United States, indicates strong correlation, due to the high correlation between the surface refractivity value and lapse rates [16].

Shen and Vilar [55] observed that lapse rate of refractivity also contributes to the correlation statistics of enhancement. When lapse rate of refractivity increases, the angle of incidence of transmitted waves decreases, helping

layer reflection to cause enhancement. When k factor decreases to normal value, the angle of incidence increases and results in smaller reflection coefficient. Similarly, high values of lapse rates were concurrent with ducting like received signals as a result of strong super-refraction.

Boithias and Battesti observed that if the modulus of the refractivity gradient increases in the portion of troposphere below the common volume, the height of common volume is reduced, lowering the scatter angle and thereby increasing the signal level [80].

The results by Ames [54] indicated good correlation between median signal levels and refractive index in lowest parts of troposphere, as expected, while the presence of heavy fog had no obvious effects on signal levels.

3.10. Correlation Between Tidal Variation and Signal Level

Gunashekar [50] observed the effect of the English Channel's semi-diurnal tides (i.e. two high and low waters in a 24 hour period) on the signal strength during periods of normal reception. A signal strength increase of approximately 1.1 dB per meter decrease in tide height at Alderney was observed, leading to an overall diurnal signal strength variation of about ±6 dB. The normal inverse relationship between the tide and signal strength is lost during periods of enhanced signal strength.

Sim observed that during times of calm sea state, Jersey-Alderney path showed a linear relationship between the signal amplitude and the tide height although the data showed some fluctuation in the signal across the linear region [11].

3.11. Correlation Between Signal Levels at Different Receiver Sites

The investigation into over-sea propagation by Gunashekar [50] involved three receivers at Alderney, Guernsey and Sark. There was concurrent increase or decrease in signal strength at Alderney, Guernsey and Sark receivers. This was indicative of similar propagation mechanisms affecting the three diverse radio paths. This correlation reduced during times of enhanced signal reception.

Sim also observed correlation between signal enhancements at both Alderney and Guernsey during his investigations on over-sea propagation [11].

3.12. Comparison with Over-Land Paths

During study of trans-horizon paths [54], it was observed by Ames et al that the summer median signal level was 48 dB below free space while winter median signal level was 73 dB below free space. Their average is approximately 61 dB as a representative annual median value. This median value was somewhat lower than the annual median value from similar over-

land measurements at 100 MHz and 1 GHz. The variation of median value (25 dB) between summer and winter was also larger than for over-land paths.

This seems to indicate that enhancement as well as seasonal variation is higher for over-sea paths than over-land paths.

3.13. Prediction Models

Propagation models are used to predict the basic transmission loss experienced by wireless signals while travelling between two antennas located on or above the Earth's irregular surface. These models have been categorised into different types during the passage of time [69, 119]. These models can be split into 4 types: (1) theoretical, (2) empirical, (3) statistical and (4) deterministic. The theoretical models are derived physically, assuming ideal conditions. Purely empirical models are derived from the measurements taken while semi-empirical models use theoretical considerations to predict propagation effects based on measurements of physical parameters other than propagation loss itself. Statistical models (or stochastic models) are relevant to small-scale statistics. They use statistical distributions to describe a range of losses for a set of paths with similar path lengths, antenna heights, frequency but different path types. On the other hand, the deterministic models are site-specific models, utilizing the local site details to compute basic transmission loss between two points. For obvious reasons, greater accuracy is expected with empirical and deterministic models. However, depending on the amount (general/specific), type (qualitative/quantitative) and detail of

information available, the amount of acceptable complexity in using a model and the accuracy required with reference to efficiency and ease-of-use, choice has to be made to select the most relevant type of propagation model to use.

3.13.1. ITU-R Recommendations

Using research inputs from around the globe, the ITU publishes its recommendations for different aspects of radio-communications. These recommendations are based on continued research and hence the recommendations keep being updated. Following is the discussion of the latest published versions of the appropriate ITU-R Recommendations.

3.13.1.1. ITU-R Recommendations P617, P452 & P526

ITU-R Recommendation P.617 [20] predicts the propagation loss for trans-horizon paths. It identifies diffraction and tropospheric scatter as main mechanisms of trans-horizon propagation. To predict the transmission loss, it deals with both these mechanisms separately.

For diffraction, P.617 recommends that for paths extending slightly beyond the horizon, ITU-R Recommendation P.526 [12] should be used to calculate transmission loss due to diffraction. The radio horizon distance is dependent on the value of the effective radius of the Earth, which depends on effective Earth radius factor ‘k’. The latter is dependent on refractivity lapse rate, which depends on weather variables of pressure, temperature and humidity. Certain combinations of these weather variables can enhance the radio horizon.

ITU-R Recommendation P.452 [21] also addresses the calculation of propagation by diffraction. This method is valid for all path types (land and sea, smooth and rough) since it uses a hybrid method based on the Deygout (principle edge) construction and an empirical correction. It assumes a series of diffraction edges of different heights. However, if all these edges are considered as zero height, the intervening terrain reduces to a 'smoothed' terrain.

Section 3 of P.617 deals with calculating transmission loss distribution for paths where tropospheric scatter mechanism is predominant. For troposcatter loss, Section 3.1 of the ITU-R Recommendation P.617 gives semi-analytical method to calculate average annual median transmission loss L(q) due to tropospheric scatter not exceeded for percentages of the time 'q' greater than 50%.

For non-exceedance time percentages less than 50%, P.617 recommends using ITU-R Recommendation P.452 [21]. ITU-R Recommendation P.452 is an interference prediction model. However, it includes a complementary set of propagation models, which ensure that the prediction accounts for all the significant propagation mechanisms through which interference signal can reach a wanted receiver. It includes the propagation mechanisms: line of sight, diffraction, tropospheric scatter and anomalous propagation (ducting, layer Reflection and refraction).

Transmission loss can be obtained from basic transmission loss by subtracting antenna gains. Hence, the transmission loss due to tropospheric scatter, not exceeded for p% of time (where p<50%) is given by:

$$L(p) = L_{bs} - G_t - G_r \quad \text{dB} \qquad (3.02)$$

Where:

L_{bs} is the transmission loss due to tropospheric scatter

G_t, G_r are the respective gains of the transmit/receive antennas

To obtain an overall distribution for troposcatter loss based on non-exceedance percentages of time from 0 to 100%, a combination of P.617 & P.452 is needed. Diffraction loss in light of relevant ITU-R Recommendations can be calculated using P.526 and also using P.452 (using sub-mechanism of diffraction only). However, the diffraction procedure of P.452 has limitations and work is ongoing to propose an improved method [62].

The overall prediction by P.452 considers all possible propagation mechanisms. It tries to identify the dominant mechanisms. It first calculates notional minimum transmission loss associated with line-of-sight propagation and over-sea sub-path diffraction, L_{minb0p}. Then it calculates the notional minimum transmission loss associated with line-of-sight propagation and trans-horizon signal enhancements L_{minbap}, then calculating notional basic transmission loss associated with diffraction and line-of-sight/trans-horizon signal enhancements (whichever is dominant), L_{bda}. It finally calculates

modified basic transmission loss L_{bam}, which takes diffraction and line-of-sight or ducting/layer-reflection enhancements into account. Basic transmission loss not exceeded for p% of time, $L_b(p)$, including effects of tropospheric scatter loss, L_{bs} and clutter losses is then calculated, given by Equation 3.03:

$$L_b = -5\log(10^{-0.2L_{bs}} + 10^{-0.2L_{bam}}) + A_{ht} + A_{hr} \text{ dB} \qquad (3.03)$$

Where:

A_{ht}, A_{hr} are the respective clutter losses due to transmitter/receiver shielding

This prediction is only valid for non-exceedance percentages less than 50%.

3.13.1.2. ITU-R Recommendation P.1546 [61]

This recommendation is used for point-to-area field strength predictions for the VHF and UHF tropospheric paths up to 1000km and antenna heights less than 3 kilometres. This recommendation provides field-strength value curves for 1 kW Effective Radiated Power (ERP) for 100, 600 and 2000 MHz exceeded for 50%, 10% and 1% of time, for land paths and cold and warm sea paths for temperate regions. Interpolation/Extrapolation of these curves is used to obtain field-strength values for any given required frequency and exceedance percentages and corrections for relevant climate are applied, based on the vertical atmospheric refractivity gradient data associated with Recommendation ITU-R P.453 [18]. The field strength versus distance curves and the associated tables are given for transmitting antenna height h1 values

of 10, 20, 37.5, 75, 150, 300, 600 and 1200 metres. Interpolation/extrapolation from the appropriate two curves is used for other values of h1. For sea paths, h1 is the height of the antenna above sea level while the curves give field-strength values for a receiving antenna with h2 equal to 10 metres. To allow for values of h2 different from the height represented by a curve a correction should be applied according to the environment of the receiving antenna.

This method is used when path profile data is not available. ITU-R Recommendation P.1812 [62] (which in principle is the same as ITU-R P.452 [21]) is preferred if profile information exists.

3.13.2. National Bureau of Standards Technical Note 101 [25]

Freeman [17] recommends and describes another method of prediction of propagation loss for trans-horizon paths, based on technical note 101 drafted by U.S. National Bureau of Standards [25]. This method identifies diffraction and tropospheric scatter as the main mechanisms achieving trans-horizon communication. It computes losses due to each of the mechanisms and then calculates combined value of basic long-term median transmission loss.

This model uses values of effective conductivity σ=5 S/m and effective relative permittivity ε=81 for seawater.

In order to determine a combined reference value for long-term median transmission loss for the path, it tries to identify the predominant mechanism based on the amount of loss. If the difference in losses from both mechanisms

is 15 dB or more, the one with lesser loss is chosen as the predominant mechanism.

However, if the values for L_{bsr} and L_{bd} are within 15 dB of each other, then it applies a correction as outlined in Freeman [17, Figure 5.24].

This method, however, does not directly provide values of loss exceeded for different percentages of time. Also, it does not use refractivity lapse rate of gradient but surface refractivity in its calculations. While high correlation has been observed between surface refractivity and signal level in temperate climates [16, 50, 55, 80], it may not hold true for other climates.

3.13.3. Experimental comparison with prediction models

The study by Gunashekar [50] has used ITU-R P.526 to predict the received signal strength. The statistics for signal levels exceeded for 99%, 90%, 50%, 10% and 1% of time were compiled. Equal importance was given to each season (more weight per datum to seasons with lesser number of recordings). The received signal levels were, in a later study, compared to the signal levels predicted by ITU-R P.1546 [61].

Sim compared the measurements with the results simulated using ITU-R P.526. This comparison suggested that the dominating propagation mechanism for Jersey-Guernsey path during calm sea days is diffraction [11].

Rudd studied short-term interference due to tropospheric signal enhancements on over-sea propagation in the English Channel and the North Sea [51]. He compared his measurement results to the ITU-R propagation models given in its recommendations P.1546 [61] & P.1812 [62], in order to examine the empirical basis of these models. Rudd observed that P.1546 was based on earlier ITU-R Recommendation P.370 [120], which was purely statistical, while P.1812 was based on P.452, which was semi-physical. While it was observed that the more complex algorithms of P.452/P.1812 agreed well with the curve-based predictions of P.370/P.1546, it was concluded that P.1812 provided a better match to measurements.

Investigation into path loss statistics and mechanisms of trans-horizon propagation on over-sea path by Shen and Vilar [56] observed that the path loss distributions of each of the mechanisms were lognormal.

Longley et al [59] presented long-term distributions of hourly-median values of transmission loss for a large number of paths from around the globe, ranging in length from 10 to 1000 km. The measured data was compared to predictions using TN101 [25] and by a modification [66] of a computer method described by Longley and Rice [65]. For paths with both transmitter and receiver horizons on the sea, a maritime temperate climate over the sea is assumed. Two paths are of particular interest, Chillerton to Alderney (121 km) and Stockland Hill to Alderney (137 km). Measurements made in 1961 and 1962 at frequencies around 200 MHz on these paths were used for analysis.

A comparison of measured results (columns 2 to 6 in Table 3-4) with prediction (columns 7 and 8 in Table 3-4) indicates that the modified version of Longley-Rice Model provides a closer prediction of the basic median transmission loss (value not exceeded for 50% of time) than TN101.

Path	**Percentage of time for which measured basic transmission loss is not exceeded (%)**					**TN101: Reference value - Basic transmission loss (dB)**	**Modified Longley-Rice: Reference value - Basic transmission loss (dB)**
	1	10	50	90	99		
Chillerton-Alderney	122.2	129.4	137.6	143.6	150.7	132.7	135.6
Stockland Hill-Alderney	136.6	144.0	147.9	150.8	155.2	140.0	145.4

Table 3-4: Comparison of measured & predicted values of transmission loss [59]

Measurements by Tawfik and Vilar [100] on 2 trans-horizon radio links, around 150 km along, operating at 10/11 GHz, were compared to five different propagation models available at that time: (1) NBS Technical Note 101 [25], (2) CCIR [101], (3) Yeh's method [102], (4) Norton's method modified by Rider [103] and (5) the French Administration method [104]. The differences between the median values of path loss measured and those predicted by the afore-mentioned propagation models indicated that the NBS method gave the best prediction, giving minimum values of mean error and standard deviation.

3.14. Interim Conclusions

Previous studies indicate that troposcatter and diffraction are the two normal propagation mechanisms on trans-horizon paths. Some studies on over-sea paths in south of UK and North Sea have observed evaporation ducts to be present almost all the time, though not becoming a dominant mechanism. Ducting as well as reflection/refraction through troposphere has been observed to exist for lesser percentages of time.

Most of the refractivity studies have used indirect measurements of refractivity (through meteorological variables), based on radiosonde measurements. The annual mean surface refractivity for the Channel Islands is ~330 N-units, while annual mean refractive index lapse rate in lowest 1 km is ~-43 N-units. The median refractivity gradient in the lowest 100m and 65m of the troposphere is ~-70 and ~-50 N-units/km respectively.

An over-water path study in the English Channels has identified evaporation ducting as a near-permanent phenomenon, existing for more than 90% of the time, in addition to the normal mechanisms of troposcatter or diffraction. The mean evaporation duct height in the Channel Islands, as determined by Gunashekar [50], is 8.3m.

Enhancements in received signals have been noticed on trans-horizon paths, particularly during summers in late afternoons and evenings. It has been observed that while ducting and anti-cyclonic conditions correlate well with

signal enhancements, the presence of ducting and/or anti-cyclonic conditions does not guarantee enhanced signal reception. Enhancement events lasting 4 hours or more have been observed over the English Channel, linked to slow-moving physical mechanisms. It has been observed that enhancements due to ducting are prominent in summer, those due to high k-factor diffraction exist throughout the year while layer-reflection/refraction based enhancements were not observed during autumn. Higher signal enhancements have been generally observed for higher frequencies.

Surface-based ducts have been observed in the Channel Islands region between heights of 84m and 102m while elevated duct at height around 1km above Bournemouth has also been observed.

Previous studies show that on longer trans-horizon paths, short-term fading follows Rayleigh distribution while long-term fading follows lognormal distribution.

Correlations have been observed between surface refractivity and refractive index lapse rate in the English Channel and the North Sea. In these cases, high correlation between signal level and refractive index lapse rate was also observed. In areas where the tide has a strong influence on path characteristics, negative correlation between tide height and signal strength has been observed. Correlation has also been observed between signal level enhancements at receiving sites separated by up to 50km.

Comparison of signal strength studies on over-land and over-sea paths indicate greater enhancement on over-sea paths.

There are many different propagation models dealing with trans-horizon propagation as whole, as well as diffraction and troposcatter individually. Investigation into propagation models has been carried out from time to time. The available relevant propagation models for trans-horizon study are ITU-R Propagation Models P.452, P.526 & P.617, and NBS Technical Note 101.

4. DESIGN OF THE EXPERIMENT

4.1. Radio Sites

This research project is based in the south of UK, over the Channel Islands and the Isle of Portland. The transmitter is installed near Ronez Quarry in the northern part of the Island of Jersey. One receiver is installed on a small island Isl De Raz, which is part of Alderney. The other receiver is placed close to the Portland Bill Lighthouse in the south of UK. Further information regarding the radio sites and paths is listed in Table 4-1:

Site Name	Longitude	Latitude	Antenna Height -m AGL (AMSL)	
			UHF	VHF
Jersey St John's Quarry	02 09 09W	49 15 39N	3 (16.5)	3.85 (17.5)
Portland Lighthouse	02 27 23W	50 30 51N	3 (12.4)	4 (13.4)
Alderney (Isl De Raz)	02 10 03W	49 43 07N	3 (12)	4 (13)
Midpoint of Jersey-Portland Path	02 18 09W	49 53 15N	N/A	N/A
Midpoint of Jersey-Alderney Path	02 09 36W	49 29 23N	N/A	N/A

Table 4-1: Radio sites and parameters of the paths

4.2. Weather and Radiosonde Stations

Meteorological information from the weather stations as well as radiosonde stations within or close to the Channel Islands region has been used extensively in this study. Table 4-2 gives the information about the primary weather stations:

Station	Source	Lat (°N)	Long (°W)	Height AMSL (m)	Distance & Bearing to nearest radio site	Distance & respective bearing to nearest sea
Portland	NNDC	50.517	2.45	52	0.5 km, SW	N/A
Alderney Airport	NNDC	49.717	2.2	89	2.4 km, E	0.5 km, NE
Jersey Airport	UKMO	49.208	2.196	84	6.7 km, NE	2 km, W
Guernsey Airport	NNDC	49.433	2.6	102	38 km, SE	1.5 km, S
CLV	BODC	49.9	2.9	5,14	55 km	N/A

Table 4-2: Primary weather stations

In addition to the primary weather sources, meteorological data was obtained from secondary sources, as shown by Table 4-3. Weather data from secondary sources was used to limited extent.

Station	Station Information	Lat (°N)	Long (°W)	Height AMSL (m)
Alderney	EGJA (NOAA)	49 43	02 12	89
CLV	62103 (NDBC)	49.9	2.9	5,14
Guernsey	EGJB (NOAA)	49 26	02 36	102
Jersey	EGJJ (NOAA)	49 13	2 12	84
Portland	Isle (UK Met Office)	50.5221	2.45562	52
Pte De La Hague	France (NNDC)	49.717	1.933	12
St. Catherine's Point	Isle of Wight (NNDC)	50.583	1.3	24

Table 4-3: Secondary weather stations

The radio sites and the weather stations are closer to each other as compared to the radiosonde stations. Figure 4-1 shows the locations of the radio sites and the weather stations:

Figure 4-1: **Locations of radio sites and weather stations [39,40]**

There are five radiosonde stations around the Channel Islands (Table 4-4):

Radiosonde Station	Latitude (N)	Longitude (-W, +E)	Height AMSL (m)
Brest	48.45	-4.42	96
Camborne	50.22	-5.33	87
Larkhill	51.2	-1.82	132
Herstmonceux	50.88	0.32	52
Trappes	48.77	2.00	167

Table 4-4: Geographical information of radiosonde stations

Further details about the proximity of these radiosonde stations to the radio sites and coast, are given by Table 4-5:

Radiosonde Station	Nearest Radio Site	Distance from Radio Site (km)	Bearing from Radio Site	Distance from coast
Camborne	Portland	210 km	West	2.25 km
Herstmonceux	Portland	200 km	East	7.5 km
Brest	Jersey	190 km	South West	20 km
Larkhill	Portland	85 km	North East	54 km
Trappes	Jersey	310 km	South East	145 km

Table 4-5: Distance parameters of radiosonde stations

Figure 4-2 shows the locations of the radiosonde stations with respect to the radio sites:

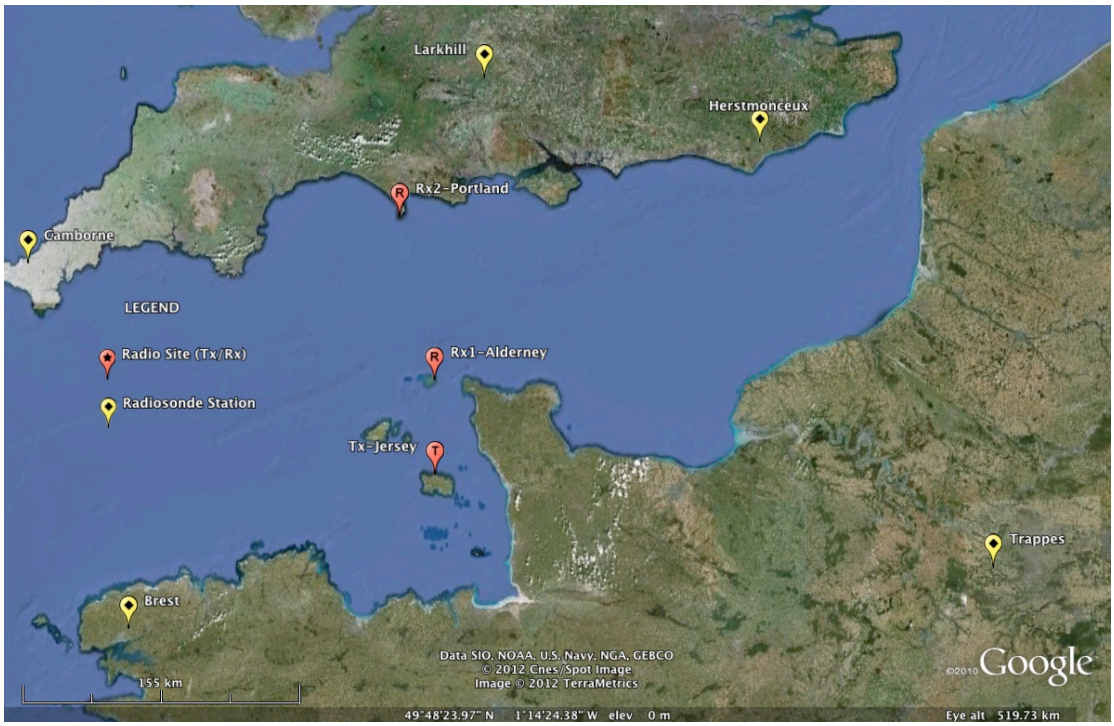

Figure 4-2: **Locations of radio sites and radiosonde stations [40]**

4.3. Radio Links – Paths and Frequencies

Two radio paths are under investigation-Jersey to Portland (140 km) and Jersey to Alderney (50 km). The bearings from the Jersey transmitter towards the Portland and Alderney receivers are 351° and 359° respectively, both bearings calculated clockwise from the North. The two paths (Jersey-Portland and Jersey-Alderney) are almost co-linear and are unobstructed. The bearings (calculated from the North) from the Portland and Alderney receivers towards the Jersey transmitter are 171° and 179° respectively.

The project has utilised two distinct frequencies, 2015 MHz (UHF) and 240.225 MHz (VHF), with vertical polarisation. The receivers were switched

between high and low frequencies via two antenna ports at specific timings, coordinated by GPS-referenced computer control. These frequencies have been identified by the ITU-R Regulations for primary use of fixed and mobile services [121].

4.4. Test Equipment

The receiving equipment used was AR5000+3 high performance wide band receiver capable of receiving frequencies from 10 kHz up to 2600 MHz. It was powered by a 13.5V DC power supply. The analogue 'S-meter' at the front of the receiver indicated the strength of received signal [29]. It gave the AGC value, which was converted to a corresponding signal strength value (in dBm) by calibration tables. The receiver sensitivity at 12 dB SINAD for SSB/CW mode for 3 kHz filter is 0.3 μV. For 50-ohm typical impedance, this is almost equal to -117.5 dBm. Hence -117.5 dBm was taken as the threshold value for receiver.

In order to ensure a very high degree of stability and for timing synchronisation, the AR5000 was fed with an external 10 MHz reference signal from GPS. It was connected to the computer hardware by RS-232 interface [34], which allowed switching the receiver 'on' and 'off' and alternating between different receiving frequencies (i.e. 240.225 MHz & 2015 MHz).

The VHF antenna used was Jaybeam Type 7043, an 8-element Yagi antenna, designed for 244 MHz, with a theoretical gain of 12.15 dBi and -3 dB beam-width of 54° [30]. The UHF antenna was Jaybeam Type 7360, a shrouded Yagi antenna, with a measured gain of 14.5 dBi and -3 dB beam-width of 28° [31].

The GPS receivers and their respective antennas used were Meinberg GPS167PC and GPS170PCI [32-33].

The transmitter for the 240 MHz signal was the NovaSource RF signal Source G6, whose typical output power was +8dBm and had minimum value of +5dBm [35]. The measured output power was +12.7dBm. The transmitter for 2 GHz signal was the NovaSource M2 RF signal Source, with a typical value of +10dBm and minimum value of +8dBm [37]. The measured output power was +9.3dBm. The radios were programmed to transmit at the specified test frequencies [36, 38], using 10 MHz reference signal from GPS for stability and accuracy.

Power amplifiers for both UHF and VHF signals were used. The UHF (2 GHz) amplifier takes a nominal input of +5dBm and maximum input of +10dBm. The nominal power output is 20dBW (100W) [47]. The tested value of net power output from the amplifier was 74 Watts going into feeder leading to the antenna.

The VHF amplifier allows a maximum input of +1dBm with a nominal output power 14dBW (25W) [46]. The constraint on the input level resulted in the use of attenuators between the VHF source and the VHF amplifier. The tested value of the net power output from the amplifier was 14 Watts going into feeder leading to antenna.

The feeder cable used for VHF & UHF was Westflex 103, which is a low loss 50-ohm coaxial cable. The cabling losses, interpolated and extrapolated for relevant frequencies and actual lengths used (approx. 20m at all sites), were 1.15 dB for VHF and 4.5 dB for UHF. The connector losses can be ignored since connectors were also present when the receivers were calibrated.

Efforts were made to align the transmitting antennas midway between the two receiver sites, creating an offset of approximately 4°. This had no effect on the VHF antenna, which has a much wider beam-width and offers approximately same gain at 4° offset from main beam. For the UHF antenna, it was observed from the manufacturer's antenna radiation patterns that this antenna orientation results in a further loss of approximately 0.5 dB.

The transmitter and receivers were connected to computer hardware based on QNX platform, which is a real-time operating system.

The antenna masts support GPS antenna, VHF Yagi antenna and UHF shrouded Yagi antenna. VHF antenna is approximately 1 metre higher than UHF antenna.

Portland and Jersey had mains power supply available. Alderney, being a remote site, had no supply available from mains. Power supply arrangements to operate the equipment at Alderney were based on solar panels and wind generator, which charged the 12 Volt batteries that provided DC power supply to the computer hardware and the receiver. The wind generator used was FM1803-2 [41].

The recorded data present on the hard disks at the receiving sites was accessed through dial-up while the transmitter was operating continuously.

4.5. Schematic and Link Budget of the Experimental Arrangement

A preliminary link budget of the links was performed using the historic median values of weather variables and the actual site and link parameters as inputs to the software 'SRTM Path Profile' [122], to estimate the median value of path loss on both paths and frequencies. The results indicated that without further amplification of signals to be received at Portland, the expected signal levels would be below the threshold level of the receiver.

In view of the above, the received signals at Portland were pre-amplified before feeding to the receiver. For the 2 GHz signal, two 'Mini-Circuits ZX60-242LN-S+' co-axial low noise amplifiers were cascaded. They take maximum input signal of +10dBm. The typical gain value for the 2 GHz signal was approximately 13dB, typical output being +16dBm [70]. For the 240 MHz signal, 'Mini-Circuits ZX-60-33LN-S+' co-axial low noise amplifier was used. It

takes a maximum input signal of +13dBm. The typical gain value for 240 MHz signal was approximately 21.75dB, typical output being +17.5dBm [71].

Figure 4-3 shows the schematic for the link components at the transmitter and receivers:

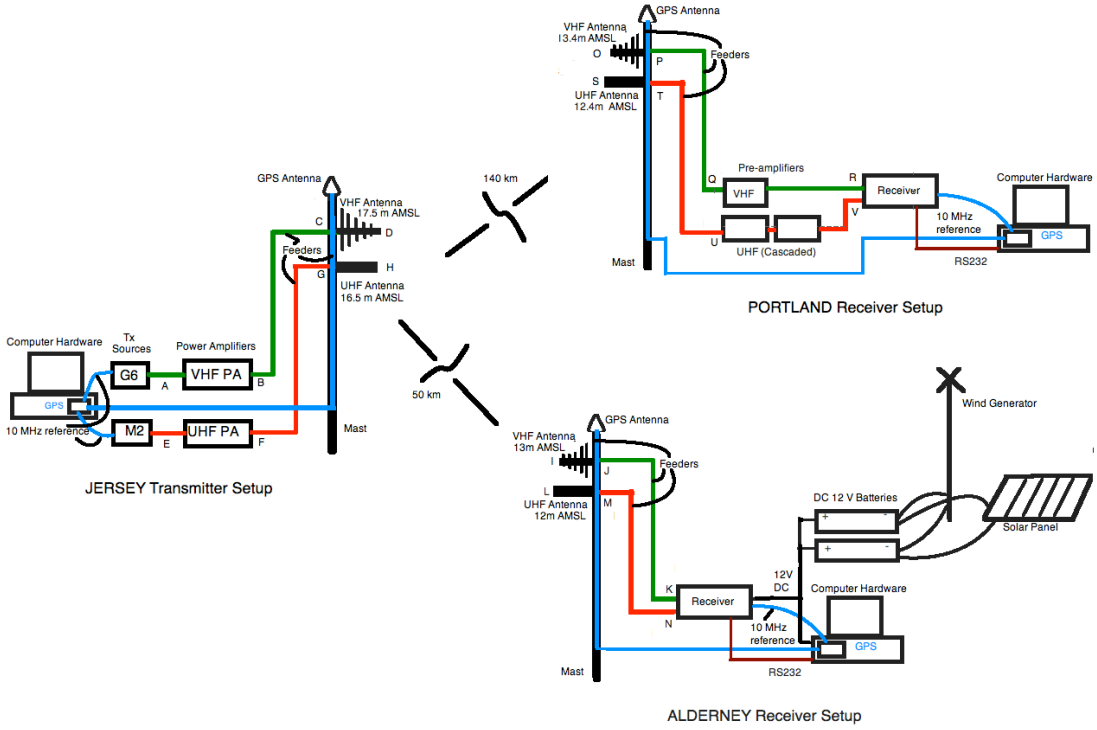

Figure 4-3: **Schematic of the experimental arrangement in the Channel Islands**

The link budget equations, with respect to different points (A through to V) on Figure 4-3, are given below:

For the VHF signal at Jersey,

P_D (dBm) = P_C (dBm) +12.15 dBi (VHF antenna gain) (4.01a)

P_C (dBm) = P_B (dBm) -1.15 dB (Feeder cable loss) (4.01b)

P_B (dBm) = P_A (dBm) + 28.8 dB (VHF amplifier gain) (4.01c)

P_A = 12.7 dBm (4.01d)

For the UHF signal at Jersey,

P_H (dBm) = P_G (dBm) +14 dBi (UHF antenna gain) (4.02a)

P_G (dBm) = P_F (dBm) -4.5 dB (Feeder cable loss) (4.02b)

P_F (dBm) = P_E (dBm) + 39.4 dB (UHF amplifier gain) (4.02c)

P_E = 9.3 dBm (4.02d)

For the VHF signal received at Portland,

$P_R=P_Q$+ 24 dB (VHF pre-amplifier gain) (4.03a)

$P_Q=P_P$-1.15 dB (Feeder cable loss) (4.03b)

$P_P=P_O$+12.15 dBi (VHF antenna gain) (4.03c)

For the UHF signal received at Portland,

$P_V=P_U$+ 21.5 dB (UHF pre-amplifier gain) (4.04a)

$P_U=P_T$-4.5 dB (Feeder cable loss) (4.04b)

$P_T=P_S$+14.5 dBi (UHF antenna gain) (4.04c)

For the VHF signal received at Alderney,

$P_K=P_J$-1.15 dB (Feeder cable loss) (4.05a)

$P_J=P_I$+12.15 dBi (VHF antenna gain) (4.05b)

For the UHF signal received at Alderney,

$P_N=P_M$-4.5 dB (Feeder cable loss) (4.06a)

$P_M=P_L$+14.5 dBi (UHF antenna gain) (4.06b)

Combining and substituting the equations above, the equations for the power levels received at both sides are:

For VHF signal at Portland,

P_{RX1V} (dBm) = 12.7 + 28.8 – 1.15 + 12.15 – P_{L1V} (dB) + 12.15 – 1.15 + 24

P_{RX1V} (dBm) = 87.5 – P_{L1V} (dB) (4.07)

Where:

P_{L1V} is the path loss experienced by the VHF signal from Jersey to Portland

For UHF signal at Portland,

P_{RX1U} (dBm) = 9.3 + 39.4 – 4.5 + 14 – P_{L1U} (dB) + 14.5 – 4.5 + 21.5

P_{RX1U} (dBm) = 89.7 – P_{L1U} (dB) (4.08)

Where:

P_{L1U} is the path loss experienced by the UHF signal from Jersey to Portland

For VHF signal at Alderney,

P_{RX2V} (dBm) = 12.7 + 28.8 – 1.15 + 12.15 – P_{L2V} (dB) + 12.15 – 1.15

P_{RX2V} (dBm) = 63.5 – P_{L2V} (dB) (4.09)

Where:

P_{L2V} is the path loss experienced by the UHF signal from Jersey to Alderney

For UHF signal at Alderney,

P_{RX2U} (dBm) = 9.3 + 39.4 – 4.5 + 14 – P_{L2U} (dB) + 14.5 – 4.5

P_{RX2U} (dBm) = 68.2 – P_{L2U} (dB) (4.10)

Where:

P_{L2U} is the path loss experienced by the UHF signal from Jersey to Alderney

4.6. Calibration

This calibration was done using IFR 2023B signal generator [123] available locally at the University of Leicester, by setting it up to the appropriate frequency and feeding into the relevant antenna terminal of the receiver. The receiver was fed with 10 MHz reference signal from the function generator.

The receivers placed at Alderney and Portland were calibrated on the sites. The receiver at Portland was first calibrated without the pre-amplifiers and then re-calibrated with the pre-amplifiers. It was observed that the pre-amplifiers introduced variations at low signal strength levels. To calibrate the receiver for these low signal levels, the median of 10 values was used as the representative value, in line with the standard practice [124].

Figures 4-4 to 4-7 show the calibration points and fitted curves using third order polynomials, the x-axis showing the signal level causing respective ‘Automatic Gain Control’ (AGC) value shown on y-axis:

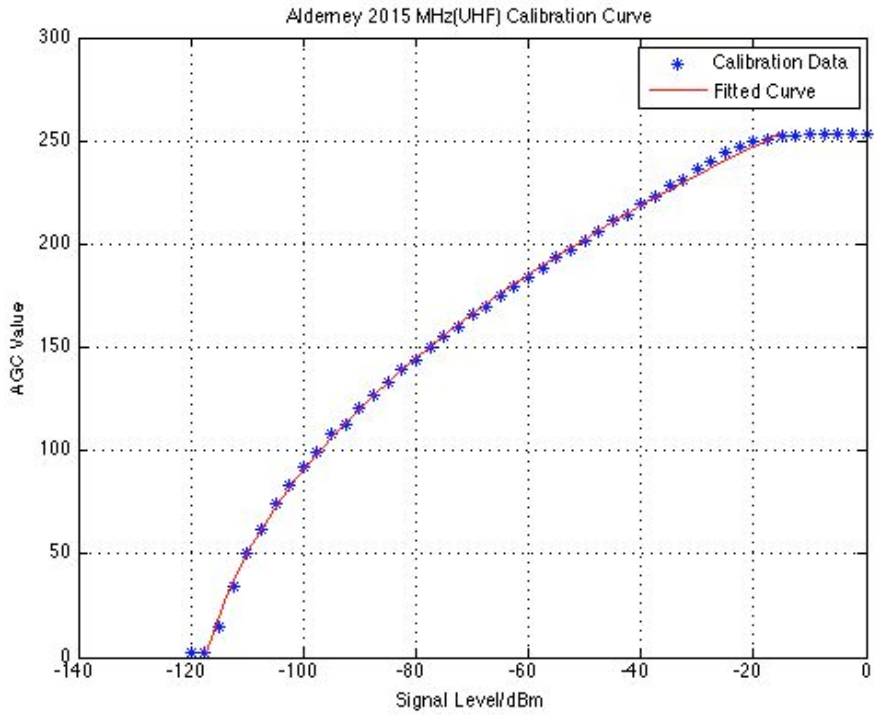

Figure 4-4: **Alderney calibration – 2 GHz (UHF)**

Based on the fitted calibration curve, the approximate limits of detectable UHF signal level (unmodulated) for Alderney are -117 dBm (lower limit) and -16 dBm (upper limit). This means that any signal values less than -117 dBm or greater than -16 dBm would be effectively interpreted as -117 dBm and -16 dBm respectively. There are 1.48% cases when signal level is less than -117 dBm while there are 0.002% cases when signal level exceeds -16 dBm.

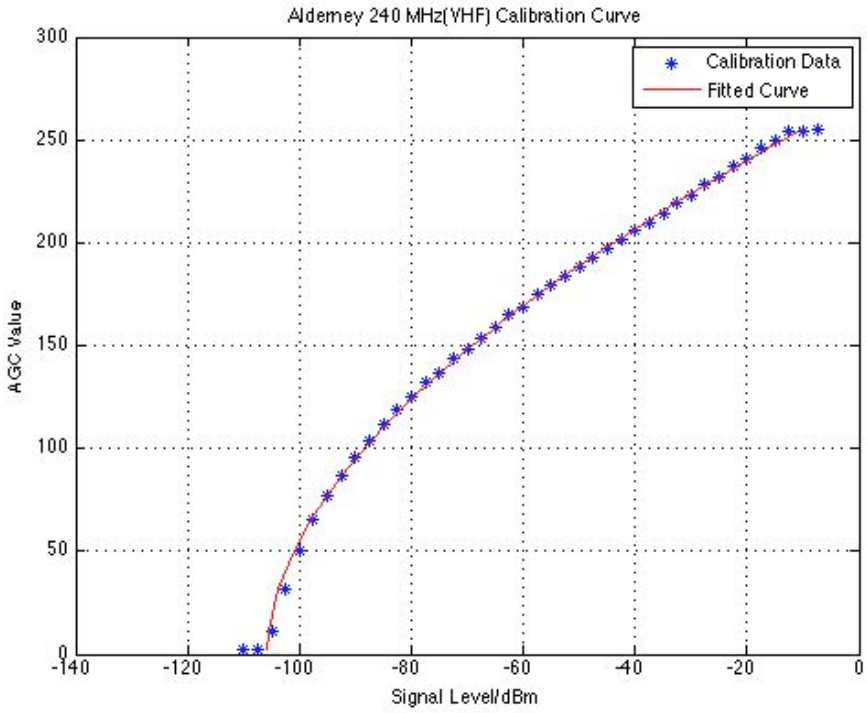

Figure 4-5: **Alderney calibration – 240 MHz (VHF)**

Based on the figure above, the limits of detectable VHF signal level limits for Alderney are -105.85 dBm (lower limit from the calibration curve) and -11 dBm (upper limit). Any signal values less than -105.85 dBm or greater than -11 dBm are interpreted as -105.85 dBm and -11 dBm respectively. There are 1.43% cases when signal level is less than -105.85 dBm while there is only one instance when the signal level is greater than -11 dBm.

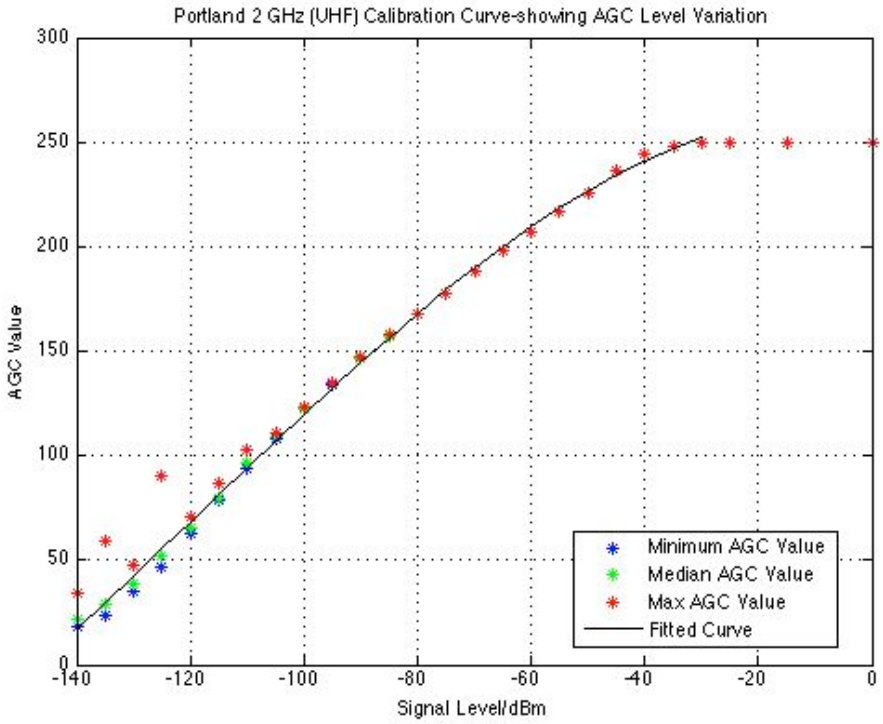

Figure 4-6: **Portland calibration with preamplifier showing AGC variation– 2 GHz (UHF)**

The interpretation of calibration curves from Portland is not like that of Alderney due to the use of pre-amplifiers at Portland. The minimum, maximum and median from the 10 AGC values corresponding to particular signal strength are shown on Figure 4-6. It can be observed that for signal strength values less than -120 dBm, there is evident variation in the corresponding set of 10 AGC values. This brings in a certain degree of uncertainty when it comes to choosing the corresponding value of signal level for a certain AGC value, as the same signal level can give different AGC values. The median of 10 values is used as representative value of AGC for corresponding signal level. This uncertainty has been addressed in greater detail later on, as shown by Figures 4-8 to 4-11 and Appendices A to D.

Also, as depicted in Figure 4-6, the curve with pre-amplifier in place does not go close to '0' AGC level because the lowest output power limit of function generator used for calibration was attained at that point.

Extrapolation is used for signal levels below -140 dBm. Hence, the limits of detectable UHF signal level for Portland are -149 dBm (lower limit from extrapolation of the calibration curve) and -33.5 dBm (upper limit). This means that signal level values less than -149 dBm or greater than -33.5 dBm are interpreted as -149 dBm and -33.5 dBm respectively. 2.15% of values are less than -149 dBm while 0.3% are greater than -33.5 dBm.

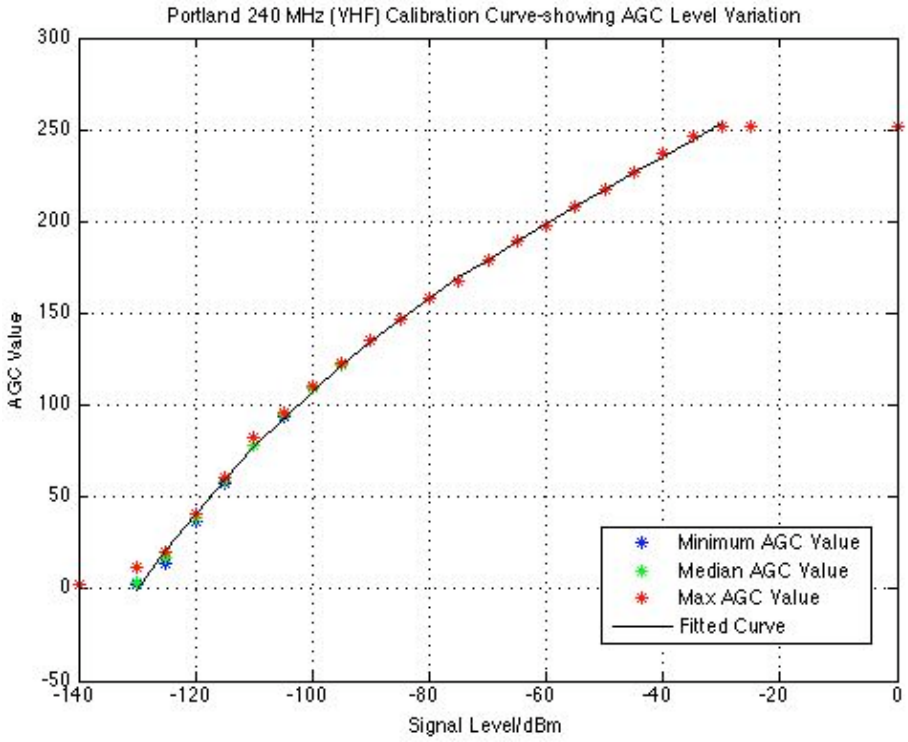

Figure 4-7: **Portland calibration with preamplifier showing AGC variation– 240 MHz (VHF)**

Based on Figure 4-7, the variation in AGC values for particular signal strength is considerably less than that with UHF signal. The variation is within

reasonable bounds and median AGC values can be used to represent signal strength levels. The limits of detectable VHF signal level limits for Portland are -133.5 dBm (lower limit from the calibration curve) and -30 dBm (upper limit). Any signal values less than -133.5 dBm or greater than -30 dBm are interpreted as -133.5 dBm and -30 dBm respectively. 3.2% of values are less than -133.5 dBm while 0.0001% values are greater than -30 dBm.

Due to the variations at low signal strength levels, the calibrations were later on repeated in greater detail, using 100 values for a particular signal level and the median of these 100 values used as the representative value for that signal level. The error analysis for low signal levels is summarised by Figures 4-8 to 4-11, which show the minimum, maximum, median and quartile AGC value for particular signal strength levels. Further statistics of possible errors that might arise due to the calibration of the receivers are presented in Appendices A to D.

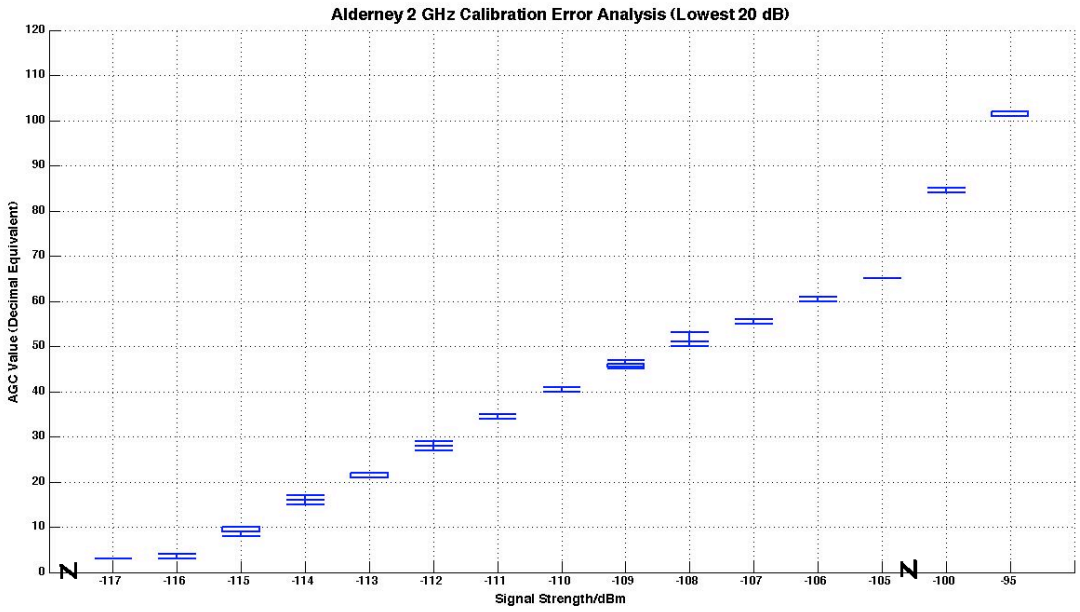

Figure 4-8: **Alderney calibration error analysis - 2 GHz (UHF)**

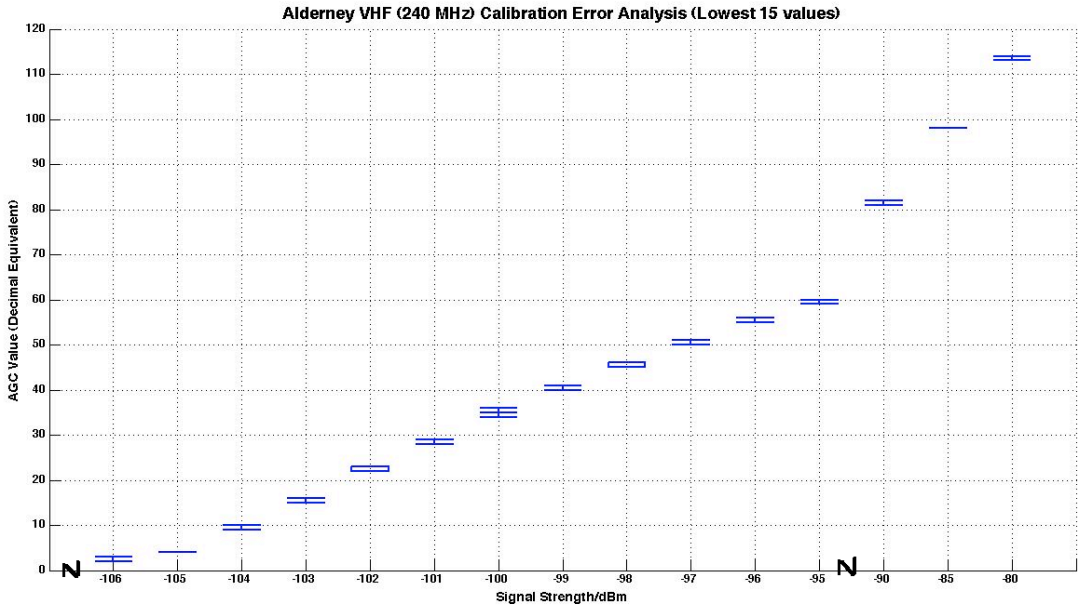

Figure 4-9: **Alderney calibration error analysis – 240 MHz (VHF)**

For both the UHF and VHF signals at Alderney, the variation within the 100 AGC values for a particular signal strength level is small. Also, there is a clear difference between the AGC values corresponding different signal strength levels.

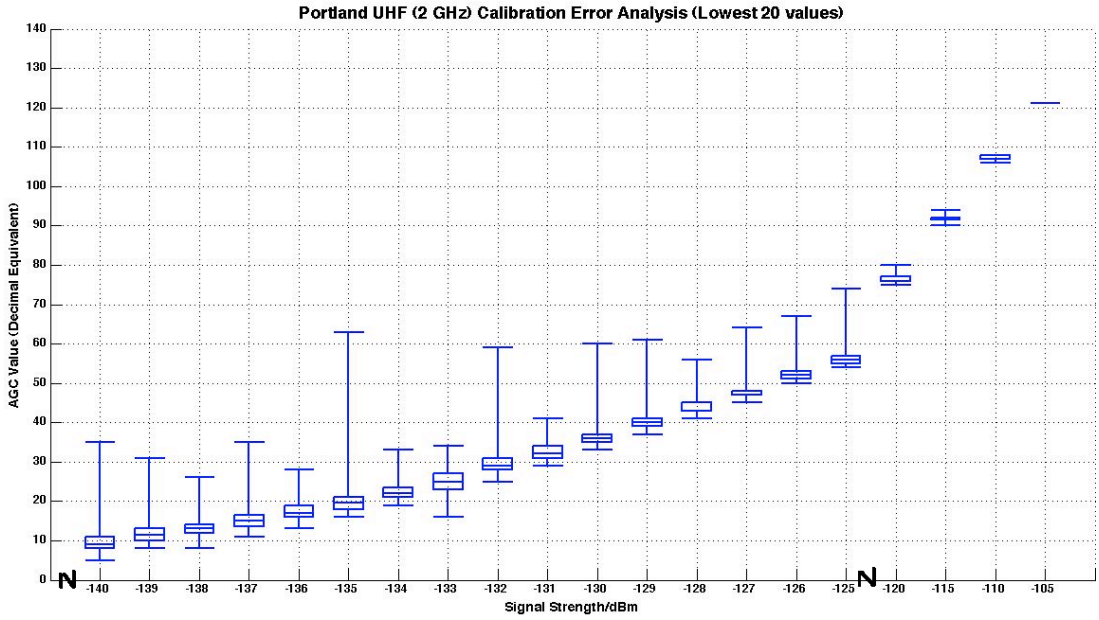

Figure 4-10: **Portland calibration error analysis – 2 GHz (UHF)**

Figure 4-10 for the calibration of UHF signal at Portland, with pre-amplifiers in place, shows considerable variation within the 100 AGC values for a particular signal strength level. This variation tends to decrease as the signal strength level increases. However, the median and quartile values (as well as the 5th, 10th, 90th and 95th percentile values in Appendix C) indicate that most of the AGC values are near the minimum of the 100-value dataset and that the median of these 100 values can be taken as a suitable representative of the 100-value dataset. The worst-case variation, i.e. the maximum value from amongst the 100-value dataset, in all cases does not exceed signal strength value of -120 dBm. This value is below the range of values considered as 'threshold' to decide between normal and anomalous propagation [See Chapter 6], at least by 12 dB.

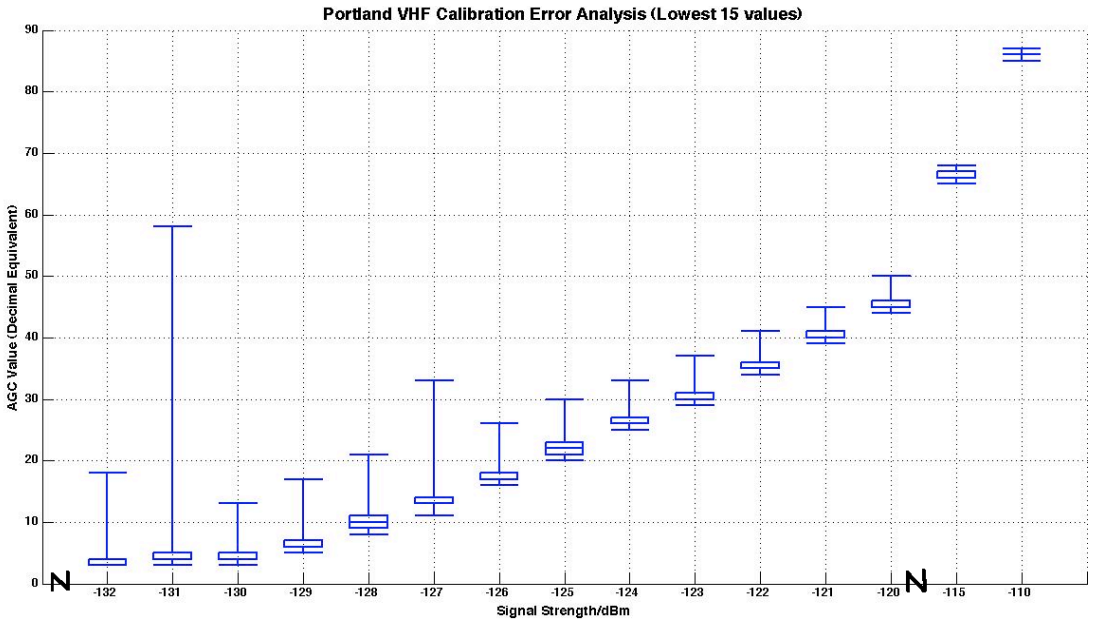

Figure 4-11: **Portland calibration error analysis – 240 MHz (VHF)**

The calibration error analysis for VHF signal at Portland follows a similar trend to that for UHF signal at Portland. Similar conclusions can be drawn from

Figure 4-11, with the worst-case variation below -115 dBm, which is at least 13 dB lower than the range of values considered as threshold to decide between normal and anomalous propagation.

Hence, despite the variations in AGC values at low signal strength levels, there is no evident impact on the detection and treatment of anomalous propagation at either of the receiving sites. The variation in AGC values gets smaller with increasing signal levels and becomes more predictable. However, these variations suggest that there are different confidence intervals attached to AGC values corresponding to a particular signal strength value. Appendices A to D help determine these intervals.

In addition, it was observed that the median values from the 10-value dataset and 100-value dataset were either the same or within 1 value of each other for 100% of the cases.

4.7. Meteorological Data from Weather Stations

Hitney et al observed that meteorological measurements with a vertical resolution of less than 10m would help in refractivity based propagation assessment [73]. As mentioned earlier in Chapter 2, refractivity can be measured directly by using a refractometer or indirectly through measurement of weather variables. The best way to measure refractivity is by using a refractometer, which is based on the principle of total-internal reflection.

However, Levy et al observed that refractometers are delicate and hard to calibrate [52].

The complexity and high price associated with refractometers makes the radiosonde the most frequently used instrument for measuring refractivity (indirectly). LIDAR (Light Detection & Ranging) measurements have opened alternative means of measuring weather variables. LIDAR is an optical remote sensing technology, using a similar principle as RADAR but using light instead of radio signal. However, the expense of equipment prohibits its widespread use [64]. Previous studies on refractivity have used measurements of weather variables made using radiosondes. In addition, an extensive global radiosonde network is in place.

Levy et al further observe that the main difficulty in indirect measurements of refractivity lies in the accurate measurement of sharp humidity gradients [52]. Due to this reason, refractivity studies based on indirect measurements of weather variables by radiosondes could have a slight degree of inaccuracy, as observed by various studies [42, 73, 74]. The Met Office uses radiosondes that measure atmospheric pressure, temperature and humidity through capacitive sensors. The accuracy of these sensors is within reasonable limits [115]. Radiosondes, going up through atmosphere at approx 5 m/s, do not usually measure wind speed and direction directly but these values are calculated by other techniques [116].

The radiosonde readings by the Met Office could not be taken at precise heights in every ascent, due to wind conditions as well as limitations of Doppler radar estimating the height. However, starting from station height, efforts were made to take readings around 200m, 850m, 1550m and further up. Usually, there were 2 daily ascents, near mid-night and mid-day (except Larkhill). Also, sometimes the height intervals between radiosonde readings can miss any important features within the interval. For the lowest 100m of the atmosphere, these potential deficiencies can be overcome to some extent by using weather data from neighbouring weather stations, which are at different heights above mean sea level up to a maximum of 102m and are recording weather at hourly intervals throughout the day. Also, the data is monitored for quality and accuracy.

Meteorological information were obtained from a number of weather stations around the Channel Islands, for the duration of the experiment. Sea level meteorological data was obtained from the Channel Lightship (aka CLV), a lightship (owned and maintained by the UK Met Office) anchored in the English Channel to the northwest of all three radio paths. The distance of the CLV to the midpoint of the Jersey-Alderney link is approximately 70 km. The nominal height at which observations were made at this station is 5.0m above mean sea level for most of the weather variables and at 14.0m AMSL for wind. Higher altitude weather data were also obtained from weather stations in Portland, and those at Jersey, Alderney and Guernsey Airports with heights of 52.0, 84.0, 89.0, and 102.0 metres AMSL respectively.

Over the period of one year of investigation (i.e., July 2009 to June 2010), the median values of weather variables recorded hourly are shown in Table 4-6:

Station	Median Value of Meteorological Variable				
	Pressure (hPa)	Temperature (°C)	Dewpoint (°C)	Relative Humidity (%)	Wind Speed (m/s)
CLV	1015.8	11.7	9.10	84.3	8.23
Portland	1009.6	11.1	8.33	85.8	6.26
Jersey	1006.3	11.6	8.30	81.1	5.66
Alderney	1005.4	12.0	9.00	81.8	5.81
Guernsey	1004.3	11.1	8.89	86.2	4.92

Table 4-6: Channel Islands - annual median values of weather variables

4.8. Tidal Data

In addition to weather variable information, information regarding tidal variations over the Channel Islands was also obtained. The sources include the original recorded tidal data at Jersey and Weymouth, obtained from the BODC and the predicted tidal information from the BBC for Portland, Jersey and Alderney. The tidal variation in the Channel Islands is large and the effect of the tide on the path link budget calculations was accounted for by considering the tidal height variations in the effective antenna heights.

4.9. Climatology of the Channel Islands

The following information is taken from Gunashekar [50], who obtained it directly from Mr Tim Lillington, Senior Meteorological Officer, Guernsey Airport Met Office (Personal Communication, 07 May 2006):

The Channel Islands have a very definite maritime climate, with only occasional continental influence. This maritime climate ensures that there is a smaller range of temperature, on both a daily and annual basis, when compared to places inland. It also slows the warming process during spring and the cooling process during the autumn.

The highest temperatures recorded are only a few degrees below those reached in mainland Britain, with 35°C being reached at sites in both Jersey and Guernsey. Alderney has a recorded maximum of 31.1°C on the 9th Aug 2003. The lowest temperatures are considerably higher than those for mainland Britain, with –9°C the lowest for Guernsey and Alderney and -11°C for Jersey.

Rainfall generally has a peak during the late autumn and winter, when the sea temperature is at its highest in relation to the air temperature. The summer tends to be the driest period, although over time the driest month has varied, but July has been one of the driest on a consistent basis.

Sunshine is, on the whole, higher than mainland Britain. This is especially noticeable in figures from spring through to early autumn, but not so obvious during the winter. The excess of summer sunshine was very much in evidence in August 2005, with up to 330hrs being recorded in the Channel Islands, which is at least 100hrs more than large parts of the UK away from SW England.

The prevailing wind is from between west and south-west, with a secondary peak from the north-east. During the summer the westerly wind is dominant with the peak for this occurring in July, which is also the month when south-east winds are at their rarest. North-east winds are dominant in April and May, while for late autumn and much of the winter south-west to south winds prevail. February is the month with the most even distribution of wind direction on average, although this hides the fact that winds can be from the east for almost the whole month, as in 1986, or the complete lack of north-east winds as in 1990.

Fog has a different annual distribution when compared to inland areas of the British Isles. The summer months and July in particular, have the highest incidence of fog, with the autumn being the least foggy season. We have, on occasion, had no fog during the autumn. A secondary peak in fog occurs during March, before the north-east wind becomes dominant. Often we have hill fog, or upslope fog, so the Airport has a much higher incidence of fog than coastal areas. Sea fog is almost non-existent in autumn and winter, increasing in frequency through late spring and early summer. We also, on occasions during the late autumn and winter, have fog advected to us from France on a south-east breeze.

Due to the proximity of the sea, the wind direction and not just air mass is important for determining our day-to-day weather. A hot air mass, as existed in early August 2003, produced 35°C with an easterly breeze on the 5th but only 19°C on the 6th with a westerly wind bringing in sea fog. In the winter the

air mass is more important, but winds from the east, with the shortest sea-track, bring the lowest temperatures.

During the late autumn and winter there is little variation in wind velocity between day and night. Spring and summer, on the other hand, have the expected peak of wind speed during the daytime and lighter winds overnight. While the speed follows the expected pattern, the wind direction does not. The wind is supposed to veer during the day as its speed increases, but we often have the wind backing with the rising speed. This tends to occur when the gradient wind is south-east. A light south-east wind at dawn is followed through the morning by a backing to the east by midday and north-east during the afternoon. It would appear that heating over France is responsible for this, with pressure falling more during the day inland than it does over the cool waters of the English Channel. This often has the effect of reversing the temperature rise expected through the early afternoon.

Sea breezes do occur regularly, although their effect can sometimes be suppressed by the influence from France. After a calm and clear night a wind following the general pressure pattern might develop. As the temperature rises the wind will start to blow onshore. At Guernsey Airport the wind often becomes variable in direction, with sea breezes coming in from different parts of the coast. The effect on the weather can be to make areas away from the coast several degrees warmer, sometimes with fog on the coast, but not inland. The most common aspect, however, is for cumulus cloud to form over the middle of the larger islands, while the smaller islands have little or no cloud.

5. RECEIVED SIGNAL STRENGTH RESULTS

This chapter deals mainly with the received signal strength data obtained during the measurement campaign. As mentioned earlier, receivers at Alderney and Portland recorded the signal strength.

5.1. Introduction

The collection of signal data started in July 2009 and was concluded in March 2011. However, data from only one year, i.e. from July 2009 until June 2010 inclusive, has been considered for the investigations that form part of this study.

The receiving system in Isl de Raz (Alderney) was operated using solar and wind-generated power. Data from the Alderney receiving site was disrupted a number of times due to wind generator failure and recurrent PC-hardware problems. As a result, data was missing during March and April 2010 while data during the period of November 2009 until February 2010 was sparse. Although the signal strength data was recorded beyond June 2010 (including the period of November 2010 to February 2011), it was observed that this data too was sparse and so could not be used in place of missing data from November 2009 to February 2010. For Portland, the data collection was generally un-interrupted and hence data for most of the year was available. The periods of missing data are considered in more detail in Section 5.7.

5.2. Signal Strength Data Types

'High-resolution data' refers to the actual raw data received and recorded. To gather this data, each receiver was recording for a 2-second period four times in a minute for each frequency, collecting 25 values during this 2-second period. This makes 100 UHF and VHF values each in a minute, translating into 6000 UHF values and 6000 VHF values recorded in an hour.

'Median data' refers to the processed data extracted from the high-resolution data, by taking the median of each set of 25 values recorded over a 2-second period. This effectively means 4 values per minute per frequency, corresponding to 240 values per hour.

'Hourly median data' refers to processed data extracted from high-resolution data, by taking median of the 6000 values recorded in one hour for each frequency.

5.3. Sample Signal Strength Data

Figure 5-1 shows a sample of raw signal levels received at both sites on 27 May 2009. This particular example shows periods of both normal signal reception and enhanced signal strength (ESS) reception. Figure 5-2 shows the predicted and/or measured tidal variation at all the three sites (Jersey, Alderney and Portland). The time axis on these and subsequent figures shows the Universal Time (UT):

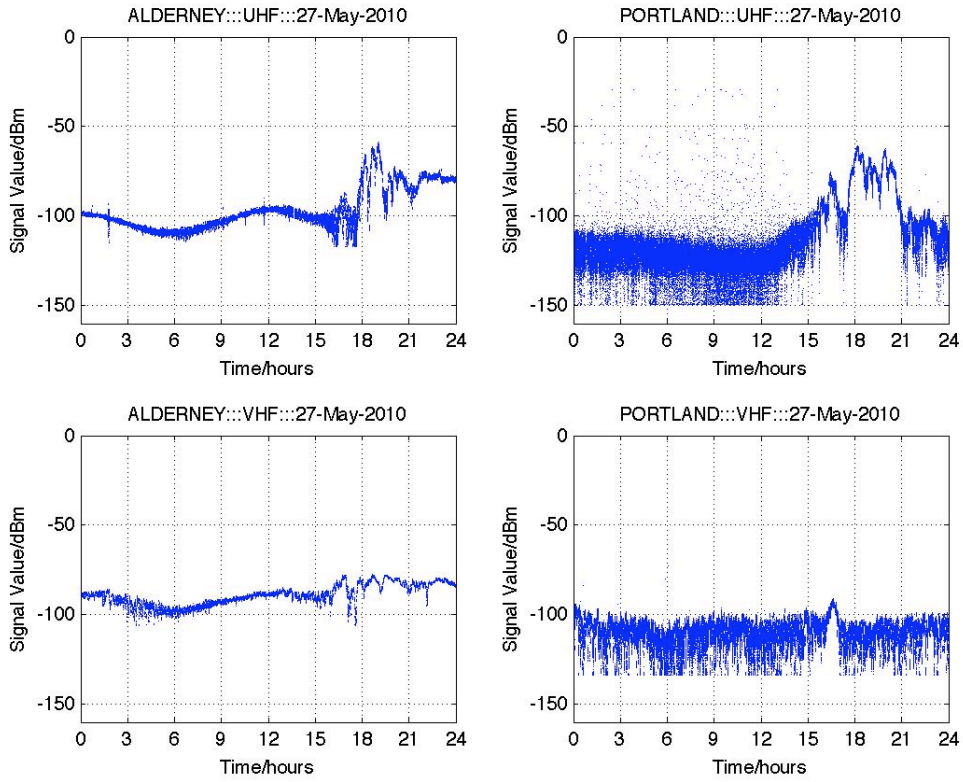

Figure 5-1: Received signal (high-resolution) – 27 May 2010

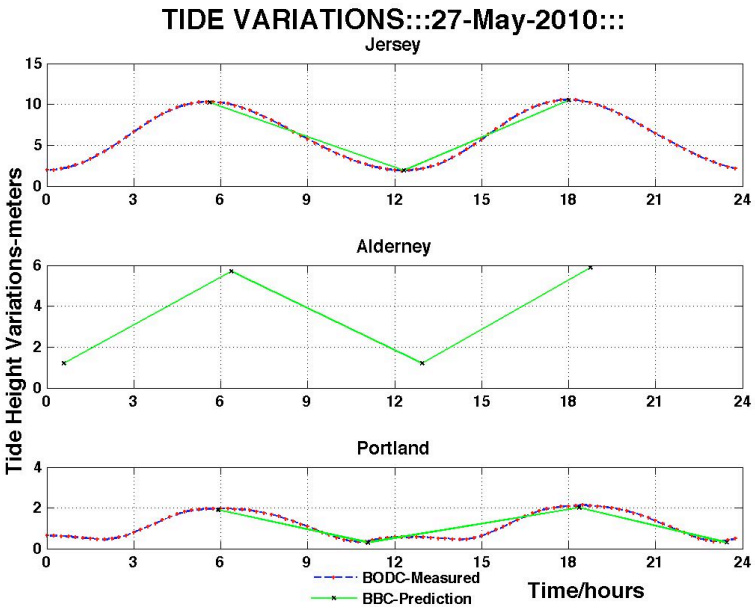

Figure 5-2: Tidal variation – 27 May 2010

For Alderney, during period of normal reception (0000 hours to 1500 hours), the signal strength shows a sinusoidal pattern, indicating dependency on the tide (i.e. high signal strength during low tides and vice versa). For periods with

enhanced signal strength, this dependency on tide disappears, as the signal from 1800 hours onwards shows.

For Portland, during period of normal reception (0000 hours to 1200 hours), the signal strength shows fast fading with deep fade margins, shown in Figure 5-2 as a wide bulk of UHF and VHF signal strengths with occasional jumps to high levels. However, periods with enhanced signal strength show lesser fading depth and sustained reception, as the UHF signal from 1800 to 2100 hours shows. There is no apparent relationship between tidal variation and signal strength for either enhanced or non-enhanced signal levels. This can be expected due to the length of the Jersey-Portland link (140 km).

5.4. Selection of Appropriate Basic Dataset

Short-lived instances of high signal strengths for the UHF signal received at Portland were observed during reception of non-enhanced signal reception (0000 hours to 1200 hours in Figure 5-2). In such instances, the signal strength was higher than the bulk of data, shown by a few dots above -100 dBm level whereas the bulk of the data was less than this level. When this fast fading (variation within 2-sec period) was investigated further, it was observed that the signal strength varies by tens of decibels, even for consecutively recorded signal values (in 2/25 second period). Figure 5-3 illustrates an example of this fast variation:

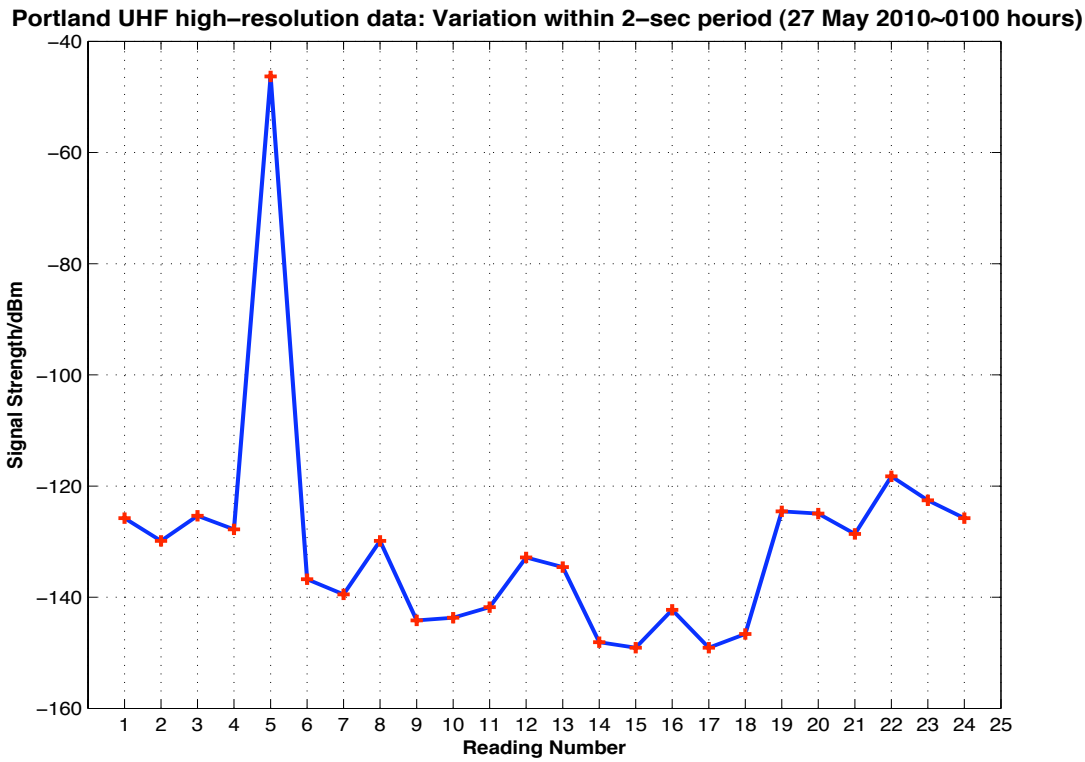

Figure 5-3: Portland UHF short-term (2-second) variation in high-resolution data – 27 May 2010 (~0100 hours)

This type of variation was observed in high-resolution data throughout the year during times of non-enhanced signal reception. Figure 5-4 shows some examples. It can be clearly observed that the highest levels from among these high-value instances effectively meant that the loss experienced by the signal while traversing from Jersey to Portland was less than free space loss.

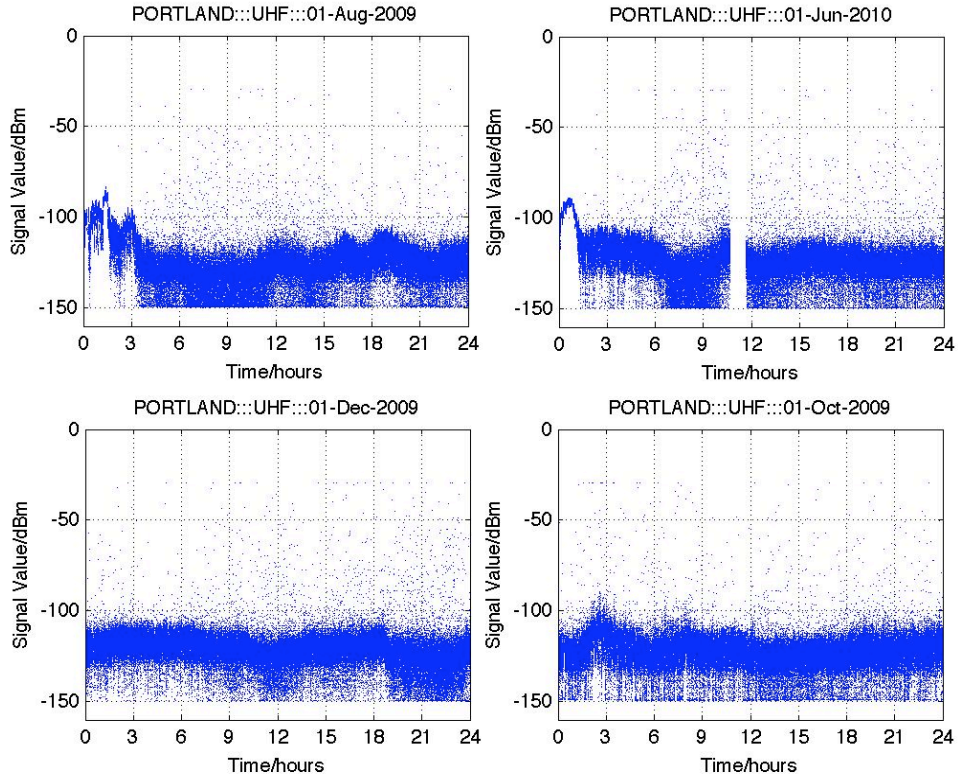

Figure 5-4: Portland UHF short-term variation in high-resolution data

However, this high-magnitude, fast fading/variation was also visible even when the Jersey transmitter was not emitting any signal. This ruled out the possibility that this was due a propagation mechanism carrying the wanted signal to the receiver without considerable loss. One such example of variation is shown in Figure 5-5 from 18 December 2009 when the UHF transmitter was off for some duration. This was confirmed by observing the simultaneous UHF signal level being received at Alderney. Figure 5-5 shows that the UHF signal received at Alderney was at the threshold level of receiver (i.e. wanted signal was not detected) while the bulk of the UHF signal received at Portland was below -125 dBm. However, there were a lot of abrupt, short-lived jumps, enabling the receiver to show received signal strengths higher than -125 dBm, going as high as the maximum levels around -30 dBm.

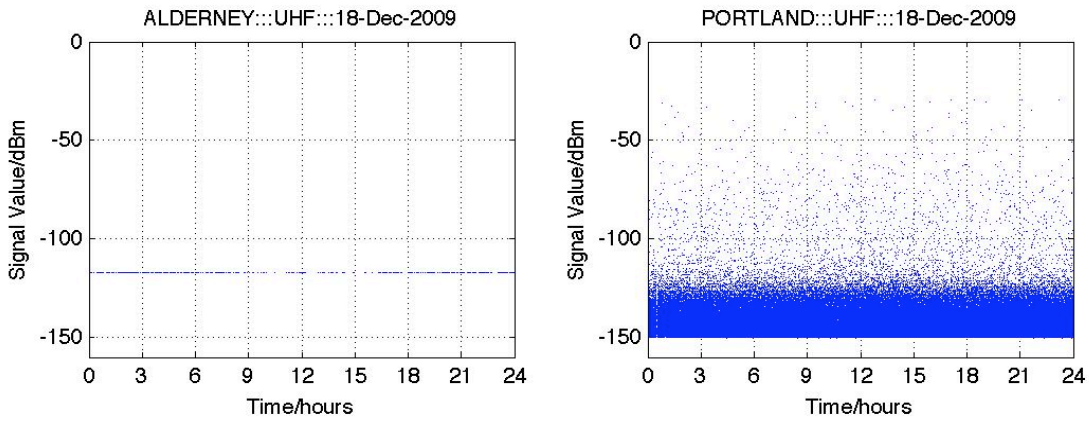

Figure 5-5: UHF received signal with Jersey UHF transmitter off- 18 Dec 2009

The shift in a single jump could be as high as 120 dB, as was observed by zooming in on high-resolution data from 18 December 2009. A few of such instances around 0400 hours are shown in Figure 5-6:

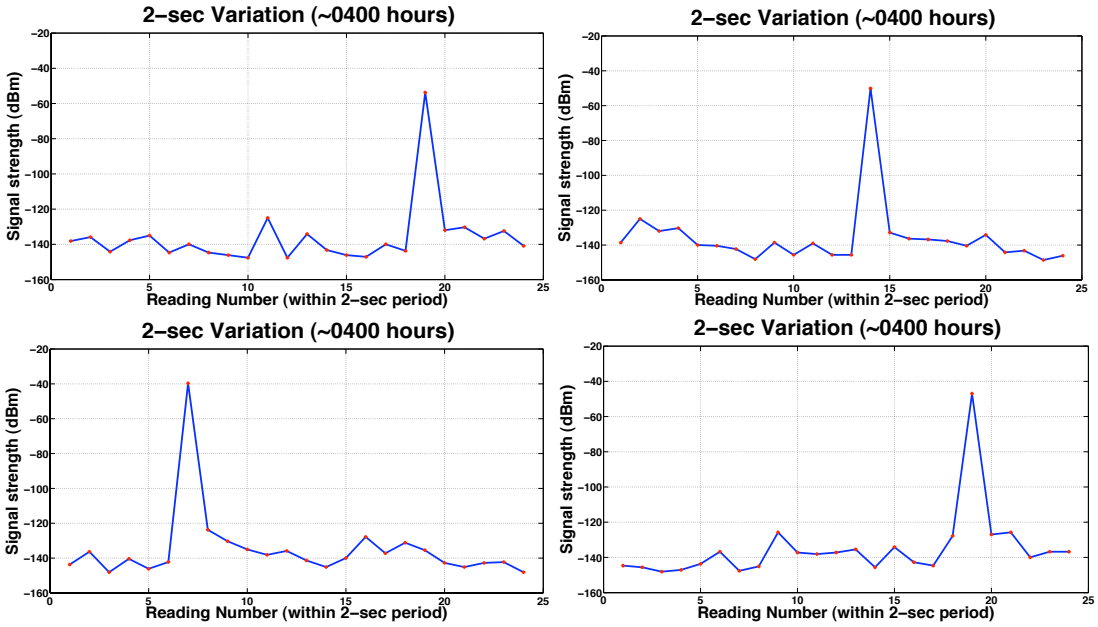

Figure 5-6: Portland received UHF signal level with Jersey UHF transmitter off – 18 Dec 2009 (~0400 hours)

There were many examples when both the receivers were not receiving valid UHF signal and it appeared to be noise. Some of these examples are shown in Figure 5-7:

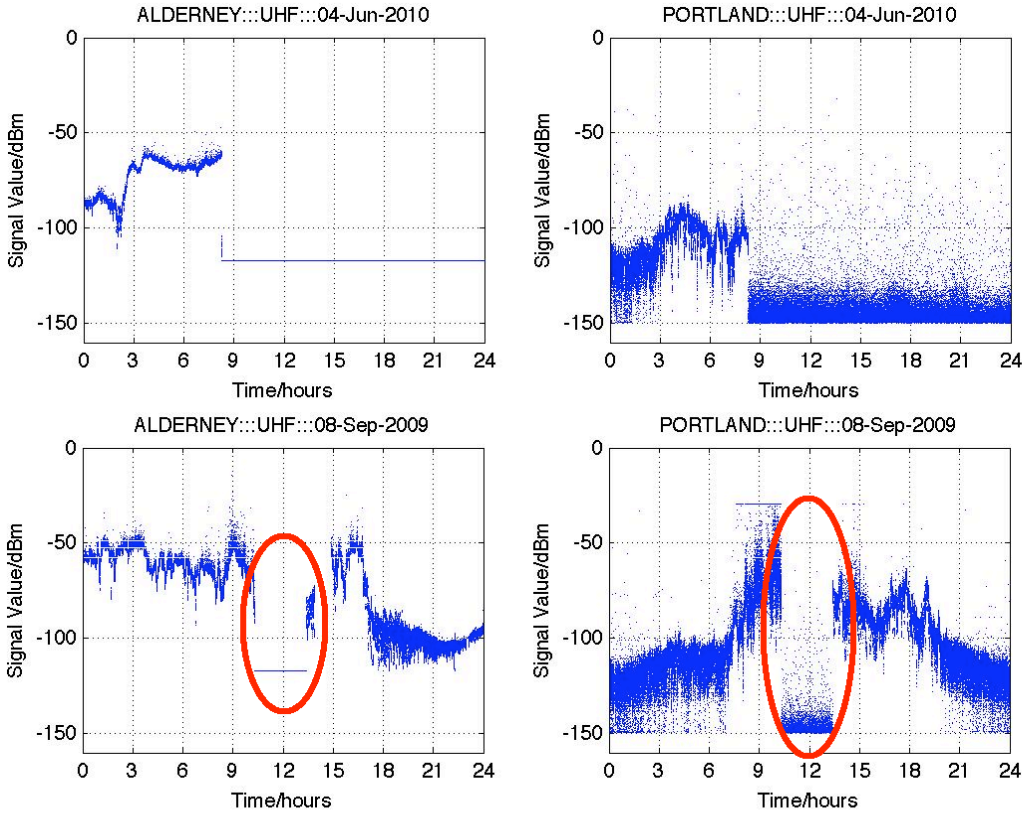

Figure 5-7: UHF signals at Alderney and Portland showing periods with Jersey UHF transmitter off

A general scan of the use of similar frequencies in the vicinity of the transmitter and receivers, performed at the start, during and after the study, did not reveal the presence of any co-frequency use. Hence, these variations could not be attributed to any unwanted transmitter (interferer) around the Channel Islands.

A possible explanation could be a non-linearity of the pre-amplifiers at Portland or contribution from a distant wireless setup whose signal is being propagated through short-lived mechanism with minimal loss. However, the

precise reason for these unpredictable, fast variations is not known. However, these variations can misrepresent enhancement when enhancement-related statistics are dealt with.

However, these anomalies of the raw data were few in number, as compared to the bulk of data, which was clearly visible to be less than -100 dBm. In a set of 25 readings, if any such anomalies were detected, they were either one or at maximum two. Hence the median of the 25 readings, the inter-quartile range and the 90% confidence interval would all give values within the bulk of data (i.e. ~-120 dBm or less). If the median value of every set of 25 values (which were recorded over a 2-second period) was used instead of high-resolution data as the basis for enhancement study, this problem was eliminated, as shown by Figures 5-8 and 5-9:

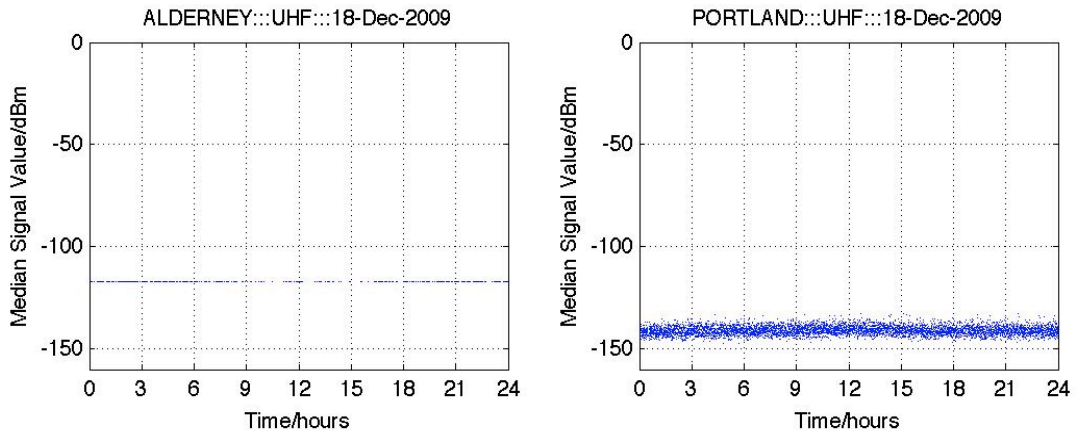

Figure 5-8: Alderney and Portland median data (UHF) – 18 Dec 2009

Figure 5-8 shows that the effect of the abrupt variations was not visible (owing to lesser number of these abnormalities as compared to bulk of data). It shows the noise floors at Alderney and Portland, Alderney's signal approximately -117 dBm and Portland's signal less than ~-140 dBm.

Figure 5-9 shows the median UHF signal strength data at Portland:

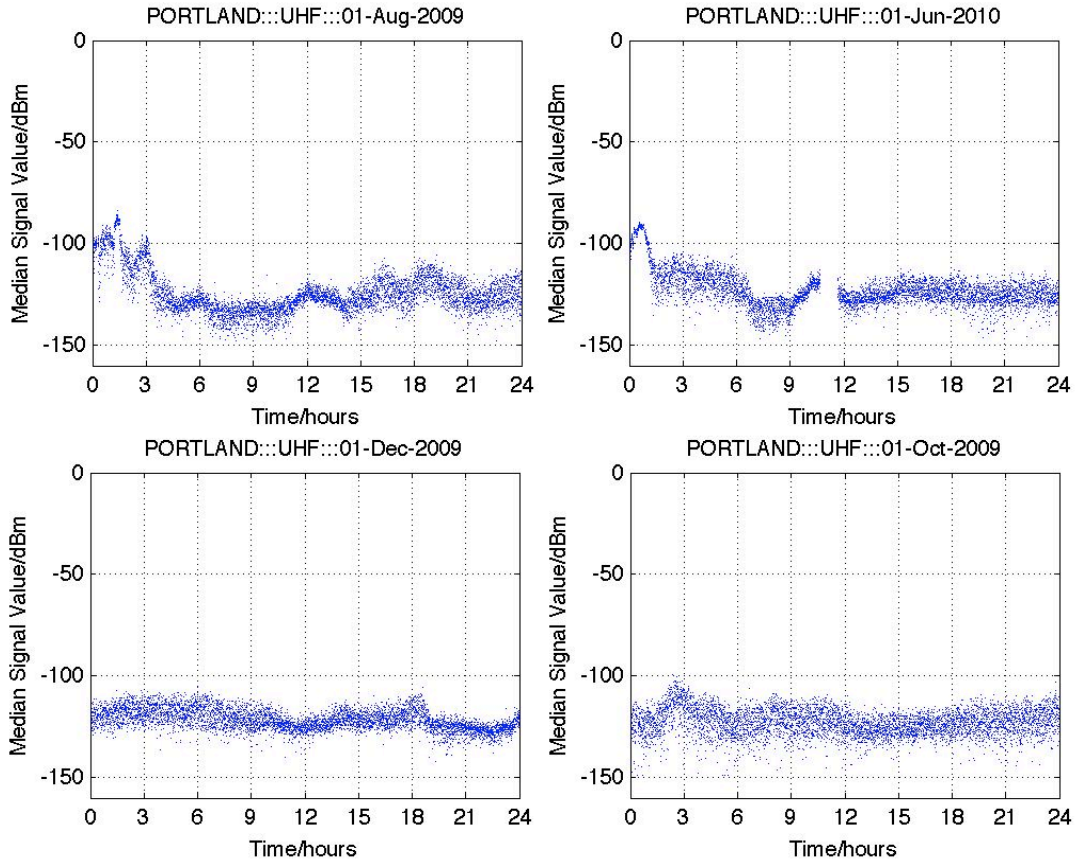

Figure 5-9: Portland UHF median data

When compared with the high-resolution data shown in Figure 5-4, it was evident that the abnormal/invalid signal strength data was removed when median values were considered.

There were also periods of time when valid signals at both frequencies were not being received at a particular receiving site, as shown in Figure 5-10. All such periods when transmission or reception was a problem were identified, because there was likelihood that at times low signal levels (near to minimum receiver threshold) were being received as a result of greater path loss and not due to any transmission problems, listed in Table 5-1.

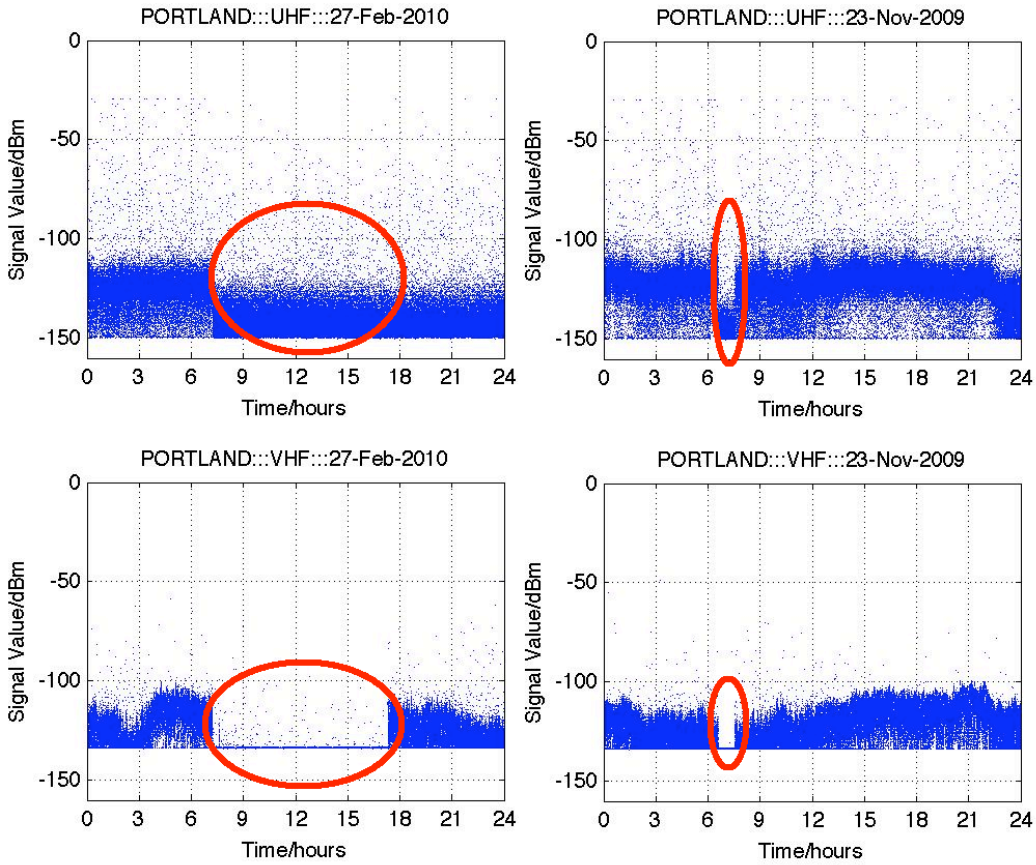

Figure 5-10: UHF and VHF signals at Portland showing common times when transmission/reception of both signals was not valid

Day & time of invalid data	Invalid signal(s)
08 Sep 2009, 10:19 to 13:23	Alderney & Portland UHF
23 Nov 2009, 06:35 to 07:34	Portland UHF & VHF
06 Dec 2009, 09:51 to 10:50	Portland UHF & VHF
14 Dec 2009, 07:23 to 08:29	Portland UHF & VHF
14 Dec 2009, 08:30 to 25 Dec 2009, 01:00	Alderney & Portland UHF
04 Feb 2010, 10:55 to 11:15	Portland UHF & VHF
04 Feb 2010, 11:15 to 05 Feb 2010, 12:26	Portland UHF
27 Feb 2010, 07:37 to 17:18	Portland UHF & VHF
27 Feb 2010, 17:18 to 02 March 2010, 09:44	Portland UHF
24 May 2010, 10:16 to 25 May 2010, 09:36	Alderney & Portland UHF
04 June 2010, 08:18 to 13 June 2010, 09:18	Alderney & Portland UHF
23 June 2010, 10:36 to 12:40	Alderney & Portland UHF
26 June 2010, 08:45 to 27 June 2010, 08:54	Alderney & Portland UHF
27 June 2010, 09:30 to 13:45	Alderney & Portland UHF
28 June 2010, 09:17 to 12:56	Alderney & Portland UHF
29 June 2010, 09:01 to 12:39	Alderney & Portland UHF

Table 5-1: Invalid data time periods

These time periods were excluded from any further data analysis, as they would adversely affect the statistics and analysis because they were not genuine/valid signal strength data.

To conclude, the high-resolution signal strength values could not be used due to the anomalies in Portland UHF data. Hence, the 'median of 2-sec' (median) dataset was selected as the appropriate dataset to use for further analysis. Also, the periods mentioned in Table 5-1 needed to be excluded prior analysing signal strength data.

5.5. Signal Strength Distributions

To specify the number of bins needed for best display of the distribution, the bin size is calculated using the central part of calibration curve, which is approximated by a linear curve. The number of bins corresponds to a change in signal strength value of 1dB and is obviously different for every distribution.

Figure 5-11 shows the distribution for the valid median UHF signal strength at Alderney recorded over the whole year (i.e. 01 July 2009 to 30 June 2010). The distribution is not symmetrical and has a long tail at the upper end. The main peak of the distribution (centred around the median value) and a long tail may suggest towards two distinct propagation phenomena. The span of the bulk of signal values (indicative of the inter-decile range of the signal strength values) is approximately 30 dB (-100 to -70 dBm):

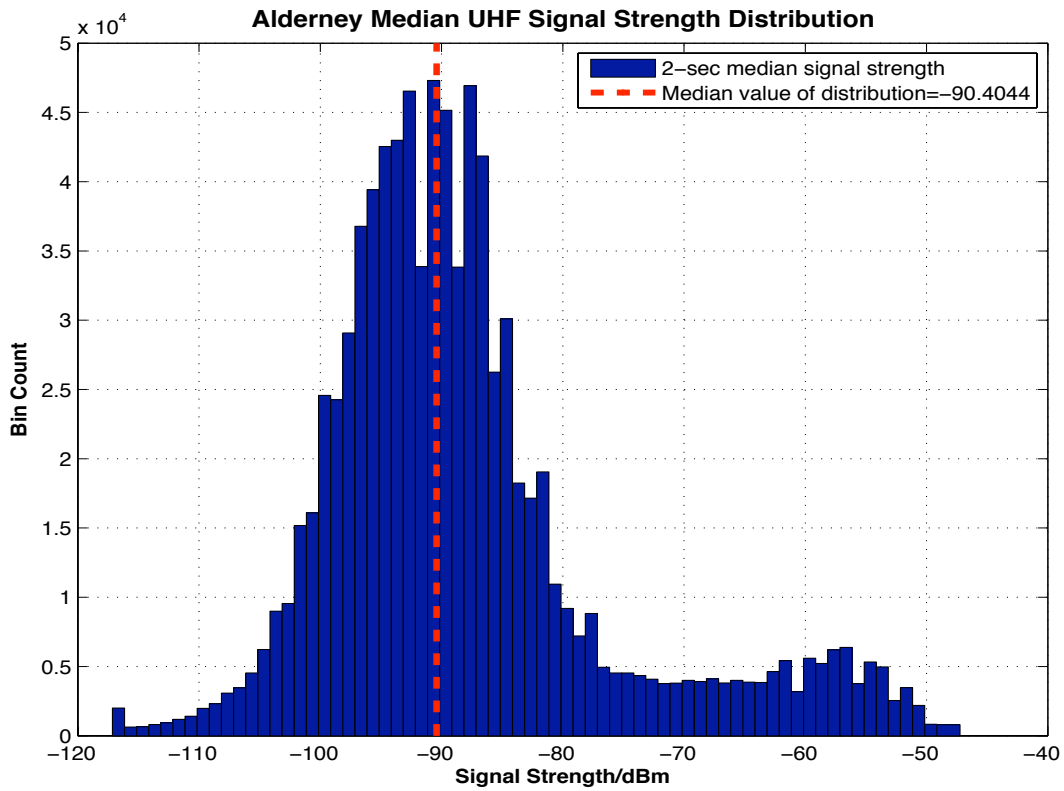

Figure 5-11: Alderney UHF median data distribution (one-year data)

Figure 5-12 shows the distribution of median VHF signal strength at Alderney:

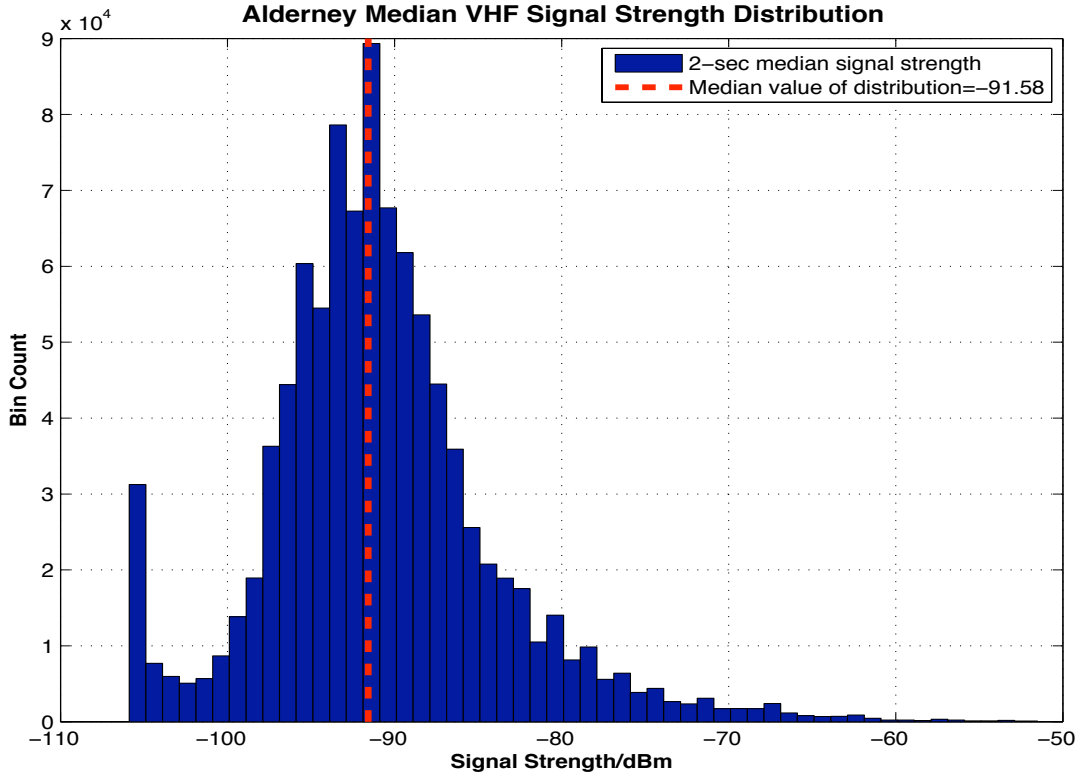

Figure 5-12: Alderney VHF median data distribution (one-year data)

The distribution is not symmetrical and has a longer tail at the upper end but not as pronounced as that for UHF. The span of the bulk of signal values is approximately 16 dB (-98 dBm to -82 dBm).

Figure 5-13 shows the distribution of median UHF signal at Portland:

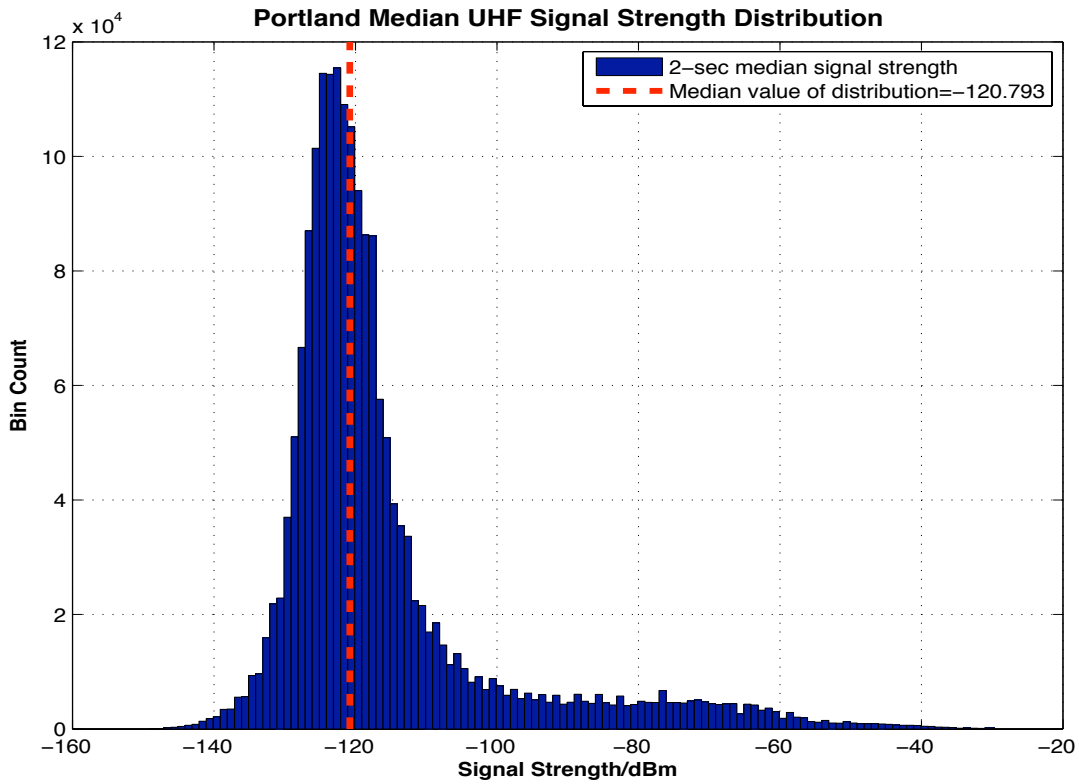

Figure 5-13: Portland UHF median data distribution (one-year data)

The distribution is not symmetrical and has a long tail at the upper end, once again indicative of two distinct propagation phenomena. The span of the bulk of signal values is approximately 33 dB (-128 dBm to -95 dBm). Figure 5-14 shows the distribution of median VHF signal at Portland:

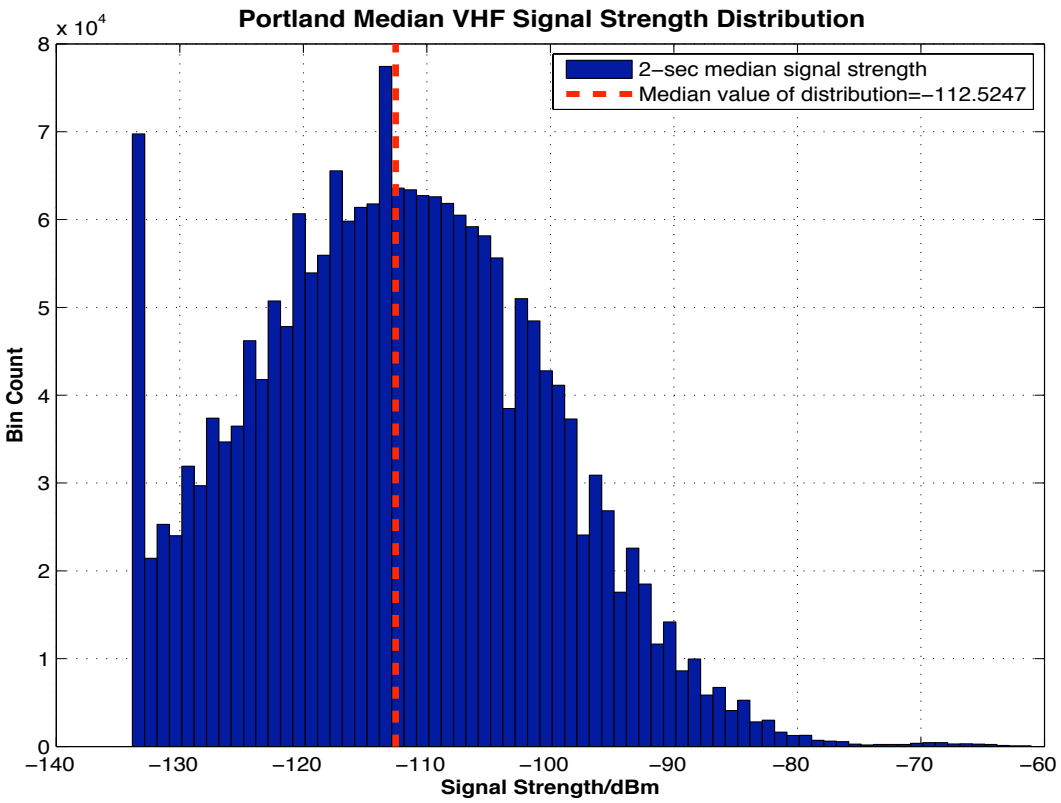

Figure 5-14: Portland VHF median data distribution (one-year data)

The distribution has a very slight, barely noticeable, longer tail towards the upper end. The span is almost 31 dB (-128 dBm to -97 dBm). It is clearly visible that VHF signal distribution has a much shorter tail than UHF signal at Portland.

5.6. Comparison Between Hourly Median Data and Median Data

A comparison of median and hourly data indicates that the basic shapes of distributions of hourly median data and median data for both UHF & VHF signals are similar. They show similar trends in terms of having longer tails at the upper ends except for VHF signal at Portland, which looks like a one big bulk without longer tails at either ends (the tiny tail of median data disappears

in hourly data). The median values from hourly and median data sets are also close to each other. These observations support the assumption that if hourly median data is used for further analysis involving meteorological data (which is only available hourly), no major detail is lost.

5.7. Missing Data

Over the one year of data considered for the study (July 2009 to June 2010), the hourly signal strength data for Alderney is available for almost 50% of time for both VHF and UHF whereas the hourly signal strength data for Portland is available for almost 97% of time for both VHF and UHF. Figure 5-15 shows the percentage of missing data for every month from July 2009 to June 2010 inclusive:

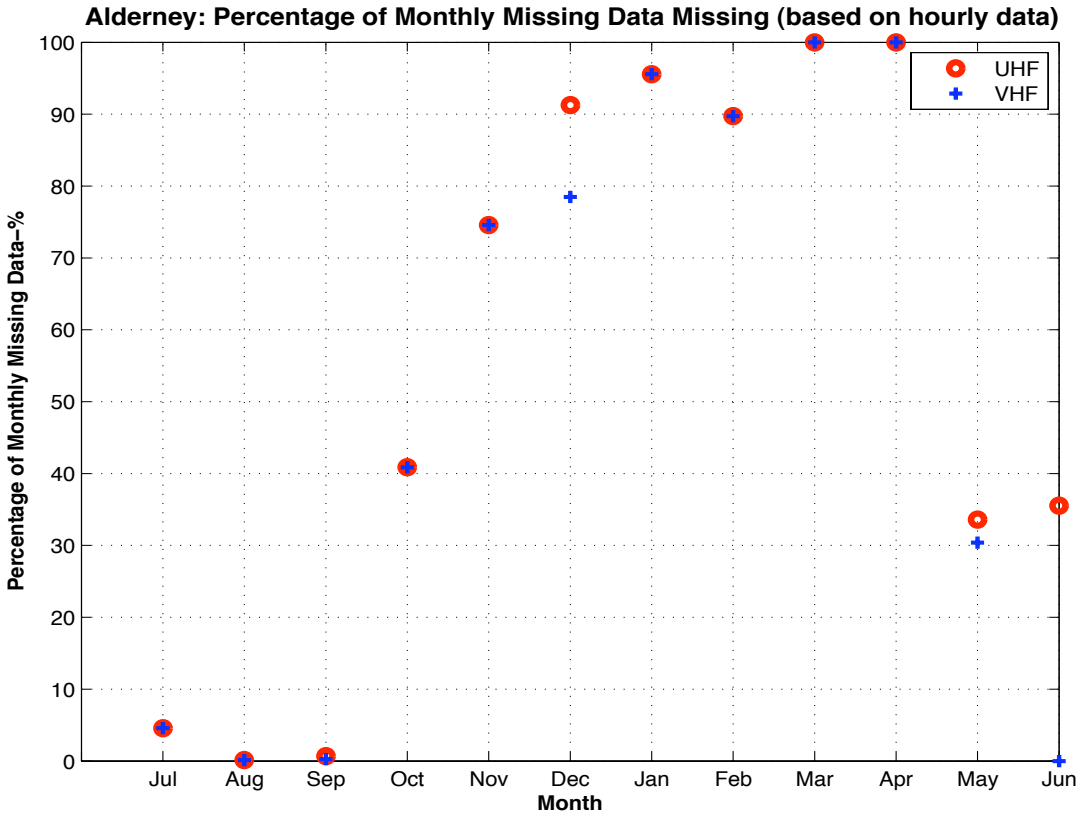

Figure 5-15: Alderney hourly median data- missing data percentage

As Figure 5-15 illustrates, more than 70% of data is missing from November onwards until April inclusive. Figure 5-16 shows the percentage of missing data at Portland, for every month from July 2009 to June 2010 inclusive:

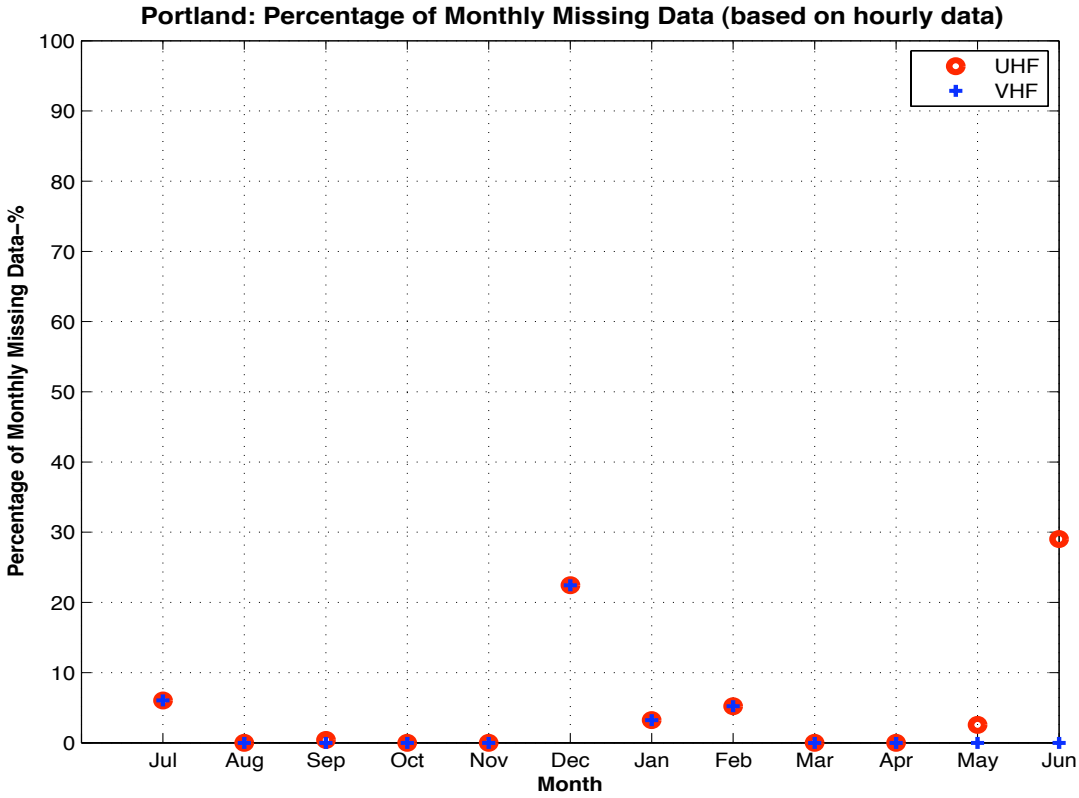

Figure 5-16: Portland hourly median data- missing data percentage

There is hardly any data missing substantially during any month, except for some in December and June, when the transmitter was not working for a few days.

5.8. *Further Statistics of Signal Data*

5.8.1. *Monthly variation of hourly signal strength*

The following figures relate to the hourly median data on monthly basis. With a maximum of 24 hourly values per day, a month can have a maximum of 744 hourly values. In the following figures, the behaviour of these hourly values has been summarised on a monthly basis.

Figure 5-17 shows the monthly variation of the hourly UHF signal at Alderney, showing quartiles, min, max and medians for every month:

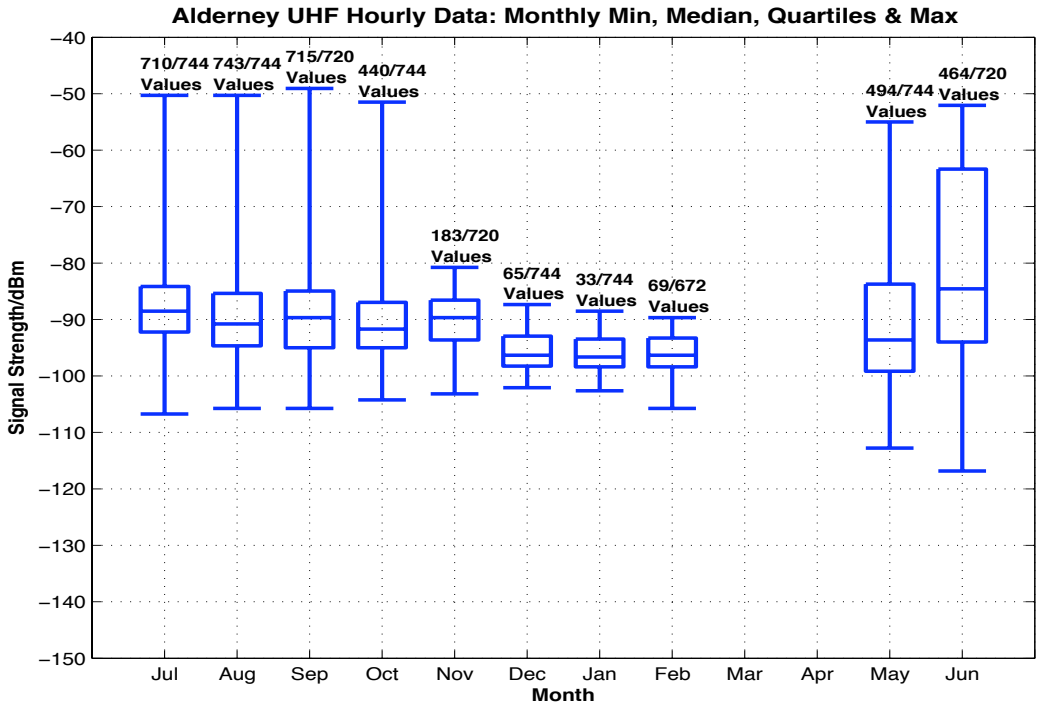

Figure 5-17: Alderney UHF hourly data- monthly box plots

The monthly median UHF signal strength is higher during summer. The inter-quartile range is markedly larger for June, as compared to rest of the months.

This is probably due to the existence of a comparable number of events with enhanced and non-enhanced signal strengths. Figure 5-18 shows the monthly variation of hourly median VHF signal at Alderney, including quartiles, min, max and medians for every month:

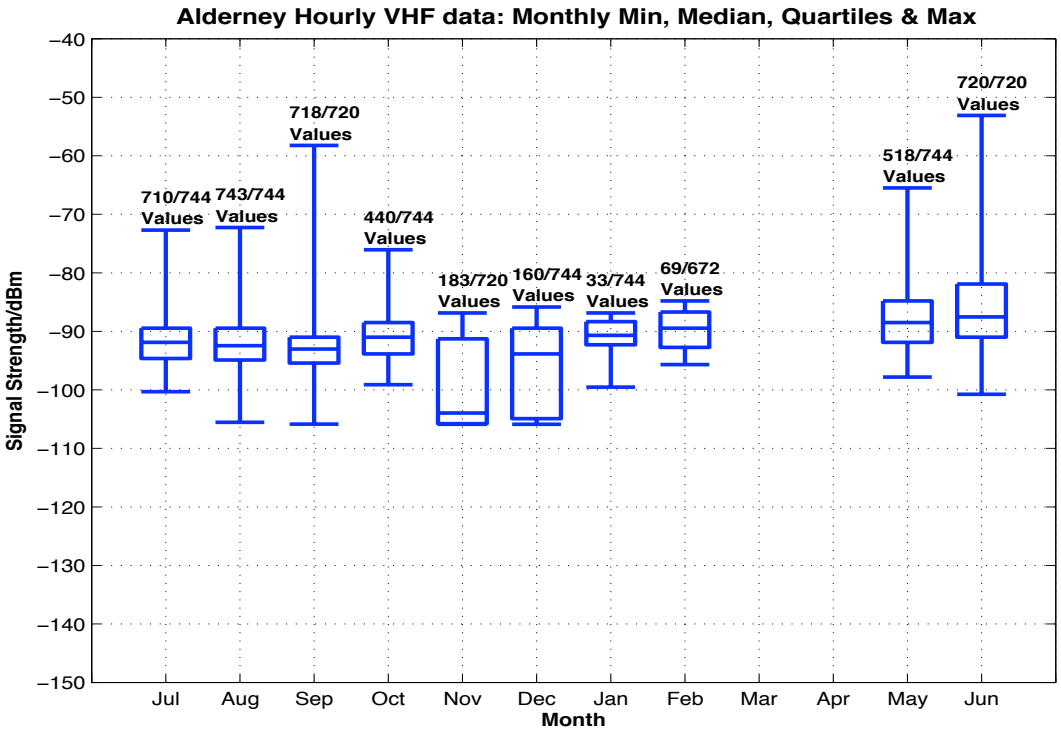

Figure 5-18: Alderney VHF hourly data- monthly box plots

The monthly median VHF signal strength is maximum for June, followed by May. Figure 5-19 shows the monthly variation of hourly median UHF signal at Portland, including quartiles, min, max and medians for every month. The monthly median UHF signal strength is maximum for June, followed by August and April. The inter-quartile range is markedly larger for June.

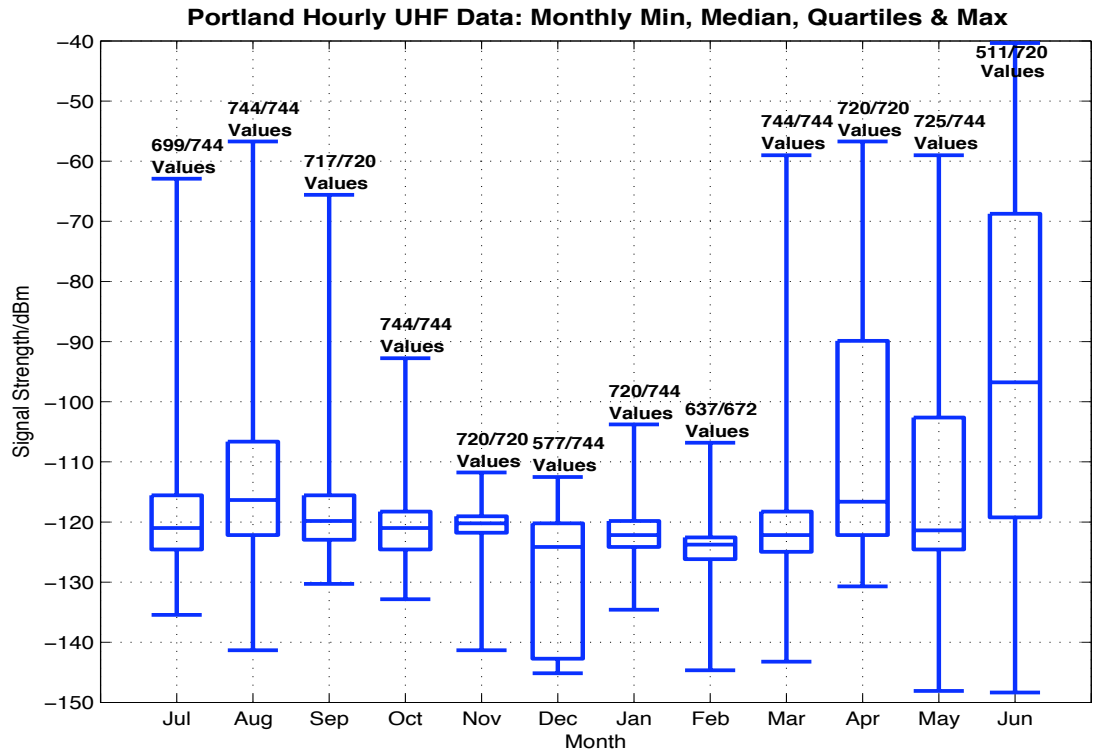

Figure 5-19: Portland UHF hourly data- monthly box plots

Figure 5-20 shows the same for hourly median VHF signal at Portland.

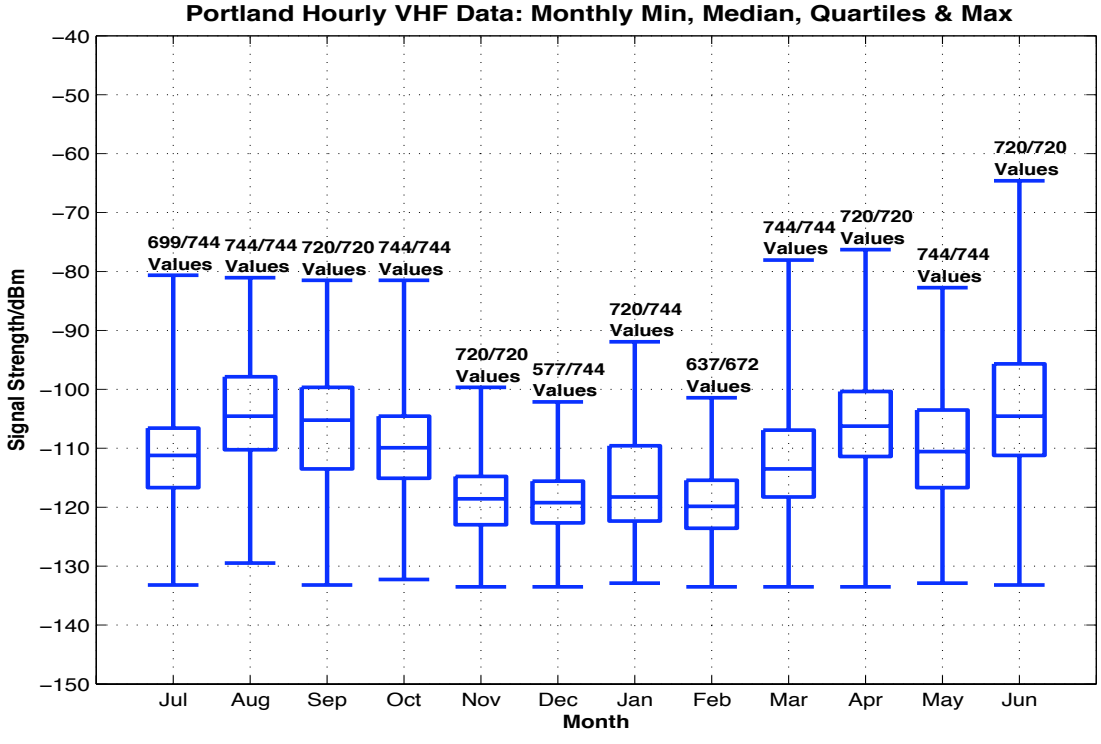

Figure 5-20: Portland VHF hourly data- monthly box plots

The monthly median VHF signal strength is maximum for June, followed by August, September and April. The inter-quartile range is minimum for December.

5.8.2. Short-term fading statistics

The following figures relate to the short-time variation of the high-resolution data, whose 25 values were recorded within the time period of 2-seconds. Considering all the 2-second sets of 25 readings each, Figure 5-21 shows the inter-decile range (IDR) of the variation of the UHF signal at Alderney within the 2-second period:

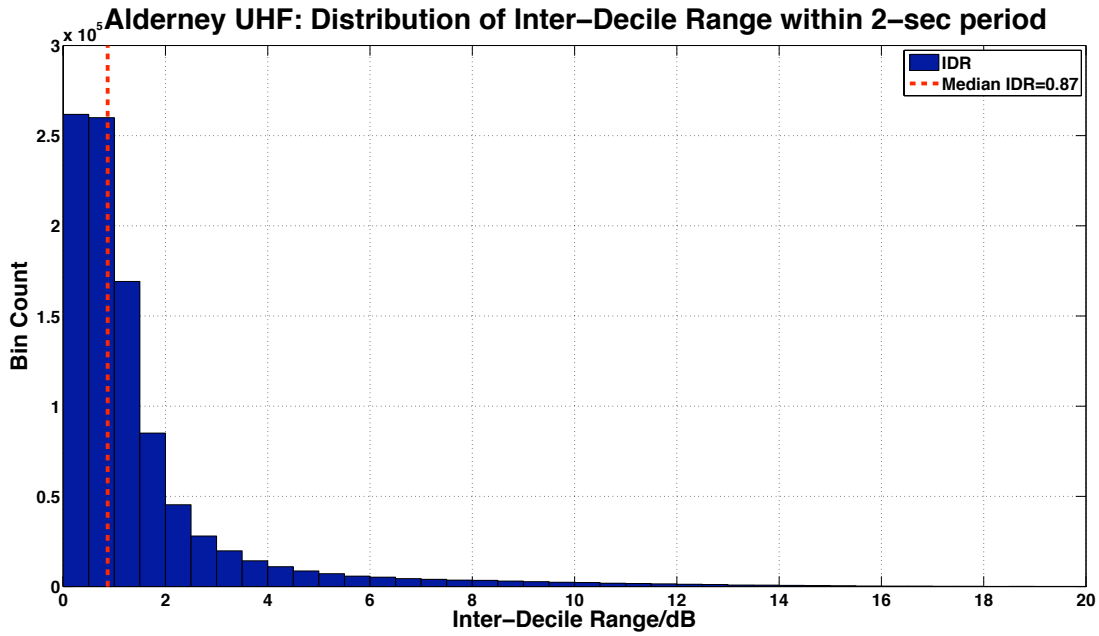

Figure 5-21: Alderney UHF IDR within 2-sec period (up to 20 dB)- histogram

The median IDR of Alderney's UHF signal over 2-second period is ~0.9 dB. Figure 5-22 shows the IDR of variation of UHF signal received at Portland within time period of 2 seconds:

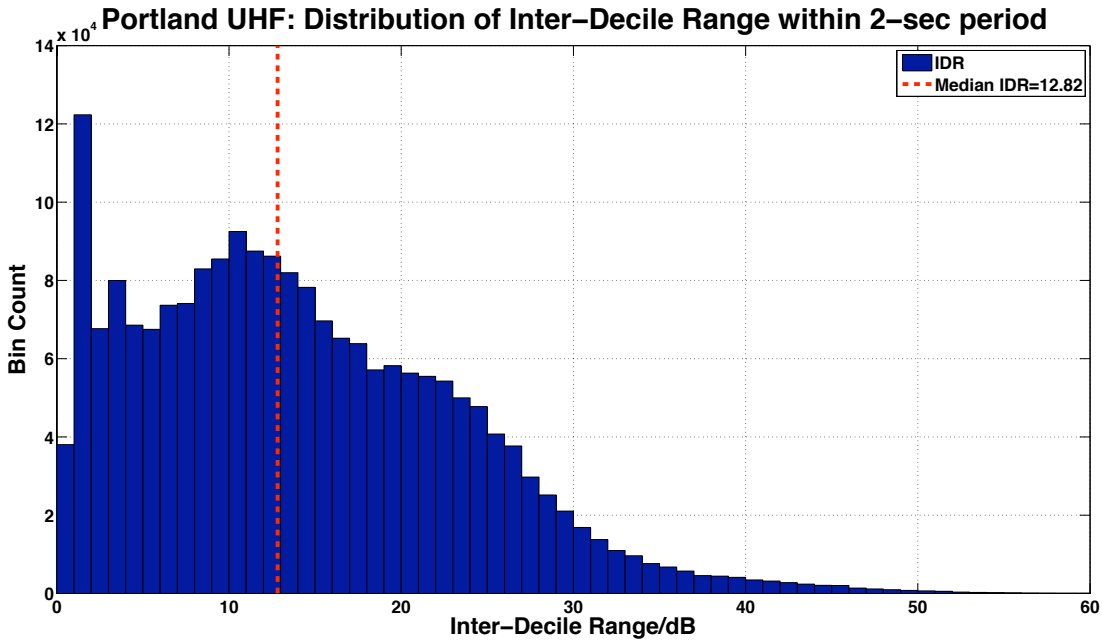

Figure 5-22: Portland UHF IDR within 2-sec period (up to 60 dB) - histogram

The median IDR of UHF signal over 2-second period is ~13 dB. Figure 5-23 shows the IDR of signal variation within 2-sec period for the median VHF signal received at Alderney, wherein the median IDR in Alderney's VHF signal over 2-second period is ~0.3 dB.

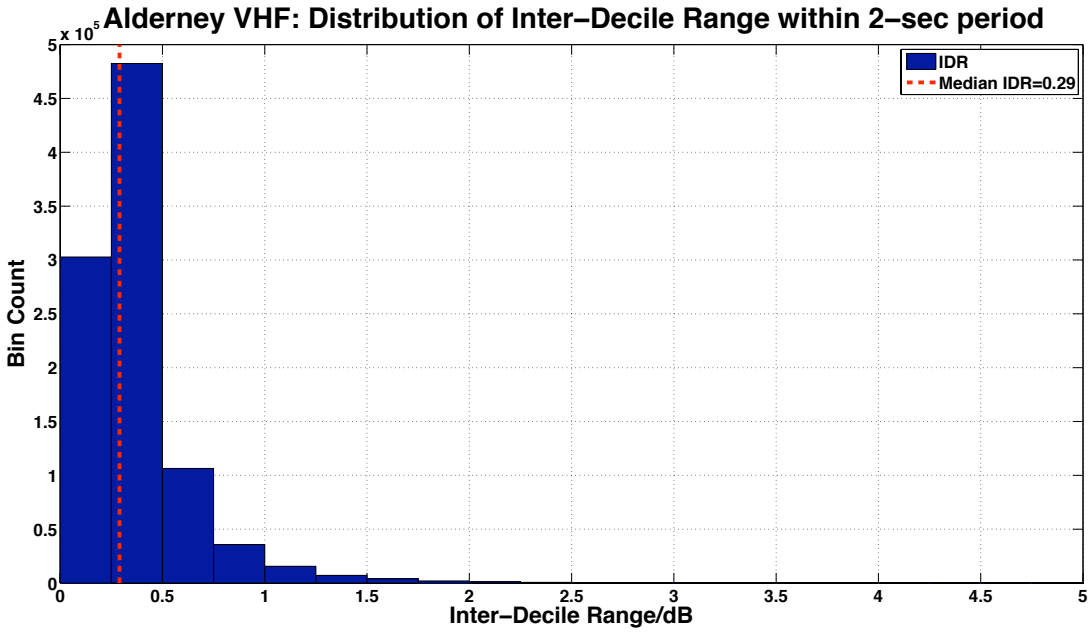

Figure 5-23: Alderney VHF IDR within 2-sec period (up to 5 dB)- histogram

Figure 5-24 shows the same for VHF signal at Portland, wherein the median IDR in Portland's VHF signal over 2-second period is ~2.3 dB.

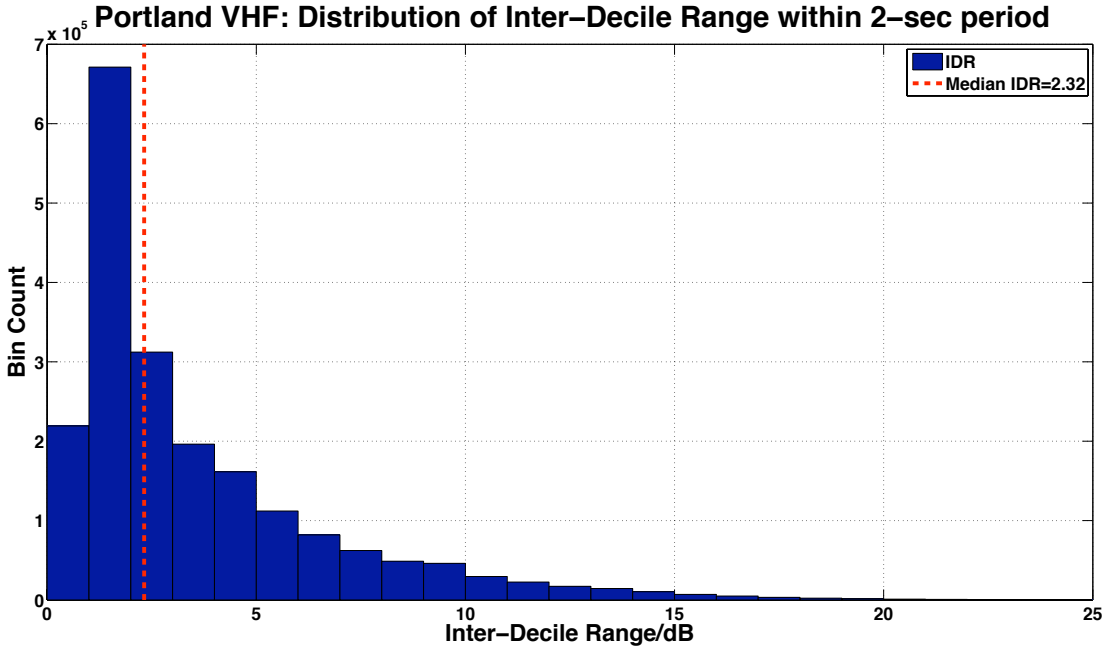

Figure 5-24: Portland VHF IDR within 2-sec period (up to 25 dB) - histogram

From the figures above, it can be observed that the short-time variation (i.e. variation within 25 values recorded within 2-seconds) is higher for Portland than Alderney. This effect is more pronounced for the UHF signal at Portland. This has been elaborated upon in Section 5.10.2.5.

As indicated by the IDRs of signal variation within the 2-second period, there is minor variation in Alderney's signals over this short period of time. On the other hand, signals at Portland show larger variation. UHF signals received at Portland (and to a lesser extent VHF signals received at Portland) show a lot of abrupt, temporary variations in signal level.

5.9. Propagation Loss

The difference between the transmitted power levels and received power levels can be used to determine the effective propagation loss incurred by the signals as they travel from Jersey to Alderney and Portland.

The basic equation used is of the following form:

$$P_R = \underbrace{P_T + G_{AMP} - L_{FEEDTX} + G_T}_{Transmitted\ EIRP} - L_{PATH} + G_R - L_{FEEDRX} + G_{PREAMP} \text{ dBm} \quad (5.01)$$

Where:

L_{PATH} is the path loss (dB)

P_R & P_T are the received and transmitted powers (dBm)

G_{AMP} & G_{PREAMP} are the amplifier and pre-amplifier gains (dB)

G_T & G_R are the transmitting and receiving antenna gains (dBi)

L_{FEEDTX} and L_{FEEDRX} are the feeder losses at transmitter and receiver (dB)

The values for Transmitted E.I.R.P. are already known and mentioned in Chapter 4. The above equation can be re-arranged for path loss L_{PATH} as follows:

$$L_{PATH} = EIRP_{TX} + G_R - L_{FEEDRX} + G_{PREAMP} - P_R \qquad \text{dB} \qquad (5.02)$$

Putting the respective values in Equation 5.02 by using Equations 4.07 to 4.10, the following values for L_{PATH} are obtained:

Receiving site	Frequency (MHz)	Path loss L_{PATH} (dB)
Portland	240	87.5 - P_R
	2015	89.7 - P_R
Alderney	240	63.5 - P_R
	2015	68.2 - P_R

Table 5-2: Path loss expression (as a function of received power)

The hourly median values of received power levels are used to generate cumulative distribution curves for the UHF and VHF signals received at Alderney and Jersey. Considering those periods when valid signals levels were being recorded at both sites, Figure 5-25 shows the cumulative distributions for the path loss, based on valid hourly data:

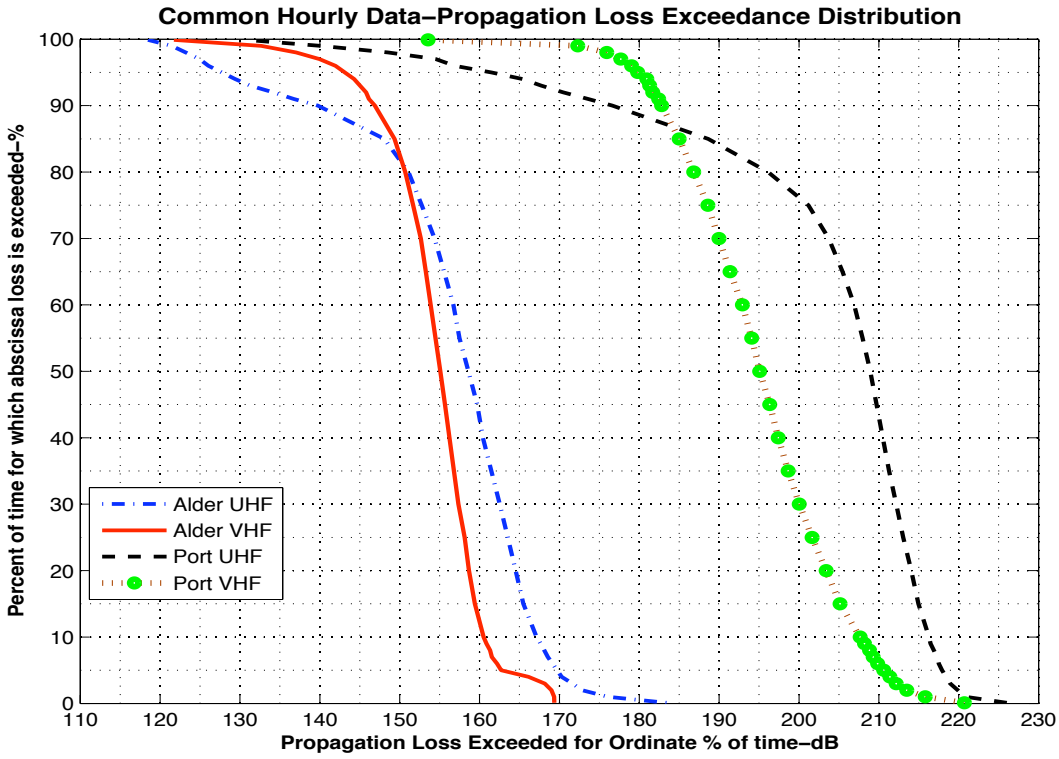

Figure 5-25: Path loss: Common valid hourly data

For Alderney, the two curves cross around 82% exceedance, from where onwards loss values exceeded by UHF signal are less than those for VHF for the same percentage of time. This points towards another propagation

mechanism wherein the comparative path loss is lesser for greater percentages of time for UHF signal than VHF. A similar trend is observed for Portland, whose cumulative distribution curve show a very long tail for UHF signal towards the higher exceedance percentages and markedly lower loss above ~87% exceedance time, indicative of an enhanced propagation phenomenon.

There is approximately 53 dB difference between the median path loss values experienced by the UHF signals whereas the difference between median VHF path loss values is about 37 dB. Also, it can be observed that the difference between the UHF path loss for Jersey-Portland path exceeded for higher percentages of time and respective values of losses for Jersey- Alderney path decreases drastically.

The comparisons between measured and predicted values are discussed in detail in the following chapter.

5.10. Received Signal Strength Enhancement

Enhancements in received signals are hard to define quantitatively, but can be understood to refer to marked departures from normal levels of reception. The following results pertaining to signal strength enhancements are based on the median data set.

5.10.1. Threshold level to decide between normal and enhanced signal

In order to differentiate between normal and enhanced signal reception during study on over-sea paths up to 50km, Gunashekar [50] used a threshold value defined as:

$$\text{Threshold} = \text{mean of all valid data} + 10 \text{ dB} \qquad (5.03)$$

The study by Shen and Vilar [55] on a 150 km English Channel path identified troposcatter as the dominant mechanism under normal atmospheric conditions and defined enhancement as signal levels above the normally observed troposcatter level.

Troposcatter and diffraction are the two long-term mechanisms that are normally prevalent over trans-horizon paths, as discussed in detail in Chapters 2 and 3. If the mechanism causing the lesser amount of median path loss is selected for each path and frequency used in this study, the expected received signal levels are shown in Table 5-3:

Receiving site	**Received signal level after median path loss (dBm)**	
	UHF	VHF
Alderney	-101.8	-78.5
Portland	-112.3	-88.5

Table 5-3: Received signal level after undergoing median path loss

The received signal levels in Table 5-3 could have been the possible candidates for the threshold levels to decide between non-enhanced and enhanced signal reception. However, a close investigation of the daily plots of

the median signal levels [Section 5.4] received throughout the year revealed that on certain days, the signal levels received at Alderney showed variation coinciding with tidal variation (i.e. two troughs and two crests in the daily signal). The maximum value of the UHF signal at Alderney during such days/periods was higher than the values given by Table 5-3. Figure 5-26 shows some of these cases:

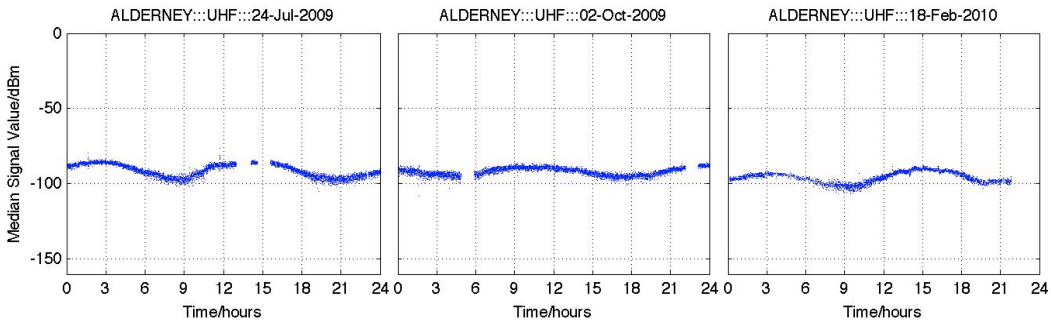

Figure 5-26: Alderney – UHF signal reception showing daily crests/troughs

On the other hand, the normal VHF signal levels at Alderney were observed to be lower than the respective value in Table 5-3. Hence, the values in Table 5-3 could not be used as the threshold values for Alderney.

Therefore, the 'representative' days for non-enhanced UHF and VHF signal reception at Alderney were identified by the eye-inspection of the whole year's data, assuming that the semi-diurnal pattern of received signal at Alderney was non-enhanced. In contrast, there were days or parts of days when the received signal levels were higher and there was no pattern in the daily signals. Figure 5-27 shows a few of such cases:

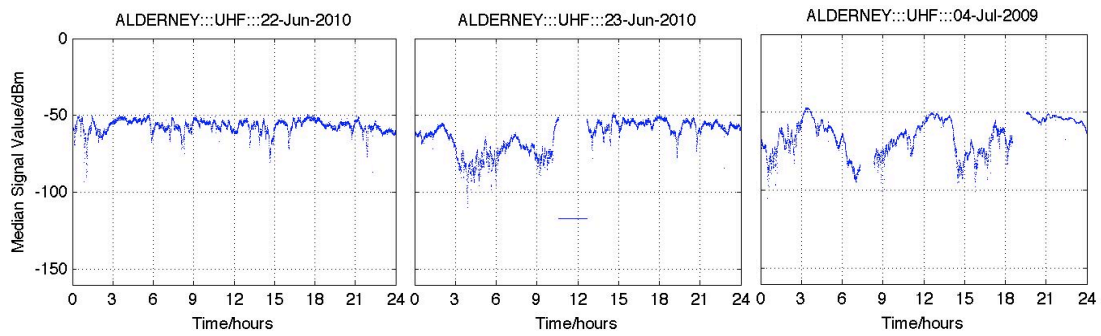

Figure 5-27: Alderney – UHF signal reception showing signal level enhancements

For the signals received at Portland, there was no apparent relationship with tidal variation. Hence, it was not easy to identify 'normal' days for Portland by looking for a pattern for non-enhanced signal reception. However, a detailed investigation of the daily signal level plots helped in identifying days/periods wherein the signal levels received were drastically different. Of these days/periods, those common with the days when the sinusoidal, semi-diurnal cycle was observed in the signals received at Alderney were selected. This effectively meant that those days/periods were picked when both Portland and Alderney received non-enhanced signals. However, with reference to Table 5-3, the observation for Portland was similar to that of Alderney, i.e. higher UHF and lower VHF signal levels were observed on such days/periods of non-enhanced signal reception. Figure 5-28 shows a few cases from Portland, with non-enhanced (a,b,c) and enhanced (d,e,f) UHF signal level reception, which indicate that a general assumption could not be made that whenever signal at Alderney was non-enhanced (or enhanced), the respective signal at Portland would be non-enhanced (or enhanced) because this was not observed at all times.

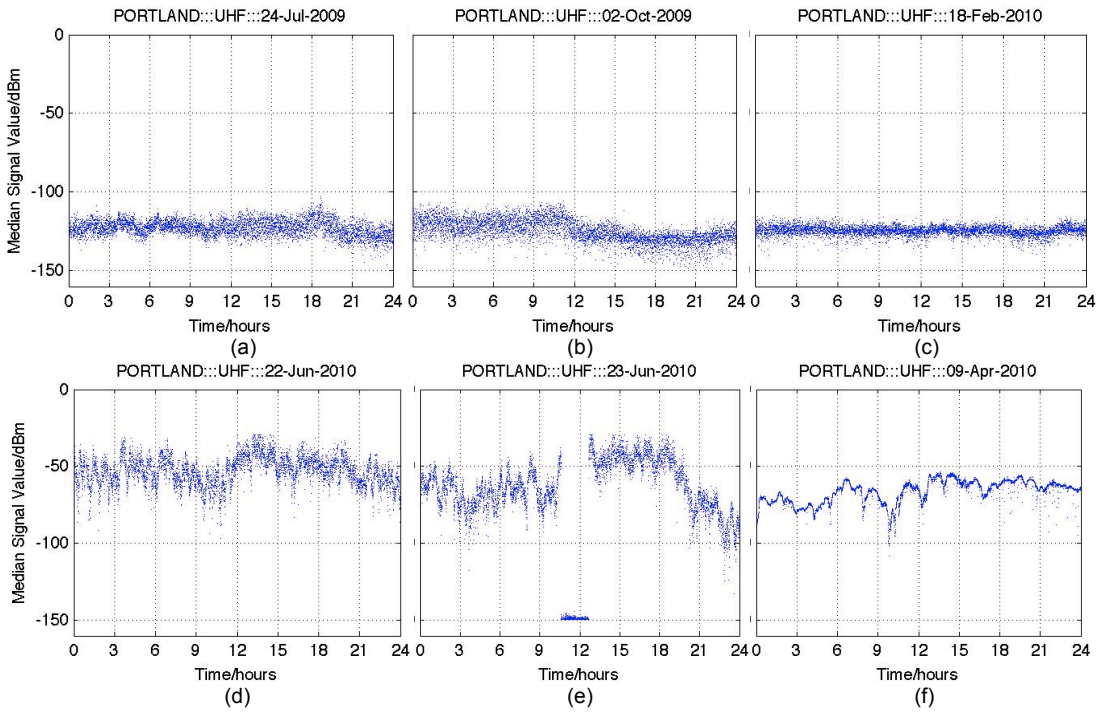

Figure 5-28: Portland – Non-enhanced/enhanced UHF signal levels

The foregoing in view, it became evident that choosing threshold values could not be based on Table 5-3 but on the observed signal levels and patterns. It was hard to draw a line on the signal strength axis and to define everything below that line as 'normal' and everything above that line as 'enhanced' signal strength. Thus, a range of threshold values was defined for each receiving site and frequency. This range was based on the maximum value the respective signal attained on a day with seemingly non-enhanced signal reception. The ranges for the threshold values were:

Receiving site	Threshold value range (dBm)	
	UHF	VHF
Alderney	-76 to -77.5	-86 to -88.5
Portland	-102 to -108	-98.5 to -102

Table 5-4: Threshold value ranges for non-enhanced/enhanced signal statistics

The highest and lowest values of threshold in the table were the respective highest and lowest 'peak' values observed during inspection of 'normal' days.

5.10.2. Enhanced signal statistics

This section deals with the basic results derived from analysing the received signal strength data with respect to enhancement.

5.10.2.1. Whole dataset

Based on the values from Table 5-4, Table 5-5 gives the percentage of time enhanced signal was observed. As Table 5-5 illustrates, VHF signals show enhancement for greater percentage of time than the UHF signals received at both the receiving sites. However, this gap reduces with selection of higher set of threshold values:

UHF threshold value (dBm)	**Occurrence frequency of enhanced signal (%)**	**VHF threshold value (dBm)**	**Occurrence frequency of enhanced signal (%)**
ALDERNEY			
-77.5	13.8	-88.5	27.7
-77	13.4	-87	21.2
-76	*12.8*	*-86*	*17.5*
PORTLAND			
-108	16.2	-102	19.5
-106	14.7	-100	14.9
-102	*12.6*	*-98.5*	*12.2*

Table 5-5: Enhancement occurrence percentage with different threshold values

Although the highest set of threshold values in the table (italicised in Table 5-5) provided a comparatively conservative standard as compared to the others, it was chosen for generating further statistics.

In addition to the 'primary' enhancements decided via threshold value of the received signal, 'secondary' enhancements of the following two types were also observed:

- Type A: The signal levels were generally lower than the threshold value but there was a marked and clear deviation in the form of a peak higher than the surrounding values
- Type B: A high tide was expected to result in a lower signal level at Alderney. Instead a higher signal level was observed

Figure 5-29 shows a few examples of these secondary enhancements:

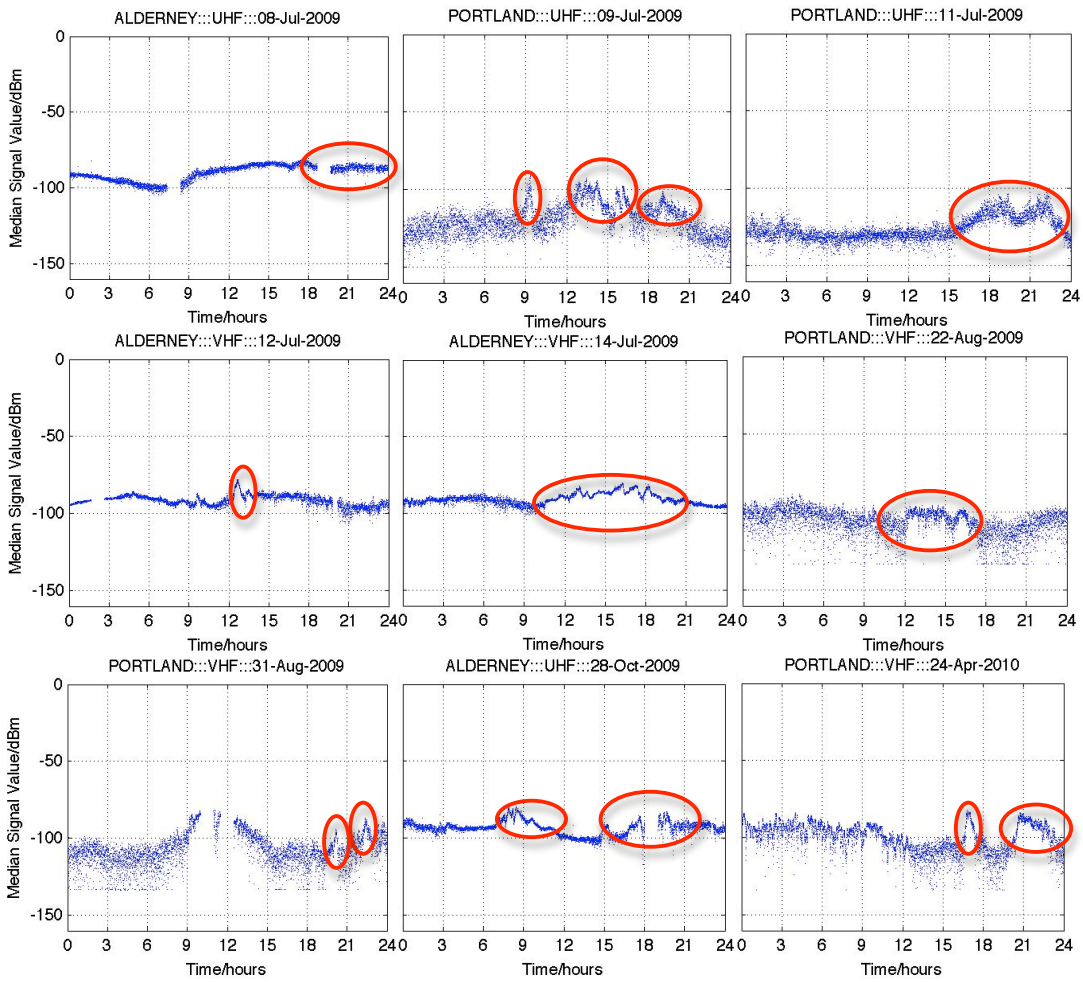

Figure 5-29: Secondary enhancement examples

Since a general filter could not be defined to identify such enhancement events, all these secondary enhancements have been identified by eye inspection of the whole year's data. When these secondary enhancements were combined with the dataset with highest threshold values from Table 5-5, the following statistics were obtained:

Receiving site	Occurrence frequency of enhanced signal (%)	
	UHF	VHF
Alderney	20.1	20.8
Portland	14.6	14.6

Table 5-6: Enhancement occurrence percentage – Primary & secondary combined

Considering the secondary enhancements as well, there is almost 7% increase in the enhancement percentage for UHF signal at Alderney, while 2 to 3% in the other cases.

5.10.2.2. Common dataset

Any 'overall' comparison between the two sites might be misleading from the results in Tables 5-5 and 5-6 since Alderney had some days/periods with valid data missing. However, when data common in time to both sites was considered, the following enhancement statistics were obtained, showing that generally, time percentages of enhancements in VHF signals are higher than those in UHF. Also, Portland shows greater percentage of enhanced UHF signals as compared to Alderney.

UHF threshold value (dBm)	Occurrence frequency of enhanced signal (%)	VHF threshold value (dBm)	Occurrence frequency of enhanced signal (%)
ALDERNEY			
-77.5	13.3	-88.5	26.0
-77	13.0	-87	20.1
-76	*12.4*	*-86*	*16.6*
PORTLAND			
-108	22.3	-102	28.9
-106	19.9	-100	22.6
-102	*16.8*	*-98.5*	*18.7*

Table 5-7: Enhancement occurrence percentage with different threshold values – Common valid data

Considering the secondary enhancements as well, the statistics of common valid median data, based on threshold levels italicised in Table 5-5, are given below:

Site	Occurrence frequency of enhanced signal (%)	
	UHF	VHF
Alderney	19.9	20.2
Portland	21.4	24.9

Table 5-8: Enhancement occurrence percentage- Primary & secondary combined (common valid data)

As compared to the enhancement percentages based on only primary signal enhancements, there is an increase in percentage enhancement of approx. 3.5 to 7.5 dB.

5.10.2.3. Monthly enhancement statistics

The analysis of enhancement, if segregated on a monthly basis, reveals more interesting results. Using the threshold values italicised in Table 5-5, the monthly breakdown of primary enhancement statistics is shown in Table 5-9:

Month	Occurrence frequency of enhanced signal (%)			
	Alderney UHF	Alderney VHF	Portland UHF	Portland VHF
July 2009	14.5 (157144)	10.7 (157140)	8.17 (166875)	5.87 (166875)
August 2009	11.2 (161306)	13.2 (161318)	19.8 (177401)	26.8 (177403)
September 2009	4.82 (158634)	5.29 (159365)	4.01 (171404)	21.2 (172140)
October 2009	1.66 (99282)	9.29 (99288)	1.78 (178102)	11.2 (178104)
November 2009	0.00 (40422)	0.15 (40421)	0.00 (170611)	0.75 (170614)
December 2009	0.00 (14007)	0.68 (26604)	0.01 (75956)	0.27 (137248)
January 2010	0.00 (6091)	1.10 (6094)	0.19 (172209)	3.51 (172207)
February 2010	0.00 (12940)	13.7 (12969)	0.04 (136084)	0.20 (149462)
March 2010	-	-	8.24 (169793)	6.15 (177624)
April 2010	-	-	32.1 (171709)	21.1 (171717)
May 2010	16.6 (118208)	31.4 (123809)	23.9 (172178)	13.5 (177765)
June 2010	38.8 (111330)	41.3 (172025)	59.9 (111051)	31.4 (171790)

Table 5-9: Monthly enhancement occurrence percentages

The enhancement is expressed as percentage of total valid data within the month, with the brackets showing number of total valid readings in the month. The maximum number of valid readings per day is 5760, making 178560 maximum possible monthly readings for '31-day' months.

In general, days from the end of spring, all of the summer and the start of autumn (almost half a year) show comparatively higher (and significant) percentage enhancements, peaking in June. It is also interesting to observe that the enhancement of signals at Portland is higher during May/June and August but is comparatively much lesser during July. This aspect has been elaborated upon later on in this section as well as in Section 7.3.

Enhanced received signal strength events can practically be of any duration, from the lowest possible resolution to hours long, as was observed in this study. It was observed that many enhancement events were of very short duration (fraction of a minute). It was observed that the signal strength levels

of most of these short-lived instances were very close to the threshold levels selected. The number of short-duration enhancement events reduced with a higher threshold value.

Hence, it was decided to segregate the short and long-duration enhancement events. It was decided to consider enhancement events at least 10 minutes long as the long-duration enhancement events and others as short-duration. This was based on two factors: Firstly, it was observed that the minimum resolution of available, reliable weather data was 10 minutes. Secondly, short-duration enhancement events were analysed on signal strength scales starting from the threshold values and increasing. It was observed that as the signal strength increased, the number of enhancement events decreased drastically. Figure 5-30 shows one such example:

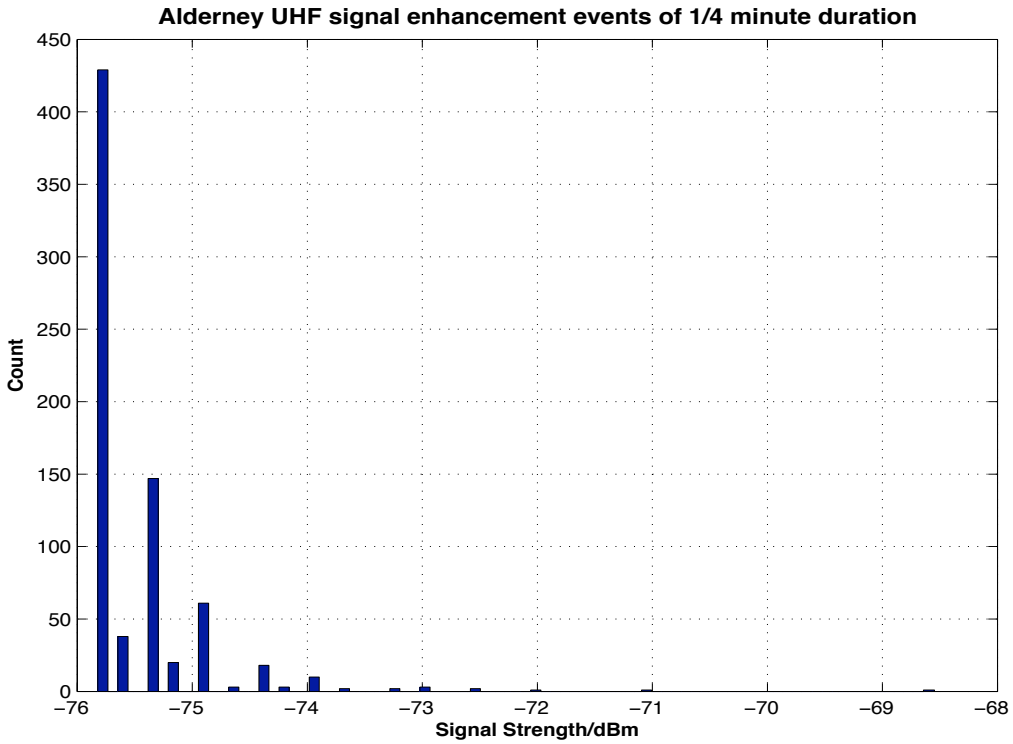

Figure 5-30: Histogram: Short-duration enhancement events of UHF signal at Alderney

This strong downward trend was observed for enhancement events lasting up to 10 minutes. Events lasting at least 10 minutes were seen to have no particular pattern with relation to signal strength levels near/higher than the threshold values.

In the following investigation of enhancement duration, an enhancement event is assumed to have ended whenever data went missing. This is especially true for Alderney because of intermittent hardware failures resulting in missing data (as explained in Chapter 4). This assumption is valid even when the last recorded value was enhanced and the first recorded value after the gap with missing data was enhanced.

Tables 5-10 to 5-17 give insight into monthly breakdown of short and long duration enhancement events:

Month & number of enhancement events		**Maximum duration of event (minutes)**				
		1/4	1/2	1	2	5
Jul 2009	403	36.2	50.6	67.0	77.4	84.4
Aug 2009	263	38.0	54.0	66.5	73.0	79.1
Sep 2009	253	51.8	73.5	81.8	88.9	92.1
Oct 2009	121	58.7	70.2	80.2	90.1	95.0
Nov 2009	0	0.0	0.0	0.0	0.0	0.0
Dec 2009	0	0.0	0.0	0.0	0.0	0.0
Jan 2010	0	0.0	0.0	0.0	0.0	0.0
Feb 2010	0	0.0	0.0	0.0	0.0	0.0
Mar 2010	NaN	-	-	-	-	-
Apr 2010	NaN	-	-	-	-	-
May 2010	372	36.6	48.4	59.7	69.1	80.4
Jun 2010	499	31.5	43.5	53.7	60.1	72.5
Whole year	*1911*	*38.8*	*53.1*	*64.8*	*73.0*	*81.5*

Table 5-10: Alderney UHF signal: Short-duration enhancement events (Percentage share of total enhancement events in the month)

Month	Minimum duration of event (m-minutes, h-hours)									
	10m	15m	30m	1h	2h	3h	6h	9h	12h	18h
Jul 2009	11.9	10.9	8.2	6.2	3.7	3.2	0.7	0.0	0.0	0.0
Aug 2009	16.0	12.9	9.5	6.8	3.8	3.0	0.8	0.4	0.0	0.0
Sep 2009	7.5	6.7	5.1	4.0	2.4	1.2	0.0	0.0	0.0	0.0
Oct 2009	3.3	2.5	2.5	2.5	0.8	0.0	0.0	0.0	0.0	0.0
Nov 2009	0.0	0.0	0.0	0.0	0.0	0.0	0.0	0.0	0.0	0.0
Dec 2009	0.0	0.0	0.0	0.0	0.0	0.0	0.0	0.0	0.0	0.0
Jan 2010	0.0	0.0	0.0	0.0	0.0	0.0	0.0	0.0	0.0	0.0
Feb 2010	0.0	0.0	0.0	0.0	0.0	0.0	0.0	0.0	0.0	0.0
Mar 2010	-	-	-	-	-	-	-	-	-	-
Apr 2010	-	-	-	-	-	-	-	-	-	-
May 2010	13.7	9.7	7.0	5.1	2.4	2.2	0.8	0.3	0.0	0.0
Jun 2010	21.6	18.4	12.4	8.4	5.0	3.4	1.6	0.4	0.0	0.0
Whole year	*14.2*	*11.8*	*8.5*	*6.1*	*3.5*	*2.6*	*0.8*	*0.2*	*0.0*	*0.0*

Table 5-11: Alderney UHF signal: Long-duration enhancement events (Percentage share of total enhancement events in the month)

Generally, the number of UHF signal enhancement events (short and long term) at Alderney is higher in summer. Most of the enhancement events are of short-duration (up to 5 minutes long). Also, longer events tend to occur more in summer than other seasons. There is hardly any signal level enhancement in winter.

Month & number of enhancement events		Maximum duration of event (minutes)				
		1/4	1/2	1	2	5
Jul 2009	1140	46.1	61.6	74.4	82.5	90.3
Aug 2009	1338	29.1	42.4	57.5	74.1	87.1
Sep 2009	478	28.5	47.3	63.2	77.4	90.0
Oct 2009	1247	47.8	64.7	75.9	85.0	94.7
Nov 2009	45	77.8	93.3	95.6	100	100
Dec 2009	106	67.0	84.9	94.3	99.1	100
Jan 2010	49	79.6	89.8	100	100	100
Feb 2010	603	48.4	66.3	83.1	94.5	99.0
Mar 2010	NaN	-	-	-	-	-
Apr 2010	NaN	-	-	-	-	-
May 2010	1991	31.2	45.4	60.8	73.1	86.1
Jun 2010	2797	33.1	47.1	61.7	74.7	85.6
Whole year	*9793*	*37.1*	*52.1*	*66.3*	*78.4*	*88.9*

Table 5-12: Alderney VHF signal: Short-duration enhancement events (Percentage share of total enhancement events in the month)

Month	Minimum duration of event (m-minutes, h-hours)									
	10m	15m	30m	1h	2h	3h	6h	9h	12h	18h
Jul 2009	5.3	4.3	2.8	1.4	0.6	0.1	0.0	0.0	0.0	0.0
Aug 2009	7.1	4.9	2.3	0.9	0.4	0.2	0.0	0.0	0.0	0.0
Sep 2009	6.1	4.4	2.3	1.7	0.8	0.4	0.0	0.0	0.0	0.0
Oct 2009	2.2	1.6	1.2	0.3	0.1	0.0	0.0	0.0	0.0	0.0
Nov 2009	0.0	0.0	0.0	0.0	0.0	0.0	0.0	0.0	0.0	0.0
Dec 2009	0.0	0.0	0.0	0.0	0.0	0.0	0.0	0.0	0.0	0.0
Jan 2010	0.0	0.0	0.0	0.0	0.0	0.0	0.0	0.0	0.0	0.0
Feb 2010	0.2	0.2	0.0	0.0	0.0	0.0	0.0	0.0	0.0	0.0
Mar 2010	-	-	-	-	-	-	-	-	-	-
Apr 2010	-	-	-	-	-	-	-	-	-	-
May 2010	7.9	5.9	3.4	1.4	0.7	0.3	0.1	0	0.0	0.0
Jun 2010	8.7	6.4	3.3	1.8	0.9	0.4	0.3	0.1	0.1	0.0
Whole year	*6.3*	*4.6*	*2.5*	*1.2*	*0.6*	*0.2*	*0.1*	*0.0*	*0.0*	*0.0*

Table 5-13: Alderney VHF signal: Long-duration enhancement events (Percentage share of total enhancement events in the month)

The trend in VHF signal enhancements at Alderney is similar to that of UHF signal. However, as compared to the UHF signal at Alderney, a greater percentage of enhanced VHF signal events at Alderney are of short duration. There are a few enhancement events in winter but all are of short duration.

Month & number of enhancement events		Maximum duration of event (minutes)				
		1/4	1/2	1	2	5
Jul 2009	1777	51.5	68.2	81.2	89.4	95.3
Aug 2009	4145	57.0	74.1	85.2	91.5	95.8
Sep 2009	1265	69.7	85.0	93.0	95.9	98.1
Oct 2009	1366	61.9	79.9	90.8	97.7	99.2
Nov 2009	1	100	100	100	100	100
Dec 2009	4	100	100	100	100	100
Jan 2010	199	69.8	85.4	95.5	99.0	100
Feb 2010	48	85.4	95.8	100	100	100
Mar 2010	897	49.2	66.3	78.6	87.7	94.6
Apr 2010	2451	44.6	61.1	74.0	84.4	92.2
May 2010	2504	40.4	57.0	71.9	82.2	91.2
Jun 2010	3511	51.8	66.8	78.2	85.9	93.3
Whole year	*18168*	*52.6*	*69.0*	*80.9*	*88.7*	*94.6*

Table 5-14: Portland UHF signal: Short-duration enhancement events (Percentage share of total enhancement events in the month)

Month	Minimum duration of event (m-minutes, h-hours)									
	10m	15m	30m	1h	2h	3h	6h	9h	12h	18h
Jul 2009	2.3	1.7	0.8	0.5	0.2	0.1	0.1	0.0	0.0	0.0
Aug 2009	2.5	1.9	1.1	0.5	0.2	0.2	0.1	0.0	0.0	0.0
Sep 2009	1.3	1.1	0.6	0.4	0.1	0.1	0.1	0.0	0.0	0.0
Oct 2009	0.3	0.1	0.1	0.0	0.0	0.0	0.0	0.0	0.0	0.0
Nov 2009	0.0	0.0	0.0	0.0	0.0	0.0	0.0	0.0	0.0	0.0
Dec 2009	0.0	0.0	0.0	0.0	0.0	0.0	0.0	0.0	0.0	0.0
Jan 2010	0.0	0.0	0.0	0.0	0.0	0.0	0.0	0.0	0.0	0.0
Feb 2010	0.0	0.0	0.0	0.0	0.0	0.0	0.0	0.0	0.0	0.0
Mar 2010	3.9	3.3	2.1	0.8	0.6	0.3	0.3	0.2	0.0	0.0
Apr 2010	4.6	3.7	2.1	1.4	0.9	0.7	0.4	0.2	0.1	0.0
May 2010	5.6	4.0	2.0	1.2	0.6	0.4	0.1	0.0	0.0	0.0
Jun 2010	3.9	2.8	1.8	0.3	0.7	0.5	0.3	0.2	0.1	0.1
Whole year	*3.2*	*2.4*	*1.4*	*0.8*	*0.5*	*0.3*	*0.2*	*0.1*	*0.0*	*0.0*

Table 5-15: Portland UHF signal: Long-duration enhancement events (Percentage share of total enhancement events in the month)

Like the enhanced signal events at Alderney, most of the enhancement events at Portland are of short duration. A greater number of enhancement events and greater percentage of longer events occur in summer.

Month & number of enhancement events		Maximum duration of event (minutes)				
		1/4	1/2	1	2	5
Jul 2009	3211	54.1	74.7	88.4	95.5	98.7
Aug 2009	8240	34.9	51.7	69.5	84.5	95.7
Sep 2009	7984	34.9	53.4	73.3	87.8	97.1
Oct 2009	4870	43.8	61.2	77.9	90.3	97.6
Nov 2009	891	72.8	91.1	98.3	100	100
Dec 2009	256	73.0	91.4	97.3	99.6	100
Jan 2010	2109	42.9	64.4	84.4	95.6	99.4
Feb 2010	155	52.3	73.5	97.4	98.7	100
Mar 2010	2084	40.6	60.3	77.8	90.0	96.6
Apr 2010	4501	36.9	55.2	73.0	86.1	95.3
May 2010	2694	34.4	48.9	66.6	81.0	92.1
Jun 2010	5579	33.9	51.1	67.6	81.1	92.4
Whole year	*42574*	*39.2*	*57.2*	*74.6*	*87.4*	*96.1*

Table 5-16: Portland VHF signal: Short-duration enhancement events (Percentage share of total enhancement events in the month)

Month	Minimum duration of event (m-minutes, h-hours)									
	10m	15m	30m	1h	2h	3h	6h	9h	12h	18h
Jul 2009	0.6	0.2	0.1	0.1	0.0	0.0	0.0	0.0	0.0	0.0
Aug 2009	1.4	0.8	0.3	0.1	0.0	0.0	0.0	0.0	0.0	0.0
Sep 2009	0.6	0.2	0.1	0.0	0.0	0.0	0.0	0.0	0.0	0.0
Oct 2009	0.9	0.4	0.1	0.0	0.0	0.0	0.0	0.0	0.0	0.0
Nov 2009	0.0	0.0	0.0	0.0	0.0	0.0	0.0	0.0	0.0	0.0
Dec 2009	0.0	0.0	0.0	0.0	0.0	0.0	0.0	0.0	0.0	0.0
Jan 2010	0.2	0.1	0.0	0.0	0.0	0.0	0.0	0.0	0.0	0.0
Feb 2010	0.0	0.0	0.0	0.0	0.0	0.0	0.0	0.0	0.0	0.0
Mar 2010	1.2	0.6	0.3	0.3	0.0	0.0	0.0	0.0	0.0	0.0
Apr 2010	2.3	1.4	0.8	0.4	0.2	0.1	0.0	0.0	0.0	0.0
May 2010	4.0	2.4	0.9	0.3	0.1	0.0	0.0	0.0	0.0	0.0
Jun 2010	3.7	2.1	0.9	0.4	0.2	0.1	0.0	0.0	0.0	0.0
Whole year	*1.6*	*0.8*	*0.4*	*0.2*	*0.1*	*0.0*	*0.0*	*0.0*	*0.0*	*0.0*

Table 5-17: Portland VHF signal: Long-duration enhancement events (Percentage share of total enhancement events in the month)

There are VHF signal enhancement events at Portland throughout the year, although most of them are of short duration. A lesser percentage of enhanced signal events is of longer duration, as compared to enhanced UHF signal events at Portland.

The cumulative distributions of the duration of enhancement events at Portland and Alderney are shown by Figure 5-31, which indicates that the UHF enhancement events last longer than the VHF enhancement events at both the receiving sites. The same trend was observed when using all valid data from both sites independently.

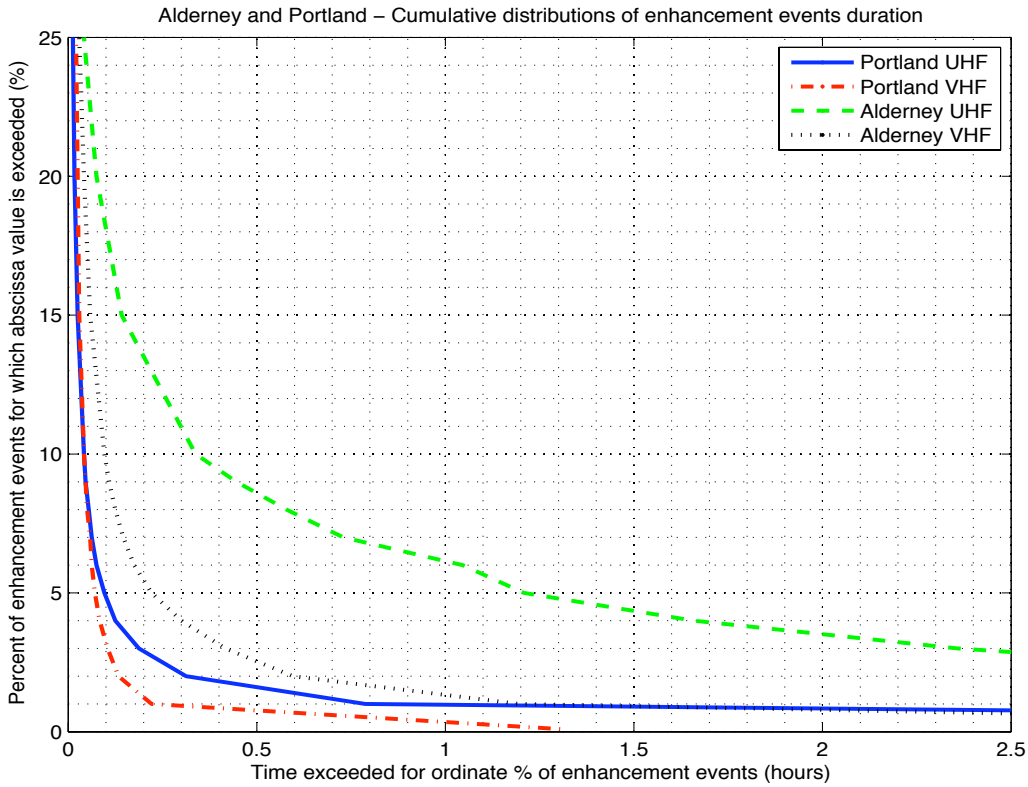

Figure 5-31: Hourly enhancement as percentage of total enhancement

According to the results of Tables 5-10 to 5-17, the clear difference between percentages of signal enhancements observed in June 2010 and August 2009 as compared to those in July 2009, as observed in Table 5-9, is insignificant for longer duration enhancement events.

It was also observed that the UHF signal received at Alderney experiences fewer enhancement events as compared to VHF and also to those at Portland. Despite intermittent hardware failures and considerably more instances of missing data at Alderney, the enhancement events at Alderney tend to last longer, as compared to enhancement events at Portland.

Comparing the longer enhancement events at both receiving sites, Alderney shows greater percentage of enhancement events than Portland for both

frequencies. Enhanced VHF signal events at Portland tend to last for least duration by comparison.

5.10.2.4. Hourly breakdown of enhancement

Figures 5-32 and 5-33 show the number of enhanced signals in a given hour expressed as a percentage of the total number of enhanced signals at Alderney and Portland respectively. For Alderney (Figure 5-32), the occurrence of enhanced UHF signal strengths peaks at 1800 hours while reaches minimum at 1000 hours. For VHF, the peak hour is 1800 while the hour with minimum share of enhancements is 0800.

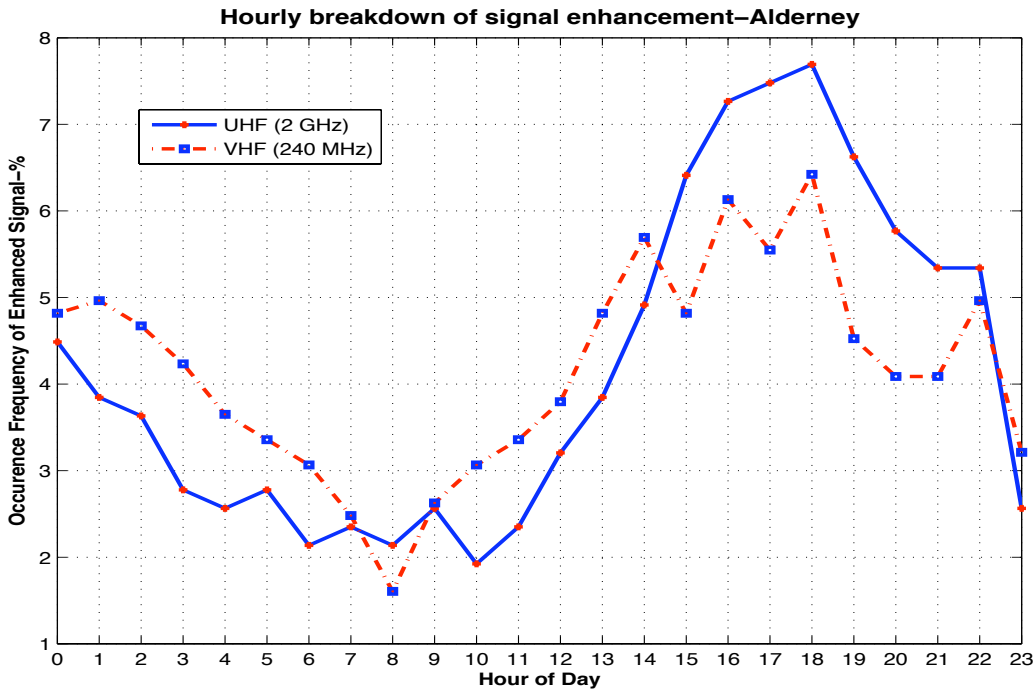

Figure 5-32: Hourly enhancement as percentage of total enhancement - Alderney

Hence enhanced signal strengths predominantly occur during late afternoon/evening periods, with 40% and 34% of UHF and VHF enhancements respectively taking place between 1400 and 1900 hours. The

general 24-hour shape has one high (1500-1800 hours) and one low (0800-1000 hours).

For Portland (Figure 5-33), the peak enhancement for UHF signal occurs between 1600 and 1700 hours while that for VHF is between 1500 and 1600 hours. The hours with minimum share of enhancement are 1000 hours for UHF while evening 1900 hours sees minimum enhancement of VHF signal at Portland. Hence the VHF signal at Portland does not have a diurnal pattern of a clear low and high separated in time as morning and late afternoon/early evening, unlike both signals at Alderney and UHF signal at Portland.

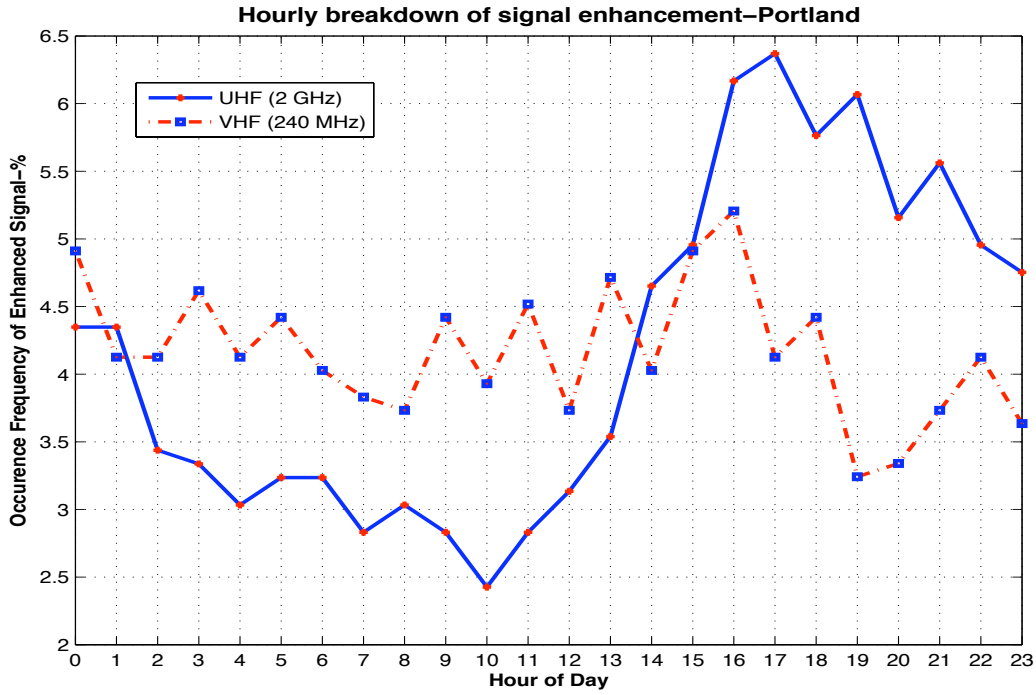

Figure 5-33: Hourly enhancement as percentage of total enhancement - Portland

A diurnal pattern was also observed by Gunashekar [50] and was attributed to temperature inversions and rapid relative humidity lapse rates between Jersey and Guernsey.

5.10.2.5. Effects of enhancement on short-term variation

As discussed earlier in Chapter 5, 25 values were being recorded over a 2-second period, four times in a minutes, at each frequency. It was observed that there were at most only a couple of readings of invalid high signal strength during an otherwise non-enhanced set of 25 readings within a 2-second period. An investigation of the IDR of the signal variation during the 2-second period is analysed here, mainly to identify any major change in behaviour of short-time signal variation during and outside periods of enhanced signal reception. Analysing the IDR effectively means that the influence of the short bursts has been excluded from this analysis. It may be noted that combined enhancement includes both primary and secondary enhancement times.

Table 5-18 shows the median values of the inter-decile range of signal variation within the 2-second period (to 2 d.p.), taken from different datasets.

Source of 2-second data	**Median value of inter-decile range (dB)**			
	Alderney UHF	Alderney VHF	Portland UHF	Portland VHF
Whole dataset	0.87	0.30	12.82	2.32
Primary enhancement times	1.78	0.00	1.81	0.81
Secondary enhancement times	0.80	0.30	4.56	1.38
Combined enhancement times	1.21	0.26	3.47	0.83
Excluding primary enhancement times	0.82	0.30	13.37	2.80
Excluding all enhancement times	0.82	0.30	13.06	2.65

Table 5-18: Median values of inter-decile range of signal level variation within 2-second period, based on set of 25 readings per 2-second period

The median values of the inter-decile range of signal level variation within 2-second period reduce during periods of enhancement, except for the UHF signal at Alderney. This shows that the UHF signal at Alderney is mostly stable (i.e. not varying a lot during 2-second period) most of the times, during and outside enhancement times. The reduction in two-second IDR is considerably pronounced for the UHF signal at Portland. Hence, enhancement tends to reduce fading depth except for UHF signal at Alderney, which shows a larger median value of short-term variation during enhancement than during periods of non-enhancements. The plots of signal enhancement (Figures 5.27 & 5.28) also show that the short-term variation in the signal level reduces during periods of enhancement.

5.10.2.6. Mutual enhancement statistics

Concurrent as well as exclusive enhancements in UHF and VHF signals were also observed at both the receiving stations. Single-frequency as well as co-frequency enhancements are observed at both sites, as shown by Table 5-19:

Enhancement parameter	Alderney	Portland
Concurrent UHF & VHF enhancement (% of annual valid received data)	8.33	5.12
UHF-only enhancement (% of annual valid received data)	2.82	4.78
VHF-only enhancement (% of annual valid received data)	7.63	4.94
Mutual enhancement events at least 10 minutes long (% of total number of enhancement events)	40.5	9.32
Mutual enhancement events at least 1 hour long (% of total number of enhancement events)	18.9	1.42
Maximum concurrent enhancement duration (hours)	~10.4	~12.5

Table 5-19: Mutual co-site enhancement parameters

Considerably higher percentage of mutual UHF and VHF signal enhancement events at Alderney last longer as compared to those at Portland. Table 5-20 below investigates the statistics involving simultaneous co-frequency enhancements at both receiving sites, showing that both sites receive simultaneous as well as non-concurrent signal enhancements.

Enhancement parameter	VHF	UHF
Concurrent enhancement at both sites (%)	8.12	9.78
Alderney-only enhancement (%)	5.79	2.00
Portland-only enhancement (%)	9.20	8.02
Mutual enhancement events at least 10 minutes long (% of total number of enhancement events)	17.4	27.3
Mutual enhancement events at least 1 hour long (% of total number of enhancement events)	2.34	10.2
Maximum concurrent enhancement duration (hours)	~11	~11.5

Table 5-20: Mutual co-frequency enhancement parameters

The results are particularly interesting for Portland, because ~9% of time for VHF and ~8% of time for UHF, Portland receives enhanced signals while respective signals being received at Alderney are non-enhanced. Looking at this from interference point-of-view, consider a radio link setup wherein VHF and UHF signals were being transmitted from Jersey and were intended to be received at Alderney. The receivers at Alderney would show non-enhanced, normal signal levels. However, these very signals transmitted from Jersey would be received at Portland in strong levels, causing potential interference to receivers in Portland operating at similar frequencies. A normal link budget calculation for receivers at Alderney would imply that since signal levels at

Alderney are not enhanced, beyond Alderney, signal levels would be even weaker. However, this experiment shows that this is not always the case. This is an important implication in radio-communications, since spatial shielding is often used as a natural screen for frequency re-use. Hence, more care is required with paths over water. This is an aspect that could be investigated further.

5.10.2.7. Median signal strength during and outside enhancement

Table 5-21 gives the values of median signal strengths during different times. The results with mean values were similar and hence not included here. In order to compare both sites, data was analysed only from days when both receivers were recording (independent results from both receiving sites are similar and hence not included here).

Dataset	Median signal strength value (dBm)			
	Alderney UHF	Alderney VHF	Portland UHF	Portland VHF
Whole dataset	-90.4	-91.7	-119.0	-108.1
Primary enhancement	-61.7	-81.5	-82.6	-94.2
Secondary enhancement	-85.2	-89.8	-112.3	-104.5
Non-enhanced times	-91.9	-92.7	-121.0	-110.9

Table 5-21: Median signal strengths during enhanced/non-enhanced times from common median dataset

The changes in median values of signal strength from when the signals are not enhanced to when they are enhanced are approx. 30 dB for UHF signal at Alderney, 11 dB for VHF signal at Alderney, 38 dB for UHF signal at Portland and 17 dB for VHF signal at Portland. The approximate gap between median UHF signal levels at Alderney and Portland during non-enhanced times is

29 dB while that for VHF signal levels is 18 dB. During enhancement, the respective gaps reduce to approx. 21 dB and 12.5 dB.

Hence, it can be observed that on average signals at Portland experienced greater enhancement in signal levels as compared to Alderney. Also, UHF signals experienced greater magnitude of level enhancement, which echoes with the lower propagation loss values for UHF (than VHF) due to the mechanisms of ducting and/or layer reflection/refraction from troposphere (excluding free space loss), as predicted by ITU P.452.

5.10.3. Propagation mechanism(s) during enhancement

Figure 5-34 shows some examples of enhanced signal strength events (marked in red) at Alderney of comparatively longer duration.

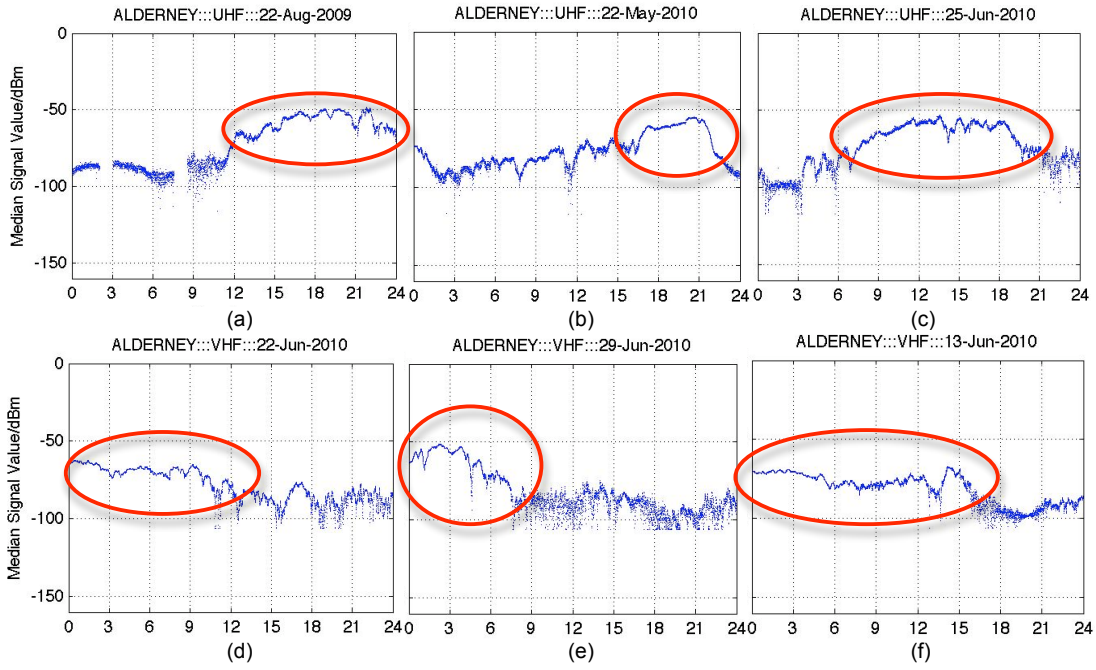

Figure 5-34: Alderney – Samples of signal strength enhancement events of longer duration (> 9 hours)

In order to identify prevalent mechanism during the enhanced signal strength events, the enhanced events were compared to the signatures identified by Shen and Vilar in their study [55], which indicated that these signatures best matched the 'ducting enhancement' events. This implied that the enhanced signal strength events were most probably due to some form of ducting.

Figure 5-35 shows the longer VHF signal level enhancement events at Portland:

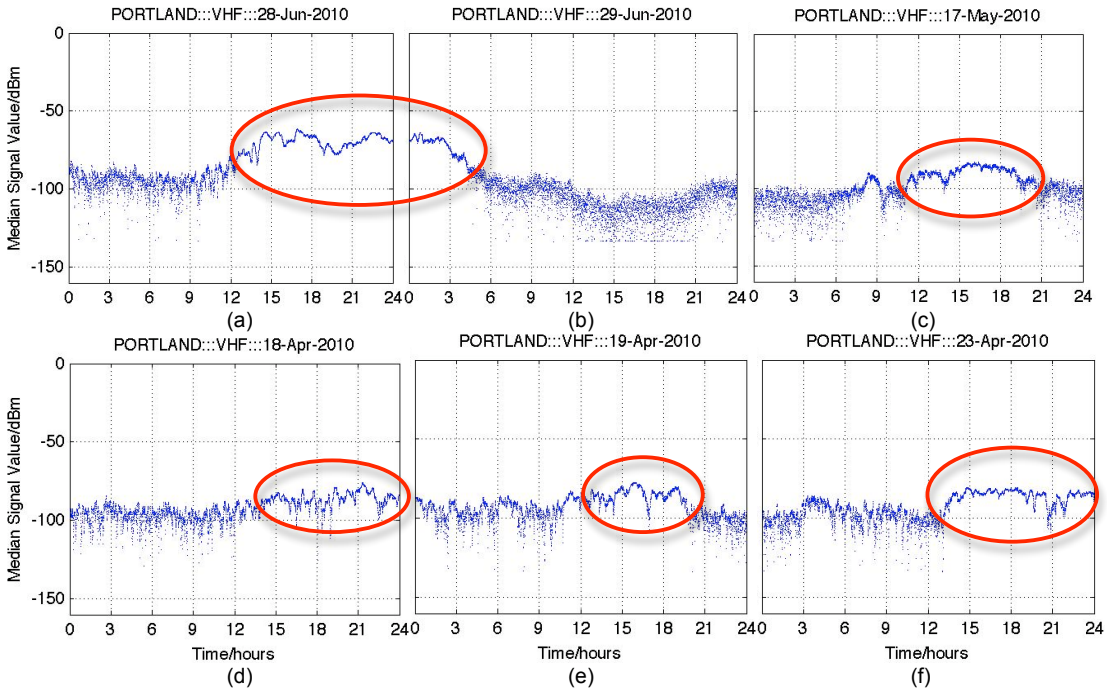

Figure 5-35: Portland – Samples of VHF signal strength enhancement events of longer duration (> 6 hours)

The signatures of enhancement events in Figure 5-35 best match the 'ducting enhancement' signatures of Shen and Vilar [55]. Figure 5-36 shows the longer UHF signal enhancement events at Portland:

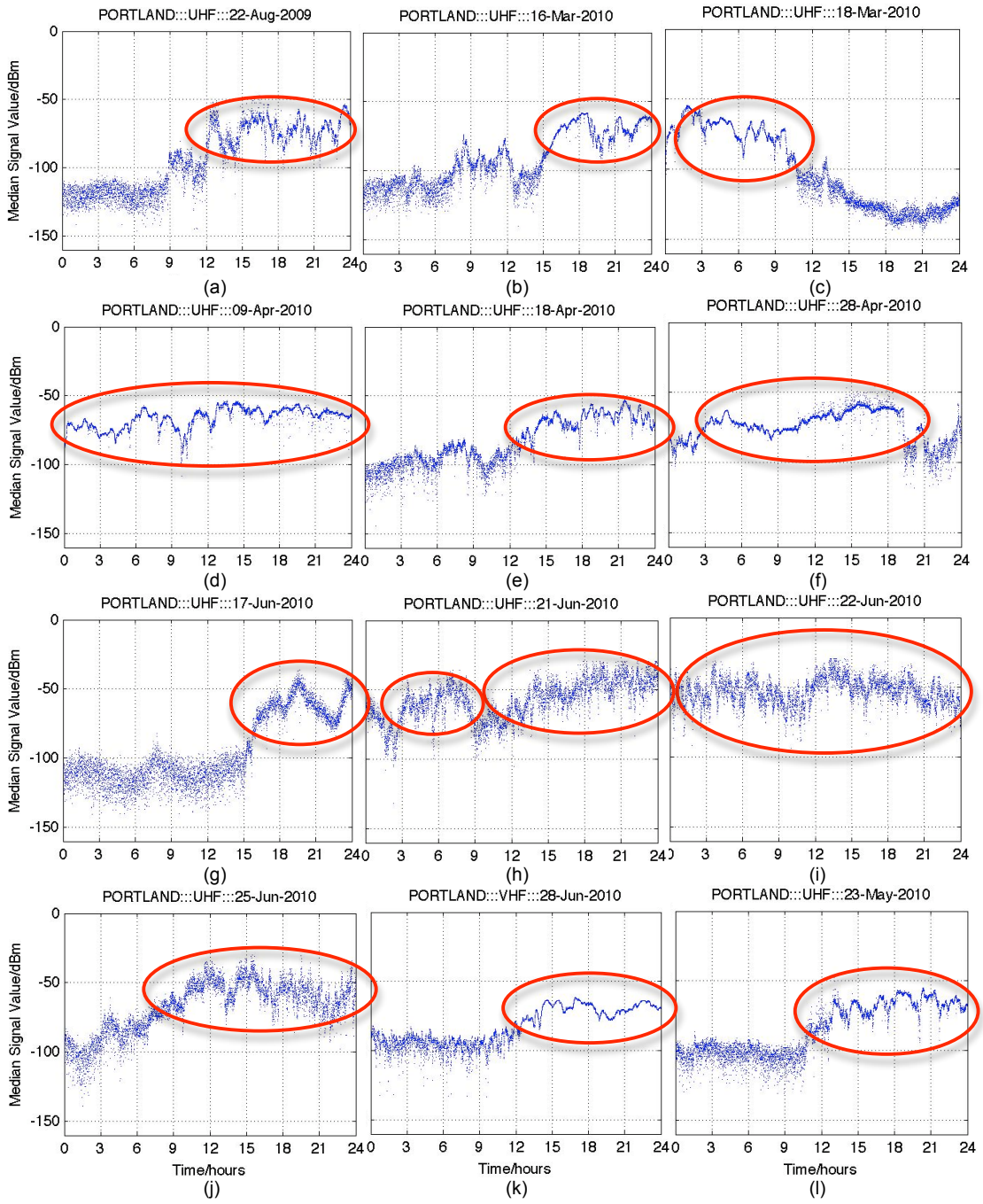

Figure 5-36: Portland – Samples of UHF signal strength enhancement events of longer duration (> 9 hours)

The signatures of most of the enhancement events in Figure 5-36 (sub figures (a) through (f), (k) & (l)) best match the 'ducting enhancement' signatures of Shen and Vilar [55]. However, enhancement the events shown by sub figures (g) through (j) do not show the same degree of signal level stability during

enhancement and appear to match the 'layer reflection enhancement' signatures.

Hence, based on signature comparison, most of the long duration signal enhancement events appear to be the result of ducting. The signatures for enhanced UHF signals at both the receiving sites also indicate a possible layer reflection mechanism. Mixed signatures (ducting and layer reflection) are also observed for all signals, although ducting signature is comparatively dominant during such events.

5.11. Interim Conclusions

The basic dataset used for further investigations is the one based on the median value of every set of 25 readings recorded over period of 2-seconds.

For comparison with meteorological data, the hourly data (median as well as values at the hour) has been used. Cumulative distributions of received signal strength of the hourly as well as the median datasets show similar trends. Cumulative path loss curves for the two frequencies and receiving sites indicates a greater degree of enhancement for UHF signals.

Most of the longer signal level enhancement events are observed in summer months. UHF enhancement events last longer than the VHF enhancement events at both the receiving sites while the enhancement events at Alderney tend to last longer, compared to those at Portland. Hourly breakdown of

enhancement events reveals a diurnal pattern, with a greater percentage of enhanced signal strengths predominantly occurring during late afternoon/evening periods and the least during morning. Generally, signal strength enhancement tends to reduce the short-time fading. Concurrent as well as isolated signal strength enhancements at both the receiving sites/frequencies have been observed, which can have implications in radio network interference management.

On average, signals at Portland experienced greater enhancement in signal levels as compared to Alderney. Also, UHF signals experienced greater magnitude of level enhancement. Most of the long duration signal enhancement events appear to be the result of ducting.

6. ANALYSIS OF HOURLY METEOROLOGICAL DATA AND MODELLING OF PROPAGATION LOSS AND EVAPORATION DUCTING

This chapter contains in-depth analysis of the hourly meteorological data, followed by modelling of the propagation loss using the same data data, comprehensive treatment of the enhanced signal strength events and ducting, with emphasis on evaporation ducting.

6.1. Horizontal Homogeneity

Gunashekar used meteorological data from several sources, including Channel Light Vessel, which was at least 50 km away from receiving sites [50]. The study was based on the assumption of horizontal homogeneity. In order to verify this assumption, the data from the Channel Light Vessel was compared to data from two nearby lightships in the English Channel (Seven Stones & Greenwich). Both these ships are more than 200km away from the Channel Light Vessel. 'Excellent' correlation of the hourly meteorological parameters was observed between the three lightships over the two years of the measurement campaign. As a result, the marine weather conditions in the British Channel Islands were approximated to those recorded at the Channel Light Vessel.

Similarly, weather data from different sources, which are geographically separated from each other, was used in this study. The values of weather

variables at hourly time instants common to all the five weather stations (Figure 4-1) were used in this analysis. Ideally, meteorological information from the sites involved in research and midpoints of the paths should be used. In the absence of this idealised arrangement, weather stations closest to the sites and the paths were used. It is, however, pertinent to mention that all the weather stations used in this study are less than 200 km away from each other (Table 4-2).

The weather variables (temperature, pressure, wind speed, wind direction and dewpoint/humidity) were measured and recorded by different weather stations, at different locations and heights, around the Channel Islands. The correlation between the concurrent values of these weather variables is summarised in Table 6-1:

Weather station pair	**Weather variable**					
	Dewp	Humid	Press	Temp	Wdir	Wspd
CLV-Portland	0.966	0.628	0.997	0.936	0.722	0.808
CLV-Jersey	0.940	0.389	0.992	0.890	0.665	0.769
CLV-Alderney	0.974	0.650	0.997	0.947	0.757	0.851
CLV-Guernsey	0.970	0.568	0.997	0.920	0.732	0.812
Portland-Jersey	0.922	0.547	0.985	0.932	0.613	0.690
Portland-Alderney	0.957	0.677	0.993	0.957	0.679	0.739
Portland-Guernsey	0.954	0.636	0.990	0.947	0.672	0.712
Jersey-Alderney	0.960	0.759	0.997	0.969	0.736	0.833
Jersey-Guernsey	0.964	0.805	0.999	0.983	0.773	0.866
Alderney-Guernsey	0.982	0.839	0.999	0.982	0.773	0.856

Table 6-1: Values of correlation coefficients between weather variables recorded at different meteorological stations

Hence, a very high correlation between pressure, temperature and dewpoint and reasonable correlation between wind direction and wind speed were observed. There was also high correlation for humidity between sites that

were geographically closer and were recording at comparable heights (e.g. Jersey, Alderney & Guernsey).

When the correlation trends were investigated on monthly/seasonal basis, it was observed that generally the correlations were higher during winter and comparatively lower during summer, though still remaining strong, especially between sites closer to each other and at comparable heights.

The high values of correlation coefficients indicated that the changes in weather conditions that took place were on sufficiently larger horizontal distance to affect all the sites of the project. Also, all these weather stations benefitted from the fact that they were coastal (except CLV which was in the middle of the sea). It was assumed that the weather variables at a fixed height and fixed time were very similar at the different weather stations of interest. Hence, a horizontal homogeneity of weather was assumed, supported by the correlation analysis. This enabled using the sea level data from the Channel Light Vessel to represent sea-level refractivity for paths under study, to relate evaporation ducting to propagation on the two over-sea paths and deriving refractivity statistics in the lowest portions of the troposphere.

6.2. Lapse Rate of Refractivity

The work by Bean et al [43] considered 268 global stations to produce contours of the average refractivity lapse rate in the lowest 1 km of atmosphere. The values of the monthly mean lapse-rates of refractivity (N-

units) for different months in the English Channel, estimated from the global contours were: 40 for January to April, 50 for May to October, between 40 & 50 for November and 40 for December. Annual mean value of lapse rate based on these monthly values was 45.4 N-units. The average annual mean value of the gradient between surface and 1km above surface, estimated from the annual contour, was 50 N-units.

The current ITU data for lapse rate of refractivity exists in the form of digital maps, derived from analysis of a ten-year (1983–1992) global dataset of radiosonde ascents. The median annual values and at times seasonal values are contained in text files in grid format. For a location different from the grid-points, the parameter at the desired location can be derived by performing a bi-linear interpolation on the values at the four closest grid-points, as described in Recommendation ITU-R P.1144 [28].

The ITU-R Recommendations use path-centre value, which is the value of the meteorological parameter for the centre of the path. The path-centres for both the experimental paths have been defined in Chapter 4. The values of average annual lapse rate of refractivity for path centre locations, obtained by the method outlined above, are approximately 43 N-units [18,28]. ITU uses positive values for lapse rate for use in its prediction models [21]. It is based on the way ITU has defined lapse rate. The lapse rate derived from ITU data, 43 N-units, is actually -43 N-units/km, when expressed as the rate of change of refractivity with height (or in other words, the vertical gradient of refractivity).

Previous research into average refractivity lapse rates in Europe carried out by Bye and Howell [42] was based on radiosonde data of 18 stations in North-West Europe from 1975 to 1981. To obtain data at a certain height, linear interpolation between previous and next reading was used. It was assumed that temperature, pressure and dewpoint vary linearly between recorded data points. The results of this research have been plotted as cumulative distributions of the average refractivity lapse rate versus percentage of occurrence for different heights up to the lowest 2km of the atmosphere. It was concluded that: (i) the atmosphere is not well mixed (independent of height) for median conditions, (ii) if super-refraction is defined as lapse rates less than -40 N-units/km, the air nearer the ground is more often super-refractive than the air higher up and (iii) the lower part of troposphere is well mixed for 5% of time, super-refractive for less than 73% of time and sub-refractive for more than 22% of time.

6.2.1. Lapse rate of refractivity from radiosonde stations

Information about the radiosonde stations used in this analysis has already been provided in Chapter 4. In order to estimate the lapse rate of refractivity, the reading at lowest height and the reading closest to 1km above sea level were used. As a daily routine, most of the radiosonde readings are taken by starting from station height and then at heights above sea level around 200m, 850m, 1550m and further up. Normally, the readings at station height and the readings around 850m (being closest to 1km) are used to determine the value of refractivity gradient. If for any reason, the reading around 850m is missing,

the reading at next higher height (around 1550m) is used. This has been done so that the height closest to 1km is used for determining the values of lapse rate of refractivity in the lowest 1km of atmosphere.

The median refractivity lapse rate (to 2 d.p.) for each radiosonde station is given in Table 6-2:

Radiosonde station	Nearest test site and distance (km)	Bearing from nearest test site	Distance from coast	Median lapse rate of refractivity ΔN (N-units/km)
Camborne	Portland, 210	West	2.25 km	-33.74
Hertsmonceux	Portland, 200	East	7.5 km	-32.75
Brest	Jersey, 190	South West	20 km	-34.61
Larkhill	Portland, 85	North East	54 km	-32.86
Trappes	Jersey, 310	South East	145 km	-32.78

Table 6-2: Median refractive index lapse rates of radiosonde stations

The median values of refractivity lapse rates for around noon and midnight for each site (except Larkhill) are given in Table 6-3, wherein the brackets show number of readings for each time:

Radiosonde station	Median lapse rate of refractivity (N-units/km) – Noon	Median lapse rate of refractivity (N-units/km) – Midnight
Camborne	-33.36 (355)	-33.90 (359)
Hertsmonceux	-31.68 (126)	-33.05 (327)
Brest	-34.74 (323)	-34.54 (346)
Larkhill	-30.95 (44)	N/A (0)
Trappes	-32.82 (359)	-32.79 (347)

Table 6-3: Median lapse rate of refractivity - Radiosonde stations

As can be observed from the median values from noon and midnight, on average there is not a lot of variation between noon and midnight lapse rates.

Figure 6-1 shows the monthly median refractivity lapse rates, from July 2009 to June 2010 inclusive, showing that the lapse rate is minimum (i.e. magnitude of lapse rate is maximum) in August and maximum in February. The maximum change between lapse rates of two consecutive months happens between May and June:

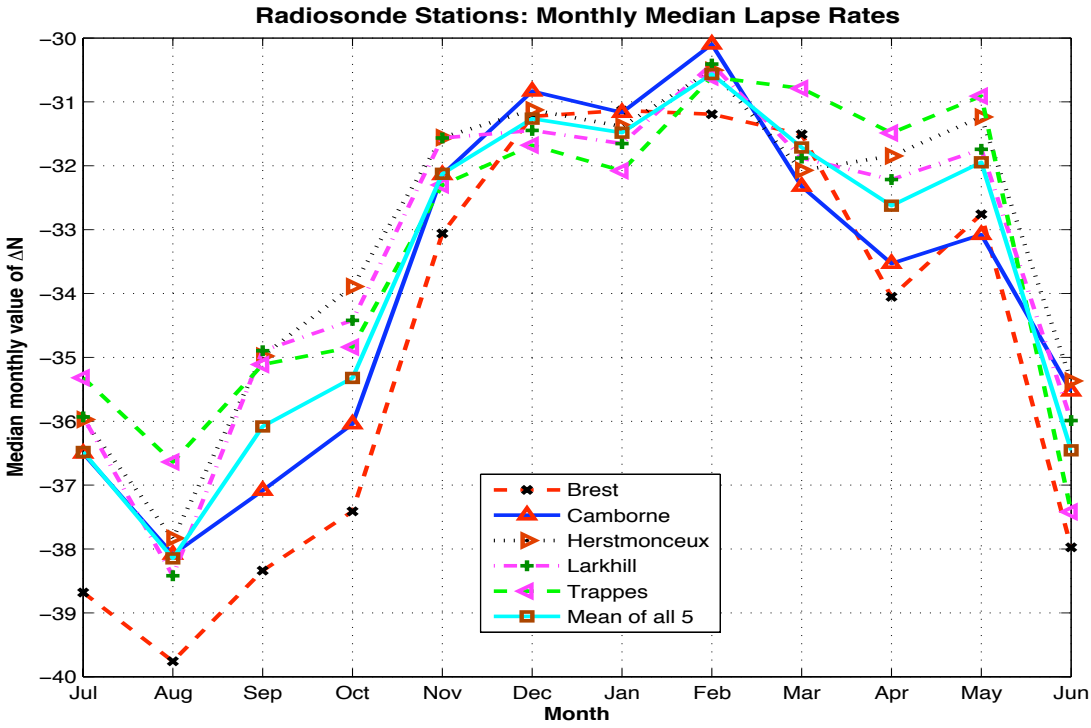

Figure 6-1: Radiosonde stations – Monthly median lapse rates of refractivity

Figure 6-2 shows the cumulative distribution of the values of lapse rate of refractivity in the lowest 1 km of atmosphere:

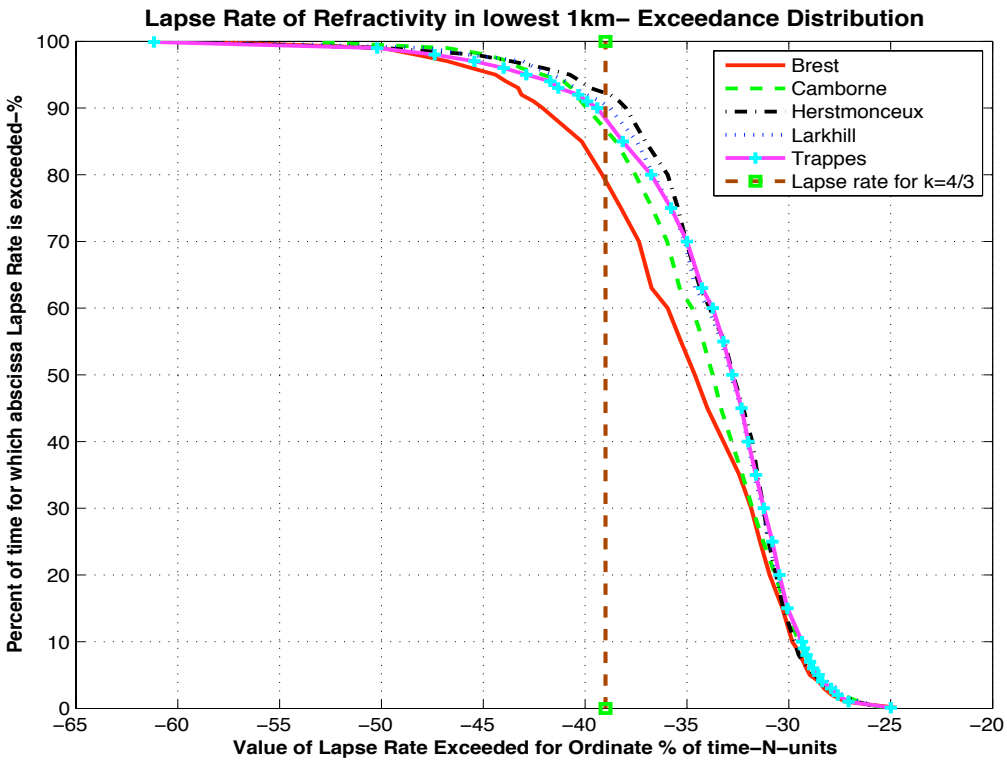

Figure 6-2: Cumulative frequency distribution: Lapse rate of refractivity – Radiosonde stations

Lapse rates leading to values of effective earth's curvature factor 'k' greater than the standard value of k=4/3 exist for almost 19.4% at Brest, 12.4% at Camborne, 7.25% at Herstmonceux, 8.9% at Larkhill and 10.7% at Trappes. Hence, since the Channel Islands are located in the vicinity of the radiosonde stations, such lapse rates can be expected between approximately 7% and 20% of time.

6.2.2. Comparison of refractivity analysis of weather stations and radiosonde stations

In the absence of any radiosonde data in very close proximity of the test sites, the weather data available from weather stations situated near to the sites can be useful. Each of the weather stations provides a set of refractivity values at

a certain height above mean sea level. The stations are listed in Chapter 4 and are at heights from sea level to 102 m above mean sea level. Although CLV is placed on sea level, the meteorological readings are taken at height of 5m while wind-related readings at 14m AMSL. A value for refractivity gradient can be obtained by using any pair of weather stations. The difference in refractivity values divided by the difference in heights of the two stations (in km) gives the normalised lapse rate of refractive index in lowest 1 km of atmosphere. These lapse rate values are hence extrapolated using refractivity gradients from lesser heights, assuming that the gradient remains constant throughout the lowest 1 km of atmosphere.

It may be noted that weather data available from various sources for Alderney was not available for almost 12 hours per day, from around 1730 to 0530 next day. Hence, the weather station pairs with Alderney as one of the sites were not included in comparison.

The refractivity results were compared to respective radiosonde data for different factors:

I. Comparison of median lapse rate from each pair with median lapse rates of neighbouring radiosonde stations
II. Comparison of median lapse rate of each pair with average annual lapse rate published by ITU
III. Comparison & correlation of monthly median lapse rates from each pair with monthly median lapse rates from neighbouring radiosonde stations

IV. Height difference of weather stations (to give as much vertical profile information about troposphere as possible)

The median refractivity gradient values for different pairs are given in Table 6-4, along with heights of the sites and approximate distances between the sites of the pair:

Weather station pair for refractivity calculations	Heights AMSL (m)	Distance between sites	Median refractivity gradient (N-units/km)
Alderney-Guernsey	89, 102	45 km	6.1
CLV-Alderney	0, 89	55 km	-34.3
CLV-Guernsey	0, 102	55 km	-30.8
CLV-Jersey	0, 84	90 km	-37.7
CLV-Portland	0, 52	75 km	-33.0
Jersey-Alderney	84, 89	50 km	22.3
Portland-Alderney	52, 89	90 km	-40.8
Portland-Guernsey	52, 102	120 km	-29.2
Portland-Jersey	52, 84	145 km	-45.2
Jersey-Guernsey	84,102	39 km	-2.2

Table 6-4: Median refractivity gradients for different pairs of weather stations

If the pairs involving Alderney are not considered (owing to the lack of data), the median lapse rate values from CLV-Guernsey, CLV-Portland, CLV-Jersey and Portland-Guernsey are close to the median values of median refractive index lapse rates for the neighbouring radiosonde stations (Ref. Tables 6-2 & 6-3) as well as to the ITU data [18, 28].

Figure 6-3 shows the monthly mean values of lapse rates of refractivity from radiosonde stations and monthly mean values of lapse rates extrapolated from the weather station pairs, excluding pairs with Alderney as a site. The comparison puts Jersey-Guernsey and Portland-Jersey as obvious outliers,

CLV-Jersey, Portland-Guernsey & CLV-Portland pairs as minor outliers to the radiosonde curves, and CLV-Guernsey as the one closest to radiosonde station curves.

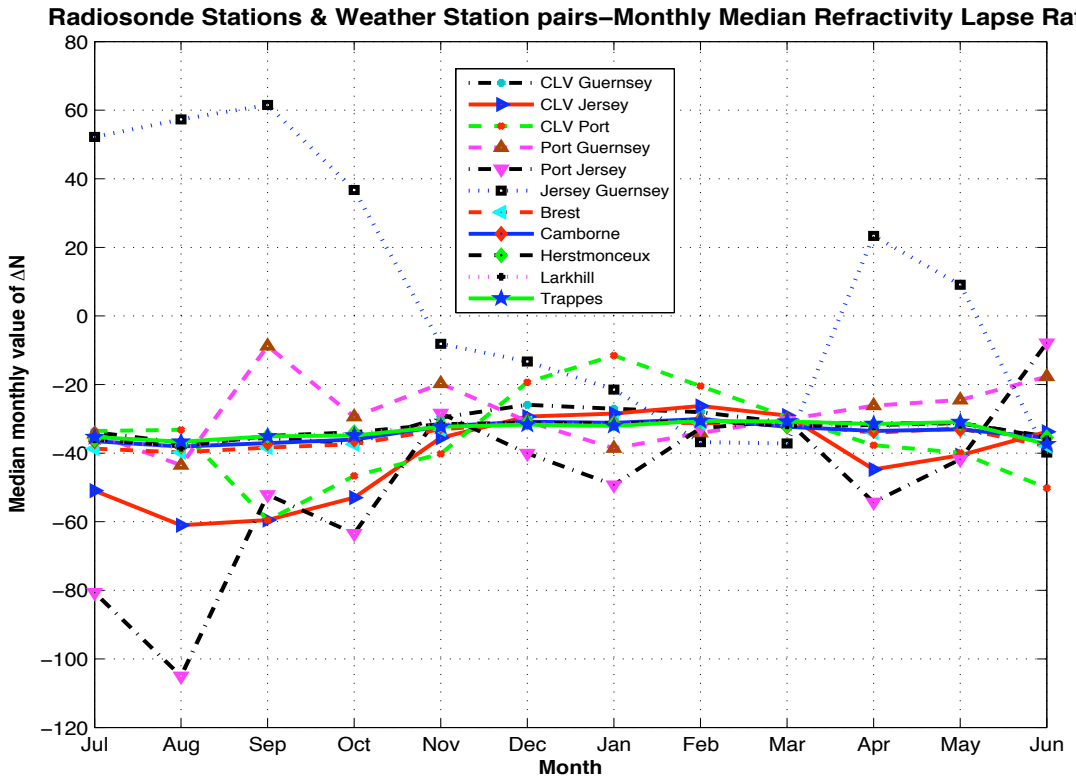

Figure 6-3: Monthly median values of lapse rate of refractivity for radiosonde stations and weather station pairs (without Alderney)

The correlation statistics between monthly median values of refractivity gradients from the three 'closest' pairs and lapse rates from three coastal radiosonde stations are summarised in Table 6-5:

Radiosonde station	**Pair used to calculate normalised refractive index lapse rate**				
	CLV-Guernsey	Portland-Guernsey	CLV-Portland	Portland-Jersey	Jersey-Guernsey
Brest	0.91	-0.14	0.67	0.61	-0.77
Camborne	0.94	-0.14	0.69	0.66	-0.81
Herstmonceux	0.84	0.06	0.47	0.66	-0.67

Table 6-5: Correlation coefficient values - Median monthly refractive index lapse rates of radiosonde stations & median monthly refractivity gradients

The correlations between the weather station pairs and radiosonde stations can be classed as strong, positive (CLV-Guernsey), reasonably positive (Portland-Jersey) and reasonable negative (Jersey-Guernsey).

Of these pairs, CLV-Guernsey & CLV-Portland cover the vertical profile from sea level (0m). CLV-Guernsey has the additional advantage that it gives a better representation of vertical profile (i.e. from 0m to 102 m) as compared to CLV-Portland (i.e. 0m to 52m).

6.2.3. Refractivity gradient in the lowest 100m of atmosphere

Normally, an indication of anomalous propagation is based on presence of ducting conditions when refractivity gradient is less than or equal to -157 N/km. However, an alternative parameter, β_0, is also employed. It is defined as the percentage of time for which the refractivity gradient is lower than -100 N/km in the first hundred metres of the atmosphere [21]. It is used to represent the probability that super-refracting 'surface' layers will occur at a given location.

The lowest part of troposphere holds special interest with reference to propagation. Previous studies have tried to model the refractive characteristics of lowest parts of the atmosphere, by using either radiososnde data from selected months of year or by using statistics based on numerical weather forecast [18, 43]. In addition, the data is now more than 60 years old. Also, the

values for the English Channel have been estimated from the global contours (isopleths) of refractivity gradients in lowest 100m of atmosphere.

The statistics published by Bean et al [43] indicate that for the areas of interest in this study, the percentage of time refractivity gradient in lowest 100m is less than or equal to -157 N-units/km, is 1% for February, between 2% & 5% in May, 2% in August and 1 % in November. Their average value is approximately 2%. The percentage of time refractivity gradient in lowest 100m of atmosphere is less than or equal to -100 N-units/km is 2% for February, 5% for May, 5% for August and 5% for November. Their average value is approximately 4.25%. Table 6-6 gives the approximate values of refractivity gradient in lowest 100m exceeded for 25%, 10%, 5% and 2% of time, for the representative months, determined by using maps given by Bean et al [43], based on five years of radiosonde data:

Percentage of time, value of refractivity gradient exceeded (%)	February	May	August	November
25	50	75	50	50
10	50	100	100	100
5	100	157	100	100
2	157	300	300	200

Table 6-6: Refractivity gradient values exceeded for different % of time in different representative months [43]

The ITU refractivity gradient statistics in the lowest 65m of atmosphere based on two years (1992-1993) of data of the numerical weather forecast [18] indicate that the value of refractivity gradient not exceeded for 50% of time in average year is between -48 and -55 for the English Channel. ITU statistics

based on radiosonde observations of five years (1955-1959) give an approximate value of -40.

Previous research by Bech et al [44] in Barcelona, Spain observed a marked super refractive minimum in August. During that month the variability of the vertical refractivity gradient also was the highest. It was also observed that midnight conditions are more super refractive than noon conditions, attributing the effect of nocturnal radiation inversions as the most probable cause.

Gunashekar investigated propagation on over-sea trans-horizon paths for frequencies around 2000 MHz with transmitter at Jersey and receivers at Alderney, Sark and Guernsey. Space diversity was employed at transmitter and receiver sites [50]. The refractivity gradient in the lowest 100m of atmosphere was calculated using refractivity values of five different weather stations, by finding the slope of the best-fit line through points on the refractivity vs. height plot for hourly data from the various sites. The mean refractivity gradient was -71 N-units/km. Refractivity gradient was observed to be sub-refractive for 5.26% of time, normal for 55.2% of time, super-refractive for 30.8% of time and trapping/ducting for 8.8% of time.

For long-term median calculations, empirical studies have established a relationship between average mean refractivity gradient for the first kilometre above the Earth's surface and the value of average monthly mean refractivity at the surface. For the United Kingdom [17],

$$\frac{\Delta \overline{N}}{\Delta h} = -3.95 \exp(0.0072 \overline{N}_S) \qquad \text{N-units/km} \qquad (6.01)$$

This equation is valid for $250 \leq N_s \leq 400$ N-units for average negative gradients near to surface.

COST 255 Report [64] observed good correlation between values of β_0 derived from radiosonde data and sea-level refractivity. The annual variations of β_0 for Brest and Trappes, France show maximum in July/August and minimum in December/January.

Airborne investigation by Levy et al [52] over the English Channel observed high correlation between dewpoint values at heights of 60m and 90m above surface. Horizontal variation of refractivity was also observed, with gradients 1 to 2 N-units/km at maximum. A strong correlation was also observed between horizontal variations of refractivity and humidity.

The pair of CLV-Guernsey can serve as a suitable source for values for refractivity gradient in the lowest 100m of atmosphere, since CLV is at sea level (though taking readings at 5m AMSL) while Guernsey is at 102m above sea level. However, due to the availability of data from stations at heights between CLV and Guernsey, it is possible to have a more detailed examination of the refractive conditions in the lowest 100m of atmosphere. It may be noted that analysis is now based on more than one set of measuring instruments. Also, if measuring stations are at short height differences from

each other or are facing in different directions, differences might be expected. However, the supplier checks data from all these stations for quality control.

Table 6-7 summarises the refractive conditions (defined in Chapter 2) in the lowest 100m of atmosphere, based on different weather station pairs (3 s.f.):

Weather station pair	**Refractive condition (% of values)**				
	Sub-refractive	Normal-refractive	Super-refractive	Ducting/ Trapping	β_0
CLV-Guernsey (0m, 102m)	3.02	95.8	1.16	0	0.23
CLV-Portland (0m, 52m)	13.9	75.7	9.56	0.86	5.60
Portland-Jersey (52m, 84m)	20	51.3	21.8	6.95	19.8
Jersey-Guernsey (84m, 102m)	48.8	41.1	8.29	1.84	6.13

Table 6-7: Refractive conditions-Lowest 100m of atmosphere

An overview of the lowest 100m, based on CLV-Guernsey pair, indicated the presence of normal-refractive gradients for almost 96% of time. A breakdown of the lowest 100m further revealed that the lowest 52m of the atmosphere was predominantly normally refractive, followed by presence of sub-refractive and super-refractive gradients. The next 32m higher up from Portland was still predominantly normal-refractive (~51% of time), sub-refractive for almost 20% of time while super-refractive/trapping for ~29% of time. The height interval from 84m to 102m showed sub-refractive gradients for ~49% of time, normal-refractive for ~41% and super-refractive/trapping gradients for ~10% of time

respectively. Hence, there are indications of the presence of high refractivity gradients within the lowest 100m of the atmosphere, especially within 52m – 84m heights AMSL.

6.2.4. Effective earth radius factor

The median value of effective earth radius factor 'k' for the Channel Islands is based on the median values of lapse rates from the radiosonde stations (Table 6-4), and is 1.273. The median value of 'k' from the most suitable pair from weather stations (CLV-Guernsey) is 1.244. Both these values are slightly less than 1.33 (4/3), the value taken globally as the median or standard value. However, since these values are based on actual readings, it is recommended that until a more accurate value is calculated, the value of 'k' as used in propagation studies in this area and its surroundings be an average of these two, i.e. k_{med}=1.259.

Also, in the lowest 100m of atmosphere (using CLV-Guernsey pair), lapse rates causing the value of 'k' to exceed 4/3 occur for almost 27% of time. If this 100m height is analysed in segments (i.e. 0-52m, 52m-84m & 84m-102m), the respective percentage of lapse rates values causing value of 'k' to exceed 4/3 occur for approximately 41%, 48%, and 25% of time.

6.2.5. Surface refractivity N_s

The work by Bean et al [43] presents maps, charts, and discussions of the worldwide variations in the radio refractive index. This pioneering data was based on inputs from radiosonde stations throughout the globe. Wherever possible, a total of 5 years of data (1955-1959) was obtained for each of the 4 representative "seasonal" months of February, May, August and November. The 5-year annual mean value of surface refractivity for the Channel Islands was ~330 N-units.

If the hourly data from weather stations is used, the median and mean values of refractivity at weather station heights (to 2 d.p.) are given by Table 6-8:

Weather station	**Station height AMSL (m)**	**Refractivity N_s (N-units) at station height**	
		Median	Mean
CLV	5	293.78	294.24
Portland	52	292.16	292.60
Jersey	84	290.80	291.02
Guernsey	102	290.72	291.24

Table 6-8: Annual median/mean values of refractivity at weather station heights

The median/mean values indicate that refractivity decreases with height, except for Jersey to Guernsey, whereby median values are very close and mean values indicate a slightly increasing trend. Also, the measurements from the neighbouring radiosonde stations give us values for N_s at different heights, starting from and above the radiosonde station heights. If only those days are selected when both noon and midnight readings are available at every

radiosonde station, the median and mean values of refractivity at station heights are summarised in Table 6-9:

Radiosonde station	Station height AMSL (m)	Refractivity N_s (N-units) at station height	
		Median	Mean
Herstmonceux	52	290.5	291.5
Camborne	87	289.1	289.8
Brest	96	289.6	290.3
Trappes	167	286.2	287.8

Table 6-9: Annual median/mean values of refractivity at radiosonde stations

The median/mean values suggest a change in refractive behaviour between Camborne and Brest (87m and 96m) wherein the average refractivity gradient is positive. Larkhill is excluded because it did not have sufficient readings at noon as well as midnight.

To obtain the values of N_0, sea level weather information from the Channel Light Vessel (CLV) was used. These readings were taken at height of 5m above mean sea level. However, they provided the best match to sea-level readings rather than using values extrapolated from surface refractivity values at higher altitudes. The monthly mean values for N_0 (to 2 d.p.) are given in Table 6-10:

Month	Average refractivity (N-units)	Month	Average refractivity (N-units)
Jul 2009	299.99	Jan 2010	290.48
Aug 2009	302.26	Feb 2010	287.35
Sep 2009	300.45	Mar 2010	291.58
Oct 2009	297.08	Apr 2010	292.73
Nov 2009	289.85	May 2010	293.51
Dec 2009	288.32	Jun 2010	298.18

Table 6-10: Monthly mean values of refractivity – CLV

The monthly mean values are higher during the summer season, decreasing through autumn to reach minimum during the winter season, increasing again during the spring to reach high peaks during the summer, agreeing with previous findings [49].

Lane [49] has used the following formula to derive values of sea-level refractivity N_0 from surface refractivity N_s:

$$N_0 = N_s e^{0.100h} \qquad \text{N-units} \qquad (6.02)$$

Where:

h is the height of the surface above mean sea level.

The study by J.A. Lane over the British Isles [49] was carried out to determine the average refractive gradient as a function of location and season. Lane observed that a standard reference atmosphere is characterised by exponential variation of refractivity with height up to several kilometres:

$$N_h = N_s e^{-bh} \qquad \text{N-units} \qquad (6.03)$$

Where:

N_s is the surface refractivity (N-units)

N_h is the refractivity at a height 'h' above surface (N-units)

The mean values of 'N_s' and 'b' for seasonal representative months were determined using 5-year radiosonde data (1951-1955), at 0200 hours and 1400 hours.

The values for Camborne and Crawley, the radiosonde stations closest to the Channel Islands, are summarised in Table 6-11:

Station	Para-meter	Time & Month							
		0200 hours				1400 hours			
		Feb	May	Aug	Nov	Feb	May	Aug	Nov
Camborne	N_s	322	333	346	328	321	333	345	328
	b	0.138	0.149	0.157	0.142	0.141	0.149	0.154	0.144
Crawley	N_s	319	329	341	326	316	326	337	325
	b	0.141	0.146	0.157	0.145	0.136	0.136	0.146	0.144

Table 6-11: Seasonal mean surface refractivity values for sites near the Channel Islands, UK [49]

It has been observed that the annual range of monthly mean surface refractivity values for both land and sea stations is around 20 N-units, while highest values for mean surface refractivity are noted in July or August.

Based on the radiosonde measurements from the 5 neighbouring radiosonde stations in the first 2 km of the atmosphere, the annual average values of the two variables 'N_s' and 'b' (to 2 d.p.) are summarised in Table 6-12.

Radiosonde station name	Station height AMSL (m)	Parameter	
		N_s (N-units)	'b' ($*10^{-4}$)
Herstmonceux	52	293.87	1.25
Camborne	87	294.01	1.27
Brest	96	295.03	1.29
Larkhill	132	293.81	1.25
Trappes	167	294.60	1.26

Table 6-12: Annual average values of surface refractivity parameters

The Channel Islands are surrounded by these five stations. Hence, an average from these five stations can be taken as the 'representative' average value for the area concerned. The average values of 'N_s' and 'b', calculated

from the table above, are N_s= 294.26 N-units and b=1.2630*10^{-4}. Here, N_s is used for sea-level, effectively meaning that these values of N_s are those of sea-level surface refractivity, N_0.

The annual mean value of surface refractivity from all the radiosonde stations is also close to the value of average annual surface refractivity calculated from Channel Light Vessel.

A monthly breakdown of mid-day and mid-night values of surface refractivity is shown in Table 6-13 (with values to 1 d.p.):

Month	Radiosonde station							
	Herstmonceux		Camborne		Brest		Trappes	
	Day	Night	Day	Night	Day	Night	Day	Night
Jul	298.7	296.1	296.5	294.9	298.1	297.0	293.4	292.6
Aug	302.6	296.8	298.6	297.0	299.6	298.5	296.5	293.8
Sep	298.9	298.1	296.3	295.3	297.8	296.0	293.4	291.5
Oct	295.4	293.2	293.5	293.2	293.9	295.1	289.7	289.1
Nov	287.0	287.7	286.8	286.0	288.3	287.9	285.4	284.8
Dec	287.3	287.2	285.7	286.2	286.7	286.8	284.8	285.4
Jan	290.3	290.7	288.6	289.3	288.0	288.7	286.8	287.7
Feb	286.8	287.7	284.4	285.4	284.3	285.3	283.1	283.9
Mar	288.5	289.6	288.1	289.1	287.0	288.9	284.9	286.3
Apr	288.5	290.7	288.6	290.0	287.9	289.7	284.0	285.4
May	287.7	289.1	290.5	291.0	290.7	291.2	286.2	287.5
Jun	298.2	293.7	290.8	294.8	294.4	293.3	294.1	292.6
Annual average	292.2	291.6	290.8	291.1	291.3	291.5	288.6	288.4

Table 6-13: Monthly mean values of surface refractivity-Radiosonde stations

Monthly analysis reveals that the surface refractivity values attain their peak day/night values during summer and are lowest during winter. The extreme months are August and February for high and low values, respectively. The annual average values do not show a great deal of difference between day

and night average annual values. A comparison between day and night values reveals seasonal trends; during summer, day mean values are higher than night mean values. This gap reduces during autumn and during winters and spring, night values exceed day values. This trend was not observed in the study by Lane [49], which had generalised the behaviour as night values exceeding day values and was based on pioneering work by Bean et al [43].

6.3. Propagation Modelling

Propagation modelling is a field of continuous research and refinement. Currently, the ITU-R propagation models dealing with trans-horizon propagation are P.617 [20], P.452 [21] & P.526 [12]. P.617 predicts troposcatter loss, P.452 predicts loss due to different mechanisms while P.526 predicts diffraction loss. Models independent of the ITU are also in use; the one relevant to this research is the NBS TN-101 [25], which predicts troposcatter and diffraction losses. These models are discussed in Chapter 3 and were implemented in MATLAB, in this study.

The term ‘Basic transmission loss’ has been repeatedly used throughout this section. It refers to the value of loss including free space loss, gaseous attenuation and the loss due to the mechanism under observation (i.e. troposcatter/diffraction/ducting etc), assuming isotropic antennas. For instance, ‘Basic transmission loss due to troposcatter’ refers to the value of free space loss, gaseous attenuation and loss due to tropospheric scatter.

6.3.1. Inputs to propagation models

The input parameters required by the different prediction models include path length, path profile information including details of any obstacles and distances to radio horizons, frequency, antenna gains and heights, tidal variation (to be incorporated within the effective antenna height), weather data for refractivity and its gradient values. Table 6-14 shows the values of common basic inputs to propagation models:

Input parameter	**Path & Frequency**			
	Jersey-Alderney		Jersey-Portland	
	UHF	VHF	UHF	VHF
Great circle path length (km)	51		141	
Frequency (MHz)	2015	240	2015	240
Transmitting/Receiving antenna gains (dBi)	14 (Tx) 14.5 (Rx)	12.15 (both Tx & Rx)	14 (Tx) 14.5 (Rx)	12.15 (both Tx & Rx)
Fraction of path over water (w)	0.999		0.999	
Distance from transmitter to its horizon d_{lt} (km)	17	17.5	17	17.5
Distance from receiver to its horizon d_{lr} (km)	14.5	15.1	14.75	15.33
Distance from transmitter to coast along path d_{ct} (km)	0.01		0.01	
Distance from receiver to coast along path d_{cr} (km)	0.005		0.1	
Distances of profile points from T_x (km)	1 to 51		1 to 141	
Heights of profile points AMSL (m)	All 0		All 0	
Longest continuous land section of path d_{tm}(km)	0.01		0.1	

Table 6-14: Input parameters for propagation models

The refractivity gradient data is hourly, giving hourly values of loss for both paths. For comparison, the interpolated value from ITU data [28] and the median refractivity lapse rate value obtained from Channel Light Vessel and

Guernsey, abbreviated as 'CG' in the tables, have been used. The 'CG' value is close to the median value from radiosonde stations.

6.3.2. Troposcatter loss

Previous studies indicate that troposcatter is the dominant mechanism on longer trans-horizon paths [17, 55, 90, 92, 94, 100]. This section deals with the calculation of median transmission loss values, as predicted by three different models- P.617 [20], P.452 [21] and TN-101 [25].

6.3.2.1. Comparison of troposcatter loss models

The median values of lapse rate of refractivity, sea-level surface refractivity, effective earth radius etc are available from the weather stations as well as from the data provided by the ITU [12,18,20,21,22,23,26,28,63]. The basic transmission loss associated with troposcatter (to 2 d.p.), as obtained from each of these models using both the median values are given in Table 6-15:

Propagation model & input dataset	**Path & Frequency**			
	Jersey-Alderney		Jersey-Portland	
	UHF	VHF	UHF	VHF
P.617 (ITU)	166.45	138.39	193.71	166.27
P.617 (CG)	169.26	140.80	195.76	167.84
P.452 (ITU)	184.38	158.72	199.73	173.54
P.452 (CG)	189.80	164.19	205.76	179.58
TN-101	169.23	141.31	197.36	169.08
TN-101 (CG)	174.63	144.86	201.26	172.98

Table 6-15: Basic median transmission loss due to troposcatter (dB)

It can be observed by comparison that P.617 predicts smallest loss values while P.452 predicts highest values for losses while the values predicted by

TN-101 tend to be within the range defined by these limits. However, the differences are less pronounced for the longer path (i.e. Jersey-Portland) as compared to those for shorter path (i.e. Jersey-Alderney).

Theoretically, P.617 includes a term that considers the impact of meteorological structure on the loss, based on the height of common volume (discussed in Chapter 2). On the other hand, P.452 includes a term dependent on the sea-level surface refractivity at path-centre. In this respect, P.617 is expected to perform better than P.452.

In terms of comparing the median values calculated from ITU parameters to those from measured path parameters (CLV-Guernsey), there is a difference of almost 2-3 dB when calculating by P.617 and 5-6 dB when using P.452. The difference in loss values determined from standard TN-101 parameters and those based on CLV-Guernsey differ by 3 to 5 dB, with the loss values from CLV-Guernsey data higher than those by standard TN-101 inputs.

6.3.2.2. Important parameters used to determine troposcatter loss

This section discusses the important parameters used in calculating the values given in Table 6-15.

ITU-R P.617

One climate from a list of nine different climates mentioned in P.617 (Climate 7b-Maritime Temperate (Oversea) in this case) is chosen to get the values for

the meteorological and atmospheric structure parameters. The value of median effective earth radius factor, k_{med}, is calculated using median value of lapse rate of refractive index, ΔN. Table 6-16 gives values of the lapse rates of refractivity in the lowest 1 km (to 2 d.p.):

Calculated Parameter	**Path**	
	Jersey-Alderney	Jersey-Portland
Average Refractivity Lapse Rate, ΔN (N-units/km) (ITU)	-42.93	-42.97
Median Refractivity Lapse Rate, ΔN (N-units/km) (CG)	-30.82	-30.82

Table 6-16: Calculated parameters for troposcatter loss for ITU-R P.617

Table 6-17 shows the values for 'Basic transmission loss due to troposcatter', not exceeded for different percentages of time equal to and higher than 50%:

Percentage of non-exceedance time (%)	**Path & Frequency**			
	Jersey-Alderney		Jersey-Portland	
	UHF	VHF	UHF	VHF
50	169.26	140.80	195.76	167.84
75	174.54	146.08	201.00	173.08
90	181.76	153.30	208.18	180.26
95	185.17	156.71	211.57	183.65
99	192.00	163.55	218.36	190.45
99.9	199.40	170.92	225.69	197.77
99.99	205.50	177.04	231.78	203.86

Table 6-17: Basic transmission loss due to troposcatter, not exceeded for different percentages of time (CLV-Guernsey)– ITU-R P.617

ITU-R P.452

ITU P.452 uses three meteorological parameters N_0, $\Delta N/\Delta h$ and β_0, which should ideally be measured at the path centre. The values of median

temperature and pressure come from the weather data. Table 6-18 gives the calculated values (to 2 d.p.):

Calculated parameter	Path	
	Jersey-Alderney	Jersey-Portland
Median surface temperature (°C)	11.5	11.5
Median pressure (hPa)	1016	1016
Refractive index lapse rate in the lowest 1 km, ΔN (N-units/km) (ITU)	-42.93	-42.97
Median refractive index lapse rate in the lowest 1 km, ΔN (N-units/km) (CG)	-30.82	-30.82
Sea-level surface refractivity, N_0 (N-units) (ITU)	328.45	328.27
Sea-level surface refractivity, N_0 (N-units) (CG)	293.89	293.89
Effective median earth radius (km) (ITU)	8769	8772
Effective median earth radius (km) (CG)	7926	7917

Table 6-18: Calculated parameters for troposcatter loss for ITU-R P.452

Table 6-19 gives the values for basic transmission loss due to troposcatter, not exceeded for different percentages of time less than and equal to 50%:

Percentage of non-exceedance time (%)	Path & Frequency			
	Jersey-Alderney		Jersey-Portland	
	UHF	VHF	UHF	VHF
50	189.80	164.19	205.76	179.58
25	185.38	159.73	201.25	175.06
10	181.88	156.23	197.74	171.56
5	179.64	153.99	195.50	169.32
1	175.10	149.45	190.97	164.78
0.1	169.50	143.85	185.37	159.18
0.01	164.51	138.86	180.37	154.19

Table 6-19: Basic transmission loss due to troposcatter, not exceeded for different percentages of time (CLV-Guernsey)– ITU-R P.452

ITU-R Recommendation P.617 is used to calculate the values of transmission loss due to tropospheric scatter, not exceeded for percentages of time greater than 50%. ITU-R P.452 calculates the values of transmission loss due to troposcatter, not exceeded for percentages of time less than 50%. Hence, by

using P.617 for non-exceedance percentages 50 to 100% and P.452 for non-exceedance percentages 0 to 50%, a troposcatter loss distribution can be created. Such a distribution can be for every single value of 'k'. However, both these models are based on the median value of 'k', which is what has been used in the above results.

TN-101

This prediction model uses the value of effective earth radius a_e, which depends on value of surface refractivity N_s [25, 17]. N_s is determined from the global minimum monthly sea level surface refractivity values, N_0 [17, Figures 5.5 & 5.7]. In this case, the value of N_s, as determined by the procedure [17, 25], is equal to that of N_0. The values for different parameters are calculated according to procedures explained in Freeman [17, Figures 5.4 to 5.15]. Table 6-20 gives the values of prominent calculated parameters:

Calculated parameter	**Path**	
	Jersey-Alderney	Jersey-Portland
Surface refractivity at path centre, N_s (N-units)	320	320
Surface refractivity at path centre, N_s (N-units) (CG)	294	294
Effective earth radius, a_e (km)	8800	8800
Effective Earth Radius, a_e (km) (CG)	8035	8035

Table 6-20: Calculated parameters for troposcatter loss for NBS TN101

6.3.3. Diffraction loss

Diffraction loss is the expected dominant mechanism on near line of sight paths and/or paths extending just beyond the horizon. This section deals with the models that predict values for diffraction loss.

6.3.3.1. Comparison of diffraction loss models

The basic transmission loss associated with diffraction (to 2 d.p.), as obtained from the relevant models using the median values are given in Table 6-21:

Propagation model & input dataset	**Path & Frequency**			
	Jersey-Alderney		Jersey-Portland	
	UHF	VHF	UHF	VHF
P.526 (ITU)	172.63	152.47	280.27	207.35
P.526 (CG)	175.27	153.43	289.11	211.36
P.452 (ITU)	168.82	141.10	220.86	177.46
P.452 (CG)	170.78	142.04	223.65	179.59
TN-101	170.94	155.38	277.10	209.18
TN-101 (CG)	171.94	153.38	287.11	210.39

Table 6-21: Basic median transmission loss due to diffraction (dB)

A comparison of the predicted values shows that P.526 predicts the highest loss values, followed closely by TN-101 and then, with larger differences for all cases except UHF signal at Alderney, by P.452, which obviously predicts the minimum values of diffraction loss.

6.3.3.2. Diffraction loss using P.526

ITU-R P.526 computes diffraction loss using the value of median effective earth radius. Table 6-22 lists the values of important calculated parameters:

Input parameter	Path	
	Jersey-Alderney	Jersey-Portland
Mean ΔN (N-units/km) (ITU)	-42.93	-42.97
Effective Median k (ITU)	1.38	1.38
Effective Median Earth Radius (km) (ITU)	8769	8772
Median ΔN (N-units/km) (CLV-Guernsey)	-30.82	
Effective Median k (CG)	1.24	
Effective Median Earth Radius (km) (CG)	7926	

Table 6-22: Input parameters for diffraction loss for P.526

The composition of ground along the paths is seawater. The properties of seawater are functions of temperature, salinity, frequency and pressure [VII, 27, 88]. ITU P.527 [88] provides the following values for seawater (average salinity) at 20°C, σ=5S/m (240MHz), σ=6S/m (2GHz) & ε=70 for both frequencies. The effective permittivity ε=83 and effective conductivity σ=4S/m [VII].

As Table 6-21 indicates, the basic median transmission loss values predicted by using the two input datasets are close, within 4 dB of each other, except for UHF on longer path where loss predicted by using CLV-Guernsey parameters is higher by 9 dB.

6.3.3.3. Diffraction loss using P.452

P.452 is based on modelling the obstacles in the path as multiple knife-edges. In this case, however, the only obstacle is the curvature of the earth - the main 'edge'.

According to Table 6-21, the difference between the median loss values of the two paths is roughly 52 dB for UHF and 37 dB for VHF. Also, the respective values predicted by using either input dataset (ITU or CG) are within 3 dB of each other.

P.452 calculates median diffraction loss value as well as non-exceedance distribution for time percentages from β_0 (defined earlier) to 50%. Table 6-23 gives the values of calculated parameter β_0:

Calculated parameter	Path	
	Jersey-Alderney	Jersey-Portland
Non-exceedance time percentage β_0 (%) (ITU)	8.5	8.3
Non-exceedance time percentage β_0 (%) (CG)	0.2	0.2
Non-exceedance time percentage β_0 (%) (Average of CP, PJ, JG)	10.5	10.5
Non-exceedance time percentage β_0 (%) (CP)	5.6	5.6
Non-exceedance time percentage β_0 (%) (PJ)	19.8	19.8
Non-exceedance time percentage β_0 (%) (JG)	6.1	6.1

Table 6-23: Calculated parameter β_0 for diffraction loss for P.452

An average of the lowest 100m gives a value close to the interpolated values from ITU. However, individual height interval sets within the lowest 100m of atmosphere reveal that the height interval between Portland and Jersey is more conducive for super-refractive/ducting conditions, as also concluded earlier in Section 6.2.3.

6.3.3.4. Diffraction loss using NBS TN101

According to the results from TN.101 in Table 6-21, the difference between the median loss values for the two paths is more than 100 dB for UHF and approx. 55-60 dB for VHF. The values predicted by using the different input datasets are close to each other except UHF for longer path, where the loss using CLV-Guernsey data is higher by 10 dB than that from the standard TN-101 inputs.

6.3.4. Ducting/Layer Reflection Loss

ITU P.452 also predicts the basic transmission loss caused by surface ducting as well as reflection and/or refraction from tropospheric layers at heights up to a few hundred metres. Table 6-24 shows the values of basic median transmission loss during such periods of anomalous propagation (ducting and layer reflection/refraction).

The difference between the values predicted by using the ITU and CG input datasets is almost 30 dB for shorter path and 19 dB for longer path. Also, the difference in loss values between the two paths is greater when using ITU parameters (20 dB for UHF, 18 dB for VHF) as compared to those by using CLV-Guernsey parameters (11 dB for UHF, 8 dB for VHF).

The results also emphasise the fact that if only the readings at sea level and 100m AMSL are considered, the value of β_0 is 0.22%. However, if readings

from different heights up to 100m are considered and then an average is used, the value of β_0 is 10.5%. This average β_0 value is also close to the ITU-interpolated average β_0 value (8.3%), and hence the respective values of loss predicted are also close to each other. The values of predicted loss for the CLV-Portland and Jersey-Guernsey height intervals are also close to each other because of close values of annual average β_0. Generally, as β_0 increases, the predicted loss value decreases:

Calculated parameter	Path & Frequency			
	Jersey-Alderney		Jersey-Portland	
	UHF	VHF	UHF	VHF
Basic median transmission loss associated with ducting and layer reflection/refraction L_{ba}, based on ITU values, (dB)	197.68	195.74	218.40	213.27
Basic median transmission loss associated with ducting and layer reflection/refraction L_{ba}, based on CG values (β_0=0.22%), (dB)	226.57	225.02	237.77	232.82
Basic median transmission loss associated with ducting and layer reflection/refraction L_{ba}, based on average of CP, PJ & JG values (β_0=10.5%), (dB)	196.16	194.14	217.40	212.20
Basic median transmission loss associated with ducting and layer reflection/refraction L_{ba}, based on CP values (β_0=5.6%), (dB)	204.02	202.14	222.19	217.06
Basic median transmission loss associated with ducting and layer reflection/refraction L_{ba}, based on PJ values (β_0=19.8%), (dB)	181.48	179.23	208.97	203.74
Basic median transmission loss associated with ducting and layer reflection/refraction L_{ba}, based on JG values (β_0=6.1%), (dB)	204.89	202.84	222.88	217.58

Table 6-24: Basic median transmission loss due to surface ducting and layer reflection/refraction- P.452

Table 6-24 illustrates that the value of β_0 has a significant role in the predicted loss values linked with ducting and layer reflection/refraction. The presence of

super-refractive gradients for a higher percent of time is more conducive to these two mechanisms. If the lowest 100m of atmosphere were to behave like the height interval between Portland and Jersey (52m to 84m), the predicted median loss values due to ducting and/or layer reflection/refraction decrease.

Also, when investigated further by excluding free space loss, it was observed that the VHF loss values were higher than the UHF loss values, by almost 16 dB for shorter path and 13 dB for longer path. This, in turn, indicated that the UHF signal, though at higher frequency, suffered lower loss than the VHF signal if the propagation mechanism was ducting and layer reflection/ refraction.

6.3.5. Combined value of transmission loss

Both P.452 and TN-101 calculate the values of combined transmission loss by considering the effects of different mechanisms. P.452 considers line of sight, diffraction, troposcatter, ducting and/or tropospheric layer reflection/refraction propagation mechanisms to calculate a net value for transmission loss:

Calculated parameter	**Path & Frequency**			
	Jersey-Alderney		Jersey-Alderney	
	UHF	VHF	UHF	VHF
Basic median transmission loss for trans-horizon path $L_b(50)$, based on ITU values (dB)	168.83	141.11	199.73	173.21
Basic median transmission loss for trans-horizon path $L_b(50)$, based on CG values (dB)	170.80	142.04	205.76	178.08

Table 6-25: Basic median transmission loss for trans-horizon path – P.452

The basic median transmission loss for trans-horizon path $L_n(0.5,50)$, depending on the climate region [17], is given by Table 6-26:

Calculated parameter	Path & Frequency			
	Jersey-Alderney		Jersey-Portland	
	UHF	VHF	UHF	VHF
Basic Long Term Median Transmission Loss for Trans-Horizon Path $L_n(0.5,50)$, based on ITU values (dB)	164.94	140.88	190.36	162.58
Basic Long Term Median Transmission Loss for Trans-Horizon Path $L_n(0.5,50)$- based on CG values (dB)	167.94	144.38	194.26	166.48

Table 6-26: Basic long-term median transmission loss for trans-horizon path $L_n(0.5,50)$ – NBS TN-101

These results are further discussed in Sections 6.3.7 and 6.4.

6.3.6. Typical transmission loss

For troposcatter, the values of predicted median transmission loss values on the shorter path (~50 km) are within the approximate ranges of 138 to 165 dB for VHF and 165 to 190 dB for UHF. For the longer path (~140 km), these values are within the ranges 166 to 180 dB for VHF and 193 to 206 dB for UHF.

For diffraction, on the other hand, the values of predicted median transmission loss values on the shorter path are in the approximate ranges of 141 to 156 dB for VHF and 168 to 176 dB for UHF. For the longer path, these values are within the ranges 177 to 212 dB for VHF and 220 to 290 dB for UHF.

Using IPS, Frazier produced path loss curves for 100 MHz, 1 GHz and 10 GHz for different antenna heights for land and sea paths [67]. Using interpolation, Table 6-27 gives the values of the basic median transmission loss for the frequencies, antenna heights and path lengths used in this study:

Calculated parameter	Path & Frequency			
	Jersey-Alderney		Jersey-Portland	
	UHF	VHF	UHF	VHF
Basic median transmission loss-IPS (dB)	174	152	200.75	183.50

Table 6-27: Basic median transmission loss (dB) – Interpolated for path lengths and antenna heights

A comparison of the values in Table 6-27 with the above-mentioned ranges indicates that the values of typical path loss interpolated from predictions by IPS [67] are within the ranges predicted by the current models.

6.3.7. Dominant trans-horizon propagation mechanism

In accordance with Equation 3.01 [Chapter 3], the respective effective distances d_e for 240 MHz and 2 GHz, the two frequencies used in this research, are 48.5 km and 24 km. Applying this hypothesis to the current research, the troposcatter loss and diffraction loss for the shorter path (Jersey to Alderney-50km) are expected to be of comparable strengths for VHF whereas troposcatter is expected to dominate on the same path at UHF. On the longer path (Jersey to Portland-140 km), troposcatter is expected to dominate at both frequencies.

Comparing the combined transmission loss values, ITU P.452 predicts diffraction as the normal propagation mechanism for Jersey-Alderney path for both frequencies and troposcatter as the normal propagation mechanism at UHF for Jersey-Portland path (141 km). For VHF on the longer path, the median loss value for diffraction and troposcatter is similar, suggesting that both mechanisms could be equally dominant.

On the other hand, comparing the combined reference values of transmission loss, TN-101 predicts troposcatter as the normal propagation mechanism for Jersey-Portland path (141 km). For the shorter path, the combined reference transmission loss values predicted are close to the values predicted for diffraction and troposcatter. The value for UHF is closer to that from diffraction while that for VHF is closer to that from troposcatter. These results, however, suggest that both mechanisms could be equally dominant.

6.4. Path Loss

Path loss values from the paths are compared to the median values predicted by different propagation models, in an attempt to identify the dominant propagation mechanism for each link/frequency.

Figure 6-4 shows the distributions for the propagation loss values (based on hourly data) exceeded for different percentages of time. The median loss values predicted by different models are also shown. It is important to remind the reader that data from Alderney is for half the year only:

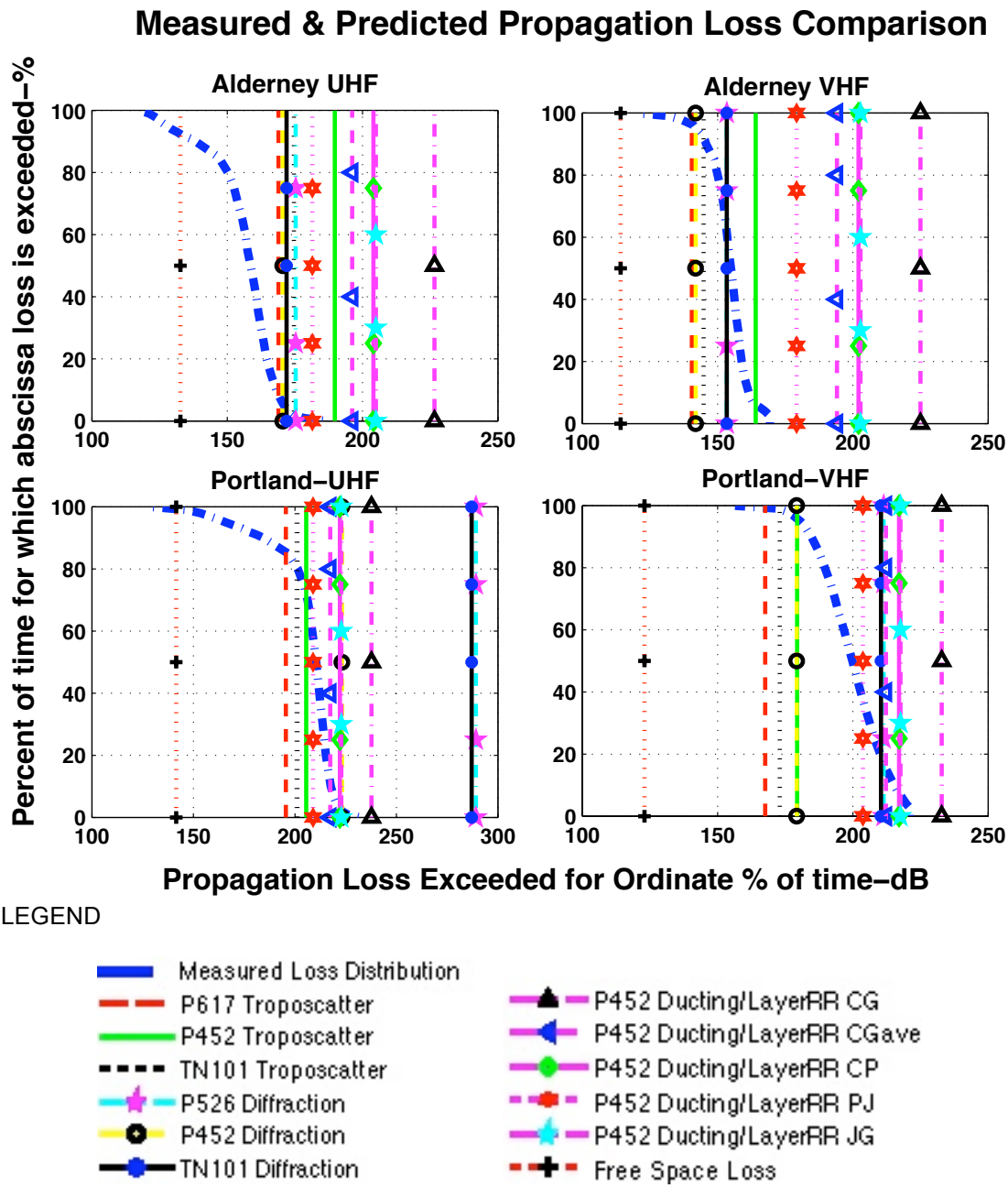

Figure 6-4: Propagation loss – Measured v/s predicted

For the UHF signal at Alderney, the measured loss is less than the FSL value for almost 8% of time. The predicted median values of ducting and/or layer reflection/refraction loss (P.452) are much higher than the values from the measured distribution. The predicted median values of diffraction and troposcatter loss lie near the lower end of the distribution. None of the predicted median values are close to the median of the distribution. The

closest values are indicative of troposcatter and diffraction as the possible mechanisms during normal (non-enhanced) signal reception. In contrast, a previous study by Gunashekar [50] observed diffraction as the pre-dominant propagation mechanism during such times.

For the VHF signal received at Alderney, the median values of diffraction loss predicted by P.526 and TN101 are close to the median of the distribution, suggesting that diffraction is the most probable propagation mechanism during non-enhanced signal reception. The median values predicted by P.452 for ducting are higher than the distribution. The predicted median troposcatter loss values from P.617 and TN.101 are near the higher extreme of the distribution while that by P.452 is near the lower extreme. The measured loss is never observed to be less than the respective FSL value. Previous research by Sim [11] observed comparable field strengths from diffraction and troposcatter for VHF signals on similar paths.

For the UHF signal at Portland, the predicted median values are indicative of troposcatter as well as ducting and/or layer reflection/refraction as the possible mechanisms during non-enhanced signal reception. The troposcatter values from all models are almost in unanimous agreement and not far from median value of the distribution. Measured loss is less than the FSL value for almost 1% of time.

For the VHF signal at Portland, none of the median values are close to the median of the distribution while the closest predicted median value is that of

ducting and/or layer reflection/refraction loss from Portland-Jersey height interval. The predicted median troposcatter loss values are within the highest 10% of the distribution whereas the predicted median diffraction and ducting/layer reflection/refraction loss values lie within the lowest 20% of the distribution of measured loss. Measured loss is never observed to be less than the FSL value.

For Alderney, P.452 predicts median troposcatter loss value at least 15 dB higher than those predicted by TN-101 and P.617. For Portland, the predicted median troposcatter loss values from all models are comparatively closer. Also, for Portland, the median diffraction loss value predicted by P.452 is lower than those predicted by P.526 and TN-101 by at least 30 dB whereas the predicted median diffraction loss values from all models are comparatively closer for Alderney.

For most of the times during normal, non-enhanced signal reception, the typical signatures of the received UHF and VHF signals at Alderney have been indicative of diffraction as the prevalent mechanism. P.452 seems to be comparatively better than P.617 and TN.101 in predicting diffraction as the mechanism prevalent during non-enhanced UHF signal reception at Alderney while the other models seem better than P.452 for predicting diffraction as the mechanism during non-enhanced VHF signal reception at Alderney.

For the signals at Portland, the predictions for the troposcatter signal levels are similar, while there is a huge difference amongst the diffraction loss values

predicted by different models. For most of the non-enhanced signal reception times, the received signals have seemed to match the typical troposcatter signature identified by Shen and Vilar [55]. This is also supported by previous studies on longer-trans horizon paths. P.452 seems to be predicting diffraction as a possible mechanism while other models rule diffraction out. In this sense, P.452 is comparatively inaccurate in predicting diffracted field over the longer path as it tends to over-estimate the diffracted median signal strength. With reference to interference prediction, if the diffracted signal is taken as the unwanted signal, other models rule out diffraction as a viable propagation mechanism, while P.452 is predicting a reasonably strong diffracted signal. Hence, P.452 can be considered to be conservative about its interference prediction from diffracted field on the longer, trans-horizon path.

The above results indicate that a comparison based on median predicted values can be sometimes conclusive. As part of future work, it might be worth splitting the data into enhanced and non-enhanced datasets and use them as inputs to the propagation models to see if further details can be revealed.

6.5. Ducting

This section investigates evaporation ducting, followed by looking at refractivity profiles within the lowest 100m of atmosphere, based on weather information gathered by five different weather stations in Channel Islands.

6.5.1. Evaporation ducting

The Paulus-Jeske method [78, 79] is used to determine the height of evaporation duct, based on the meteorological data available from Channel Light Vessel (Ref Section 3.6). It uses the values of meteorological variables air temperature, sea temperature, relative humidity and wind speed to calculate the duct height.

The world average evaporation duct height is approximately 13m [77], while the long-term mean duct thickness at northern latitudes is roughly 8m [73], with the North Sea having 5-6 m high evaporation ducts [72, 87]. The mean evaporation duct height near Lorient, France is 7.8m [97].

The study by Gunashekar [50] calculated the height of evaporation duct using Paulus-Jeske (P-J) and Naval Postgraduate School (NPS) Models, based on meteorological data available from Channel Light Vessel. Although it was concluded that NPS model performed better than the P-J Model, the P-J model was used for further analysis. The software AREPS was also used for surface-based ducting statistics and comparison with P-J model. The mean Paulus-Jeske evaporation duct height over the two years of measurement (using hourly weather data from the Channel Light Vessel) was 8.3m, with maximum duct height being 23.7m. Zero duct heights corresponded to cases of sub-refraction.

Figure 6-5 shows the histogram of the hourly values of evaporation duct height:

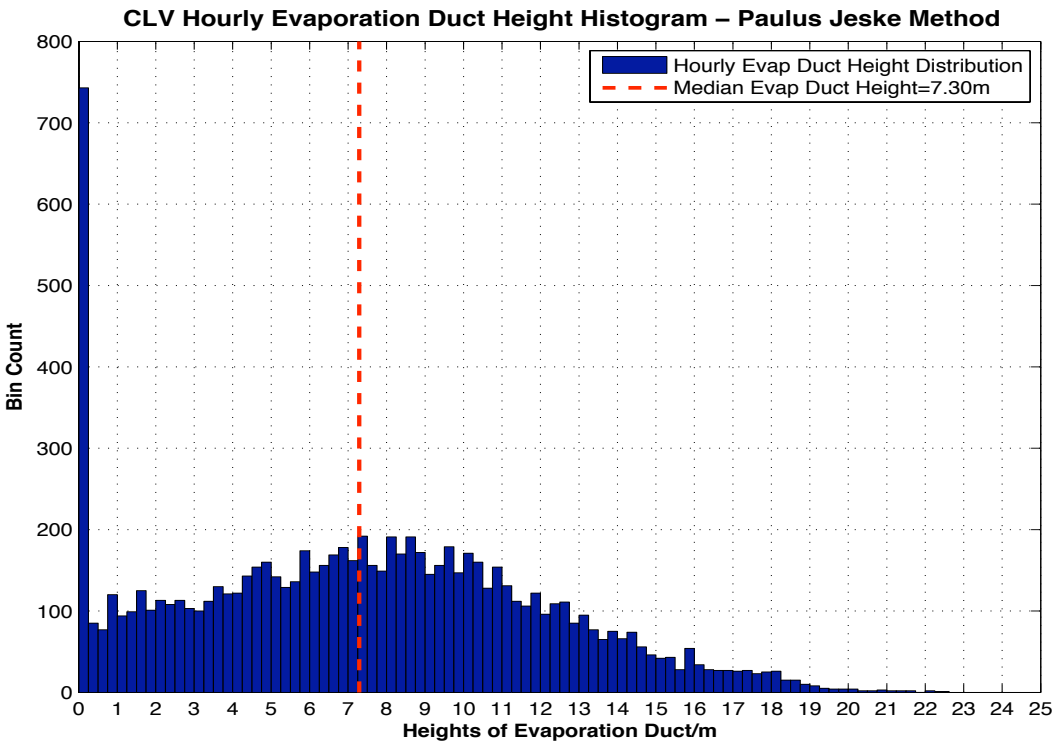

Figure 6-5: CLV – Histogram of evaporation duct height

There were 743 instances when the calculated height of evaporation duct was 0.25m or less, of which the values was zero in 662 cases. Hence, 7.6% of the evaporation duct height values were zero. This effectively meant that in all the other cases, amounting to more than 92%, there was some degree of evaporation ducting. This augmented the notion that evaporation ducting is a near-permanent phenomenon on over-sea paths around the area of the test links [50]. 10% of values exceeded height of 13.5m while 90% exceeded height of 0.6m, hence giving an inter-decile range of 12.9m. The annual mean/median height of the evaporation duct (as per P-J model) was 7.3m.

Figure 6-6 shows the daily/monthly mean values of evaporation duct height:

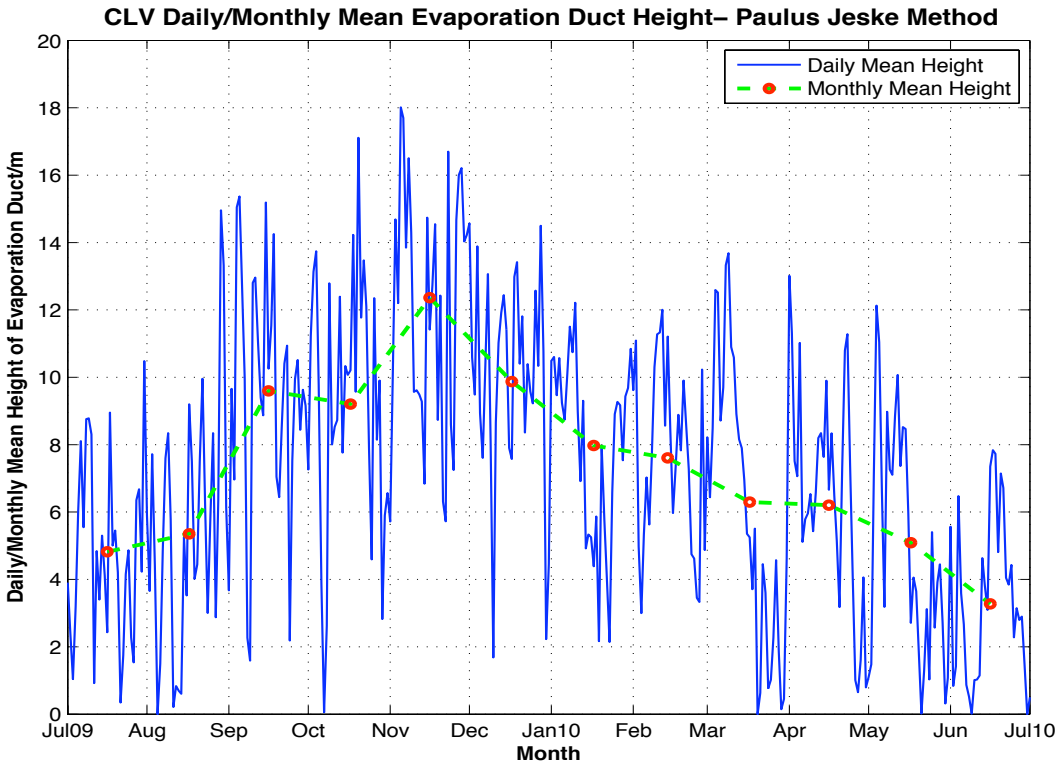

Figure 6-6: CLV – Daily/Monthly mean evaporation duct height

The values of monthly mean evaporation duct height are higher during the autumn season, reaching peak in November, while minimum was observed during the summer, going as low as ~3m in June. It can be observed that the daily average evaporation duct are highly variable from day to day.

Figure 6-7 shows the hourly mean duct height from all the months. It can be observed that there are seasonal as well as hourly max/min trends. During summer months (June to August), the mean hourly duct heights reach minimum during early morning time (~ 0300 to 0600 hours) while attaining maximum values in afternoon/evening around 1400 to 1900 hours. During the autumn months (September to November), the hourly means can attain maximum values any time after 0900 hours whereas there is no particular time

window for the occurrence of minimum values. During the winter (December to February), higher duct height levels are observed in afternoon/evening times while in December peaks are also observed before noon (0900 to 1100 hours). In spring season (March to May), the maximas are around early morning as well as afternoon while minimas do not show a noticeable pattern.

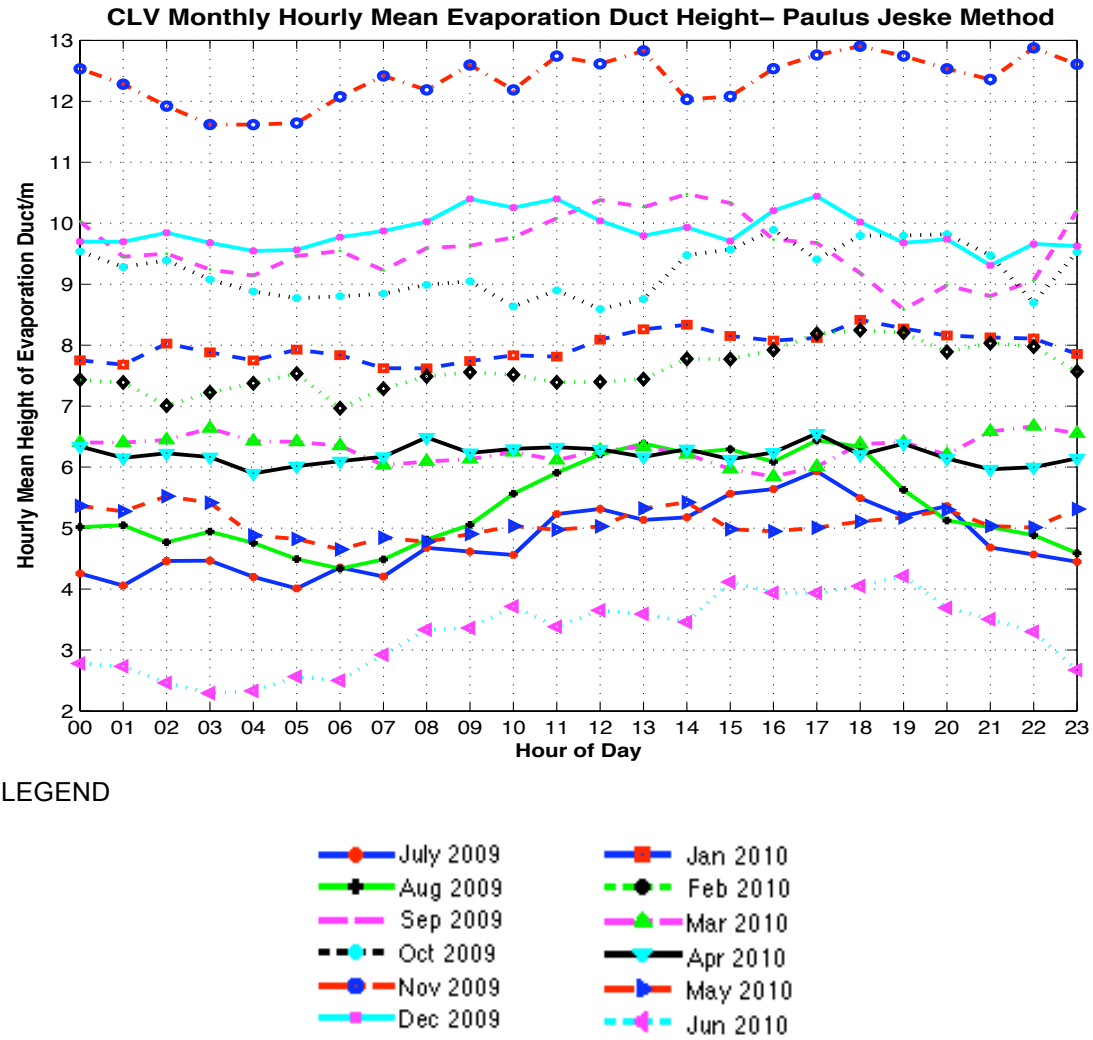

Figure 6-7: CLV – Monthly hourly mean evaporation duct height

Figure 6-8 shows the variation of the hourly duct height over the whole year, showing hourly maximum, minimum, median values and IQR:

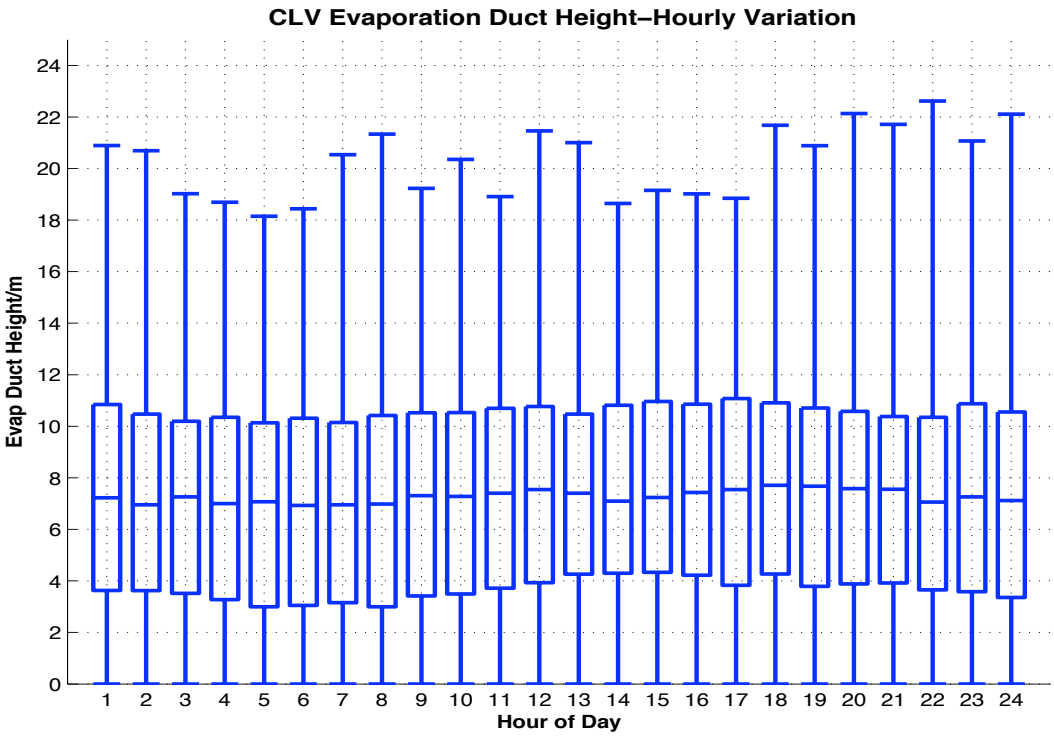

Figure 6-8: CLV – Annual hourly evaporation duct height variation

Figure 6-8 illustrates that the estimated duct heights can reach high values at any time of the day during one year of observation on such paths and that there is no systematic change with time.

6.5.2. Ducting/Super-refractive conditions in the lowest part of atmosphere

The breakdown of the lowest 100m of the atmosphere in the English Channel shows interesting change of refractive conditions with height, as discussed in Section 6.2.3 and summarised by Table 6-7. Part of the atmosphere between Portland and Jersey (i.e. 52m-84m height AMSL) shows the presence of ducting and super-refractive gradients for almost 30% of time.

Previous estimates suggest the presence of greater lapse rates in the lowest 65m of atmosphere than in the lowest 100m of atmosphere [18]. The observations by this study tend to agree with this notion.

6.6. Interim Conclusions

Strong correlation between meteorological variables recorded at neighbouring weather stations supports the assumption of horizontal homogeneity, which has been used for the analysis of weather data with respect to received signal strength data.

Meteorological data by the radiosonde stations around the Channel Islands indicates the presence of lapse rates of refractivity in the lowest 1 km of atmosphere causing 'k' factor to be greater than 4/3 for 7% to 20% of time in the year. The value of median effective earth radius factor is 1.27.

On a monthly average basis, the refractivity conditions within the lowest 84m (i.e. CLV to Jersey Airport) are positively correlated to the lapse rates of refractivity from the coastal radiosonde stations while the conditions within the height interval 84m to 102m (i.e. Jersey Airport and Guernsey Airport) are negatively correlated to those from radiosonde stations. On average, the height interval from 52m AMSL up to 84m AMSL is comparatively more conducive for super-refraction and ducting than the other sections within the lowest 102m of atmosphere.

The average value of surface refractivity obtained from radiosonde stations decreases with height, except for between height interval 87m to 96m (i.e. between Camborne and Brest), when it increases slightly with height. The midday monthly average values of surface refractivity are greater than the midnight monthly average values in summer. This trend reverses during winter. The average value of sea level surface refractivity is approx 294 N-units, which is almost 10% lower than the interpolated value obtained from the ITU data, which is approx 328 N-units.

Different mechanisms (e.g. diffraction, troposcatter, ducting, layer reflection etc) can enable propagation of radio signals on the two paths investigated. The path loss values obtained from the prediction models considered can help infer the most probable propagation mechanism by selecting the model with loss values closest to the actual path loss observed. However, the median path loss values predicted by different propagation models are sometimes indicative of different propagation mechanisms. ITU model P.452 tends to predict higher diffracted signal strengths at Portland than the other models.

The annual mean/median height of the evaporation duct (as per the P-J model) is 7.3m, with the highest daily/hourly median values in November and lowest in June.

7. RELATIONSHIPS BETWEEN METEOROLOGICAL PARAMETERS AND RECEIVED SIGNAL STRENGTH

This chapter contains in-depth analysis of correlations between signal and weather data and comparisons (if applicable) to previous research. The weather data used is hourly. Hence, any comparisons with signal levels can be made with 'hourly' signal dataset only. For hourly signal data, there are two possible datasets: the 'median' hourly data (based on the median of the signal strength values within the hour) and the 'spot' hourly data (signal data at the instant of the completed hour). Unless otherwise stated, the spot hourly data is used in the following investigations.

7.1. Correlation Between Signal Level and Evaporation Ducting

Evaporation ducting is a near-permanent phenomenon observed on the paths involved in this research (Ref Section 6.5). The heights of evaporation duct, based on hourly data available from CLV, have been estimated using the Paulus Jeske (P-J) Method [78, 79]. CLV is not exactly within the line of the paths between transmitter and receivers. However, in the absence of a source that is recording weather variables at the midpoints of the over-sea paths, the data available from CLV is used, based on the assumption of horizontal homogeneity (See Section 6.1).

The estimated P-J evaporation duct heights and the corresponding hourly signal strengths at the respective antennas at Alderney and Portland are plotted against each other, as shown in Figure 7-1. These plots are based on

using the hourly median data from the whole year. For reference, the median signal levels due to different propagation mechanisms, as predicted by different propagation models (Section 6.3), are also indicated:

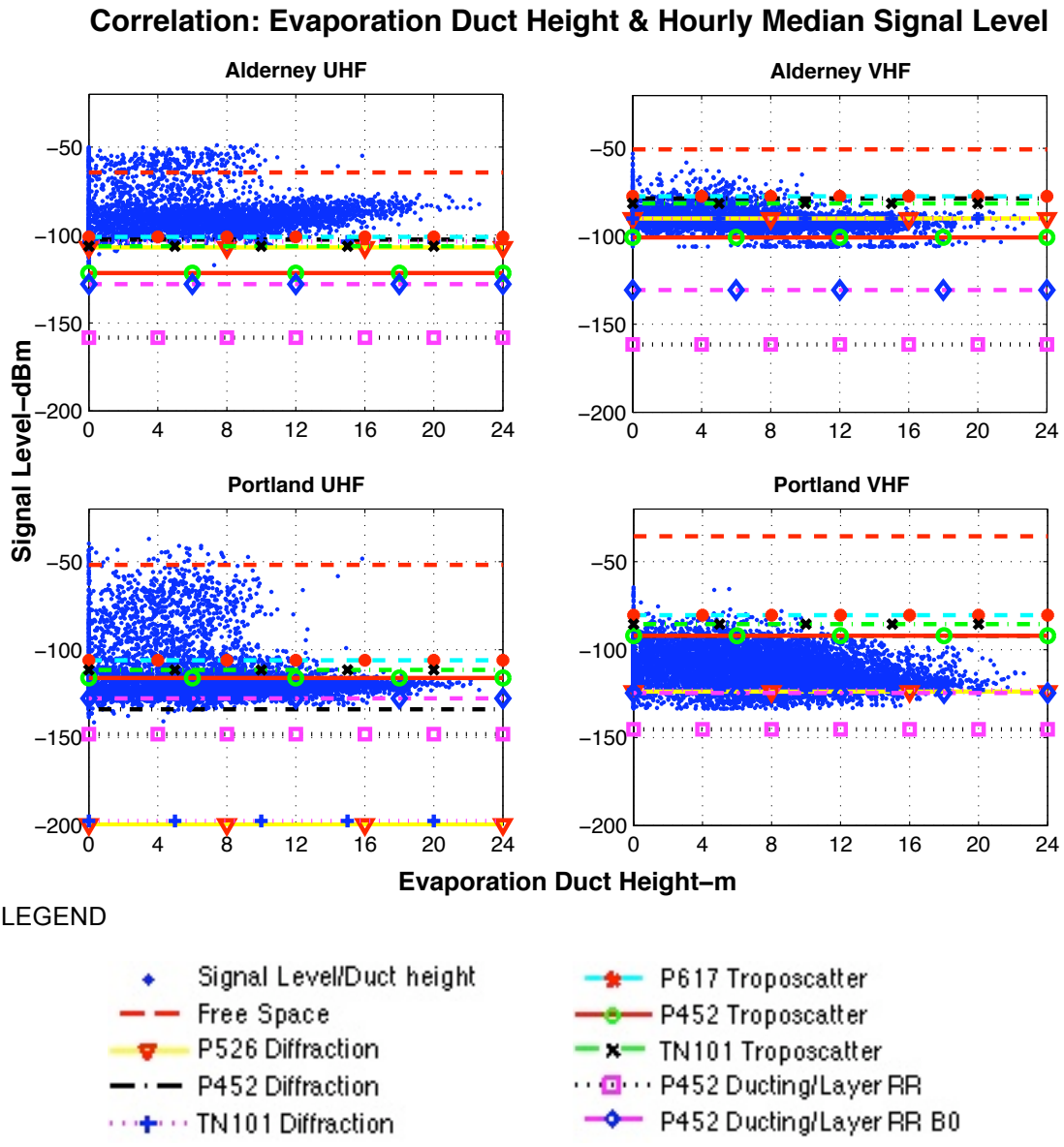

Figure 7-1: Received signal level v/s P-J evaporation duct height

The different mechanisms and values mentioned in the legend have been discussed earlier in Sections 6.3 and 6.4.

The conclusions about the most probable propagation mechanisms are similar to those in Chapter 6, Section 6.4. In addition, an overall conclusion from Figure 7-1 is that there is hardly any correlation between the hourly data from the whole year and hourly evaporation duct height. If the major cluster of data (i.e. non-enhanced signal) is observed, the UHF signal received at Alderney has a slight degree of positive correlation with the evaporation duct height while the VHF signals at both sites have a lesser, negative correlation with evaporation duct height.

If correlation analysis is repeated with different subsets of data categorised as indicated in Table 7-1, the following results are obtained:

Dataset	**Receiving site & frequency**			
	Alderney-UHF	Alderney-VHF	Portland-UHF	Portland-VHF
Whole 'hourly spot' data	-0.01	-0.28	-0.17	-0.21
Data from primary enhancement times	0.07	-0.16	0.00	-0.21
Data from secondary enhancement times	0.10	-0.01	-0.11	-0.04
Data excluding primary enhancement times	0.35	-0.14	0.18	-0.09
Non-enhanced data (data excluding combined enhancement times)	0.41	-0.13	0.19	-0.09

Table 7-1: Correlation coefficients: Evaporation duct height and signal data

The results from Table 7-1 indicate that the non-enhanced UHF signal at Alderney is positively correlated with evaporation duct height. This correlation almost disappears during times of enhanced signal reception.

Gunashekar [50] observed that evaporation ducting was supporting propagation of 2 GHz signals during the times when enhanced signal strengths were not being observed. Though diffraction was the dominant mechanism during such times, evaporation ducting was also prevalent and contributed to higher than diffraction signal strength levels that were still not high enough and hence not considered to be ESS events. The above results tend to match the findings by Gunashekar.

The non-enhanced VHF signals at both the receiving sites have, if any, low (negative) correlation with evaporation duct heights, which remains similar during enhancement. The non-enhanced UHF signal at Portland has low positive correlation with evaporation duct height while hardly any correlation with evaporation duct height during signal enhancement.

If only enhancement events lasting at least 1 hour are considered for this analysis, the results are similar to those in Table 7-1 for the UHF signals received at both sites, while for the VHF signals, the (negative) correlation during enhancement is greater than the values in Table 7-1 (the value of correlation coefficient is -0.30 for primary enhanced VHF signal at Alderney while -0.32 for the primary enhanced VHF signal at Portland).

Comparing these results to the previous relevant ducting studies [55, 89], enhancements in frequencies beyond 3 GHz have often been attributed to evaporation ducting. Also, the study by Bean et al [43] identified minimum and median trapping frequencies for ducting for different times of the year for

coastal city of Bordeaux, France. The lower frequency used in this project (240 MHz) is close to the minimum winter trapping frequency ~200 MHz. The higher frequency (2 GHz), however, is above the median trapping frequencies throughout the year and hence has a higher probability of being supported by ducting.

Simple correlation analysis of the signal levels during transition times (from non-enhanced to enhanced signal reception) values of evaporation duct at those times has been inconclusive, with no correlation with weather at any of the sites.

The median height of the evaporation duct and the effective heights AMSL (including the effects of tidal variations) of the transmitting and receiving antennas during and outside periods of enhanced signal strength reception and non-enhanced are summarised in Table 7-2:

Signal Type	Height variable (h)	Enhanced times	Non-enhanced times
Alderney UHF	Evaporation duct	3.9	7.6
	Tx antenna (Jersey)	16.7	16.5
	Rx antenna (Alderney)	12.2	12.0
Alderney VHF	Evaporation duct	3.8	7.8
	Tx antenna (Jersey)	18.6	17.3
	Rx antenna (Alderney)	14.1	12.8
Portland UHF	Evaporation duct	4.2	8.0
	Jersey antenna (Tx)	16.6	16.4
	Alderney antenna (Rx)	12.5	12.3
Portland VHF	Evaporation duct	4.6	7.9
	Jersey antenna (Tx)	17.9	17.4
	Alderney antenna (Rx)	13.8	13.3

Table 7-2: Median heights (metres) during enhancement events and periods of non-enhanced signal strength

It can be observed that while the median transmitter/receiver antenna heights are similar during periods of enhanced as well as non-enhanced signal reception, the median evaporation duct height decreases considerably during periods of signal enhancement. The results from the table indicate that during times when the signals are not enhanced, they have a greater chance of getting coupled into the evaporation duct than when they are enhanced, because of comparatively lesser height difference.

Table 7-3 gives the median values of signal strengths observed for different configurations of the antennas, with respect to the evaporation duct height:

Signal Type	**Antenna Configuration**						
	Rx < educt	Rx > educt	Tx < educt	Tx > educt	Tx > educt, Rx < educt	Tx, Rx < educt	Tx, Rx > educt
Alderney UHF	-89.7	-92.7	-87.7	-92.6	-90.4	-87.7	-92.7
Alderney VHF	-94.9	-92.9	-95.9	-93.3	-94.6	-95.9	-92.9
Portland UHF	-120.8	-122.8	-120.2	-122.4	-120.8	-120.2	-122.8
Portland VHF	-118.4	-114.9	-118.6	-115.4	-118.4	-118.6	-114.9

Table 7-3: Median signal strengths (dBm) during periods of non-enhanced signal strength, based on different antenna configurations with respect to evaporation duct height

It can be observed from Table 7-3 that the median value of the non-enhanced UHF signal strength at both the receiving sites was higher when both of the antennas were located within the evaporation duct as compared to those

cases when either or both antennas were higher than the evaporation duct height. The difference was more prominent for Alderney than Portland.

In contrast, the results for VHF signals at both the sites suggest that higher signal strengths were achieved when the antennas were not located within the evaporation duct. This observation was more prominent for Portland.

Hence, evaporation ducting appears to be more conducive for propagation of UHF signals than VHF signals. Generally, evaporation ducting helps in increasing the received UHF signal levels, if the antennas are located within the duct. For a comparison between the roles of the transmitter and receiver antennas, the transmitter antenna being within evaporation duct helps in higher received signal strengths.

7.2. Correlation Between Signal Level and Tidal Variations

The instantaneous tide heights at Jersey, Alderney and Portland have been used to estimate the tide height at the centre of the two paths, i.e. Jersey to Alderney and Jersey to Portland. It is assumed that the peaks (and troughs) of tidal variation at the midpoints of the paths occur halfway in time between the times of occurrence of tidal peaks (and troughs) at respective ends of the links and that the height of tide at the midpoints of the paths is the average of the two ends. The correlation between the estimated tide heights and the corresponding hourly signal strengths at the respective antennas at Alderney

and Portland are shown in Figure 7-2, using the hourly median data from the whole year.

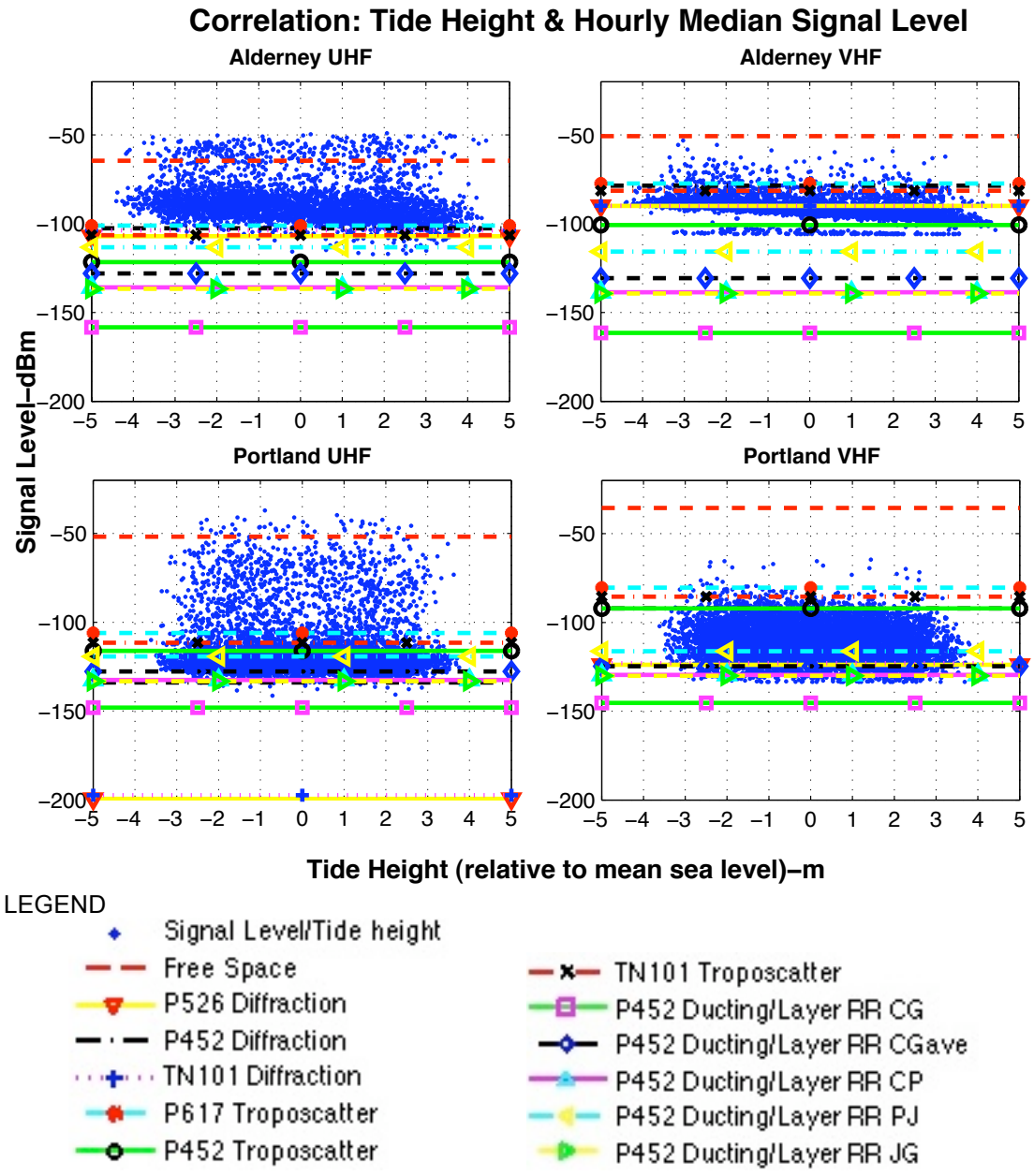

Figure 7-2: Received signal level v/s tide height

The bulk of UHF signal data at Alderney (between -80 dBm and -100 dBm) seems to have some degree of negative correlation with relative tide height. There is indication of stronger negative correlation between VHF signal at Alderney and tide height, for the bulk of data between -80 dBm and -100 dBm.

There is hardly any hint of correlation between UHF signal at Portland and tide height. If any, there is low correlation between VHF signal at Portland and tide height. Lesser influence of tides is expected on the signals at Portland due to the length of the path (~140 km). Similar results are obtained when using 'spot hourly' signal data. Hence, they have not been included here.

If the correlation analysis is repeated with different subsets of data categorised according to Table 7-1, the following values for correlation coefficients are obtained. Similar results are obtained if the analysis is repeated with the 'spot hourly' data from the days when sufficient data from both sites was available:

Dataset	**Receiving Site & Frequency**			
	Alderney-UHF	Alderney-VHF	Portland-UHF	Portland-VHF
Whole 'hourly spot' data	-0.21	-0.39	-0.02	-0.11
Data from primary enhancement times	0.04	-0.04	0.01	-0.09
Data from secondary enhancement times	-0.25	-0.36	0.16	-0.05
Data excluding primary enhancement times	-0.37	-0.43	-0.02	-0.08
Non-enhanced data	-0.40	-0.44	-0.02	-0.08

Table 7-4: Correlation coefficients: Relative tide height and signal data

It is clear from the values of Table 7-4 that the non-enhanced signals at Alderney have high, negative correlations with tidal variation, which disappear during primary signal level enhancements, agreeing with previous findings [50]. Reasonable, negative correlation during secondary enhancements might be indicative of a propagation mechanism involving diffraction and also

causing signal enhancement. The signals received at Portland have hardly any correlation with tide heights during normal and enhanced signal reception.

7.3. Correlation Between Signal Level and Weather Variables

The weather data available is in hourly time resolution. Hence, the study of correlation between weather and signal level data is based on hourly signal strength value (both hourly median and hourly spot values). Tables 7-5 to 7-9 give the values of correlation coefficients based on hourly weather data from weather stations and hourly datasets:

Weather variable (Jersey)	**Receiving site & frequency**			
	Alderney-UHF	Alderney-VHF	Portland-UHF	Portland-VHF
Dewpoint	0.06	0.08	0.12	0.32
Humidity	-0.48	-0.17	-0.29	-0.16
Pressure	0.04	0.07	0.26	0.52
Temperature	0.41	0.21	0.29	0.41
Wind Speed	-0.02	-0.29	-0.28	-0.43

Table 7-5: Correlation coefficients: Jersey weather and hourly median signal

Weather variable (Alderney)	**Receiving site & frequency**			
	Alderney-UHF	Alderney-VHF	Portland-UHF	Portland-VHF
Dewpoint	0.12	0.08	0.14	0.34
Humidity	-0.41	-0.18	-0.25	-0.10
Pressure	0.02	0.07	0.26	0.52
Temperature	0.39	0.21	0.27	0.42
Wind Speed	0.04	-0.31	-0.28	-0.42

Table 7-6: Correlation coefficients: Alderney weather & hourly median signal

Weather variable (Portland)	Receiving site & frequency			
	Alderney-UHF	Alderney-VHF	Portland-UHF	Portland-VHF
Dewpoint	0.18	0.11	0.17	0.37
Humidity	-0.10	0.00	-0.11	-0.02
Pressure	0.04	0.10	0.26	0.50
Temperature	0.29	0.13	0.24	0.40
Wind Speed	-0.05	-0.38	-0.32	-0.39

Table 7-7: Correlation coefficients: Portland weather & hourly median signal

Weather variable (CLV)	Receiving site & frequency			
	Alderney-UHF	Alderney-VHF	Portland-UHF	Portland-VHF
Air Temperature	0.24	0.03	0.16	0.36
Dewpoint	0.21	0.12	0.19	0.37
Humidity	0.07	0.21	0.15	0.24
Pressure	0.02	0.09	0.24	0.48
Sea Temperature	0.13	-0.11	0.05	0.24
Wind Speed	-0.08	-0.40	-0.36	-0.45
ASTD	0.26	0.21	0.28	0.37

Table 7-8: Correlation coefficients: CLV weather & hourly median signal

Weather variable (Guernsey)	Receiving site & frequency			
	Alderney-UHF	Alderney-VHF	Portland-UHF	Portland-VHF
Dewpoint	0.13	0.08	0.14	0.35
Humidity	-0.40	-0.15	-0.23	-0.04
Pressure	0.03	0.08	0.26	0.52
Temperature	0.39	0.19	0.27	0.41
Wind Speed	-0.06	-0.33	-0.29	-0.40

Table 7-9: Correlation coefficients: Guernsey weather & hourly median signal

It was observed that the hourly median signal values and hourly spot signal values follow the same trends in variations, giving values of correlation coefficients close to each other (hence those from spot hourly instants not shown). It is worth reminding the reader that weather data available from Alderney is mostly for 12 hours every day, i.e. from 0500 hours to 1700 hours.

The UHF signal at Alderney has reasonable correlations with temperature (positive) and humidity (negative) measured at neighbouring stations (i.e. Alderney, Jersey and Guernsey). The VHF signal received at Alderney has reasonable (negative) correlation with wind speed.

On the other hand, the UHF signal at Portland indicates some degree of negative correlation with wind speed and low positive correlations with pressure and temperature. The VHF signal received at Portland shows relatively stronger correlations with pressure, temperature, dewpoint (positive), and wind speed (negative).

It can be observed that meteorological variables impact the received signal strengths. It has been observed that the conditions that would generally increase the probability of receiving higher strength signals are: increase in temperature, ASTD, sea-level humidity and decrease in wind speed and humidity at heights above sea level. Increase in pressure tends to increase the signal strengths received at Portland. These variations can lead to the formation of temperature inversion layers and negative humidity gradients (Ref Section 2.2.1), which can be instrumental in creating ducts to trap radio signals and propagate them without considerable loss.

If data from only the days when both Alderney and Portland were receiving data is used, the results show similar general trends as above. However, this is a very general picture since it considers the whole dataset, including times of normal and enhanced reception. If correlation analysis is repeated with

different subsets of data categorised according to Table 7-1, the following results are obtained. Once again, the 'spot hourly' data is used.

Alderney UHF

Dataset	Jersey: Weather variable				
Alderney UHF	Dewp	Humid	Press	Temp	Wspd
Overall hourly spot data	0.05	-0.46	0.03	0.39	-0.02
Primary enhancement times	-0.10	-0.24	0.02	0.18	-0.12
Secondary enhancement times	0.13	-0.25	0.00	0.28	0.17
Excluding primary enhancement times	-0.03	-0.40	-0.03	0.23	0.32
Non-enhanced data	-0.06	-0.42	-0.04	0.21	0.35

Table 7-10: Correlation coefficients: Alderney UHF signal v/s Jersey weather

Dataset	Alderney: Weather variable				
Alderney UHF	Dewp	Humid	Press	Temp	Wspd
Overall hourly spot data	0.10	-0.41	0.02	0.38	0.05
Primary enhancement times	-0.06	-0.32	0.00	0.28	-0.06
Secondary enhancement times	0.12	-0.34	-0.11	0.33	0.44
Excluding primary enhancement times	0.07	-0.37	-0.03	0.29	0.36
Non-enhanced data	0.04	-0.38	-0.04	0.27	0.38

Table 7-11: Correlation coefficients: Alderney UHF signal v/s Alderney weather

There is hardly any correlation with dewpoint and pressure variations. The non-enhanced signal has reasonable, negative correlation with humidity, which decreases during times of enhancement. There is low, positive correlation with temperature at all times. There is low, positive correlation with wind speed when signal experiences no enhancement, but this relationship disappears during primary signal enhancement. The results are similar with Guernsey and Portland weather stations are hence not included.

Table 7-12 investigates UHF signal at Alderney with conditions at CLV:

Dataset	CLV: Weather variable						
Alderney UHF	ATemp	STemp	ASTD	Dewp	Humid	Press	Wspd
Overall hourly spot data	0.23	0.12	0.25	0.20	0.07	0.03	-0.07
Primary enhancement times	0.20	0.17	0.12	0.14	-0.08	0.02	-0.14
Secondary enhancement times	0.30	0.25	0.20	0.23	-0.00	-0.05	0.18
Excluding primary enhancement times	0.25	0.28	0.02	0.09	-0.18	-0.04	0.29
Non-enhanced times	0.26	0.31	-0.02	0.07	-0.23	-0.05	0.32

Table 7-12: Correlation coefficients: Alderney UHF signal v/s CLV weather

UHF signals received at Alderney have low, positive correlation with air and sea temperatures at CLV (comparatively better during non-enhanced periods). There is hardly any correlation with dewpoint, ASTD and pressure. Low correlation of non-enhanced signal with humidity (negative) and wind speed (positive) disappear during enhancement.

Alderney VHF

Tables 7-13 and 7-14 show the statistics derived from VHF signal received at Alderney and weather conditions observed at Jersey and Alderney:

Dataset	Jersey: Weather variable				
Alderney VHF	Dewp	Humid	Press	Temp	Wspd
Overall hourly spot data	0.07	-0.16	0.07	0.19	-0.27
Primary enhancement times	0.03	-0.05	0.21	0.07	-0.26
Secondary enhancement times	0.09	-0.07	0.13	0.14	-0.12
Excluding primary enhancement times	0.07	-0.10	-0.02	0.15	-0.15
Non-enhanced data	0.07	-0.10	-0.02	0.15	-0.14

Table 7-13: Correlation coefficients: Alderney VHF signal v/s Jersey weather

Dataset	Alderney: Weather variable				
Alderney VHF	Dewp	Humid	Press	Temp	Wspd
Overall hourly spot data	0.06	-0.18	0.05	0.18	-0.28
Primary enhancement times	0.10	-0.06	0.22	0.13	-0.25
Secondary enhancement times	-0.08	-0.10	-0.03	-0.02	0.00
Excluding primary enhancement times	0.05	-0.12	0.00	0.13	-0.17
Non-enhanced data	0.04	-0.13	0.00	0.13	-0.16

Table 7-14: Correlation coefficients: Alderney VHF signal v/s Alderney weather

VHF signals received at Alderney have hardly any correlation with dewpoint, temperature and humidity. Non-enhancement signal has almost zero correlation with pressure while enhanced signal has low, positive correlation with pressure. Weak, negative correlation with wind speed during periods of non-enhanced reception gets slightly stronger (staying negative) during primary enhancement. The results with Portland and Guernsey are similar and hence left out.

Table 7-15 investigates VHF signal at Alderney with conditions at CLV.

Dataset	CLV: Weather variable						
Alderney VHF	ATemp	STemp	ASTD	Dewp	Humid	Press	Wspd
Overall hourly spot data	0.03	-0.10	0.22	0.12	0.20	0.08	-0.37
Primary enhancement times	0.20	0.11	0.27	0.22	0.11	0.10	-0.16
Secondary enhancement times	0.14	0.11	0.12	0.19	0.18	0.16	-0.01
Excluding primary enhancement times	0.28	0.25	0.12	0.15	-0.10	-0.04	0.16
Non-enhanced times	0.27	0.25	0.12	0.13	-0.11	-0.03	0.17

Table 7-15: Correlation coefficients: Alderney VHF signal v/s CLV weather

The results indicate that pressure at CLV is hardly correlated with VHF signal level at Alderney. Non-enhanced signal has weak, positive correlations with air and sea temperatures (which decrease during enhancement), and hardly any correlation with other variables. Enhanced signal has weak positive correlations with ASTD and dewpoint.

Portland UHF

Dataset	Jersey: Weather variable				
Portland UHF	Dewp	Humid	Press	Temp	Wspd
Overall hourly spot data	0.11	-0.27	0.25	0.27	-0.26
Primary enhancement times	-0.06	-0.29	0.05	0.18	-0.12
Secondary enhancement times	-0.01	-0.14	0.11	0.11	-0.16
Excluding primary enhancement times	-0.02	-0.17	0.14	0.06	-0.05
Non-enhanced data	-0.03	-0.17	0.14	0.05	-0.04

Table 7-16: Correlation coefficients: Portland UHF signal v/s Jersey weather

Dataset	Portland: Weather variable				
Portland UHF	Dewp	Humid	Press	Temp	Wspd
Overall hourly spot data	0.16	-0.10	0.24	0.22	-0.30
Primary enhancement times	0.03	-0.12	0.05	0.11	-0.21
Secondary enhancement times	0.02	-0.02	0.14	0.04	-0.29
Excluding primary enhancement times	0.02	-0.16	0.13	0.08	-0.01
Non-enhanced data	0.00	-0.16	0.13	0.07	-0.01

Table 7-17: Correlation coefficients: Portland UHF signal v/s Portland weather

There is little correlation of the UHF signals at Portland with dewpoint while weak, negative correlation with humidity (which increases slightly during enhancement) exists. The non-enhanced signal has hint of low, positive correlation with pressure, which disappears during enhancement. The enhanced signal has weak correlation with temperature (positive) and wind speed (negative) while non-enhanced signal hardly had any correlation with these variables. The results with Guernsey (not included) are similar.

Table 7-18 deals with Portland's UHF signal and weather at CLV:

Dataset	CLV: Weather variable						
Portland UHF	ATemp	STemp	ASTD	Dewp	Humid	Press	Wspd
Overall hourly spot data	0.15	0.05	0.27	0.17	0.14	0.23	-0.34
Primary enhancement times	0.13	0.05	0.27	0.08	-0.08	0.06	-0.21
Secondary enhancement times	-0.01	-0.06	0.17	0.01	0.03	0.13	-0.26
Excluding primary enhancement times	0.08	0.11	-0.03	0.00	-0.14	0.13	-0.03
Non-enhanced times	0.06	0.10	-0.04	-0.01	-0.15	0.13	-0.02

Table 7-18: Correlation coefficients: Portland UHF signal v/s CLV weather

There is hardly any correlation of UHF signal at Portland with dewpoint, temperatures, pressure and humidity during times of primary enhancement as well as non-enhanced signal reception. Non-enhanced signal is uncorrelated with wind speed and ASTD while enhanced signal has weak correlations with ASTD (positive) and wind speed (negative).

Portland VHF

Tables 7-19 and 7-20 relate to investigation of correlation of VHF signal received at Portland with weather recorded:

Dataset	Jersey: Weather variable				
Portland VHF	Dewp	Humid	Press	Temp	Wspd
Overall hourly spot data	0.26	-0.15	0.44	0.34	-0.36
Primary enhancement times	0.03	-0.09	-0.08	0.11	-0.10
Secondary enhancement times	0.12	-0.10	0.18	0.19	-0.22
Excluding primary enhancement times	0.17	-0.09	0.37	0.23	-0.24
Non-enhanced data	0.17	-0.09	0.37	0.23	-0.24

Table 7-19: Correlation coefficients: Portland VHF signal v/s Jersey weather

Dataset	Portland: Weather variable				
Portland VHF	Dewp	Humid	Press	Temp	Wspd
Overall hourly spot data	0.31	-0.02	0.42	0.34	-0.33
Primary enhancement times	0.10	0.09	-0.09	0.06	-0.08
Secondary enhancement times	0.16	0.04	0.17	0.17	-0.16
Excluding primary enhancement times	0.19	-0.07	0.36	0.24	-0.20
Non-enhanced data	0.19	-0.07	0.36	0.23	-0.20

Table 7-20: Correlation coefficients: Portland VHF signal v/s Portland weather

The VHF signal received at Portland is uncorrelated with humidity. Non-enhanced data has a small, positive correlation with pressure, which disappears during primary enhancement. Comparatively weaker correlations with dewpoint and temperature (positive), and wind speed (negative) during non-enhanced times become weaker during primary enhancement times. Results with Alderney and Guernsey are similar and hence not included here.

Table 7-21 shows the results with CLV:

Dataset	CLV: Weather variable						
Portland VHF	ATemp	STemp	ASTD	Dewp	Humid	Press	Wspd
Overall hourly spot data	0.30	0.20	0.31	0.31	0.20	0.41	-0.37
Primary enhancement times	0.05	-0.02	0.19	0.11	0.18	-0.10	-0.12
Secondary enhancement times	0.15	0.17	-0.03	0.14	0.06	0.17	-0.20
Excluding primary enhancement times	0.10	0.03	0.16	0.08	0.00	0.19	-0.23
Non-enhanced times	0.10	0.04	0.15	0.07	0.00	0.18	-0.22

Table 7-21: Correlation coefficients: Portland VHF signal v/s CLV weather

There is little correlation of the VHF signal with temperatures and dewpoint while a weak positive correlation with ASTD is observed. The non-enhanced

signal has weak correlations with pressure (positive) and wind speed (negative) while the enhanced signal had weak positive correlation with humidity.

Hence, it can be observed that in many cases the relationships between signal and weather variables change when signals get enhanced. However, some conditions observed that were common to almost all the signals were that the signal strengths tended to increase with temperature, ASTD and sea-level humidity and decrease with increasing wind speed and station-level humidity at heights higher than sea-level. It is possible that the change in weather conditions play a part in signal level enhancements, by giving rise to certain phenomena such as ducting or high k-factor diffraction or refraction, that are conducive to propagation without considerable loss.

Tables 7-22 to 7-25 give the median values of weather variables during times of enhancement and non-enhanced signal reception. The second column in these tables gives the annual median values of different weather variables recorded at the Channel Light Vessel.

While Portland had weather and received signal data available for most of the year, the received signal data as well as the meteorological data recorded at Alderney had some missing information. Hence, the median values from Alderney during or outside periods of signal level enhancement are not close to the median values from the CLV. The results from other weather stations are similar for common variables (hence are not included):

Weather variable	Annual median value at CLV	Median values of weather variables recorded at CLV for times common with times of valid UHF signal reception at Alderney	
		Enhanced	Non-enhanced
ASTD (°C)	-0.4	0.7	-0.5
Air Temp (°C)	11.7	15.6	10.9
Dewpoint (°C)	9.1	14.0	8.4
Humidity (%)	84.3	91.4	83.5
Pressure (hPa)	1015.8	1019.3	1015.2
Sea Temp (°C)	12.1	14.7	11.7
Wind-speed (m/s)	8.2	5.1	8.7

Table 7-22: CLV Weather: Comparison of median values of weather variables for UHF signal at Alderney

Weather variable	Annual median value at CLV	Median values of weather variables recorded at CLV for times common with times of valid VHF signal reception at Alderney	
		Enhanced	Non-enhanced
ASTD (°C)	-0.4	0.5	-0.6
Air Temp (°C)	11.7	14.9	10.7
Dewpoint (°C)	9.1	13.1	8.2
Humidity (%)	84.3	91.4	83.1
Pressure (hPa)	1015.8	1019.4	1014.8
Sea Temp (°C)	12.1	13.8	11.5
Wind-speed (m/s)	8.2	4.6	8.7

Table 7-23: CLV Weather: Comparison of median values of weather variables for VHF signal at Alderney

Weather variable	Annual median value at CLV	Median values of weather variables recorded at CLV for times common with times of valid UHF signal reception at Portland	
		Enhanced	Non-enhanced
ASTD (°C)	-0.4	0.4	-0.6
Air Temp (°C)	11.7	12.4	11.2
Dewpoint (°C)	9.1	10.9	8.4
Humidity (%)	84.3	89.7	82.9
Pressure (hPa)	1015.8	1020.2	1014.2
Sea Temp (°C)	12.1	11.9	12.0
Wind-speed (m/s)	8.2	5.1	8.7

Table 7-24: CLV Weather: Comparison of median values of weather variables for UHF signal at Portland

Weather variable	Annual median value at CLV	Median values of weather variables recorded at CLV for times common with times of valid VHF signal reception at Portland	
		Enhanced	Non-enhanced
ASTD (°C)	-0.4	0.2	-0.6
Air Temp (°C)	11.7	15.0	10.8
Dewpoint (°C)	9.1	12.6	8.1
Humidity (%)	84.3	90.0	82.9
Pressure (hPa)	1015.8	1020.0	1013.8
Sea Temp (°C)	12.1	14.6	11.5
Wind-speed (m/s)	8.2	5.1	8.7

Table 7-25: CLV Weather: Comparison of median values of weather variables for VHF signal at Portland

The general observation from Tables 7-22 to 7-25 and from similar analysis involving the other weather stations is that during enhancement, the median and mean values of the weather variables change considerably. The following changes to weather conditions from periods of non-enhanced signal reception to enhanced signal reception have been observed:

- Increase in temperature and dewpoint
- Increase in ASTD (Air-sea temperature difference)
- Increase in pressure
- Decrease in humidity at stations at higher altitudes while increase in sea-level humidity (with average humidity conditions at Portland almost staying similar), creating a negative humidity gradient
- Decrease in wind speed

These results also agree with the findings by Gunashekar [50]. Also, it was earlier observed (Section 5.10.2.3.) that there were fewer enhancement events in July 2009 than in August 2009 and June 2010. When this was

investigated further on a monthly basis, it was observed that during the month of July, on average the values of pressure on all the weather stations were less than those in August 2009 and June 2010 while comparatively higher wind speeds were observed during July 2009. Since high pressure and low wind speeds are observed prevalent conditions during signal level enhancements, it is anticipated that the reduced percentage of enhancement events can be attributed to these two factors.

7.4. Correlation Between Signal Level and Surface Refractivity

The values of surface refractivity at different weather stations are determined by using hourly weather data from respective weather stations. Table 7-26 gives the correlation statistics of sea level surface refractivity at CLV (N_0) and signal levels at the two receiving sites:

Dataset	**Receiving site & frequency**			
	Alderney-UHF	Alderney-VHF	Portland-UHF	Portland-VHF
Hourly Spot Data	0.18	0.17	0.25	0.46
Primary enhancement times	0.15	0.25	0.09	0.10
Secondary enhancement times	0.17	0.19	0.14	0.29
Excluding primary enhancement times	0.02	0.10	0.06	0.34
Non-enhanced data	-0.01	0.09	0.04	0.34

Table 7-26: Correlation coefficients: CLV surface refractivity & signal data

The non-enhanced signals are generally uncorrelated with N_0, except for the VHF signal at Portland, which is (weakly) positively correlated. During enhancement periods, correlation increases for signals at Alderney, more noticeably for VHF, while the correlation decreases during enhancement of VHF signal at Portland. Results from other stations are similar.

This is suggestive that VHF signal levels normally received at Portland (non-enhanced) tend to increase with sea-level/higher level surface refractivity. Previous research by Fitzsimons [125] on a 87 km trans-horizon, coastal path in Cyprus operating at 4.7 GHz observed reasonable (positive) correlation between weekly median signal level and surface refractivity (~0.6) and reasonable (negative) correlation with wind speed (~-0.4) recorded at three neighbouring weather stations. It was discussed that reasonable correlation with a surface parameter was not possible if troposcatter was the only propagation mechanism. It was hence projected that reflection through layers of lower atmosphere might also be the prevalent mechanism. The results for the non-enhanced VHF signal at Portland are similar and hence similar suggestions can be made about the VHF signal at Portland.

Tables 7-27 and 7-28 give the median values of surface refractivity during periods of enhanced signal levels as well as non-enhanced signal reception, showing that in general, the surface refractivity increases during signal enhancement periods, for all stations from sea level up to 102m AMSL:

Weather Station	UHF		VHF	
	Enhanced	Normal	Enhanced	Normal
CLV (0m)	301.2	293.3	300.3	293.2
Portland (52m)	299.1	291.8	298.0	291.7
Jersey (84m)	295.0	290.3	294.9	290.2
Guernsey (102m)	296.5	290.3	295.6	290.1

Table 7-27: Surface Refractivity: Comparison of median values at Alderney

Weather Station	UHF		VHF	
	Enhanced	Normal	Enhanced	Normal
CLV (0m)	297.7	293.1	300.0	292.9
Portland (52m)	295.7	291.6	297.6	291.4
Jersey (84m)	293.3	290.3	294.7	289.9
Guernsey (102m)	293.7	290.1	295.7	289.8

Table 7-28: Surface Refractivity: Comparison of median values at Portland

During enhanced signal strength reception periods, the average surface refractivity at Guernsey is slightly greater than that at Jersey, in contrast with the gradual decrease-with-height trend observed otherwise. During normal signal reception, the average vertical profile of surface refractivity is that of decrease with altitude.

7.5. Correlation Between Signal Level and Refractivity Gradients

Refractivity gradients (or normalised lapse rates of refractivity) have been determined from the hourly refractivity values. Different pairs of weather stations have been used to determine these normalised lapse rates. Table 7-29 gives the results from correlation analysis of signal with the refractivity gradients based on readings at sea level and 102m heights. The results are not indicative of any trends, during/outside periods of signal enhancement:

Dataset	Receiving site & frequency			
	Alderney-UHF	Alderney-VHF	Portland-UHF	Portland-VHF
Hourly Median Data	-0.13	-0.08	-0.20	-0.19
Hourly Spot Data	-0.16	-0.09	-0.21	-0.17
Primary Enhancement times	-0.14	-0.12	-0.18	-0.07
Secondary Enhancement times	-0.13	0.05	-0.12	-0.11
Excluding primary enhancement times	-0.11	-0.04	0.00	-0.10
Non-enhanced data	-0.13	-0.04	0.01	-0.10

Table 7-29: Correlation coefficients: Signal level and normalised lapse rate of refractivity based on CLV & Guernsey

If the weather station pairs in order of increasing height AMSL are used, the results are given by Tables 7-30 to 7-32:

Dataset	Receiving site & frequency			
	Alderney-UHF	Alderney-VHF	Portland-UHF	Portland-VHF
Hourly Median Data	-0.05	-0.06	-0.09	-0.13
Hourly Spot Data	-0.07	-0.07	-0.10	-0.10
Primary Enhancement times	0.04	-0.06	-0.14	-0.04
Secondary Enhancement times	-0.08	-0.05	0.04	0.06
Excluding primary enhancement times	-0.12	-0.06	0.04	-0.08
Non-enhanced data	-0.13	-0.07	0.05	-0.08

Table 7-30: Correlation coefficients: Signal level and normalised lapse rate of refractivity based on CLV & Portland

Dataset	Receiving site & frequency			
	Alderney-UHF	Alderney-VHF	Portland-UHF	Portland-VHF
Hourly Median Data	-0.22	-0.09	-0.19	-0.21
Hourly Spot Data	-0.20	-0.08	-0.17	-0.19
Primary Enhancement times	-0.17	-0.16	-0.11	-0.11
Secondary Enhancement times	-0.13	0.03	-0.10	-0.19
Excluding primary enhancement times	-0.15	-0.03	-0.11	-0.09
Non-enhanced data	-0.16	-0.03	-0.11	-0.09

Table 7-31: Correlation coefficients: Signal level and normalised lapse rate of refractivity based on Portland & Jersey

The results from CLV-Portland and Portland-Jersey pairs have no noticeable trends different to what has been observed above. The overall deduction from these tables is that signal levels have, if any, very weak negative correlation with refractivity gradients in lowest 84m of atmosphere.

Dataset	Receiving site & frequency			
	Alderney-UHF	Alderney-VHF	Portland-UHF	Portland-VHF
Hourly Median Data	0.21	0.08	0.14	0.23
Hourly Spot Data	0.19	0.07	0.13	0.19
Primary Enhancement times	0.05	0.10	0.07	0.08
Secondary Enhancement times	0.09	0.03	0.03	0.12
Excluding primary enhancement times	0.23	0.07	0.11	0.12
Non-enhanced data	0.24	0.07	0.11	0.12

Table 7-32: Correlation coefficients: Signal level and normalised lapse rate of refractivity based on Jersey & Guernsey

Table 7-32 shows that the non-enhanced UHF signal at Alderney has weak, positive correlation with the lapse rate of refractivity between Jersey and Guernsey. There are no other noticeable trends.

The overall refractive conditions within the lowest 100m have been discussed earlier in Chapter 6 (Section 6.2). However, if only those hourly instants are considered when a valid signal was received and the refractive gradients of those instants are analysed, the following results are obtained. The number in brackets in first row corresponds to the number of valid hourly readings:

Weather station pair	**Refractive condition**	**Alder UHF** (3568)	**Alder VHF** (3892)	**Port UHF** (7830)	**Port VHF** (8452)
CLV-Guernsey	Sub-refractive	4.43	5.15	2.37	2.80
	Normal	93.44	92.74	96.40	96.00
	β_0	0.48	0.44	0.25	0.23
	Super-refractive	2.13	2.11	1.23	1.21
	Ducting	0.00	0.00	0.00	0.00
CLV-Portland	Sub-refractive	12.51	13.02	12.34	13.35
	Normal	70.93	70.60	76.81	76.02
	β_0	8.77	8.81	5.70	5.64
	Super-refractive	14.88	14.79	9.92	9.74
	Ducting	1.68	1.59	0.93	0.89
Portland-Jersey	Sub-refractive	21.83	23.65	19.11	19.84
	Normal	36.24	36.57	50.50	50.88
	β_0	32.13	30.34	21.05	20.19
	Super-refractive	28.28	27.19	22.73	22.14
	Ducting	13.64	12.59	7.66	7.14
Jersey-Guernsey	Sub-refractive	63.47	61.04	50.82	49.13
	Normal	25.55	26.58	39.90	40.74
	β_0	7.31	8.04	5.61	6.12
	Super-refractive	7.90	9.20	7.59	8.37
	Ducting	3.08	3.17	1.69	1.76

Table 7-33: Percentage of time different refractivity gradients are observed between different weather station pairs, for all times when a valid signal was received

If only the readings at sea level and 102m (CLV & Guernsey respectively) are considered, the refractivity gradients appear to be highly-normally refractive. There is hardly any indication of the presence of super-refractive/ducting gradients. However, a breakdown of this height into height-wise pairs reveals that super-refractive and ducting gradients are present for considerable percentages of time when valid signals were recorded at either receiving sites, especially within the 52m to 84m height interval.

If only the non-enhanced data is considered for the analysis of prevalent refractive conditions, the following results are obtained:

Weather station pair	**Refractive condition**	**Alder UHF** (2790)	**Alder VHF** (2725)	**Port UHF** (6451)	**Port VHF** (6640)
CLV-Guernsey	Sub-refractive	3.40	4.12	1.99	2.23
	Normal	95.77	94.66	97.51	97.32
	β_0	0.07	0.22	0.05	0.05
	Super-refractive	0.83	1.22	0.50	0.46
	Ducting	0.00	0.00	0.00	0.00
CLV-Portland	Sub-refractive	12.52	13.05	12.98	14.12
	Normal	70.83	71.17	77.69	76.73
	β_0	8.69	8.62	4.84	4.76
	Super-refractive	15.22	14.14	8.62	8.41
	Ducting	1.42	1.64	0.71	0.73
Portland-Jersey	Sub-refractive	21.67	22.53	18.69	20.57
	Normal	39.26	39.29	54.71	53.99
	β_0	29.05	28.34	17.28	16.44
	Super-refractive	28.33	27.87	21.35	20.74
	Ducting	10.74	10.30	5.25	4.70
Jersey-Guernsey	Sub-refractive	63.66	63.03	48.77	45.94
	Normal	26.79	26.59	42.99	43.91
	β_0	5.93	6.30	4.59	6.09
	Super-refractive	7.01	8.10	7.14	8.67
	Ducting	2.54	2.29	1.10	1.48

Table 7-34: Percentage of non-enhanced time periods different refractivity gradients are observed between different weather station pairs

The deductions from Table 7-34 are similar to those from Table 7-33. Table 7-35 shows the refractivity gradients prevalent during time periods of primary signal enhancement:

Weather station pair	Refractive condition	Alder UHF (468)	Alder VHF (685)	Port UHF (989)	Port VHF (1018)
CLV-Guernsey	Sub-refractive	10.48	8.41	4.40	5.07
	Normal	78.82	85.55	89.88	89.06
	β_0	3.28	1.62	1.43	1.52
	Super-refractive	10.70	6.05	5.73	5.88
	Ducting	0.00	0.00	0.00	0.00
CLV-Portland	Sub-refractive	13.55	13.02	8.37	10.57
	Normal	68.39	65.83	72.76	72.10
	β_0	10.11	10.65	11.02	9.16
	Super-refractive	14.84	19.23	16.53	15.81
	Ducting	3.23	1.92	2.35	1.51
Portland-Jersey	Sub-refractive	22.40	27.87	21.34	15.20
	Normal	18.55	27.24	29.31	35.12
	β_0	51.81	38.43	39.12	40.57
	Super-refractive	27.38	22.99	29.96	29.14
	Ducting	31.67	21.89	19.40	20.55
Jersey-Guernsey	Sub-refractive	62.47	56.11	59.38	63.37
	Normal	16.48	24.92	24.57	24.42
	β_0	16.70	13.95	12.18	8.11
	Super-refractive	13.27	12.23	10.34	8.42
	Ducting	7.78	6.74	5.71	3.79

Table 7-35: Percentage of enhancement time periods different refractivity gradients are observed between different weather station pairs

The results from only 0m and 100m readings apparently reveal no ducting gradients and super-refractive gradients for about 10% or less of enhancement time. It does not appear that in general the lowest 100m of atmosphere is contributing to signal level enhancements as it still appears to be dominantly normally-refractive, with a slight increase in super-refractive as well as sub-refractive gradients (and a corresponding decrease in normally-refractive gradients) as compared to times of normal (non-enhanced) signal

reception. However, once again, a detailed investigation of the lowest 100m reveals interesting results.

The conditions in the lowest 52m are similar for periods of both normal and enhanced signal reception, being slightly more sub-refractive, slightly less normally-refractive (though still remaining predominantly normally-refractive), equally/slightly more conducive for super-refraction and ducting. These changes are comparatively more pronounced for signals at Portland than those at Alderney. However, for both sites and frequencies, the refractivity gradients within the lowest 52m of atmosphere are those of ducting for ~3% or less of enhancement times. Hence, it cannot be really concluded that this part of atmosphere is enabling ducting.

Within the next 32m of the atmosphere (between Portland and Jersey), the refractivity gradients are similarly sub-refractive and super-refractive for the UHF signal at Alderney. However, there is a considerable decrease in percentage share of normally-refractive gradients and a corresponding increase in those of ducting. For the VHF signal at Alderney, the conditions are now slightly more sub-refractive and correspondingly lesser super-refractive, accompanied with a decrease in normally-refractive gradients and a corresponding increase in those of ducting. In comparison with Table 7-34 (non-enhanced signal reception), the conditions are now slightly more sub-refractive, more super-refractive and ducting while correspondingly lesser normally-refractive for the UHF signal at Portland. For the VHF signal at Portland, the conditions are now less sub-refractive and normally-refractive,

while more conducive to super-refraction and ducting. In general, by comparison to non-enhanced signals, the conditions for all the signals are now more conducive to ducting.

The next higher 18m of atmosphere (between Jersey and Guernsey) show similarly dominant sub-refractive conditions for the signals at Alderney. For Portland, this section of atmosphere was sub-refractive and normally-refractive for comparative percentages of time during non-enhanced periods. During signal enhancements, however, this section of atmosphere is clearly dominantly sub-refractive. The conditions are comparatively more supportive of super-refraction and ducting than during non-enhanced signal reception, with ducting and super-refractive gradients accounting for ~21% or less of enhancement time.

Hence, during enhanced signal reception, a general increase in super-refractive and ducting gradients is observed within the lowest 100m of atmosphere, notably between the heights of 52m and 84m. This also re-enforces the observation that in order to have better understanding of vertical profile of atmosphere, observation of meteorological parameters at regular height intervals is essential.

Table 7-36 gives the median values of normalised lapse rates and k-factor (in brackets) during periods of enhanced as well as normal (non-enhanced) UHF signal reception at Alderney:

Pair used for lapse rate	Alderney UHF	
	Enhanced	Non-enhanced
CLV-Guernsey (0m-102m)	-45.8 (1.41)	-30.5 (1.24)
CLV-Portland (0m-52m)	-39.8 (1.34)	-32.5 (1.26)
Portland-Jersey (52m-84m)	-109.1 (3.27)	-43.3 (1.38)
Jersey-Guernsey (84m-102m)	42.1 (0.79)	-4.4 (1.03)

Table 7-36: Normalised lapse rate of refractivity and k-factor: Comparison of medians for UHF signal at Alderney

A general overview of the atmosphere by comparing values at sea level and those at Guernsey (102m) indicates that median conditions remain normally-refractive during or outside signal enhancement. A breakdown of this vertical profile reveals that the lowest 52m remains, on average, normally-refractive. The part within 52m-84m height changes behaviour, from being normally-refractive on average during normal (non-enhanced) reception to being super-refractive during signal enhancement. Correspondingly, the average value of k-factor also increases within this height interval, suggesting that refraction/reflections from layers of atmosphere within this height due to high k-factor could be possible propagation mechanisms during enhancement. The average conditions within 84m to 102m interval are almost sub-refractive/normally-refractive during normal signal reception but change to sub-refractive during enhancement.

Tables 7-37 to 7-39 analyse other signals from this study for similar analysis. The deductions from these tables are similar to those from Table 7-36, except that the average conditions within the 52m to 84m height interval during signal level enhancement are not clearly super-refractive, though the median value is close to the boundary value of -79 N-units/km between normally/super-refractive conditions:

Pair used for lapse rate	Alderney VHF	
	Enhanced	Non-enhanced
CLV-Guernsey (0m-102m)	-39.1 (1.33)	-30.4 (1.24)
CLV-Portland (0m-52m)	-43.4 (1.38)	-32.4 (1.26)
Portland-Jersey (52m-84m)	-63.3 (1.68)	-43.8 (1.39)
Jersey-Guernsey (84m-102m)	15.9 (0.91)	-3.9 (1.03)

Table 7-37: Normalised lapse rate of refractivity and k-factor: Comparison of medians for UHF signal at Alderney

Pair used for lapse rate	Portland UHF	
	Enhanced	Non-enhanced
CLV-Guernsey (0m-102m)	-41.4 (1.36)	-29.8 (1.23)
CLV-Portland (0m-52m)	-42.4 (1.37)	-31.8 (1.25)
Portland-Jersey (52m-84m)	-78.1 (1.99)	-42.1 (1.37)
Jersey-Guernsey (84m-102m)	19.9 (0.89)	-5.7 (1.04)

Table 7-38: Normalised lapse rate of refractivity and k-factor: Comparison of medians for UHF signal at Portland

Pair used for lapse rate	Portland VHF	
	Enhanced	Non-enhanced
CLV-Guernsey (0m-102m)	-39.0 (1.33)	-29.9 (1.24)
CLV-Portland (0m-52m)	-38.7 (1.33)	-31.9 (1.25)
Portland-Jersey (52m-84m)	-78.5 (2.00)	-41.4 (1.36)
Jersey-Guernsey (84m-102m)	29.1 (0.84)	-7.1 (1.05)

Table 7-39: Normalised lapse rate of refractivity and k-factor: Comparison of medians for VHF signal at Portland

For all the above cases (Tables 7-36 to 7-39), there are differences between mean and median values (mean values not included). However, these differences are insignificant and do not affect the deductions made above.

In order to identify any straight-forward relationships between signal levels and lapse rate during transition times (from non-enhanced to enhanced signal reception), correlation analysis of the signal level with values of lapse rates at those times has been inconclusive, with no particular correlation with any lapse rate pair.

7.6. Correlation Between Signal Levels Received at Alderney and Portland

There have been instances when both sites show simultaneous enhancements in signals while at times only one site shows enhancement. Also, at times, both signals at one site have shown mutual enhancements. Hence, the correlation between the high-resolution signal strength datasets may be usefully analysed, as Table 7-40 shows:

Dataset	UHF	VHF
Whole median data	0.58	0.34
Primary enhancement times	0.22	0.50
Secondary enhancement times	0.02	0.00
Excluding primary enhancement times	0.05	0.00
Non-enhanced data	0.05	0.00

Table 7-40: Correlation coefficients: Co-frequency signals at Alderney & Portland

Analysing co-frequency signals at the two receiving sites, there is hardly any correlation between the respective signals at Alderney and Portland during non-enhanced signal reception. However, correlation increases during primary enhancement, with this correlation more evident for VHF signals. This suggests that during times of signal enhancement, there is a higher chance of having a higher signal at Portland when signal at Alderney goes high than during times of non-enhanced signal reception. This tendency is stronger for the enhanced VHF signal than enhanced UHF signal. The correlation coefficient values from the whole dataset indicate that as a general trend, UHF

signals at Alderney and Portland have a greater tendency of increasing/decreasing simultaneously than the VHF signals at these two sites.

Dataset	Alderney	Portland
Whole median data	0.52	0.50
Primary enhancement times	0.16	0.35
Secondary enhancement times	0.29	0.03
Excluding primary enhancement times	0.24	0.22
Non-enhanced data	0.24	0.22

Table 7-41: Correlation coefficients: Mutual co-site signals at Alderney & Portland

The non-enhanced VHF and UHF signals at both sites are weakly, positively correlated. During periods of enhanced signal reception, this correlation decreases for Alderney while increases for Portland. Hence, enhanced UHF and VHF signals at Portland have a greater tendency of increasing/decreasing simultaneously than the enhanced signals at Alderney. The correlation coefficient values from the whole dataset indicate that as a general trend, VHF and UHF signals at both the receiving sites have a higher tendency of increasing/decreasing simultaneously.

7.7. Interim Conclusions

The non-enhanced UHF signal at Alderney tends to increase with evaporation duct height. This relation is not observed for other signals or during enhancement periods. During periods of signal enhancement, generally the

evaporation duct heights are lower than within periods of non-enhanced reception. During non-enhanced signal reception, comparatively higher median UHF signal strengths were observed when both transmitter and receiver antennas were located within the duct. In contrast, higher median VHF signal strengths were observed when antennas were above the evaporation duct.

The non-enhanced UHF and VHF signals at Alderney are reasonably, negatively correlated with tidal variation. This trend is not visible during primary signal level enhancements.

Investigations into correlations between signal level and meteorological variables observed at different weather stations reveal that relationships between signal and weather tend to change as signals become enhanced. The general weather conditions observed to be prevalent during enhanced signal strength were increases in temperature, dewpoint, ASTD, pressure, sea-level humidity and surface refractivity and a decrease in wind speed and higher-altitude humidity. The non-enhanced VHF signal at Portland was moderately positively correlated with surface refractivity, indicative of layer reflection/refraction as propagation mechanism other than troposcatter during such times.

A detailed investigation of the lowest 100m of the atmosphere, with respect to enhanced and non-enhanced signal strengths observed at the receiving sites, shows an increase in super-refractive and ducting gradients when signal

levels were enhanced. These changes were most prominent between the heights of 52m and 84m, indicating that the ducting signatures observed in enhanced signals might possibly be attributed to the gradients within this region of the atmosphere.

The simultaneous non-enhanced signals at both the receiving sites do not tend to increase/decrease together. However, the simultaneous enhanced VHF signals at both the receiving sites tend to increase together. This is indicative that the propagation mechanism for both might be the same. Also, the mutually enhanced UHF and VHF signals at Portland have a greater tendency to increase/decrease simultaneously than those at Alderney. The general trend in variation of signal strengths over the whole year is that co-frequency/co-site signals tend to vary simultaneously.

8. CONCLUSIONS

This study investigates over-sea VHF and UHF propagation, focusing on signal enhancement events, relationships of received signals with the local meteorology and issues pertaining to co-frequency interference, made possible by the rather novel, co-linear configuration of the two over-sea links/paths in the English Channel. The observations and subsequent analysis are based on a year of recording of VHF and UHF signal strengths at two receiving sites, Alderney and Portland.

The work done as part of this research has generally contributed to the existing knowledge in radio systems planning by verifying a few similar previous findings and making new contributions as well as improving the accuracy and understanding of different issues. This study has relied on high-resolution signal and meteorological observations together with an understanding of the propagation mechanisms. It is recommended that, unless more refined studies are undertaken in the region of interest, the findings from this study be preferred over the historic values, due to the reasons discussed in detail in relevant sections.

It is expected that these results would form the stepping-stone of further investigations into relevant subject areas, as well as enable to answer some of the current ITU-R questions pertaining to propagation data and prediction methods for trans-horizon systems, spectrum management and frequency sharing/coordination studies for similar paths/frequencies.

8.1. Summary

A summary of key results obtained from this study are listed below:

- Signal level enhancements have been observed for both receiving sites (Alderney and Portland) and frequencies (240 MHz, 2 GHz), for 12-21% of time when valid signals were received.

- The occurrence of signal enhancement events has a seasonal trend; most of the events lasting at least 10 minutes were observed in summer, late spring and early autumn but there were few enhancements in the other months of the year. A greater percentage of enhanced VHF signal events at both the receiving sites were of short duration.

- Considering those times of year when both receivers were recording valid data, Portland experiences enhancement more often than Alderney, for both VHF and UHF signals. However, most of the events at Portland are of short-duration. If only the longer enhancement events are analysed, about 6% of enhancement events for UHF signal at Alderney last at least 1 hour. The corresponding percentage for VHF signal at Alderney is 1% while those at Portland are 1% and 0.2% for UHF and VHF respectively. Hence, enhanced UHF signal events tend to last longer than enhanced VHF signal events at both the sites. Also, those at Alderney tend to last longer than those at Portland.

- The occurrence of simultaneous signal strength enhancements on Alderney and Portland suggests that the mechanisms responsible for enhancement can sometimes exist at relatively large scale. This happens for around 8% of time for VHF signals and around 10% of time for the UHF signals. Mutual enhancement at both frequencies occurs for ~8% of time at Alderney and 5% of time at Portland while independent enhancement of one frequency while other was non-enhanced occurs ~3% to 8% of the time. These results indicate that at times, the mechanisms responsible for enhancement could be different and conducive to enhancement of signals at one particular site and/or frequency. These results have implications with reference to spectrum and interference management. For example, if Alderney were intended receiver and was receiving VHF or UHF signals at non-enhanced (normal) levels, Portland can potentially receive enhanced signals for at least 8% of time. Hence, un-intended receivers at Portland would get interference from the enhanced signals, although the levels recorded at Alderney were non-enhanced. Hence, a greater care is required when dealing with co-linear paths over-water under similar conditions.

- Portland experienced greater enhancement in signal levels as compared to Alderney while UHF signals experienced greater magnitude of level enhancement as compared to VHF signals. Hence, the mechanisms/conditions responsible for signal level enhancements were found to be comparatively more effective at UHF.

- The occurrence of enhancement was analysed on hourly basis and a diurnal pattern was observed for all signals except the VHF signal at Portland, with a maxima at afternoon/early evening and a minima in morning.

- Enhancement reduces the short-time (fast) fading, most considerably for the UHF signal at Portland, followed by VHF signals at Portland and Alderney respectively.

- According to the results of Shen and Vilar [55], the ‘signatures’ of most of the enhanced events are indicative of ducting.

- It is appreciated and was observed that meteorological measurements at short height intervals give a more accurate and better picture of vertical profile of atmosphere, which does not become visible with larger increments, which is usually the case with available radiosonde measurements. However, it is hard to co-locate weather stations recording at fixed heights. Hence, usually a compromise needs to be made between co-location and lesser height interval by using horizontal homogeneity of weather stations at different locations. In this study it was shown that this was a valid assumption for the geographical area considered. Very strong correlations were observed between meteorological variables recorded at neighbouring weather stations, supporting the assumption of horizontal homogeneity, which was subsequently used for the analysis of weather data with respect to

received signal strengths. The correlations were comparatively stronger in winters and between stations that were closer to each other, vertically and horizontally.

- The median value of lapse rate of refractivity in the lowest 1km of atmosphere for the English Channel, determined from relevant radiosonde data, is -33.5 N-units/km, which is different from the values from previous studies and relevant ITU-R recommendations and procedures by almost 25% (The estimated median value from ITU is ~-43 N-units/km). The calculated median value of lapse rate in turn implies that the respective median value of effective earth radius factor 'k' is 1.27. This is slightly less than the normally used median value of 1.33. Lapse rates in the lowest 1km causing value of 'k' to exceed the standard value have been observed for 7-20% of time. In contrast, the normalised lapse rates within the lowest 100m of atmosphere causing values of 'k' to exceed 4/3 occur for approximately 25 to 48% of time.

- The refractivity gradients within sections of the lowest 100m can follow trends similar or different to those within the lowest 1km of atmosphere. The height interval from 52m to 84m, represented by weather stations at Portland and Jersey, has been observed to be most conducive for super-refraction and ducting. Based on annual median/median readings from radiosonde and weather stations, the height interval from 84m to 102m seems more conducive for sub-refraction.

- The annual mean/median sea level surface refractivity for the English Channel, determined from the CLV data as well as radiosonde data, is ~294 N-units. The current ITU-R datasets and procedures estimate this value to be almost 10% higher at ~328 N-units. The sea level surface refractivity has seasonal trends, with higher monthly mean values in summer than in winter. During summer, the mean values of surface refractivity at noon are higher than those at midnight. This trend reverses during winter and was not observed by previous studies.

- Different mechanisms (e.g. diffraction, troposcatter, ducting, layer reflection etc) can enable propagation of radio signals on the two paths investigated. The path loss values obtained from the prediction models considered can help infer the most probable propagation mechanism by selecting the model with loss values closest to the actual path loss observed. However, the median path loss values predicted by different propagation models are sometimes indicative of different propagation mechanisms.

- The median troposcatter and diffraction loss values predicted by TN-101 lie within the bounds of median values predicted by ITU-R propagation models, suggesting that despite its general assumptions, it is reasonably accurate for median loss predictions. This also supports the recommendations by previous studies for the usage/accuracy of this prediction model.

- The median loss values predicted by sub-model of P.452 associated with ducting and/or layer reflection/refraction were higher for VHF than UHF signals. Hence, P.452 predicts that the UHF signal, though at higher frequency, suffers lesser loss as compared to VHF signal if the propagation mechanism is ducting and/or layer reflection/refraction.

- On the longer path, the median diffraction loss values predicted by P.452 are considerably lower than the other models, which rule out diffraction as a mechanism prevalent on the longer path. The observations seem to agree more with the other models than P.452.

- Evaporation ducting is a near-permanent phenomenon, observed to exist for almost 90% of time with varying duct heights estimated using Paulus-Jeske method. The duct heights reach maximum values during autumn and minimum during summer.

- The mean Paulus-Jeske evaporation duct height over one year of measurement, using bulk weather measurements from Channel Light Vessel), is 7.3m. This value is consistent with previous studies [50, 72, 73, 87, 97].

- UHF signal at Alderney has reasonable correlation with estimated evaporation duct heights during periods of non-enhanced signal reception, suggesting that evaporation ducting is prevalent as normal mechanism during these times. However, it has not been observed to

be the dominant mechanism, though the presence of the antennas within the duct increases the received signal strengths. Based on median effective antenna heights and duct heights, there is a greater probability of non-enhanced signals getting trapped into the ducts than the signals during main enhancement periods. Evaporation ducting appears to be more conducive for propagation of UHF signals as compared to VHF signals. Previous studies also predict similar behaviour [43, 55, 89].

- The tidal variation in the English Channel contributes to the signal strengths received on the shorter trans-horizon path (Jersey-Alderney) of approx. 50 km length at both VHF (240 MHz) and UHF (2 GHz). There is an inverse relationship between signal strength and tide height. This effect is only visible on the shorter path, indicating that diffraction around the bulge of the earth is the pre-dominant mechanism for this path.

- The normally inverse relationship between tide height and signal strength observed at Alderney is lost during primary signal enhancements, indicating that a mechanism other than diffraction prevails during such times.

- The longer path (Jersey-Portland) does not show this tide height-signal relationship and the signature of the non-enhanced signal best matches the troposcatter signature identified by Shen and Vilar [55], indicating

that diffraction is not responsible for propagation of wireless signals on this 140 km path.

- The sea level meteorological conditions observed during enhanced signal propagation are: increase in difference between air and sea temperatures, increase in pressure, dewpoint & humidity and decrease in wind speed. At other stations, decrease in humidity and similar conditions are observed. Such variations are supportive of the formation of temperature inversion layers and negative humidity gradients, which can further create ducts to trap radio signals and propagate them over long distances without considerable loss, as has been observed on both the receiving sites.

- The non-enhanced VHF signal received at Portland was observed to be positively related to surface refractivity. This is suggestive of refraction through layers of lower atmosphere as a possible prevalent mechanism during those times.

- High signal strengths are observed when the average surface refractivity values increase. Also, high signal strengths were observed when the median normalised k-factor values based on refractive index lapse rates in the lowest 100m were higher. These are indicative of the presence of mechanisms involving high k-factor refraction and reflection from layers of atmosphere during high signal strengths.

- Ducting and super-refractive gradients have been observed between CLV (sea-level) and Guernsey Airport (102m), more prominently between Portland (52m) and Jersey (84m).

- The reasonable, positive value of correlation between simultaneously enhanced VHF signals at both the receiving sites suggests that there is a higher probability of having an enhanced VHF signal at Portland/Alderney when the VHF signal at Alderney/Portland is enhanced. The non-enhanced signals do not show any such trend. Also, the enhanced UHF and VHF signals at Portland have a greater tendency of increasing/decreasing simultaneously than the enhanced signals at Alderney.

8.2. Recommendations for Future Work

Research is a continuous process. Taking leads from results of this research, there is further scope of work. The present research has made extensive use of the weather data available from nearby weather stations, based on the assumption of horizontal homogeneity. However, collocated meteorological measurements at short height intervals could be more useful. Ideally, static ship-borne/buoy measurements at path centres and transmit/receive terminals can be arranged, with tall masts accommodating several sensors located at different heights. Also, ship-borne receivers can be utilised for planned runs of ships conducted at noon, sunset, sunrise and midnight to give more insight into specific changes in meteorological variables taking place at these times. If

possible, these can be complemented with airborne measurements for vertical profiles of refractivity, for heights of 200m up to 1.5 km, to help in the understanding the structure of lowest 1km of atmosphere in more detail.

Similar over-land setups can also be investigated for comparative parameters. At the same time, it is suggested that studies in coastal areas (within 15 km of sea), inland areas (more than 50 km from sea) and different terrain (e.g. sand) be carried out. The lowest portions of atmosphere over paths dominated by sands could have an interesting structure, due to the volatile weather conditions normally prevalent in such areas.

In order to extend the understanding of frequency dependence of various phenomena observed, it is recommended to extend similar measurements to wider range of frequencies, paying special regard to the frequency bands marked by ITU for fixed, point-to-point communication, though higher frequencies are expected to get adversely affected by atmospheric attenuation. Also, a new wide-range propagation model has been recently proposed in the form of a draft ITU-R recommendation [126]. In principle, this model is similar to the ITU-R P.452, having sub-models to deal with different mechanisms. However, it addresses a few of the limitations of P.452 as well as including a few mechanisms not part of P.452. The ITU-R recommends the use of this draft model for frequency-sharing studies. It is recommended that the data made available from this study be used to test the newly proposed ITU-R recommendation.

Use has also been made of the data from the radiosonde stations around the English Channel. If high-resolution data from at least 5 years can be available for these radiosonde stations, this can further refine the relevant findings of this research.

APPENDIX A. ALDERNEY UHF CALIBRATION ERROR ANALYSIS (LOWEST 50 dB)

A. Signal Level (dBm)	B. Calibration values (Decimal equivalent)	C. Median Decimal Value	D. Standard Deviation	E. 5th percentile	F. 95th percentile	G. 90%confidence interval (F-E)	H. 10th percentile	I. 90th percentile	J. 80% confidence interval (I-H)	K. Min Decimal Value	L. Max Decimal Value
-120	03x98,04x2	3	0.1407	3	3	0	3	3	0	3	4
-118	03x100	3	0	3	3	0	3	3	0	3	3
-117	03x100	3	0	3	3	0	3	3	0	3	3
-116	04x99,03x1	4	0.1	3	3	0	3	3	0	3	4
-115	09x65,10x34,8	9	0.4935	10	9	1	10	9	1	8	10
-114	16x96,17x2,15x2	16	0.201	16	16	0	16	16	0	15	17
-113	21x51,22x49	21	0.5024	22	21	1	22	21	1	21	22
-112	28x96,27x2,29x2	28	0.201	28	28	0	28	28	0	27	29
-111	34x85,35x15	34	0.3589	35	34	1	35	34	1	34	35
-110	40x99,41	40	0	40	40	0	40	40	0	40	41
-109	46x74,45x25,47	46	0.1	46	45	1	46	45	1	45	47
-108	51x98,50,53	51	0.2245	51	51	0	51	51	0	50	53
-107	56x93,55x7	56	0.2564	57	56	1	56	56	0	55	56
-106	60x77,61x23	60	0.423	61	60	1	61	60	1	60	61
-105	65x100	65	0	65	65	0	65	65	0	65	65
-100	85x99,84	85	0.1	85	85	0	85	85	0	84	85
-95	102x58,101x42	102	0.496	102	101	1	102	101	1	101	102
-90	116x99,115	116	0.1	116	116	0	116	116	0	115	116
-85	129x96,130x3,128	129	0.2	129	129	0	129	129	0	128	130
-80	142x95,141x4,144	142	0.2836	142	142	0	142	142	0	141	144
-75	153x97,154x3	153	0.1714	153	153	0	153	153	0	153	154
-70	164x96,165x4	164	0.1969	164	164	0	164	164	0	164	165

APPENDIX B. ALDERNEY VHF CALIBRATION ERROR ANALYSIS (LOWEST 50 dB)

A. Signal Level (dBm)	B. Calibration values (Decimal equivalent)	C. Median Decimal Value	D. Standard Deviation	E. 5th percentile	F. 95th percentile	G. 90%confidence interval (G-F)	H. 10th percentile	I. 90th percentile	J. 80% confidence interval (J-I)	K. Min Decimal Value	L. Max Decimal Value
-110	3x100	3	0	3	3	0	3	3	0	3	3
-109	3x100	3	0	3	3	0	3	3	0	3	3
-108	3x99,4	3	0.1	3	3	0	3	3	0	3	4
-107	3x96,2x4	3	0.1969	3	3	0	3	3	0	3	4
-106	3x99,2	3	0.1	3	3	0	3	3	0	2	3
-105	4x100	4	0	4	4	0	4	4	0	4	4
-104	9x78,10x22	9	0.4163	10	9	1	10	9	1	9	10
-103	16x87,15x13	16	0.338	16	15	1	16	15	1	15	16
-102	22x66,23x34	22	0.4761	23	22	1	23	22	1	22	23
-101	29x94,28x6	29	0.2387	29	28	1	29	29	0	28	29
-100	35x97,34x2,36	35	0.1738	35	35	0	35	35	0	34	36
-99	40x96,41x4	40	0.1969	40	40	0	40	40	0	40	41
-98	46x54,45x46	46	0.5009	46	45	1	46	45	1	45	46
-97	50x85,51x15	50	0.3589	51	50	1	51	50	1	50	51
-96	55x99,56	55	0.1	55	55	0	55	55	0	55	56
-95	60x97,59x3	60	0.1714	60	60	0	60	60	0	59	60
-90	81x99,82	81	0.1	81	81	0	81	81	0	81	82
-85	98x100	98	0	98	98	0	98	98	0	98	98
-80	113x99,114	113	0.1	113	113	0	113	113	0	113	114
-75	126x98,124,127	126	0.2245	126	126	0	126	126	0	124	127
-70	139x99,138	139	0.1	139	139	0	139	139	0	138	139
-65	150x93,151x7	150	0.2564	151	150	1	150	150	0	150	151
-60	162x68,161x32	162	0.4688	162	161	1	162	161	1	161	162

APPENDIX C. PORTLAND UHF CALIBRATION ERROR ANALYSIS (LOWEST 50 dB)

A. Signal Level (dBm)	B. Calibration values (Decimal equivalent)	C. Median Decimal Value	D. Standard Deviation	E. 5th percentile	F. 95th percentile	G. 90%confidence interval (F-E)	H. 10th percentile	I. 90th percentile	J. 80% confidence interval (I-H)	K. Min Decimal Value	L. Max Decimal Value
-140	9x21,10x10,11x17,12x5,13x2,14x4,8x18,7x13,6x3,5,17x2,15,19,24,35	9	3.7965	16	7	9	13.5	7	6.5	5	35
-139	10x17,11x21,12x16,13x12,14x6,15x4,8x4,9x8,16x3,17x3,18,19,20,23,30,31	11.5	3.7082	18.5	9	9.5	16	9	7	8	31
-138	13x15,14x15,15x12,10x11,11x12,13x22,16x5,17,8x2,19,20,23,26x2	13	2.892	18	10	8	16	10	6	8	26
-137	16x13,17x7,18x4,12x11,13x12,14x20,15x17,11x2,19x2,20x2,21x5,22,23,24,34,35	15	3.8281	21.5	12	9.5	20.5	12	8.5	11	35
-136	16x18,17x22,18x16,19x7,20x7,21x4,14x7,15x7,22x2,23x2,24,25,27,13x4,28	17	2.7864	23	14	9	21	14	7	13	28
-135	18x24,19x18,20x14,21x20,16x2,17x6,22x5,24x3,23x2,26x2,25,27,34,63	19.5	5.0084	25.5	17	8.5	23	18	5	16	63
-134	20x14,21x14,22x27,23x17,24x10,25x5,19x3,26x2,28x2,32x2,27,30,31,33	22	2.7326	29	20	9	25.5	20	5.5	19	33
-133	24x21,25x19,26x17,27x12,28x6,29x5,22x2,23x9,32x3,34x3,30,33	25	3.5938	32	23	9	29	23	6	22	33
-132	27x13,28x23,29x14,30x15,31x9,26x5,32x4,33x5,34x3,36x2,25x2,38,39,41,47,59	29	4.4256	37	26	11	33.5	27	6.5	25	59
-131	31x23,32x25,33x21,34x12,35x4,37x5,38x2,40x2,30x2,29x2,41,36	32	2.2361	37.5	31	6.5	36.5	31	5.5	29	41
-130	35x19,36x24,37x25,38x10,39x5,34x10,40x2,33,41,43,46,60	36	3.0288	40	34	6	39	34	5	33	60
-129	39x28,40x26,41x12,42x7,43x2,44x5,38x9,37x3,45x2,47x2,46,48,49,61	40	3.1087	46.5	38	8.5	44	38	6	37	61
-128	42x16,43x36,44x17,45x9,46x7,47x2,48x3,49x3,41x2,50x2,52,54,56	43	2.6019	49.5	42	7.5	48	42	6	41	56
-127	47x36,48x25,49x10,50x2,45x3,46x17,52x2,56x2,51,53,64	47	2.4538	52	46	6	49	46	3	45	64
-126	50x22,51x27,52x25,53x10,54x6,55x2,57x2,59x2,56,61,62,67	52	2.7218	58	50	8	54.5	50	4.5	50	67
-125	56x31,55x26,57x15,58x9,59x6,54x8,60,63,66,71,74	56	2.9082	59.5	54	5.5	59	55	4	54	74
-120	76x55,75x18,78x7,77x17,79x2,80	76	0.9625	78	75	3	77.5	75	2.5	75	80
-115	92x66,91x24,93x7,94x2,90	92	0.6416	93	91	2	92	91	1	90	94
-110	107x70,108x29,106	107	0.4731	108	107	1	108	107	1	106	108
-105	121x100	121	0	121	121	0	121	121	0	121	121
-100	134x86,133x13,135	134	0.3562	134	133	1	134	133	1	133	135
-95	146x75,145x25	146	0.4352	146	145	1	146	145	1	145	146
-90	157x99,158	157	0.1	157	157	0	157	157	0	157	158

APPENDIX D. PORTLAND VHF CALIBRATION ERROR ANALYSIS (LOWEST 50 dB)

A. Signal Level (dBm)	B. Calibration values (Decimal equivalent)	C. Median Decimal Value	D. Standard Deviation	E. 5th percentile	F. 95th percentile	G. 90%confidence interval (F-E)	H. 10th percentile	I. 90th percentile	J. 80% confidence interval (I-H)	K. Min Decimal Value	L. Max Decimal Value
-135	3x91,2,7,8,10x5,18	3	2.1982	10	3	7	3	3	0	2	18
-134	3x91,4x2,6,8,10,11x3,13	3	1.8829	9	3	6	3	3	0	3	13
-133	3x78,2,4x7,5x4,10,11x4,12x2,13,14,16	3	2.7902	11.5	3	8.5	7.5	3	4.5	2	16
-132	3x66,4x14,10x2,12x4,15,11,18,5x5,14x2,16,13,9,6	3	3.4514	13.5	3	10.5	11.5	3	8.5	3	18
-131	4x47,5x17,3x12,6x5,7x3,8x2,10,12x3,13x3,15x4,16,21,58	4	6.3129	15	3	12	12.5	3	9.5	3	58
-130	3x4,4x42,5x30,6x13,7x3,8x3,11,12,13x3	5	1.9714	9.5	4	5.5	7	4	3	3	13
-129	5x7,6x28,7x41,8x10,9x3,10,12,14,15x2,16x3,17x3	7	2.8312	16	5	11	11	6	5	5	17
-128	8x4,9x30,10x37,11x15,12x6,13x3,17x3,18,21	10	2.083	15	9	6	12	9	3	8	21
-127	12x18,13x37,14x26,15x12,11x2,20,21,22x2,33	13	2.6769	17.5	12	5.5	15	12	3	11	23
-126	16x6,17x38,18x37,19x8,20x5,21x2,22,23,25,26	18	1.6267	21	16	5	20	17	3	16	26
-125	21x28,22x41,23x15,20x4,24x2,25x2,27,28x2,29x3,30x2	22	2.1046	28.5	21	7.5	24.5	21	3.5	20	30
-124	25x18,26x37,27x24,28x16,30x2,31x2,33	26	1.4117	29	25	4	28	25	3	25	33
-123	30x37,31x46,32x9,29,33,34x2,35,36,37x2	31	1.367	34	30	4	32	30	2	29	37
-122	35x26,36x51,37x14,34x4,38x2,39x2,41	36	1.0384	37.5	35	2.5	37	35	2	34	41
-121	40x35,41x36,42x17,39x5,43x2,44x3,45x2	41	1.1828	43.5	40	3.5	42	40	2	39	45
-120	44x12,45x53,46x22,47x7,48x4,49,50	45	1.0952	48	44	4	47	44	3	44	50
-115	66x62,67x33,68x3,65x2	66	0.5801	67	66	1	67	66	1	65	68
-110	85x10,86x88,87x2	86	0.3387	86	85	1	86	85.5	0.5	85	87
-105	102x92,103x6,101x2	102	0.2814	103	102	1	102	102	0	101	103
-100	117x99,116	117	0.1	117	117	0	117	117	0	116	117
-95	130x100	130	0	130	130	0	130	130	0	130	130
-90	142x78,143x22	142	0.4163	143	142	1	143	142	1	142	143
-85	154x99,153	154	0.1	154	154	0	154	154	0	153	154

REFERENCES

1. Ofcom (2007), “The International Communications Market 2007”, *Research Document*, Ofcom, London, UK. 12 December.

2. Ofcom (2007), “Choice, competition, innovation: Delivering the benefits of the digital dividend”, *News Release*, Ofcom, London, UK, 13 December.

3. ITU (1994), “Calculation of free-space attenuation”, *Recommendation ITU-R P.525-2*, ITU, Switzerland, August.

4. Friis,H.T. (1946), “A note on a simple transmission formula”, *Proceedings of the Institute of Radio Engineers*, Vol 34, p. 254, May

5. ITU (2008), “The Radio Regulations”, *The Radio Regulations-Edition of 2008*, Article 1

6. Hall, M.P.M, Barclay, L.W. and Hewitt, M.T. (1996), “Propagation of Radiowaves”. *Short Run Press Ltd., Exeter*, Chapter 1,4 (D.F.Bacon), Chapter 6 & 8 (K.H.Craig) and Chapter 7 (J.W.F.Goddard).

7. Griffiths, J. (1987), “Radio Wave Propagation and Antennas, An Introduction”. *Prentice Hall*, pg.74-76

8. White, I. (1992), “The VHF/UHF Book”. DIR Publishing, Chapter 2.

9. Collin, R. E. (1985), “Antennas and Radiowave Propagation”, *McGraw Hill Book Company*, Chapters 1 & 6

10. Huang, Y and Boyle, K. (2008), “Antennas-From Theory to Practice”, *John Wiley & Sons Ltd*, West Sussex, UK, Chapter 3

11. Sim, C. Y. D. (2002), “The propagation of VHF and UHF radio waves over sea paths”, *Thesis (PhD)*, University of Leicester, UK

12. ITU (2009), “Propagation by Diffraction”, *Recommendation ITU-R P.526-11*, ITU, Switzerland, October.

13. Struzak, R. (2006), “Radio-wave Propagation Basics”, *ICTP-ITU-URSI School on Wireless Networking for Development*, The Abdus Salam International Centre for Theoretical Physics ICTP, Italy, February.

14. Olsen, R.L., Rogers, D.V., Hulays, R.A. and Kharaldy, M.M.Z. (1993), “Interference due to Hydrometeor Scatter on Satellite Communication Links”, *IEEE Proceedings*, No 6, Vol 81, June.

15. Garlington, T. (2006), Microwave Line-of-Sight Transmission Engineering, *Technical Publication*, US Army Information Systems Engineering Command, Transmission Systems Directorate, USA, June.

16. Bean, B.R. and Dutton, E.J. (1966), "Radio Meteorology". *National Bureau of Standards Monograph 92*, US Department of Commerce, March.

17. Freeman, R.L. (2007), "Radio System Design for Telecommunications", *Third Edition*, John Wiley & Sons, Chapters 1, 5. January.

18. ITU (2003), "The radio refractive index: its formula and refractivity data", *Recommendation ITU-R P.453-9*, ITU, Switzerland.

19. ITU (1999), "The concept of Transmission Loss for Radio Links", *Recommendation ITU-R P.341-5*, ITU, Switzerland.

20. ITU (1992), "Propagation Prediction Techniques And Data Required For The Design Of Trans-Horizon Radio-Relay Systems", *Recommendation ITU-R P.617-1*, ITU, Switzerland.

21. ITU (2009), "Prediction procedure for the evaluation of interference between stations on the surface of the Earth at frequencies above about 0.1 GHz", *Recommendation ITU-R P.452-14*, ITU, Switzerland. October

22. ITU (2009), "Attenuation by atmospheric gases", *Recommendation ITU-R P.676-8*, ITU, Switzerland. October

23. ITU (2007), "Effects of tropospheric refraction on radiowave propagation", *Recommendation ITU-R P.834-6*, ITU, Switzerland. January

24. ITU (1994), "Definitions of terms relating to propagation in non-ionized media", *Recommendation ITU-R P.310-9*, ITU, Switzerland. August

25. Rice, P.L., Longley, A.G., Norton, K.A. and Barsis, A.P. (1967), "Transmission Loss Predictions for Tropospheric Communication Circuits", *Vols 1 & 2*, USA. January

26. ITU (2009), "Annual Mean Surface Temperature", *Recommendation ITU-R P.1510-2*, ITU, Switzerland. October

27. Meissner, T. and Wentz F. (2004), "The Complex Dielectric Constant of Pure and Sea Water from Microwave Satellite Observations", *IEEE Transactions On Geoscience And Remote Sensing*, Vol. 42, No. 9, Sep

28. ITU (2009), "Guide to the application of the propagation methods of Radiocommunication Study Group 3", *Recommendation ITU-R P.1144-5*, ITU, Switzerland, October

29. AOR Ltd (1999), “AR5000, AR5000c, AR5000+3”, *Product Information Leaflet*, AOR Ltd, Japan

30. Jaybeam Ltd, “Type 7043 VHF/UHF 8 Element Yagi High Gain end mounted”, *Product Datasheet*, Jaybeam Limited, UK

31. Jaybeam Wireless, “7360008-Cellular Yagis-1900-2170 Yagis, ideal for repeaters and linear coverage systems”, *Product Datasheet*, Jaybeam Wireless, UK

32. Meinberg (2009), “GPS167PC: GPS Receiver for Computers (ISA-Bus)”, *Product Information Brochure*, Meinberg Radio Clocks, Germany

33. Meinberg (2009), “GPS170PCI: GPS Clock for Computers (PCI/PCI-X Bus)”, *Product Information Brochure*, Meinberg Radio Clocks, Germany

34. AOR Ltd (1999), “AR5000 RS-232C Command List”, *Technical Document*, AOR Ltd, Japan

35. Nova Engineering (2008), “NovaSource G6 RF Signal Source User Manual”, *User Manual*, Version 1.3, L-3 Communications, Nova Engineering

36. Nova Engineering (2008), “NovaSource G6 RF Signal Source Programming the NovaSource G6”, *Application Note*, Revision 2.0, L-3 Nova Engineering

37. Nova Engineering (2007), “NovaSource M2 RF Signal Source User Manual”, *User Manual*, Version 3.3, L-3 Communications, Nova Engineering

38. Nova Engineering (2005), “NovaSource M2”, *Application Note*, Revision 1, L-3 Nova Engineering, April

39. Google Earth (2010), “Channel Islands”, 49° 42’ N and 2° 0’ W, GOOGLE EARTH, November

40. Google Earth (2011), “English Channel”, 49° 42’ N and 2° 0’ W, GOOGLE EARTH, June

41. Marlec (2007), “FM1803-2 Furlmatic Windcharger”, *Technical Document*, Marlec Engineering Co Ltd, UK, May

42. Bye, G.D. and Howell, R.G. (1989), “Average Radio Refractive Index Lapse Rate Of The Lower Troposphere For Locations In NW Europe”, *Sixth International Conference on Antennas and Propagation 1989*, pp 229-233, Vol 2, April

43. Bean, B.R., Cahoon, B.A., Samson, C.A. and Thayer, G.D. (1966), “A World Atlas of Atmospheric Radio Refractivity”, *Institute for Telecommunication Sciences and Aeronomy,* Boulder, Colorado, USA

44. Bech, J., Codina, B., Lorente, J. and Bebbington, D. (2002), “ Monthly and daily variations of radar anomalous propagation conditions: How ‘normal’ is normal propagation?”, *Proceedings of ERAD 2002,* pp35–39, Delft, Netherlands

45. Ford B.W. (1996), “Atmospheric Refraction: How Electromagnetic Waves Bend in the Atmosphere and Why It Matters”, US Navy

46. AR Worldwide (2008), “Model KMW1080”, *Technical Specification*, AR Worldwide, Modular RF, Washington, USA

47. Accelonix (2008), “E/NPA/2G/100W”, *Technical Specification*, Accelonix Narrow band amplifier specification sheet, UK

48. Hall, M.P.M (1979), “Effects of the Troposphere on Radio Communication”, *IEEE Electromagnetic Waves Series*, First Edition, ISBN 0-906048-25-7, Exeter, UK

49. Lane, J.A. (1961), “The radio refractive index gradient over the British Isles”, *Journal of Atmospheric and Terrestrial Physics*, Vol.21, pp.157-166

50. Gunashekar, S.D. (2006), “An Investigation Of The Propagation Of 2 GHz Radio Waves Over Sea Paths”, *Thesis (PhD)*, University of Leicester, UK

51. Rudd, R (2009), “Statistics of Anomalous Tropospheric Propagation at UHF frequencies”, *IEEE 3rd European Conference on Antennas and Propagation 2009 (EuCap2009),* pp.3862-3864, 23-27 March

52. Levy, M.F., Craig, K.H., Champion, R.J.B., Eastment, J.D. and Whitehead, N.W.M. (1991), “Airborne Measurements of Anomalous Propagation over the English Channel”, *IEE Seventh International Conference on Antennas and Propagation 1991 (ICAP 91)*, pp 173-176, Vol 1, April

53. BBC (1972), “UHF Medium Distance Tropospheric Propagation Measurements over the English Channel”, *BBC Research Department Report No. 1972/6*, March

54. Ames, L.A., Newman, P., Rogers, T.F. (1955), “VHF Tropospheric Overwater Measurements For Beyond the Radio Horizon”, *Proceedings of the IRE*, Vol. 43, pp. 1369-1373, October

55. Shen, X.D. and Vilar, E. (1995), “Anomalous Transhorizon Propagation and Meteorological Processes of a Multilink Path”, *Journal of Radio Science*, Vol 30, pp. 1467-1479, October

56. Shen, X.D. and Vilar, E. (1996), “Path loss statistics and mechanisms of transhorizon propagation over a sea path”, *Electronics Letters*, Vol 32, No. 3, pp 259 – 261, February

57. Joy, W.R.R. (1958), “The Long-Range Propagation of Radio Waves at 10 cm Wavelength”, *IEE Proceedings*, Vol 105, pp 153-157

58. Ndzi, D., Austin, J. and Vilar, E. (1997), “Fading Statistics on an Over-the-Sea Transhorizon Link”, *1997 High Frequency Postgraduate Student Colloquium*, University of Leeds, September

59. Longley, A.G., Reasoner, R. K. and Fuller, V. L. (1971), “Measured And Predicted Long Term Distributions Of Tropospheric Transmission Loss”, *Telecommunications Research & Engineering Report 16*, US Department of Commerce, July

60. Smith, Jr., E.K., and S. Weintraub (1953), “The Constants in the Equation for Atmospheric Refractive Index at Radio Frequencies” *Proceedings of the IRE*, Vol. 41, pp. 1035-1037

61. ITU (2009), “Method for point-to-area predictions for terrestrial services in the frequency range 30 MHz to 3 000 MHz”, *Recommendation ITU-R P.1546-4*, October

62. ITU (2009), “A path-specific propagation prediction method for point-to-area terrestrial services in the VHF and UHF bands”, *Recommendation ITU-R P.1812-1*, October

63. ITU (2005), “Reference standard atmospheres”, *Recommendation ITU-R P.835-4*, March

64. COST (2002), “COST 255 – Radiowave propagation modelling for new satellite communication services at Ku-band and above”, *Final Report*, CCLRC, March

65. Longley, A.G. and Rice, P.L. (1968), “Prediction of Tropospheric Radio Transmission Loss Over Irregular Terrain: A Computer Method-1968”, *ESSA Technical Report ERL 79-ITS 67*, July

66. Longley, A. G. and Reasoner, R.K. (1970), “Comparison of propagation measurements with predicted values in the 20 to 10,000 MHz range”, *ESSA Tech Report ERL 148 - ITS 97*

67. Frazier, W.E. (1984), “Handbook Of Radio Wave Propagation Loss (100 - 10,000 MHz)”, *NTIA REPORT 84-165*, December

68. Longley, A.G. (1976), “Location Variability of Transmission Loss– Land Mobile and Broadcast Systems”, *Office of Telecommunications OT Report 76-87*, May

69. Weissberger, M., 'Meidenbauer, R., Riggins, H. and Marcus, S. (1982), “Radio Wave Propagation: A Handbook Of Practical Techniques For Computing Basic Transmission Loss And Field Strength”, *Handbook,* EMC Analysis Centre, Department of Defense, USA, September

70. Mini-Circuits (2009), “Coaxial Low Noise Amplifier ZX60-242LN+”, *Specification Sheet*, Mini-Circuits USA

71. Mini-Circuits (2009), “Coaxial Low Noise Amplifier ZX60-33LN+”, *Specification Sheet*, Mini-Circuits USA

72. Barclay, L.W. (Editor) (2003), “Propagation of Radiowaves”, *The Institution of Electrical Engineers*, 2nd Edition, London, United Kingdom

73. Hitney, H.V., Richter J.H., Pappert R.A., Anderson K.D. and Baumgartner, G.B., Jr. (1985), “Tropospheric Radio Propagation Assessment”, *Proceedings of the IEEE*, Vol. 73, No. 2, pp. 265-283

74. Helvey, R. (1983), “Radiosonde errors and spurious surface-based ducts,” *IEE Proceedings*, Vol. 130, No. 7, pp. 643-648, December

75. Glevy, D.F. (1976), “An assessment of radio propagation affected by horizontal changes in refractivity,” *Naval Electronics Lab. Cen. Tech. Note 3153*, May

76. Rowden, R.A., Tagholm, L.F. and Stark, J.W. (1958), “A Survey of Tropospheric Wave Propagation Measurements by the BBC, 1946-1957”, *IEE Paper No.2517*

77. Hitney, H.V. and Vieth, R. (1990), “Statistical Assessment of Evaporation Duct Propagation”, *IEEE Transactions on Antennas and Propagation*, Vol 38, No. 6, June

78. Jeske, H. (1965) “Die Ausbrietung elektromagnetischer Wellen im cm- bis m-Band iiber dem Meer unter besonderer Beriicksichtigung der meterologischen Bedingungen in der maritimen Grenzschicht,” *Hamburger Geophysikalische Einzelschriften*, Hamburg

79. Paulus, R.A. (1985) “Practical application of an evaporation duct model,” *Radio Science*, Vol. 20, No. 4, pp. 887-896, July-Aug

80. Boithias, L. and Battesti, J. (1983), “Propagation due to tropospheric inhomogeneities”, *IEE Proceedings*, Vol. 130, No. 7, December

81. Patterson, W.L. (1998), “Advanced Refractive Effects Prediction System (AREPS)”, *User’s Manual*, Version 1.0, SPAWAR, US Navy, April

82. Hitney, H.V. (2002), “Evaporation duct assessment from meteorological buoys” *Radio Science*, Vol. 37, No. 4, 1055, 10.1029/2000RS002325

83. Babin, S.M., Young, G.S., and Carton, J.A. (1997), “A New Model of the Oceanic Evaporation Duct”, *Journal of Applied Meteorology*, Vol. 36, pp. 193-204, March

84. Baumgartner Jr., G.B., Hitney, H.V. and Pappert, R.A. (1983), “Duct propagation modelling for the integrated-refractive-effects prediction system (IREPS)”, *IEE Proceedings – Part F*, Vol. 130, No. 7, pp. 630-642

85. Patterson, W.L., Hattan, C.P., Lindem G.E., Paulus R.A., Hitney H.V., Anderson K.D. and Barrios, A.E (1994), “Engineer’s Refractive Effects Prediction System (EREPS)”, *Technical Document 2648*, Version 3.0, US Navy

86. Space and Naval Warfare Systems Command (SPAWAR) (2004), “User’s Manual (UM) for Advanced Refractive Effects Prediction System (AREPS)”, *Technical Document,* Atmospheric Propagation Branch, San Diego, US Navy

87. Skolnik, M.I. (1980), “Introduction to Radar Systems”, *Third Edition*, McGraw-Hill Inc.

88. ITU (1992), “Electrical Characteristics Of The Surface Of The Earth”, *Recommendation ITU-R P.527-3*, March

89. Wickerts, S., and Nilsson, L. (1973), “The Occurrence of Very High Field Strengths at Beyond the Horizon Propagation Over Sea in the Frequency Range 60-5000 MHz,” *Modern Topics in Microwave Propagation and Air-Sea Interaction*, edited by Zancla, A., pp. 217-240, D. Reidel Publishing Company

90. Gough, M.W. (1979), “UHF Signal Strength Measurement as a guide to Atmospheric Structures”, *The Marconi Review*, Vol.42, Number 214, pp. 135-152

91. Castel, F.D., Editor (1965), “Progress in Radio Science”, *Elsevier Publishing Company*, 1960-1963, Volume 2 – Radio and Troposphere, pp. 127-135

92. Stark, J.W. (1965), “Simultaneous long distance tropospheric propagation measurements at 560 and 774 MHz over the North Sea”. *Radio and Electronic Engineering*, Vol.30, pp. 241-255, October.

93. Roda, G. (1988), “Troposcatter Radio Links”, *Artech House Inc*, Chapter 1,3,4 and 6.

94. Goldhirsh, J. and Musiani, H. (1999), “Signal level statistics and case studies for an over-the-horizon mid-Atlantic coastal link operating at C-band”, *Radio Science*, Volume 34, Number 2, pp 355-370, March-April.

95. Anderson, K.D. (1987), “Worldwide Distributions of Shipboard Surface Meteorological Observations for EM Propagation Analysis,” *NOSC Technical Document 1150 (ADA188771)*, 40 pp., Naval Ocean Systems Center, San Diego, CA, Sep

96. Paulus, R.A. and Anderson, K.D. (2000), “Application Of An Evaporation Duct Climatology In The Littoral”, *Proceedings of the Battlespace Atmospherics and Cloud Impact on Military Operations*, BACIMO 2000, Fort Collins, CO, 25-27 April

97. Christophe, F., Douchin N., Hurtaud Y., Dion D., Makarushka R., Heemskerk H., and Anderson K. (1995), “Overview of NATO/AC 243/Panel 3 Activities Concerning Radiowave Propagation in Coastal Environments,” *AGARD CP-567 (ADA296641)*, Propagation Assessment in Coastal Environments, February.

98. Goldhirsh, J., Dockery G.D., and Musiani B.H. (1994), “Three years of C band signal measurements for overwater, line-of-sight links in the mid-Atlantic coast,” *Radio Science*, Vol 29, Number 6, pp 1421-1431.

99. Laven, P.A., Taplin D.W., and Bell C.P. (1970), “ Television reception over sea paths: the effect of the tide,” *BBC Research Department Report (Report No. RA-62, Serial No. 1970/22)*, Research Department, Engineering Division, The British Broadcasting Corporation.

100. Tawfik, A.N. and Vilar, E. (1993), “X-Band Transhorizon Measurements of CW Transmissions Over the Sea-Part I: Path Loss, Duration of Events, and Their Modelling”, *IEEE Transactions On Antennas And Propagation*, Vol. 41, No. 11, November

101. CCIR (1986), “Propagation data required for transhorizon radio relay systems,” *Report 238-5*, pp. 367-388, Geneva.

102. Yeh, L.P. (1960), “Simple methods for designing troposcatter circuits,” *IEEE Transactions on Communication Systems*, Vol. CS-8, pp. 193-198, September.

103. Rider, G.C. (1962), “Median signal level prediction for tropospheric scatter,” *Marconi Review*, Vol. 146, pp. 203-210

104. Boithias, L. (1983), “Radio Wave Propagation,” *Mcgraw-Hill*, North Oxford Academic, London.

105. Tawfik, A.N., Vilar, E. and Martin, L. (1993), "Correlation Of Transhorizon Signal Level Strength With Localised Surface Meteorological Parameters", *Eighth International Conference on Antennas and Propagation (ICAP 93)*, Herriot-Watt University, Edinburgh, pp. 335-339, March/April

106. Gunashekar, S.D., Warrington, E.M. and Siddle, D.R. (2008), "Propagation of 2 GHz Radio Waves Over the English Channel: Analysis of Cases of Sub-Refraction", *Proceedings of the XXIX General Assembly of the International Union of Radio Science (URSI) 2008*, Chicago, USA, 7-16 August

107. Ofcom (2012), "Telecommunications Market Data Tables Q3 2011", *Communications Market Report*, Ofcom, London, UK. 02 February.

108. Ofcom (2011), "The International Communications Market 2007", *Research Document*, Ofcom, London, UK. 14 December.

109. ITU (2007), "Radiometeorological data required for the planning of terrestrial and space communication systems and space research application", *ITU-R Question*, ITU, Switzerland.

110. ITU (2007), "Methods for predicting propagation over the surface of the Earth", *ITU-R Question*, ITU, Switzerland.

111. ITU (1995), "Propagation data and prediction methods required for trans-horizon systems", *ITU-R Question*, ITU, Switzerland.

112. ITU (2012), "Work programme and Questions of Radiocommunication Study Groups", *ITU-R Resolution*, ITU, Switzerland

113. Kerr, D.E. (1990), "Propagation of short radio waves", *The Institution of Electrical Engineers*, Electromagnetic Waves Series 24, pp 5, UK

114. Lerner, L.S. (1997), "Physics for Scientists and Engineers", *Vol 2*, pp 947 – 952, USA

115. Vaisala (1997), "RS80 Radiosondes", *Technical Specifications*, Finland

116. BADC (2007), "BADC Help File: Radiosonde Data", *BADC*, Apr

117. Lehpamer H. (2004), "Microwave Transmission Networks-Planning, Design and Deployment", *McGraw-Hill Professional Engineering Series*, pp 36-38

118. Al-Nuaimi, M., Richter, J. and Gkionis, A. (2002), "Influence Of Metrology On The Trans-Horizon Illumination Of Obstacles And Their Site Shielding Factor", *Proceedings of the 27th General Assembly*, International Union of Radio Science (URSI), pp1611-1614, Aug

119. Iskander, M. F. and Yun, Z. (2002), “Propagation Prediction Models for Wireless Communication Systems”, *IEEE Transactions On Microwave Theory And Techniques,* Vol. 50, No. 3, March

120. ITU (1995), “VHF and UHF propagation curves for the frequency range from 30 MHz to 1 000 MHz. Broadcasting service”, *Recommendation ITU-R P.370-7*, suppressed in October 2001, superseded by P.1546, October

121. ITU (2001), “Radio Regulations 1-Articles”, *ITU-R Radio Regulations*, *Edition of 2001*, pp 9

122. Willis, M.J. (2011), “SRTMPathProfile”, *Version 0.54*

123. IFR (1999), “IFR 2023A/B, 2025”, *Technical Document*, *Issue 1*, IFR Ltd, Longacres House, Norton Green Road, Stevenage, Herts., UK

124. Bell, S. (1999), “A Beginner's Guide to Uncertainty of Measurement”, *Measurement Good Practice Guide No. 11 (Issue 2)*, National Physical Laboratory, UK, Aug, pp 4-5

125. Fitzsimons, T.K. (1968), “Observations of tropospheric-scatter path loss at C band frequencies and meteorological conditions in Cyprus”, *IEE Proceedings*, Vol. 115, No. 7, July

126. ITU (2012), “A general purpose wide-range terrestrial propagation model in the frequency range 30 MHz to 50 GHz”, *Recommendation ITU-R P.2001*, February

INTERNET REFERENCES

I. “electromagnetic spectrum.” Babylon Dictionary. Babylon Dictionary Online. Babylon Dictionary, 2011. 09 June 2011. <http://dictionary.babylon.com/electromagnetic_spectrum/>

II. "telecommunications media." Encyclopædia Britannica. Encyclopædia Britannica Online. Encyclopædia Britannica, 2011. Web. 09 June 2011. <http://www.britannica.com/EBchecked/topic/585825/telecommunications-media>.

III. “Fresnel Zone.” Averse. Wikipedia, 2011. Web. 15 June 2011. <http://commons.wikimedia.org/wiki/File:Fresnelsche_zone.gif>

IV. http://www.dxfm.com/Content/propagation.htm

V. “Wave Propagation.” *Communication Systems*, Wikipedia. Wikibooks Online Book. 17 June 2011. <http://en.wikibooks.org/wiki/Communication_Systems/Wave_Propagation>

VI. “Doppler Radar Beam.” How Radar Works, NOAA. Online School for Weather. 19 June 2011. <http://www.srh.noaa.gov/jetstream/doppler/beam_max.htm>

VII. “Tables of Physical & Chemical Constants”, (1995), 16th edition. Section 2.7.9 Physical Properties of sea water. Kaye & Laby Online. Version 1.0 (2005). 23 June 2011. <http://www.kayelaby.npl.co.uk/general_physics/2_7/2_7_9.html>

VIII. “Relative Humidity and Dewpoint Temperature from Temperature and Wet-Bulb Temperature ”, (2010), NOAA, <http://www.srh.noaa.gov/images/epz/wxcalc/rhTdFromWetBulb.pdf

IX. “Anticyclone”, (2011), National Weather Service, NOAA, <http://www.nws.noaa.gov/glossary/index.php?word=anticyclone>

LIST OF PUBLICATIONS

The following is a list of the various publications that have been produced during the duration of work reported in this thesis:

Mufti, N., Siddle, D.R. and Warrington, E.M. (2009), “Modelling UHF and VHF Signals and Interference at Cold-Sea Paths”, *URSI Festival of Radio Science*, University of Birmingham, Birmingham, UK, December.

Mufti, N., Siddle, D.R. and Warrington, E.M. (2010), “Radio, the atmosphere and the sea - Prediction of interference between radio signals on over-sea links”, *Festival of Postgraduate Research*, University of Leicester, Leicester, UK, June.